VOLUME 38 SECOND SERIES NUMBER 5 1931

ics Lib.

THE PHYSICAL REVIEW

A JOURNAL OF EXPERIMENTAL AND THEORETICAL PHYSICS

CONDUCTED BY

THE AMERICAN PHYSICAL SOCIETY

BOARD OF EDITORS

Managing Editor, JOHN T. TATE, University of Minnesota, Minneapolis
Assistant Editor, J. W. BUCHTA, University of Minnesota, Minneapolis
E. U. CONDON, C. J. DAVISSON, F. K. RICHTMYER, K. F. HERZFELD, A. W. HULL,
F. W. LOOMIS, A. J. DEMPSTER, DAVID M. DENNISON, J. C. SLATER

SEPTEMBER 1, 1931

First Spark Spectrum of Rubidium (Rb II) — O. LAPORTE, G. R. MILLER, AND R. A. SAWYER — 843
Nuclear Spin of Potassium — F. W. LOOMIS AND R. W. WOOD — 854
Isotope Separation in the Spectra of Li I — D. S. HUGHES — 859
Energy Relations in Complex Spectra — DAVID R. INGLIS — 862
Ultra-Ionization Potentials in Mercury Vapor — A. G. SHENSTONE — 873
Excitation Probabilities for Electrons in Helium, Neon, and Argon — L. C. VAN ATTA — 876
Effect of Temperature on the Continuous Band Spectrum of Mercury Vapor — W. M. NIELSEN — 888
Spectral Fluorescence Efficiencies of Certain Substances with Applications to Heterochromatic Photographic Photometry — GEORGE R. HARRISON AND PHILIP A. LEIGHTON — 899
Effect of Varying Concentrations of Certain Electrolytes on the Violet Band of the Raman Spectra of Water — C. C. HATLEY AND DIXON CALLIHAN — 909
Satellites of *M*-Series X-ray Lines — F. R. HIRSH, JR. — 914
New Effect Produced by Action of X-rays on Matter — G. I. POKROWSKI — 925
X-ray Study of the Magnetic Character of Liquid Crystalline Para-Azoxyanisol and a Comparison with the Isotropic Liquid — G. W. STEWART — 931
Measurements on the Vapor Stream from the Cathode of a Vacuum Arc — W. E. BERKEY AND R. C. MASON — 943
Electrodeless Discharge: Method of Measuring Induced Current, Variation of Current with Pressure for Various Gases — CHARLES T. KNIPP AND JULIAN K. KNIPP — 948
Life of Metastable Mercury and Evidence for a Long-Lived Metastable Vibrating Nitrogen Molecule — M. L. POOL — 955
Ionization of Kr and Xe by Positive Alkali Ions and the Ionization Potentials of Ne, A, Kr, and Xe — OTTO BEECK AND J. CARLISLE MOUZON — 967
Aging of Ions in Air and Nitrogen — JOHN ZELENY — 969
Reflection of Mercury from Alkali Halide Crystals — H. A. ZAHL AND A. ELLETT — 977
Low Temperature Rotational Heat Capacities and the Relative Amounts of the Nuclear Singlet, Triplet and Quintet Symmetry Modifications of Methane — D. S. VILLARS AND G. SCHULTZE — 998
Acoustic Resonator Interferometer: I. The Acoustic System and its Equivalent Electric Network — J. C. HUBBARD — 1011
On the Strain-Energy Function for Isotropic Bodies — C. KAPLAN — 1020
On the Increase in Surface Area Due to Crystal Faces Developed by Etching — LEWI TONKS — 1030
Crystal Structure of Sodium Nitrite, $NaNO_2$ — G. E. ZIEGLER — 1040
Light of the Night Sky — JOSEPH KAPLAN — 1048
Stability of the Atmosphere of a Rotating Star — ROSS GUNN — 1052
Dielectric Constants of Certain Organic Liquids at Medium Frequency — W. R. PYLE — 1057
Letters to the Editor — 1071

Relation Between the Scattering of X-rays by Gases and Crystals, *G. E. M. Jauncey and G. G. Harvey*—1071; Reflection of Electrons by a Special Potential Field, *E. L. Hill*—1072; Quantization of Large Scale Events, *David L. Watson*—1072; The Emission of Positive Ions from Cu and Ag, *H. B. Wahlin*—1074; The Alternating Intensities of N_2 Bands, *Harold C. Urey*—1076; The Red CN Band System, *F. A. Jenkins, Yale K. Roots, and Robert S. Mulliken*—1075; Reaction Due to Gas Molecules Leaving the Cathode of an Arc, *B. Wallman*—1077; Angular Distribution of Photoelectrons, *A. Sommerfeld*—1078; The Effect of Piezoelectric Oscillation on the Intensity of X-ray Reflections from Quartz, *S. Nishikawa, Y. Sakisaka and I. Sumoto*—1078; A New Criterion for Predissociation, *Joseph Kaplan*—1079; Predissociation in Nitrogen and Excitation of the Green Auroral Line, *Joseph Kaplan*—1079

Book Reviews — 1081

PUBLISHED BY THE AMERICAN PHYSICAL SOCIETY
EDITORIAL OFFICE: MINNEAPOLIS, MINN.

THE AMERICAN PHYSICAL SOCIETY

OFFICERS OF THE SOCIETY

President:	W. F. G. Swann	Bartol Research Foundation, Philadelphia, Pa.
Vice-President:	Paul D. Foote	The Gulf Companies, Pittsburgh, Pa.
Secretary:	W. L. Severinghaus	Columbia University, New York City
Treasurer:	G. B. Pegram	Columbia University, New York City
Editor:	John T. Tate	University of Minnesota, Minneapolis, Minn.
Local Secretary for the Pacific Coast:	L. B. Loeb	University of California, Berkeley, Calif.

THE PHYSICAL REVIEW

Published by the American Physical Society. Executive office: University of Minnesota, Minneapolis, Minn. Two volumes annually, twelve issues per volume.

First series. From July 1, 1893, to January 1, 1913, the Review was conducted by Edward L. Nicholas, Ernest Merritt and Frederick Bedell, with the financial support of Cornell University. The first four volumes were issued annually; subsequent volumes, semi-annually; thirty-five volumes in all.

Second series. On January 1, 1913, the Review was transferred to the American Physical Society as announced on the first page of the new series which was then begun. Since then it has been conducted by a Board of Editors elected by the Society. Semi-annual volumes begin in January and July. Since July 1, 1929, the Review has been issued twice a month.

Contributors are referred to page 2 of the advertisements for further information.

Annual subscription, throughout the Postal Union, $12.00 in advance.

General index, 1893-1920, $4.00, in advance.

Back Volumes, $9.00 per volume; Back Numbers, $1.50 per copy for issues prior to July 1, 1929 (Vols. 1-33), $.75 per copy for issues subsequent thereto. Postage is free if remittance accompanies order; otherwise postage is extra. No bound volumes can be supplied. The Review offers to purchase a limited number of First Series, Vol. 1, No. 1 (at $2.00 each); Second Series, Vol. 7, No. 1, January 1916; Vol. 7, No. 2, February 1916; Vol. 7, No. 4, April 1916; and Vol. 7, No. 5, May 1916 (at $2.00 each).

Advertisements. Rates will be supplied by the Editor on request. Copy for each number must be received at Minneapolis two weeks prior to the dates of issue; old copy is used until new copy is received. Send electrotypes direct to the printers, George Banta Publishing Co., Menasha, Wis.

Discount of ten percent is allowed to members of the American Physical Society on purchase of back numbers.

Changes of Address and Complaints of failure to receive the Review, in the case of members of the Physical Society, should be addressed to the Treasurer; in the case of other subscribers, to the Editor. New copies can be sent free in response to complaint of non-delivery only if notice of non-delivery is received within three months of date of issue.

Editorial Correspondence should be addressed to the Physical Review, University of Minnesota, Minneapolis, Minn.

Entered at the post office at Menasha, Wis., as second class matter.
Acceptance for mailing at special rate of postage provided for in section 1103, Act of October 3, 1917, authorized September 6, 1926.

THE
PHYSICAL REVIEW

THE FIRST SPARK SPECTRUM OF RUBIDIUM (Rb II)

By Otto Laporte, George R. Miller, and Ralph A. Sawyer
University of Michigan

(Received July 23, 1931)

Abstract

The resonance lines of Rb II have been photographed in the extreme ultraviolet region with the vacuum spectrograph. The mode of excitation was the hollow cathode discharge in helium, and in addition, the hot spark was employed with rubidium hydroxide in cored aluminum electrodes. The values of the wave-lengths of the ultraviolet lines for Rb II were obtained from third order measurements. The visible region was photographed with various glass and quartz spectrographs. With the separations of the resonance lines as guides, the classification scheme given by Reinheimmer was found to be correct, but incomplete. Some lines taken from Otsuka's data were fitted into the scheme. The coupling is of an intermediate type approaching that of (*jj*) form. Levels of the $4p^5 4d$, $4p^5 5s$, $4p^5 5p$, $4p^5 5d$, and $4p^5 6s$ configurations were identified. Their separations were compared with Kr I. It was also attempted to separate the $^3P_2$ and $^3P_1$ terms due to $4p^5(5s, 6s)$ from the $4p^5(4d, 5d)$ levels. The limit of excitation furnished by metastable helium falls exactly between the various levels caused by the $4p^5 5p$ configuration, thus providing a check on the interpretation of the classification. The ionizing potential of Rb II was calculated to be 27.3 volts.

I. Experimental Procedure

A PRELIMINARY exposure of Rb II excited in the hollow cathode discharge in helium was photographed in the vacuum region with a 1 m vacuum spectrograph and the positions of the resonance lines were noted. Their intensities were not sufficient to give wave-length determinations from second and third order measurements hence the hot spark was employed for producing the excitation using rubidium hydroxide in cored aluminum electrodes.

An E_1 Hilger quartz prism spectrograph was used for the region λ2470 to λ4300 with an iron comparison spectrum as standards. Due to its higher dispersion, the E_1 glass prism spectrograph was used for the regions λ4100 to λ5800 with an iron comparison spectrum, and λ5800 to λ8000 with an argon comparison spectrum. The reductions of wave-lengths were made by means of a Hartmann formula.

II. Analysis of the Rb II Spectrum

In Table I we give the spectral levels to be expected in Rb II for the two limiting cases of Russell-Saunders and of (*jj*) coupling. Rb II, however, belongs like many other spectra to an intermediate type where neither case is completely realized.

The positions of the levels due to various configurations are largely influenced by the principal quantum number of the valence electron and by the degree of ionization; i.e according to whether we consider Kr I, Rb II, Sr III, the configurations will yield levels of different positions relative to each other. To illustrate this point a schematic Moseley diagram of the energy levels of Kr I and its isoelectronic analogues is given in Fig. 1.

TABLE I. *Electron configurations and theoretical terms of the Rb II spectrum.*

Electron configuration	Russell-Saunders						(*jj*)		Number of levels
$4p^5$	^2P						$^2P_{1\frac{1}{2}}$	$^2P_{\frac{1}{2}}$	
$4p^6$				$^1S_0$			0		(1)
$4p^55s$ $4p^56s$ $4p^57s$ —		$^1P_1$			$^3P_{210}$		12	01	(4)
$4p^55p$ $4p^56p$ $4p^57p$ —	$^1S_0$	$^1P_1$	$^1D_2$	$^3S_1$	$^3P_{210}$	$^3D_{321}$	12 0123	01 12	(10)
$4p^54d$ $4p^55d$ $4p^56d$ —	$^1P_1$	$^1D_2$	$^1F_3$	$^3P_{210}$	$^3D_{321}$	$^3F_{432}$	0123 1234	12 23	(12)
$4p^54f$ $4p^55f$ $4p^56f$ —	$^1D_2$	$^1F_3$	$^1G_4$	$^3D_{321}$	$^3F_{432}$	$^3G_{543}$	1234 2345	23 34	(12)

In this diagram the $(\nu/R)^{1/2}$ of the term values of the levels arising from one configuration and referred to $4p^5$ are represented by approximately straight lines as functions of the atomic number. Since we know the position of the levels in Kr I[1] and since for larger values of Z the slope of these Moseley curves approaches the value $1/n$ (n being the total quantum number of the valence electron) we are able to get a rough idea concerning the mutual position of the levels with respect to each other. It is seen that the Moseley lines of the configurations $4p^6$ and $4p^54d$ form a screening doublet because they involve valence electrons of the same principal quantum number 4. Similarly the configurations $4p^55s$ and $4p^55p$ form a screening doublet since their respective valence electrons have the same total quantum number 5. However, it is characteristic for this isoelectronic series that due to their higher total quantum number, the configurations $4p^55s$ and $4p^55p$ diverge from the Moseley line belonging to $4p^5$ and cross the Moseley line belonging to $4p^54d$. In the limit of high ionizations the configurations $4p^54d$ will be nearest to the ground level $4p^6$ while the configurations $4p^55s$ and $4p^55p$ are more and more removed from $4p^6$ an $4p^54d$. In Kr I the configuration $4p^55s$ is still nearest to

[1] W. F. Meggers, T. L. de Bruin, C. J. Humphreys, Bureau of Standards, J. of Res. **3**, 731 (1929).

the ground level $4p^6$, but as is seen from the diagram it must be expected that in Rb II the configurations $4p^5 5s$ and $4p^5 4d$ will just be overlapping whereas for higher ionizations $4p^5 4d$ will lie below $4p^5 5s$. We shall see in the next chapter that indeed in Rb II, $4p^5 5s$ and $4p^5 4d$ overlap, thus complicating considerably the analysis of the spectrum. For the same reason, the configurations $4p^5 6s$ and $4p^5 5d$ overlap also.

The $4p^5 5p$ levels lie in a distinct group about in the middle between the lower $4p^5 5s$ and $4p^5 4d$ levels and the upper $4p^5 6s$ and $4p^5 5d$ levels.

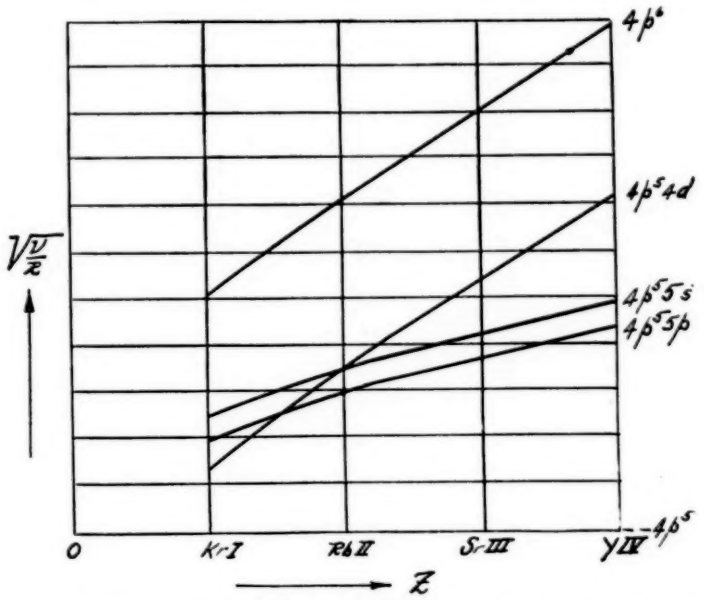

Fig. 1. Schematic Moseley diagram of "average" values of $(\nu/R)^{1/2}$ plotted against atomic number, Z.

III. Identification of Levels and Configurations in Rb II

1. Using the separations of the resonance lines obtained in the extreme ultraviolet region as a guide, the classification was extended to the visible region and is presented in Table II.

The first and second columns contain the spectroscopic notations[2] of the levels arising from the $4p^5 4d$, $4p^5 5d$ and $4p^5 5s$, $4p^5 6s$ configurations respectively, while the third column contains the J values of these levels. The fourth column contains the relative term values of the levels of these configurations and are referred to the $4p^6\ {}^1S_0$ level. The heads of the remaining columns are designated with the spectroscopic notations[2] and relative term values (referred to $4p^6\ {}^1S_0$) of the levels due to the $4p^6$ and $4p^5 5p$ configurations. In the body of the table are the wave numbers of the spectral lines, followed in parenthesis by their intensities. Below each wave number is the discrepancy

[2] Since it is impossible to assign L and S values to the levels, the levels were numbered according to their order, and the inner quantum number was given as lower index to this number. The odd configurations are indicated with a small zero as upper index.

TABLE II. *Classification of lines of Rb II.*

$4p^5(4d, 5s)$ d	s	J		$4p^6$ $^1S_0$ J=0	$4p^55p$ 1_1 J=1	2_2 2	3_2 3	4_1 1	5_2 2	6_0 0	7_2 1	8_2 2	9_1 1	10_0 0
			Rel. Term	0	154279.25	156742.20	156900.72	158156.66	158717.04	161205.13	163929.47	164972.81	165094.55	167367.30
1_1°		1	126453.53			30289.10*(13) .43		31703.10*(0) −.03	32263.90*(2) .39	34751.50*(2) −.10				
2_2°		2	128693.70		25585.57 (1) .24			29463.06 (7) .10	30023.60*(2) .26					
	$^3P_2$°	2	133347.29		20932.20 (9) −.05	23395.24 (8) .33	23553.65 (10) .22	24809.60 (5) .23	25369.90 (10) .15			31625.30*(1) −.22	31747.20*(5) −.06	
	$^3P_1$°	1	134875.14	134875.00(15) −.14	19404.19 (6) .08	21867.06 (10) 0		23281.81 (8) .29	23842.03 (9) .13	26330.36 (7) .37		30097.85 (0) .18	30219.30*(0) −.11	32762.00*(1) −.16
3_2°		2	136665.21								27264.20 (1) −.06	28307.70 (2) .10	28429.50*(2) .16	
4_0°		0	138799.56		15479.57 (6) −.05			19357.24 (2) .14			25129.87 (7)		26295.03 (5) .04	
5_1°		1	140615.18	140613.00 (9) −2.18	13663.97 (1) −.10	16126.94 (2) .08		17541.59 (6) .11	18101.78 (6) −.08	20590.06 (3) .11	23314.33 (8) −.04	24357.76 (8) .13	24479.35 (6) −.02	27022.13(4) .01
	$^3P_0$°	0	141879.24								22050.27 (3) .04		23215.29 (2) −.02	
$6_{1,2}$°		1,2	143027.39								20902.12 (7) .04		22067.14 (6) −.02	
	$^1P_1$°	1	143467.00	143464.00 (5) −3.00				14689.64 (1) −.02	15249.87 (2) −.17	17738.19 (6) .06	20462.51 (5) .04	21506.03 (8) .22	21627.53 (5) −.02	24170.43 (7) .13
7_2°		2	143960.94					14195.70 (2) −.02	14755.95 (9) −.15			21012.03 (5) .16	21133.62 (5) .01	
$8_{1,2}$°		1,2	145630.06					12526.30 (30) −.30	13087.10 (50) .12					
$4p^5(5d, 6s)$														
	$^3P_2$°	2	179740.11		25460.86 (4) 0	22997.95 (4) .04	22839.52 (5) .13	21583.30 (2) −.15	21023.18 (5) .11					
	$^3P_1$°	1	180173.33		25894.08 (2) .10	23431.17 (5) .04		22016.54 (5) −.13	21456.37 (4) .08	18968.24 (3) .04				
1_1°		1	184205.27		29926.12 (1) .20	27463.03 (1) −.04		26048.48 (1) −.13	25488.32 (3) .09	23000.14 (1) 0				
2_2°		2	184841.65		30562.60*(7)	28099.26 (0) −.19	27940.95 (1) .02	26684.87 (3) −.12	26124.74 (4) .13					
3_2°		3	185131.62			28389.40 (3) −.02	28230.85 (2) −.05		26414.60 (0) .02					
4_1°		2	185622.53		31343.70*(0) .42	28880.35 (2) −.02	28721.60*(3) −.21	27465.78 (4) −.09	26905.64 (1) .15					
5_2°		3	186010.87			29268.66 (6) −.04	29110.01 (0) −.14		27293.89 (4) .06					
6_1°		1	187340.37								23410.97 (4) .04	22367.53 (5) −.03	22245.92 (4) .10	19703.16 (0) .09
	$^1P_1$°	1	188622.28					30465.30*(5) −.32		27417.12 (3) −.03	24692.70 (0) .07	23649.57 (0) .10	23527.88 (1) .15	
7_1°		1	189006.27			32263.90*(2) −.17			30289.10*(3) −.03	27801.5 (1) −.36				
$8_{1,2}$°		1,2	192380.15								28450.50*(3) −.12	27407.39 (0) .05	27285.88 (4) .28	

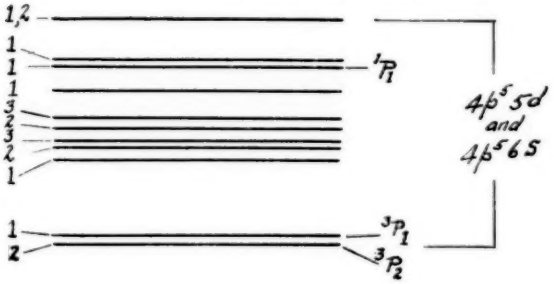

Fig. 2 – Energy Diagram for Rb II

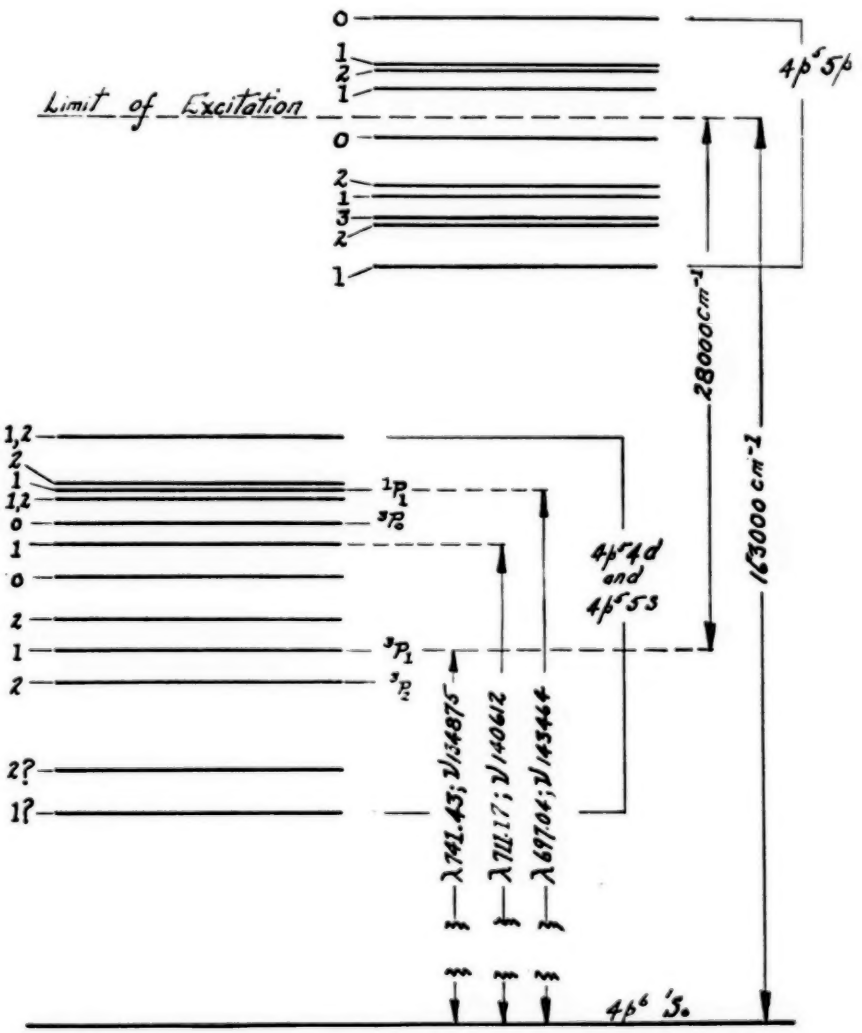

Fig. 2. Energy diagram for Rb II.

(observed value minus calculated value) between the observed wave number and the wave number calculated from the positions assigned to the levels. The scheme is essentially that of Reinheimmer's[3] with some additional lines (marked with an asterisk) taken from the tables of Otsuka[4] that fit very well into the classification.

2. The energy diagram of Rb II is represented by Fig. 2 and all levels are drawn to scale except the $4p^6\ {}^1S_0$. The numerals on the left of the groups are the inner quantum numbers (J), while the term symbols to the right of the lower and upper groups designate the s levels. (See paragraph 5 below for identification of the s levels.) The three resonance lines representing transitions from the $4p^6$ to $4p^5 5s$ and $4p^5 4d$ levels are indicated. The limit of excitation of metastable helium falls about midway between the two groups of levels of the $4p^5 5p$ configuration.

3. Table III contains a list of Rb II lines classified in this investigation. In the first three columns are the intensities as obtained by the three investi-

TABLE III. *Wave-length list of Rb II lines.*

Intensity			λ air I.A.	ν vac.	Classification
M	O	R			
5			697.04 (vac.)	143464	$4p^6\,{}^1S_0 - 5s\,{}^1P_1^\circ$
9			711.17 (vac.)	140613	$4p^6\,{}^1S^\circ - 4d\,{}^1_1$
15			741.43 (vac.)	134875	$4p^6\,{}^1S_0 - 5s\,{}^3P_1^\circ$
	2		2876.73	34751.5	$4d\,{}^1_1{}^\circ - 5p6_0$
	1		3051.43	32762.0	$5s\,{}^3P_1^\circ - 5p10_0$
	2		3098.55	32263.9	$4d\,{}^1_1{}^\circ - 5p5_2\ (5p2_2 - 5d7_1^\circ)$
	5		3148.98	31747.2	$5s\,{}^3P_2^\circ - 5p9_1$
	0		3153.36	31703.1	$4d\,{}^1_1{}^\circ - 5p4_2$
	1		3161.11	31625.3	$5s\,{}^3P_2^\circ - 5p8_2$
	0		3185.51	31343.7	$5p1_1 - 5d4_2^\circ$
	7		3271.03	30562.6	$5p1_1 - 5d2_2^\circ$
	5		3281.49	30465.3	$5p4_1 - 6s\,{}^1P_1^\circ$
2	3		3300.73	30289.1	$4d\,{}^1_1{}^\circ - 5p2_2\ (5p5_2 - 5d7_1^\circ)$
	0		3308.20	30219.2	$5s\,{}^3P_1^\circ - 5p9_1$
2	8	0	3321.545	30097.85	$5s\,{}^3P_1^\circ - 5p8_2$
	2		3329.91	30023.6	$4d\,{}^2_2{}^\circ - 5p5_2$
		1	3340.605	29926.12	$5p1_1 - 5d1_1^\circ$
1	7	2	3393.111	29463.06	$4d\,{}^2_2{}^\circ - 5p4_2$
		0	3415.648	29268.66	$5p2_2 - 5d5_3^\circ$
		0	3434.263	29110.01	$5p3_3 - 5d5_3^\circ$
		2	3461.574	28880.35	$5p2_2 - 5d4_2^\circ$
	3		3480.71	28721.6	$5p3_3 - 5d4_2^\circ$
	3		3513.88	28450.5	$5p7_1 - 5d8_{1,2}^\circ$
	2		3516.53	28429.50	$4d3_2^\circ - 5p9_1$
		3	3521.439	28389.40	$5p2_2 - 5d3_3^\circ$
0	9	2	3531.602	28307.70	$4d3_2^\circ - 5p8_2$
		2	3541.216	28230.85	$5p3_3 - 5d3_3^\circ$
		0	3557.800	28099.26	$5p2_2 - 5d2_2^\circ$
		1	3577.959	27940.95	$5p3_3 - 5d2_2^\circ$
	1		3595.91	27801.5	$5p6_0 - 5d7_1^\circ$
		4	3639.860	27465.78	$5p4_1 - 5d4_2^\circ$
		1	3640.225	27463.03	$5p2_2 - 5d1_1^\circ$
		3	3646.321	27417.12	$5p6_0 - 6s\,{}^1P_1^\circ$
		0	3647.616	27407.39	$5p8_2 - 5d8_{1,2}^\circ$
		4	3662.784	27293.89	$5p5_2 - 5d5_3^\circ$
		4	3663.859	27285.88	$5p9_1 - 5d8_{1,2}^\circ$

[3] H. Reinheimmer, Ann. d. Physik **71**, 162 (1923).
[4] O. Otsuka, Zeits. f. Physik **36**, 786 (1926).

TABLE III (*Continued*).

Intensity			λ air I.A.	ν vac.	Classification
M	O	R			
		1	3666.774	27264.20	$4d3_2^\circ - 5p7_1$
		4	3669.622	27022.13	$4d5_1^\circ - 5p10_0$
		1	3715.640	26905.64	$5p5_2 - 5d4_2^\circ$
		3	3746.381	26684.87	$5p4_1 - 5d2_2^\circ$
		0	3784.714	26414.60	$5p5_2 - 5d3_3^\circ$
		1	3796.393	26333.34	
50		7	3796.823	26330.36	$5s^3P_1^\circ - 5p6_0$
		1	3797.170	26327.96	
		1	3797.276	26327.23	
		5	3801.925	26295.03	$4d4_0^\circ - 5p9_1$
		4	3826.708	26124.74	$5p5_2 - 5d2_2^\circ$
		1	3837.910	26048.48	$4p4_1 - 5d1_1^\circ$
4		2	3860.796	25894.08	$5p1_1 - 6s^3P_1^\circ$
		1	3907.350	25585.57	$4d2_2^\circ - 5p1_1$
		3	3922.259	25488.32	$5p5_2 - 5d1_1^\circ$
2		4	3926.489	25460.86	$5p1_1 - 6s^3P_2^\circ$
50		10	3940.568	25369.90	
		1	3940.915	25367.67	$5s^3P_2^\circ - 5p5_2$
		1	3941.099	25366.48	
2		7	3978.207	25129.87	$4d4_0^\circ - 5p7_1$
7		5	4029.562	24809.60	$5s^3P_2^\circ - 5p4_1$
		0	4048.640	24692.70	$5p7_1 - 6s\ P_1^\circ$
3		6	4083.927	24479.35	$4d5_1^\circ - 5p9_1$
6		8	4104.313	24357.76	$4d5_1^\circ - 5p8_2$
2		7	4136.125	24170.43	$5s^1P_1^\circ - 5p10_0$
		1	4192.566	23845.05	
20		9	4193.097	23842.03	$5s^3P_1^\circ - 5p5_2$
		1	4193.467	23839.93	
		1	4193.612	23839.10	
		0	4227.222	23649.57	$5p8_2 - 6s^1P_1^\circ$
		1	4243.888	23556.69	
25		10	4244.436	23553.65	$5s^3P_2^\circ - 5p3_3$
		1	4244.800	23551.63	
		1	4244.981	23550.62	
		1	4249.085	23527.88	$5p9_1 - 6s^1P_1^\circ$
		5	4266.622	23431.17	$5p2_2 - 6s^3P_1^\circ$
		4	4270.303	23410.97	$5p7_1 - 5d6_1^\circ$
		1	4272.640	23398.17	
20		8	4273.176	23395.24	$5s^3P_2^\circ - 5p2_2$
		1	4273.524	23393.33	
		1	4273.703	23392.35	
0		8	4288.005	23314.33	$4d5_1^\circ - 5p7_1$
		1	4293.484	23284.58	
20		8	4293.994	23281.81	$5s^3P_1^\circ - 5p4_1$
		1	4294.362	23279.82	
		1	4294.567	23278.71	
		2	4306.299	23215.29	$5s^3P_0^\circ - 5p9_1$
		1	4346.582	23000.14	$5p6_0 - 5d1_1^\circ$
		4	4346.996	22997.95	$5p2_2 - 6s^3P_2^\circ$
3		5	4377.150	22839.52	$5p3_3 - 6s^3P_2^\circ$
		5	4469.516	22367.53	$5p8_2 - 5d6_1^\circ$
		4	4493.949	22245.92	$5p9_1 - 5d6_1^\circ$
1		6	4530.358	22067.14	$4d6_{1,2}^\circ - 5p9_1$
		3	4533.824	22050.27	$5s^3P_0^\circ - 5p7_1$
		5	4540.771	22016.54	$5p4_1 - 6s^3P_1^\circ$
15		10	4571.790	21867.16	$5s^3P_1^\circ - 5p2_2$
		1	4572.162	21865.38	
1		5	4622.447	21627.53	$5s^1P_1^\circ - 5p9_1$
		2	4631.918	21583.30	$5p4_1 - 6s^3P_2^\circ$
5		8	4648.562	21506.03	$5s^1P_1^\circ - 5p8_2$
		4	4659.320	21456.37	$5p5_2 - 6s^3P_1^\circ$
1		5	4730.479	21133.62	$4d7_2^\circ - 5p9_1$
		5	4755.329	21023.18	$5p5_2 - 6s^3P_2^\circ$

TABLE III (*Continued*).

Intensity			λ air I.A.	ν vac.	Classification
M	O	R			
3		5	4757.853	21012.03	$4d7_2^\circ - 5p8_2$
20		9	4775.998	20932.20	$5s^3P_2^\circ - 5p1_1$
		1	4776.410	20930.39	
0		7	4782.871	20902.12	$4d6_{1,2}^\circ - 5p7_1$
10		3	4855.361	20590.16	$4d5_1^\circ - 5p6_0$
		5	4885.627	20462.51	$5s^1P_1^\circ - 5p7_1$
		0	5073.919	19703.16	$5p10_0 - 5d6_1^\circ$
10		6	5152.094	19404.19	$5s^3P_1^\circ - 5p1_1$
0		2	5164.592	19357.24	$4d4_0^\circ - 5p4_1$
		3	5270.508	18968.24	$5p6_0 - 6s^3P_1^\circ$
20		6	5522.789	18101.78	$4d5_1^\circ - 5p5_2$
15		6	5635.994	17738.91	$5s^1P_1^\circ - 5p6_0$
5		6	5699.159	17541.59	$4d5_1^\circ - 5p4_1$
		2	6199.093	16126.94	$4d5_1^\circ - 5p2_2$
8		6	6458.347	15479.57	$4d4_0^\circ - 5p1_1$
2		2	6555.625	15249.87	$5s^1P_1^\circ - 5p5_2$
15		9	6775.062	14755.95	$4d7_2^\circ - 5p5_2$
		1	6805.646	14689.64	$5s^1P_1^\circ - 5p4_1$
		2	7042.450	14195.70	$4d7_2^\circ - 5p4_1$
8		1	7316.505	13663.97	$4d5_1^\circ - 5p1_1$
50			7664.43	13087.10	$4d8_{1,2}^\circ - 5p5_2$
30			7698.57	12526.30	$4d8_{1,2}^\circ - 5p4_1$

gators; in the fourth column are the frequencies in vacuum; the last column contains the classification. $(4p^5)$ is omitted in the classification since it is common to all configurations lying above the $4p^6\ {}^1S_0$ ground state. The odd configurations are indicated by an upper index°.

4. As far as the identification of the levels whose term values are written down at the top of Table II is concerned, there seems to be no ambiguity to assign them to the configuration $4p^55p$. Not only does their number (namely 10) agree with what is to be expected theoretically, but also the individual inner quantum numbers are exactly those which the configuration is to yield (compare Table I) In addition to that, a very convincing argument in favor of the present identification is given by a consideration of the change of separation when going from Kr I to Rb II

In the following figure (Fig. 3), the relative term values of the ten p terms of Kr I are drawn referred to their center of gravity, and analogously the relative term values of the ten p terms of Rb II are plotted referred to the center of gravity but reduced in scale to the magnitude of the relativisitic doublet p^5 of Kr I by multiplication with 5220/8500. This method is the same as that used by Mack, Laporte, and Lang.[5] As may be seen from this diagram, there is a very good correspondence between the two respective groups of levels. It is interesting to note that the two crossings-over which occur take place between levels which in both spectra have very small separations between them. It is also interesting to note the beginning of (jj) coupling since in both spectra, the largest separation divides the ten p levels into two groups of four and six levels each with the inner quantum numbers 011223 and 0112 respectively. This division is exactly the one required by (jj) cou-

[5] J. E. Mack, O. Laporte, and R. J. Lang, Phys. Rev. **31**, 748 (1928).

pling as is seen from Table I. In the limit of very high ionization, the levels will be arranged in four groups, namely 12, 0123, 01, 12.

5. So far the discussion has been confined to the even levels. The odd levels offer the singular problem of separating the levels due to $4p^5 5s$ from those due to $4p^5 4d$. To be sure, this is impossible from a strictly theoretical point of view due to the complete overlapping of the two configurations, just as it is impossible to assign L or S values unless there is decided Russell-Saunders coupling. In our case we were guided by the three resonance lines, two of which would have to involve the difference $^3P_1 - {}^1P_1$. For fairly pronounced

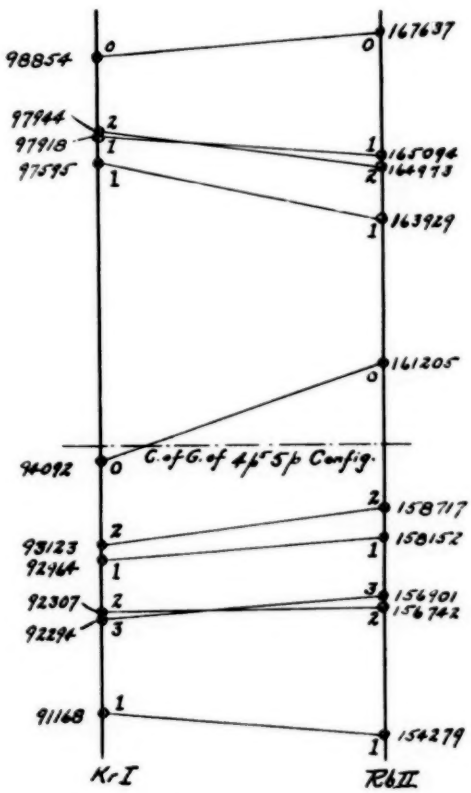

Fig. 3. The $4p^5 5p$ configurations of Kr I and Rb II referred to the center of gravity and reduced to the same magnitude of the relativistic doublet $4p^5$.

(jj) coupling, this difference could be expected to be equal to $^3P_2 - {}^3P_0$ which distance was estimated to be in the neighborhood of 7500 cm^{-1}. The nearest approach to this were the two resonance lines $\nu\nu$134875, 143646 with $\Delta\nu = 8589$ cm^{-1}. Thus the levels 134875 cm^{-1} and 143467 cm^{-1} were decided on as $^3P_1$ and $^1P_1$. After that, the levels 133347 cm^{-1} and 141879 cm^{-1} immediately suggested themselves as $^3P_2$ and $^3P_0$. A confirmation of this identification is the fact that according to Reinheimmer[3] the levels $^3P_2$ and $^3P_1$ show a characteristic hyperfine structure. It must nevertheless be admitted that the identification of the level 141879 cm^{-1} as $^3P_0$ is not very certain and rests

mainly upon an order of magnitude agreement with Houston's formula.[6]

Exact agreement with Houston's formula cannot be expected, since the p^5s overlap with p^5d. Compare Laporte and Inglis[7] for disagreement in case of K II where the analogous situation occurs.

After the identification of the $4p^55s$ levels, we are left with eight levels with the following inner quantum numbers: 0; 1?; 2?; 1; 2; 2; 1, 2; 1, 2. A question mark following two of the levels means that while there is a sufficient number of combinations of these levels to fix the quantum numbers unambiguously, the reality of the levels as such, is somewhat doubtful due to the fact that their combinations do not appear strongly enough in the hollow cathode discharge. On the other hand, the notation 1, 2 means that due to an insufficient number of combinations of these levels, their inner quantum number cannot be determined completely, while nevertheless the levels seem real. On the whole the result of Table I is not unsatisfactory. Counting one of the 1, 2 levels as having $J=1$, and the other as having $J=2$, we get: one level with $J=0$, three levels with $J=1$, and four levels with $J=2$ which is indeed the required number for $4p^54d$ according to Table I. Although a thorough search for levels with $J=3$ was made, none could be established satisfactorily, at least not with the present data. Their combinations appear not to lie within our region of observation.

6. We come now to a corresponding discussion of the levels due to $4p^56s$ and $4p^55d$ configurations. Since from the previous discussion we have a fairly accurate estimate of the $4p^5\ {}^2P$ separation, namely:

$$4p^55s({}^3P_2 - {}^3P_0) = 8532\ \text{cm}^{-1}$$
$$4p^55s({}^3P_1 - {}^1P_1) = 8592\ \text{cm}^{-1},$$

we now have to search for two $J=1$ levels which should show the same separation, with the lower one of the two having $J=2$ level nearby. The levels with relative term values 180173.33 cm^{-1} and 188622.28 cm^{-1} were chosen as ${}^3P_1$ and ${}^1P_1$ respectively. They show the separation $4p^56s$ $({}^3P_1 - {}^1P_1) = 8448.85$ cm^{-1}. This choice also fixes the level 179740.11 cm^{-1} as being ${}^3P_2$. A search for the level ${}^3P_0$ which ought to lie a little below ${}^1P_1$ has been unsuccessful. This is not surprising since even the combinations with ${}^1P_1$ are rather weak.

Having thus selected the levels belonging to $4p^56s$, there remain for the configuration $4p^55d$ eight levels with inner quantum numbers: 1; 2; 3; 1; 2; 3; 1; 1, 2 while the theory leads one to expect one level with $J=0$, three levels with $J=1$, four levels with $J=2$, three levels with $J=3$, and one level with $J=4$.

It is seen by comparison that level "1, 2" with relative term value 192380.15 cm^{-1}, the inner quantum number of which cannot be decided from its combinations (compare Table I), must be given $J=2$. This leaves one more level with $J=2$ and one level with $J=3$ undiscovered. Needless to say the level $J=4$ cannot be established from its one combination with the $4p^55p$ group.

[6] W. V. Houston, Phys. Rev. **33**, 297 (1929).
[7] O. Laporte and D. R. Inglis, Phys. Rev. **35**, 1337 (1930).

7. The separations between the first and second series members of $^3P_2$ and $^3P_1$ are found to be equal to 46393 cm^{-1} and 45298 cm^{-1} respectively. Using the Rydberg term tables for spark spectra,[8] these differences were each fitted into a Rydberg sequence thus giving two independent determinations of the absolute scale:

$5s^3P_2 - 6s^3P_2 = 46393\ cm^{-1}$	$5s^3P_1 - 6s^3P_1 = 45298$
$^3P_2 = 88556$	$^3P_1 = 86926\ cm^{-1}$
$5s(^3P_2 - {}^3P_1) = 1528$	
$^3P_1 = 87028\ cm^{-1}$	

The agreement is very good; we take as average value $^3P_1 = 86977$. By adding the frequency of the resonance line λ741.43, $\nu 134875\ cm^{-1}$ ($^1S_0 - {}^3P_1$) to the $^3P_1$ term value, we obtain

$$^1S_0 = 221852\ cm^{-1}$$

as the calculated term of the normal rubidium ion and corresponds to an ionizing potential of 27.3 volts. Mohler[9] gives 25.2 volts.

8. The available energy of metastable helium atoms is about[10] 163000 cm^{-1}. Since 134875 cm^{-1} are expended in exciting the first resonance line, then only the remaining energy of about 28000 cm^{-1} will be available to excite additional levels. Thus the limit of excitation falls between level 161205 and level 163929 cm^{-1}.

This is in complete agreement with the experimental facts. Numerous strong lines given by Reinheimmer[3] which represent transitions from $4p^55p$ towards $4p^55s$ do not appear in the hollow cathode discharge in helium because they come from one of the ten $4p^55p$ levels which lies beyond the just mentioned limit of excitation. (For example, the line representing the transition $4p^55s\ ^3P_2{}^0 - 4p^55p\ 9_1 = 31747.2$ does not appear in this investigation.) On the other hand many of Reinheimmer's lines appear strongly on our plates also because they involve a $4p^55p$ level that lies inside the limit of excitation (for example, the line $4p^55s\ ^1P_1{}^0 - 4p^55p\ 6_0 = 17738.19$ has intensity 6 in Reinheimmer's data, and appears with an intensity of 15 in the hollow cathode discharge in helium). To be sure, a few lines whose initial levels lie beyond the excitation limit appear weakly in the hollow cathode discharge also because there is always a small number of ionized helium atoms present to furnish a much higher energy of excitation of Rb^+.

A corresponding analysis of Cs II is being made at the present time[11] and will be published in the near future.

[8] F. Paschen, J.O.S.A. and R.S.I. **16,** 231 (1928).

[9] F. L. Mohler, Phys. Rev. **28,** 46 (1928).

[10] For convenience in spectroscopic discussion, the energy is given in ν units. It may be converted to equivalent volts by multiplying by 1.2345×10^{-4}.

[11] See preliminary communication, Phys. Rev. **37,** 845 (1931).

THE NUCLEAR SPIN OF POTASSIUM

By F. W. Loomis[1] and R. W. Wood[2]
The Alfred Loomis Laboratory, Tuxedo Park, New York

(Received July 20, 1931)

Abstract

Photographs of certain bands in the absorption spectrum of the potassium molecule show branches with alternating intensities. Moreover, comparison of the line spacings with those calculated by extrapolating observations on lithium and sodium show that all lines of each branch are present and the phenomenon of alternating missing lines does not occur. This disproves the assertion, based on failure of certain observers to find hyperfine structure, that the nuclear spin of K^{39} is zero.

RECENTLY searches have been made for hyperfine structure of potassium arc lines by Schüler and Brück[3] and of spark lines by Frisch.[4] In neither case was any hyperfine structure detected. The conclusion has been drawn,[5] that the nuclear spin of the principal isotope of potassium, K^{39}, is zero. This, if true, would be of considerable significance because it constitutes one of the very few reported exceptions to Heitler and Herzberg's rule[6] that the spins of the nuclei are even or odd multiples of half a Bohr unit according as the number of protons in the nucleus is even or odd.

The authors have therefore thought it worth while to attack the problem by the method of band spectra; that is, to determine whether or not alternate lines of the K_2 band spectrum are missing as they should be if the nuclear spin is zero.

It is true that measurements and analyses of the rotational structure of the potassium molecule have already been reported by Smith[7] and by Fredrickson and Watson;[8] but these were made in the same way and published at the same time as their analyses of the molecular spectra of sodium, and we have since shown[9] that the spectroscopic resolution of both investigators was insufficient, the "series" illusory and the reported constants wholly meaningless. It seemed probable that this was also true of their measurements of the potassium spectrum, and the present investigation has shown that this is in fact the case.

The spectrum was photographed in the fourth order of the Tuxedo laboratory forty foot spectrograph, using a particularly fine seven-inch plane grat-

[1] The University of Illinois.
[2] The Johns Hopkins University.
[3] Schüler and Brück, Zeits. f. Physik **58,** 735 (1929).
[4] Frisch, unpublished, but mentioned by Frisch and Kronig.[5]
[5] Frisch and Kronig, Naturwiss **19,** 444 (1931).
[6] Heitler and Herzberg, Naturwiss **17,** 673 (1929).
[7] Smith, Proc. Roy. Soc. **A106,** 400 (1924).
[8] Fredrickson and Watson, Phys. Rev. **30,** 429 (1927).
[9] Loomis and Wood, Phys. Rev. **32,** 223 (1928).

ing with 15000 lines per inch. The spectrograph has recently been completely thermostated and the mounting redesigned by Mr. Alfred Loomis and is now very convenient to operate and capable of giving high definition with long exposures.

The potassium was contained in an iron tube, with windows fastened to the ends with sealing wax, evacuated to a few millimeters of residual gas (principally hydrogen), heated at the center with a flame and cooled at the ends with water to protect the windows. It is necessary to adjust the temperature rather closely, so that the band spectrum is developed, but does not become too complex. The solar spectrum was used as a source and also as a comparison. The absorption spectrum of potassium was photographed in the region from 6440 to 6700A, which region contains the strong (2,0) (1,0) (1,1) (0,1) and (0,2) bands of the red system, and other weak ones.

Some of the bands, notably the (0,2) band, are so well resolved that it is possible to pick out the consecutive lines of a branch on mere examination of the plate. In these branches a definite alternation of intensities can be seen. It persists over the whole of the region which is free from overlapping bands and the only lines which do not fit into it are those for which there is evidence of superposition. There can be no doubt that the alternation is real. Moreover, the lines are obviously members of a single branch, probably the Q branch, because it is the strongest. They are not lines of P and R branches with a fortuitous phase relation to each other, for the weaker lines remain midway between the stronger ones for the whole observable length of the branch.

The existence of this alternation of intensities shows at once that the nuclear spin cannot be zero, as the failure to find hyperfine structure of the atomic lines was thought to indicate.

The exact value of the spin could be found from the ratio of alternate intensities by the accepted formula that this ratio is equal to $s/(s+1)$. Unfortunately our present measurements do not permit the quantitative determination of this ratio. It is probably safe to say, however, that it is not as pronounced as 1:3; i.e. that $s>\frac{1}{2}$. Probably $s=1,1\frac{1}{2}$ or 2, but this cannot be relied upon. We hope to measure the alternation of intensities at a future time.

Further evidence that alternate lines of the bands are not missing, and hence that the nuclear spin is not zero, can be obtained from a study of the spacing of the lines in the branches. If one assumes that the spin is not zero, and all lines are present, then the second differences of the frequencies of the lines in a branch should be very approximately equal to $2C$, where $C=B'-B''$ in the usual band spectrum notation. If the spin were zero and alternate lines were missing the second differences between the lines which appeared would be $8C$. The second differences observed are, for all the branches of all the bands studied, about -0.016 cm^{-1}, yielding $C=-0.008$ cm^{-1} on the first, and correct, assumption, or $C=-0.002$ on the second. Now we do not yet know the true C of the potassium molecule, but a comparison with the accurately known values for lithium and sodium (see Table I) is sufficient to

show that the value -0.002 cannot be correct, whereas -0.008 is a quite reasonable extrapolation.

A still more definite test would be to compare the extrapolated values of B' and B'', the two larger quantities of which C is the relatively small difference. Pending the result of a complete analysis of our plates, which we expect to publish later, B' and B'' can best be estimated as follows: Mecke has noticed that the quantity B_0/ω_0 does not change much during a transition, or in other words, that $B_0'\omega_0''/B_0''\omega_0'$ is usually approximately unity. In the case of lithium[10] it is 1.07. In sodium[9] it is 1.04. Let us extrapolate its value for potassium as 1.02 which should not be wrong by more than a few percent, and is certainly more than sufficiently accurate for our purpose. Now[11] $\omega_0''=92.64$ and $\omega_0'=74.73$ so that we find $B''_0/B'_0=1.21$. With this value for the ratio of the B's it is possible to calculate the values of the B's themselves which correspond to each of the above assumptions about C. The results are given in Table I.

TABLE I. *Values in parenthesis are estimates based on the extrapolation for* $B_0'\omega_0''/B_0''\omega_0'$.

	Li_2	Na_2	K_2(if $s>0$)	K_2(if $s=0$)
M	7	23	39	
$-C$	0.1162	0.0289	0.008	0.002
$-MC$	0.81	0.66	0.31	0.08
$B_0'\omega_0''/B_0''\omega_0'$	1.07	1.04	(1.02)	
B_0'	0.5532	0.1254	(0.038)	(0.0095)
B_0''	0.6694	0.1543	(0.046)	(0.0115)
MB_0'	3.87	2.88	(1.48)	(0.37)
MB_0''	4.69	3.55	(1.79)	(0.45)

It will be seen that the values deduced on the assumptions that $s>0$ and that all lines are present are plausible, while those deduced from the alternative assumption are not. This is particularly apparent in lines 4, 8 and 9 in which the constants have been multiplied by the atomic weight M.

We may say then, with considerable certainty, that the spin of the potassium nucleus (K^{39}) is not zero. And it is perhaps permissible to doubt the inferences, as to non-existence of nuclear spin, that have been drawn in other cases from failure to find hyperfine structure.

[10] Harvey and Jenkins, Phys. Rev. **35,** 789 (1930).
[11] Crane and Christy, Phys. Rev. **36,** 421 (1930).

THE ISOTOPE SEPARATION IN THE SPECTRA OF Li I

By D. S. Hughes
University of Chicago

(Received June 18, 1931)

Abstact

Three lines of the Li I spectrum were examined for possible isotope components. A faint component was found on the long wave-length side of the lines 6708A and 3232A. The measured separation of this component and the doublet is in good agreement with the calculated separation of the Li_6 and Li_7 lines. No components other than the regular doublet were observed for the line 6104A. This is in accord with the theory since the calculated separation for this line is below the limit of resolution of the apparatus used.

IN view of the prediction of an observable separation between the spectral lines of Li_6 and Li_7,[1] it was decided to investigate the arc spectrum. Schüler and Wurm[2] have examined the first line of the principal series, 6708A, and found it to be a triplet. Since the long wave-length member of this triplet was very weak and could not be accounted for on the basis of any accepted theory of line structure it was ascribed to Li_6. The magnitude of the separation was such that the long wave member of the Li_7 doublet coincided with the short wave member of Li_6 doublet, causing the line to appear as a triplet.

Since it is very difficult to secure sharp emission lines from Li, the first two lines of the principal series were examined in absorption. The line 6104A, which is not absorbed, was photographed in emission, with a hollow cathode discharge tube. With large currents through the tube the line would, because of self reversal, appear as a triplet. However, on decreasing the current the appearance of the line would change until with 0.5 amperes passing through the tube it appeared as a doublet.

The first vacuum furnace for vaporizing the lithium in the absorption experiments was a seamless steel tube 2 inches in diameter and 26 inches long. The central 13 inches were wound with resistance wire and the ends wound with 1/4 inch copper tubing through which water was circulated to cool the wax with which the quartz windows were fastened on. Later a longer furnace was constructed with 48 inches of resistance winding.

This design does not permit a determination of vapor density. The metallic vapor diffuses to the ends and condenses so that the vapor pressure is zero there. The average density depends upon the number of atoms evaporating per second, which is a function of the area and condition of the lithium surface as well as of the temperature. Due to the fact that Li attacks glass and quartz at temperatures above about 200°C, it did not seem feasible to construct tubes which could be kept hot at the ends.

[1] D. S. Hughes and Carl Eckart, Phys. Rev. **36,** 694 (1930).
[2] H. Schüler and E. Wurm, Naturwiss. **15,** 971 (1927).

Two grating were used in this investigation, a 6-inch plane grating with 15,000 lines to the inch and a 6-inch concave grating, with a radius of curvature of 21 feet, and the same number of lines to the inch. The plane grating was first used in a littrow mounting with a 10-inch concave mirror having a focal length of 15 feet. This mounting gave a dispersion of about 0.566A/mm in the fourth order of 6708A.

Using this mounting and a carbon arc as a continuous source the photographs of 6708A, shown in Figure 1 were obtained. The upper photograph was taken when the furnace was at a dull red heat. The current through the resistance winding was decreased by small steps and the successive photographs taken. Components *a* and *b* are ascribed to Li_7 and component *c* to

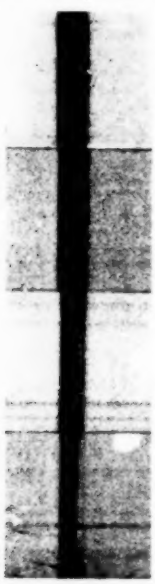

Fig. 1. Absorption of Li 6708A in lithium vapor. Temperature of furnace is highest for the top photograph. 6 inch plane grating, dispersion 0.566 A/mm in fourth order.

Li_6. According to this interpretation *b* is really composed of two lines, the long wave-length member of the Li_7 doublet and the short wave-length member of the Li_6 doublet.

In the hope of resolving the nuclear spin lines a new grating mounting was constructed with an 18-inch concave mirror of focal length 25 feet. With this mounting a dispersion of 0.326 A/mm was secured in the fourth order at 6708A. The longer furnace was constructed so that a lower temperature of the absorbing column could be used and hence sharper lines obtained. The photograph shown in Figure 2 was taken with this arrangement. The microphometer curves of the plates, however, did not reveal any structure.

Since the mirror used in the 25-foot mounting was silver plated and did not reflect 3232, it was necessary to use the concave grating for the examination of the second line of the principal series. The dispersion in the fourth order at 3232A was 0.652 A/mm. The carbon arc which had proved to be a

very intense and convenient source for 6708A was found to be too weak for use at this wave-length. The intensity of the continuous hydrogen spectrum was also of insufficient intensity. It was then decided to attempt to use the Li emission line as a continuous source. The line, which was obtained by placing

Fig. 2. Absorption of Li 6708A in lithium vapor. A longer tube and lower temperature than for Fig. 1. 6 inch concave grating, dispersion 0.326 A/mm in fourth order.

a small quantity of lithium carbonate in a copper arc, was very broad and with a current of 4 amperes through the arc, showed no signs of self-reversal.

Several plates of the line at 3232A were taken with this arrangement. Figure 3 shows the microphotometer traces of these plates. The portion of the trace between *A* and *B* represents the absorption line. In the original

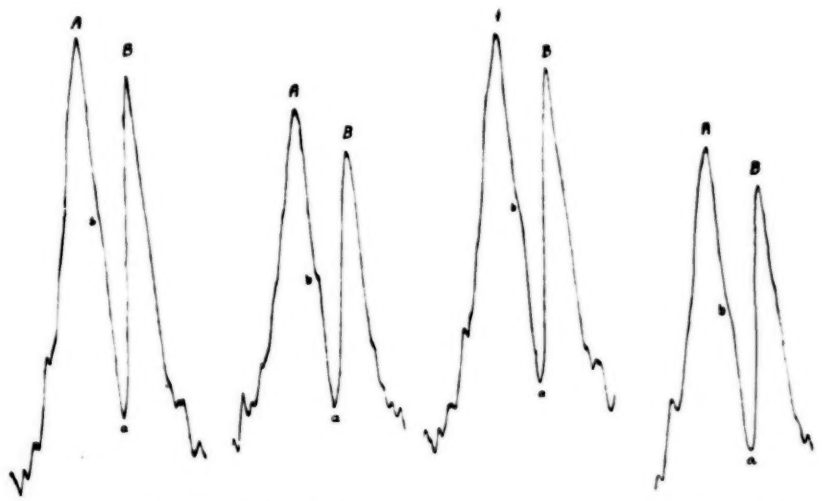

Fig. 3. Microphotometer of absorption of Li 3232A in lithium vapor. The portion of the trace between *A* and *B* represents the absorption line. It is to be noted that the component *b* is present in each trace and is thereby distinguished from the accidental motions of the galvanometer.

negative the resolution was sufficient to allow the separation to be measured. The component *a*, is ascribed to Li_7 and component, *b*, to Li_6. Although this line should be a doublet, due to electron spin the observed doubling was as-

cribed to the isotope effect rather than to the spin for two reasons; first, relative intensity (the component b is much weaker than a and disappears entirely if the temperature of the furnace is lowered slightly); second, the spacing (the separation in Figure 3 is about 0.058A, the separation due to electron spin for this line as calculated from the regular doublet law is about 0.01 A).

The change in frequency due to the finite mass of the nucleus in the case of a one-electron system is.

$$\delta\nu = -m\nu_0/M \tag{1}$$

where m is the electronic mass, M is the mass of the nucleus, and ν_0 is the frequency of the line, calculated by neglecting the motion of the nucleus In the case of more complicated atoms this same effect is still present. Two isotopes of an element should emit lines of slightly different frequencies, as given by the following equation

$$\delta\nu = \left(\frac{m}{M_1} - \frac{m}{M_2}\right)\nu \tag{2}$$

M_1 and M_2 are the nuclear masses of the isotopes, and is the frequency of the line. In the case of two and three-electron systems, however, there is an additional effect which displaces only the P levels[2], and hence only lines arising from or terminating upon a P level. The value of this additional effect for three-electron systems in which one electron is in a P orbit and the other two are in $1s$ orbits is given by

$$\delta\nu_1 = -\frac{128}{3}\frac{m}{M}R_\infty Z_1^5 Z_2^5 n^2(n^2-1)\frac{(Z_1 n - Z_1)^{2n-4}}{(Z_1 n + Z_2)^{2n+4}} \tag{3}$$

where Z_1 is the effective nuclear charge for the $1s$ electrons, Z_2 the effective nuclear charge for the p electron, n the principal quantum number of the p electron, m the electronic mass, M the mass of the nucleus and R_∞ Rydberg's number for an atom with an infinitly heavy nucleus. Equations (2) and (3) give changes in energy which are opposite in sign and in the case of Li I are of the same order of magnitude. This leads to a very small displacement of the P levels and hence to a comparatively large effect in lines arising from p levels and terminating upon s levels.

The results of the calculations and measurements are presented in the following table.

TABLE I.

Line	Transition	Δ_1	Δ_2 (obs)	Δ_2 (cal)
6707.86A	$2P-1S$	0.155A	0.156A	0.123A
6103.59	$3D-2P$	0.112	0.00	0.049
3232.67	$3P-1S$	(0.01)*	0.058	0.042

* Calculated from the regular doublet law.

Δ_1 is the regular doublet separation, Δ_2 is the isotope separation. The values of Z_1 and Z_2 used in calculating the fifth column were taken from the work on screening by Eckart.[3] The disagreement between the observed and calculated displacement is probably to be ascribed to the unresolved nuclear spin lines of Li_7. Since the Li_6 nucleus has no spin,[4,5] the spin of the Li_7 nucleus will lead to a relative displacement of its lines. This interpretation seems to be in accord with the fact that the fractional disagreement is approximately the same for 6708A and 3232A.

The best evidence for this interpretation would be a calculation of the relative vapor densities of the two isotopes from the intensities of the absorption lines. One method of doing this would be to find the reduction in length of the absorbing column necessary so that the intensity of the Li_7 lines in the short column would be the same as the intensity of the Li_6 lines in the long column, with the same conditions of vapor density and temperature in each column. Due to the difficulty already pointed out in connection with the vapor pressure it did not seem to be possible to make measurements of this sort.

A fair agreement has been found between the calculated and observed separation of Li_6 and Li_7 lines for two lines of the Li I spectrum. In the case of 6104A no lines were observed that could not be ascribed to Li_7. Considering the small calculated displacement the Li_6 lines were probably masked by the Li_7 lines, since the width of the emission lines was of the order of magnitude of the calculated separation.

This work was carried out under the direction of Professor H. G. Gale, and the author wishes to express his gratitude to him for his encouragement and many helpful suggestions. The author also wishes to express his appreciation to Professor Carl Eckart, who suggested the problem and to Professor G. S. Monk for his advice in connection with the spectroscopic technique.

[3] Carl Eckart, Phys. Rev. **36,** 878 (1930).
[4] H. Schüler, Zeits. f. Physik **58,** 741 (1929).
[5] A. Harvey and F. A. Jenkins, Phys. Rev. **35,** 798 (1930).

ENERGY RELATIONS IN COMPLEX SPECTRA

By David R. Inglis
University of Michigan

(Received July 17, 1931)

Abstract

The manner in which the energy levels of extreme (*jj*) coupling are split up by interaction of the electrons is calculated, and the results serve in special cases to determine energies in the condition intermediate between (*jj*) and (*LS*) coupling. Single-electron wave functions appropriate to large spin-orbit interaction are selected, and antisymmetric atomic wave functions are formed of them. With these the diagonal elements of the matrix of electrostatic interaction are reduced to combinations of radial integrals, the same integrals met by Slater in (*LS*) coupling. Some configurations have only one such radial integral to express electrostatic interaction. It serves as a parameter in the extension to intermediate coupling by a method of Goudsmit. Coefficients in the general equation for the energies are determined by the energies in extreme couplings. Knowledge of electrostatic energies in (*jj*) coupling, as here calculated, extends the applicability of the method to configurations having three states with the same angular momentum.

Introduction

THEORETICAL relationships between the separations of the levels of a configuration in the two extreme couplings are well known.[1,2] They are obtained by considering a single type of interaction at a time. Houston introduced both electrostatic and spin-orbit interaction and solved completely the problem of two electrons, one of them an *s*-electron. The energies of the two states with the same J are solutions of a ternary quadratic equation. Goudsmit[3] has suggested a simplified method of solution for such problems. Even in more complicated configurations the energies are roots of homogeneous equations, and in some cases it is possible to determine the coefficients from a knowledge of the energies in extreme couplings. For several configurations, the separations due to spin-orbit interaction are known in terms of a parameter both in (*jj*) coupling, where they are large, and in (*LS*) coupling, where they are relatively small. The electrostatic separations are known in extreme (*LS*) coupling, where they are large.[1] This knowledge sufficed to determine the coefficients for the configurations p^2 and p^4, where the equations for general coupling are quadratic or linear. It will be shown that knowledge of the electrostatic energies in (*jj*) coupling, where they are small, completes the determination of the coefficients of a cubic equation with one electrostatic parameter. The ensuing calculation of such energies will thus make it possible to determine for intermediate coupling the levels of some configurations having three states with the same value of J.

[1] J. C. Slater, Phys. Rev. **34**, 1293 (1929).
[2] Pauling and Goudsmit, Theory of Line Spectra, McGraw-Hill, 1930.
[3] S. Goudsmit, Phys. Rev. **35**, 1325 (1930).

Electrostatic Energy in (*jj*) Coupling

1. Wave functions for (jj) coupling. The calculation of the electrostatic energy of the states is quite similar to that done by Slater for (*LS*) coupling, but here the appropriate wave functions are less simple. We are dealing with the smaller of two interactions. First we determine the wave functions stabilized for the larger spin-orbit interaction. This initial perturbation is a sum of functions of single-electron coordinates. The problem thus reduces to the selection of single-electron wave functions $u(nljm_j/)$ appropriate to spin-orbit interaction. Each such stabilized wave function is a linear combination of the two[4] simple single-electron wave functions $u(nlm_lm_s/)$ with the same value of total angular momentum m_j. These are $u(nlm_j-\frac{1}{2}/r\theta\phi)\ \delta(\frac{1}{2}/\sigma)$ and $u(nlm_j+\frac{1}{2}/r\theta\phi)\ \delta(-\frac{1}{2}/\sigma)$ which we abbreviate $u(m_j-\frac{1}{2}/)\ \delta(\frac{1}{2}/\sigma)$ and $u(m_j+\frac{1}{2}/)\ \delta(-\frac{1}{2}/\sigma)$. To calculate the perturbation energy matrix $v_{ij} = fu(i/)\ (\boldsymbol{l}\cdot\mathbf{s})\ u(j/)$ we use the relations

$$l_x \pm il_y = e^{\pm i\phi}\left(\pm\frac{\partial}{\partial\theta} + i\frac{\cos\theta}{\sin\theta}\frac{\partial}{\partial\phi}\right);\quad l_z = -i\frac{\partial}{\partial\phi}$$

$$\frac{\partial}{\partial\theta}P_l^m(\cos\theta) = m\frac{\cos\theta}{\sin\theta}P_l^m(\cos\theta) - P_l^{m+1}(\cos\theta).$$

With these and the operators[5] representing spin we obtain

$$v_{11} = \tfrac{1}{2}(m_j - \tfrac{1}{2});\quad v_{22} = -\tfrac{1}{2}(m_j + \tfrac{1}{2})$$
$$v_{21} = v_{12} = \mp\tfrac{1}{2}\{(l - m_j + \tfrac{1}{2})(l + m_j + \tfrac{1}{2})\}^{1/2}.$$

Of the double sign here and in the following formulas, the upper sign is for positive values of m_j, the lower for negative m_j. (Positive roots of the radicals are implied). In either case the energies are $\frac{1}{2}l$, $-\frac{1}{2}(l+1)$. The normalized linear combinations are

$$(2l+1)^{-1/2}\{(l + m_j + \tfrac{1}{2})^{1/2}u(m_j - \tfrac{1}{2}/)\delta(\tfrac{1}{2}/\sigma) \mp (l - m_j + \tfrac{1}{2})^{1/2}u(m_j + \tfrac{1}{2}/)\delta(-\tfrac{1}{2}/\sigma)\}$$
$$(2l+1)^{-1/2}\{(l - m_j + \tfrac{1}{2})^{1/2}u(m_j - \tfrac{1}{2}/)\delta(\tfrac{1}{2}/\sigma) \pm (l + m_j + \tfrac{1}{2})^{1/2}u(m_j + \tfrac{1}{2}/)\delta(-\tfrac{1}{2}/\sigma)\}.$$

In each case the first combination belongs to the state with $j = l+\frac{1}{2}$, the second has $j = l-\frac{1}{2}$. The stabilized wave function may then be written as an explicit expression in its quantum numbers, as follows:

$$u(nljm_j/) = (2l+1)^{-1/2}\{[l + \tfrac{1}{2} + 2(j-l)m_j]^{1/2}u(nlm_j - \tfrac{1}{2}/)\delta(\tfrac{1}{2}/\sigma) - 2(j-l)(m_j/|m_j|)[l + \tfrac{1}{2} - 2(j-l)m_j]^{1/2}u(nlm_j + \tfrac{1}{2}/)\delta(-\tfrac{1}{2}/\sigma)\} \quad (1)$$

[4] J. H. Bartlett, Jr., Phys. Rev. **35**, 230 (1930).

[5] A convenient explicit formulation of the Pauli spin operations is:

$$s_x\delta(m_s/\sigma) = \tfrac{1}{2}\delta(m_s/-\sigma)$$
$$s_y\delta(m_s/\sigma) = im_s\delta(m_s/-\sigma)$$
$$s_z\delta(m_s/\sigma) = m_s\delta(m_s/\sigma)$$

where the unit is $h/2\pi$ and $m_s = \pm\frac{1}{2}$.

The coefficients may be abbreviated:

$$u(n'l'j'm_j'/) = f'u(m_j' - \tfrac{1}{2}/)\delta(\tfrac{1}{2}/\sigma) + g'u(m_j' + \tfrac{1}{2}/)\delta(-\tfrac{1}{2}/\sigma). \qquad (1')$$

The two functions $u(m_j - \frac{1}{2}/\ )$ and $u(m_j + \frac{1}{2}/\ )$ have the same radial part, so the radial part of the stabilized function may be separated from the rest. This fact later assumes importance in leading us to the radial integrals of Slater's paper.

2. Electrostatic energy. The next step is identical with a part of Slaters' work (reference 1, Part 2, §2), being independent of the specialization of the single-electron wave functions. $u(n/\ )$ may be the wave function for any state of which the four quantum numbers are represented by n. The fundamental states of the atom have as wave functions antisymmetric cominations of products of these single-electron wave functions. The integrals $\int u^* H u$ contain many terms, the number of which is reduced by consideration of the orthogonality of the electronic wave functions. The diagonal elements of the matrix of electrostatic interaction reduce to

$$\sum(\text{pairs of } n\text{'s})\{J(n;n') - K(n;n')\}$$

where

$$\begin{aligned} J(n;n') &= \int u^*(n/1)u^*(n'/2)(e^2/r_{12})u(n/1)u(n'/2) \\ K(n;n') &= \int u^*(n/1)u^*(n'/2)(e^2/r_{12})u(n/2)u(n'/1). \end{aligned} \qquad (2)$$

3. Energy in (jj) coupling. The integrals (2) must now be determined for the special case of (jj) coupling. The electron wave functions $u(n/\ )$ are $u(nljm_j/\ )$ of (1). A summation over the spin coordinates accompanies the integration. The summation having been made; $K(nljm_j; n'l'j'm_j') =$

$$\begin{aligned} &f^2f'^2\int (e^2/r_{12})u^*(m_j - \tfrac{1}{2}/1)u^*(m_j' - \tfrac{1}{2}/2)u(m_j - \tfrac{1}{2}/2)u(m_j' - \tfrac{1}{2}/1) \\ &+ fg'gf\int (e^2/r_{12})u^*(m_j - \tfrac{1}{2}/1)u^*(m_j' + \tfrac{1}{2}/2)u(m_j + \tfrac{1}{2}/2)u(m_j' - \tfrac{1}{2}/1) \\ &+ gf'fg'\int (e^2/r_{12})u^*(m_j + \tfrac{1}{2}/1)u(m_j' - \tfrac{1}{2}/2)u(m_j - \tfrac{1}{2}/2)u(m_j' + \tfrac{1}{2}/1) \\ &+ g^2g'^2\int (e^2/r_{12})u^*(m_j + \tfrac{1}{2}/1)u(m_j' + \tfrac{1}{2}/2)u(m_j + \tfrac{1}{2}/2)u(m_j' + \tfrac{1}{2}/1) \\ &\quad = f^2f'^2K(nlm_j - \tfrac{1}{2}; n'l'm_j' - \tfrac{1}{2}) + g^2g'^2K(nlm_j + \tfrac{1}{2}; n'l'm_j' + \tfrac{1}{2}) \\ &\quad\quad + ff'gg'L(nlm_j; n'l'm_j') \end{aligned} \qquad (3)$$

where

$$L(nlm_j;n'l'm_j') = 2\int (e^2/r_{12})u^*(m_j - \tfrac{1}{2}/1)u^*(m_j' + \tfrac{1}{2}/2)u(m_j + \tfrac{1}{2}/2)u(m_j' - \tfrac{1}{2}/1)$$

Similarly,

$$J(nljm_j;\, n'l'j'm_j') = f^2f'^2J(nlm_j - \tfrac{1}{2};\, n'l'm_j' - \tfrac{1}{2}) + f^2g'^2J(nlm_j - \tfrac{1}{2};\, n'l'm_j' + \tfrac{1}{2}) + g^2f'^2J(nlm_j + \tfrac{1}{2};\, n'l'm_j' - \tfrac{1}{2}) + g^2g'^2J(nlm_j + \tfrac{1}{2};\, n'l'm_j' + \tfrac{1}{2}). \quad (4)$$

The integrals J and K are Slater's integrals. He has tabulated the results of the angular integrations. L is a new integral. It contains, in general, four different sets of unperturbed, single-electron quantum numbers nlm_l. There are, however, only two different sets of principal quantum numbers nl, so that the radial integrals are the same as some of those that Slater met. Introducing the expansion for $(1/r_{12})$ into the definition of L, along with the spherical harmonics for $u(nlm_l/—)$, we get

$$L(m_j;\, m_j') = L(nlm_j;\, n'l'm_j') = c^k(lm_j - \tfrac{1}{2};\, l'm_j' - \tfrac{1}{2})c^k(lm_j + \tfrac{1}{2};\, l'm_j' + \tfrac{1}{2})G^k(nl,\, n'l')$$

where

$$c^k(lm;\, l'm') = \frac{1}{2}\left\{\frac{(k - |\, m - m'\,|\,)!}{(k + |\, m - m'\,|\,)!}\right\}^{1/2}\left\{(2l+1)\frac{(l - |\, m\,|\,)!}{(l + |\, m\,|\,)!}\right\}^{1/2} \left\{(2l'+1)\frac{(l' - |\, m'\,|\,)!}{(l' + |\, m'\,|\,)!}\right\}^{1/2}\int_{-1}^{1} P_l^{|m|}(x)P_{l'}^{|m'|}(x)P_k^{|m-m'|}(x)\,dx$$

$G^k(nl,\, n'l')$ is a radial "exchange" integral defined by Slater. (If we consider the radial wave function $R(nl/r)$ normalized to unity,[6] we define F^k and G^k without the factor $(4\pi)^2$). It is entirely fitting that we should have the same radial integrals in the two extreme couplings; another result would be inconsistent with sum rules.

The coefficients c^k are related thus to Slater's coefficients:

$$a^k(lm,\, l'm') = c^k(lm,\, lm)c^k(l'm',\, l'm')$$

$$b^k(lm,\, l'm') = \{c^k(lm,\, l'm')\}^2$$

c^k may thus be had, except for sign,[7] by taking the square roots of the values of b^k tabulated by Slater.

(2) says that the energy is the sum of the interactions of pairs of electrons. The interaction energy of two electrons in specified states is had by evaluating (3) and (4) with the aid of tables of a^k, b^k, and c^k. The energies so calculated for electrons in the various s, p, and d states, are listed in Table I.

[6] Condon and Shortley, Phys. Rev. **37**, 1025 (1931); §2.

[7] To get c^k, the square root of b^k is to be taken with the negative sign for the following values of $(l, m; l', m'; k)$: (1, ±1; 1, ±1; 2), (1, ±1; 2, ±1 or ±2; 3), (1, ±1; 2, 0; 1), (2, ±2; 2, ±2; 2), (2, ±2; 2, ±1; 4), (2, ±2; 2, 0; 2), (2, ±2; 2, ±1; 4), and (2, ±1; 2, ±1; 4); otherwise positive. Also, b^3(1, ±1; 2, ±2) is 45/245, not 9/245. The formulation of c^k was suggested by consideration of non-diagonal matrix elements by workers at M.I.T. and Harvard, kindly communicated by M. H. Johnson.

TABLE I. *Interaction energy of pairs of electrons.*
(NOTE: the table is also valid when the signs both of m_j and of m_j' are changed.)

	l	j	m_j	l'	j'	m_j'	$-G^0$	$-G^1/9$	$-G^2/25$
ss	0	1/2	1/2	0	1/2	1/2	1	0	0
	0	1/2	1/2	0	1/2	−1/2	0	0	0
ps	1	3/2	3/2	0	1/2	1/2	0	3	0
	1	3/2	3/2	0	1/2	−1/2	0	0	0
	1	3/2	1/2	0	1/2	1/2	0	2	0
	1	3/2	1/2	0	1/2	−1/2	0	1	0
	1	1/2	1/2	0	1/2	1/2	0	1	0
	1	1/2	1/2	0	1/2	−1/2	0	2	0
ds	2	5/2	5/2	0	1/2	1/2	0	0	5
	2	5/2	5/2	0	1/2	−1/2	0	0	0
	2	5/2	3/2	0	1/2	1/2	0	0	4
	2	5/2	3/2	0	1/2	−1/2	0	0	1
	2	5/2	1/2	0	1/2	1/2	0	0	3
	2	5/2	1/2	0	1/2	−1/2	0	0	2
	2	3/2	3/2	0	1/2	1/2	0	0	1
	2	3/2	3/2	0	1/2	−1/2	0	0	4
	2	3/2	1/2	0	1/2	1/2	0	0	2
	2	3/2	1/2	0	1/2	−1/2	0	0	3

	l	j	m_j	l'	j'	m_j'	$F^2/25$	$-G^0$	$-G^2/25$
pp	1	3/2	3/2	1	3/2	3/2	1	1	1
	1	3/2	3/2	1	3/2	1/2	−1	0	2
	1	3/2	3/2	1	3/2	−1/2	−1	0	2
	1	3/2	3/2	1	3/2	−3/2	1	0	0
	1	3/2	3/2	1	1/2	1/2	0	0	1
	1	3/2	3/2	1	1/2	−1/2	0	0	4
	1	3/2	1/2	1	3/2	1/2	1	1	1
	1	3/2	1/2	1	3/2	−1/2	1	0	0
	1	3/2	1/2	1	1/2	1/2	0	0	2
	1	3/2	1/2	1	1/2	−1/2	0	0	3
	1	1/2	1/2	1	1/2	1/2	0	1	0
	1	1/2	1/2	1	1/2	−1/2	0	0	0

	l	j	m_j	l'	j'	m_j'	$F^2/105$	$-G^1/225$	$-G^3/1225$
dp	2	5/2	5/2	1	3/2	3/2	10	90	15
	2	5/2	5/2	1	3/2	1/2	−10	0	50
	2	5/2	5/2	1	3/2	−1/2	−10	0	75
	2	5/2	5/2	1	3/2	−3/2	10	0	0
	2	5/2	5/2	1	1/2	1/2	0	0	25
	2	5/2	5/2	1	1/2	−1/2	0	0	150
	2	5/2	3/2	1	3/2	3/2	−2	36	36
	2	5/2	3/2	1	3/2	1/2	2	54	49
	2	5/2	3/2	1	3/2	−1/2	2	0	10
	2	5/2	3/2	1	3/2	−3/2	−2	0	45
	2	5/2	3/2	1	1/2	1/2	0	0	50
	2	5/2	3/2	1	1/2	−1/2	0	0	125
	2	5/2	1/2	1	3/2	3/2	−8	9	54
	2	5/2	1/2	1	3/2	1/2	8	54	24
	2	5/2	1/2	1	3/2	−1/2	8	27	2
	2	5/2	1/2	1	3/2	−3/2	−8	0	60
	2	5/2	1/2	1	1/2	1/2	0	0	75
	2	5/2	1/2	1	1/2	−1/2	0	0	100
	2	3/2	3/2	1	3/2	3/2	7	9	9
	2	3/2	3/2	1	3/2	1/2	−7	6	36
	2	3/2	3/2	1	3/2	−1/2	−7	0	90
	2	3/2	3/2	1	3/2	−3/2	7	0	180
	2	3/2	3/2	1	1/2	1/2	0	75	0
	2	3/2	3/2	1	1/2	−1/2	0	0	0
	2	3/2	1/2	1	3/2	3/2	−7	6	36
	2	3/2	1/2	1	3/2	1/2	7	1	81
	2	3/2	1/2	1	3/2	−1/2	7	8	108
	2	3/2	1/2	1	3/2	−3/2	−7	0	90
	2	3/2	1/2	1	1/2	1/2	0	50	0
	2	3/2	1/2	1	1/2	−1/2	0	25	0

TABLE I. (*continued*)

	l	j	m_j	l'	j'	m_j'	$F^2/1225$	$F^4/441$	$-G^0$	$-G^2/1225$	$-G^4/441$
dd	2	5/2	5/2	2	5/2	5/2	100	1	1	100	1
	2	5/2	5/2	2	5/2	3/2	−20	−3	0	120	4
	2	5/2	5/2	2	5/2	1/2	−80	2	0	60	9
	2	5/2	5/2	2	5/2	−1/2	−80	2	0	0	14
	2	5/2	5/2	2	5/2	−3/2	−20	3	0	0	14
	2	5/2	5/2	2	5/2	−5/2	100	1	0	0	0
	2	5/2	3/2	2	5/2	3/2	4	9	1	4	9
	2	5/2	3/2	2	5/2	1/2	16	−6	0	48	10
	2	5/2	3/2	2	5/2	−1/2	16	−6	0	108	5
	2	5/2	3/2	2	5/2	−3/2	4	9	0	0	0
	2	5/2	1/2	2	5/2	1/2	64	4	1	64	4
	2	5/2	1/2	2	5/2	−1/2	64	4	0	0	0
	2	5/2	5/2	2	3/2	3/2	70	0	0	30	1
	2	5/2	5/2	2	3/2	1/2	−70	0	0	40	6
	2	5/2	5/2	2	3/2	−1/2	−70	0	0	0	21
	2	5/2	5/2	2	3/2	−3/2	70	0	0	0	56
	2	5/2	3/2	2	3/2	3/2	−14	0	0	36	4
	2	5/2	3/2	2	3/2	1/2	14	0	0	2	15
	2	5/2	3/2	2	3/2	−1/2	14	0	0	32	30
	2	5/2	3/2	2	3/2	−3/2	−14	0	0	0	35
	2	5/2	1/2	2	3/2	3/2	−56	0	0	27	10
	2	5/2	1/2	2	3/2	1/2	56	0	0	6	24
	2	5/2	1/2	2	3/2	−1/2	56	0	0	25	30
	2	5/2	1/2	2	3/2	−3/2	−56	0	0	12	20
	2	3/2	3/2	2	3/2	3/2	49	0	1	49	0
	2	3/2	3/2	2	3/2	1/2	−49	0	0	98	0
	2	3/2	3/2	2	3/2	−1/2	−49	0	0	98	0
	2	3/2	3/2	2	3/2	−3/2	49	0	0	0	0
	2	3/2	1/2	2	3/2	1/2	49	0	1	49	0
	2	3/2	1/2	2	3/2	−1/2	49	0	0	0	0

The first columns list the quantum numbers specifying a pair of electronic states, and they are followed in the other columns by the energy coefficients belonging to the pair of states. To get the interaction energy of the states, $J(nljm_j; n'l'j'm_j') - K(nljm_j; m'l'j'm_j')$, we multiply the integral at the head of each column by the coefficient listed in its column, and add the products. In the case of more than two electrons, we must make a summation of these energies over the pairs of electron states, according to (2).

This gives us the diagonal elements of the matrix of interaction energy. Because the wave functions are stabilized for spin-orbit interaction, non-diagonal elements exist only between states of the same magnetic energy—the states that are degenerate at the introduction of our present perturbation. M_J is a constant of the motion, so the energy matrix is considered only in the squares characterized by the same set of $(nlj)(n'l'j') \cdots (n''l''j'')$ and the same M_J. The sum of the diagonal terms, which we now know, is the sum of the energies of the states with this set of electronic quantum numbers and with $J \geqq M_J$. By taking differences[8] of such diagonal sums we get energies of the individual states $(nlj)(n'l'j') \cdots (n''l''j'')J$.

[8] Example: In Table II, the $J=4$ level of *pd* has the energy of the first *dp* state of Table I. The sum of the energies of this and the next level, $J=3$, is the sum of the second and seventh *dp* states of Table I, namely, $-12\ F^2/105 - 36\ G^1/225 - 86\ G^3/1225$; and this, minus the energy for $J=4$, is the energy for the $J=3$ level.

4. Examples of electrostatic separations in (jj) coupling. This calculation has been carried out for several configurations, involving the interactions of two, three, or six electrons. When the optical electrons are an almost-closed shell and one other electron, as in the configuration p^5p', there are two sets of parameters of electrostatic interaction. The integrals $F^k(nl, nl)$ and $G^k(nl, nl)$ express the interaction of the equivalent electrons in the almost-closed shell, and in the result contribute the same energy to each level of the configuration, so do not affect the separations. The integrals $F^k(nl, n'l')$ and $G^k(nl, n'l')$ express the interaction of the single electron with the electrons of the almost-closed shell, and give interesting separations.

Fig. 1 illustrates schematically the roles played by the electrostatic and spin-orbit interactions near extreme couplings, for the example p^5d. The calculations described above give the coefficients of $F^k(nl; n'l')$ and $G^k(nl; n'l')$

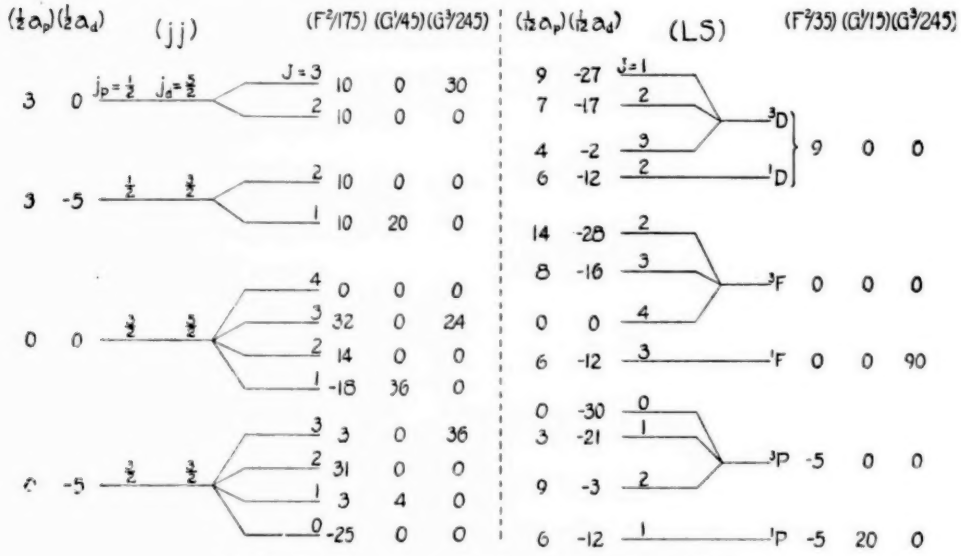

Fig. 1. Energy scheme of p^5d near extreme couplings.

listed on the left side, and for the right side the method of Slater is used. a_p and a_d are the usual parameters of spin-orbit interaction ($energy = a_p(\boldsymbol{l}_p \cdot \mathbf{s}_p)$) and their contributions are given by the vector model. ($J=4$) has been taken as reference level.

The (jj) electrostatic energies for the configurations pp', pd, dd', p^5s, and p^5p' are given in Table II. Corresponding energies in (LS) coupling, with which comparison may be made as regards sum rules, have been given by Slater[1] or by Condon and Shortley,[6] except for p^5p and p^5d. For p^5d they are listed in Fig. 1, and for p^5p they are

$$^1S, {}^3S = -2F^2/5 + 2G^0 - 2G^2/5 \pm 3G^0$$

$$^1P, {}^3P = F^2/5 - G^0 - 2G^2/5$$

$$^1D, {}^3D = -F^2/25 - G^0 - 4G^2/25 \pm 6G^2/25.$$

In the case of p^5d it happens that the four levels with $J=2$ involve only one parameter of electrostatic interaction. For p^5s and d^9s the results are just the same as for ps and ds, respectively, and the latter have been given by Houston. Experiment shows that the integral $G^k(nl; n'O)$ changes its sign between these cases,[9] due to the change in the radial parts of the electronic wave functions.

TABLE II. *Electrostatic energies for various configurations*

j	j'	J	$F^2/25$	G^0	$G^2/25$
3/2	3/2	3	1	−1	−1
		2	−3	1	−3
		1	1	−1	−1
		0	5	1	5
3/2	1/2	2	0	0	−1
		1	0	0	−5
1/2	3/2	2	0	0	−1
		1	0	0	−5
1/2	1/2	1	0	−1	0
		0	0	1	0

pp'

j	j'	J	$F^2/25$	G^0	$G^2/25$
3/2	3/2	3	−1	−1	−10
		2	3	−1	− 6
		1	−1	−1	−10
		0	−5	3	−10
3/2	1/2	2	0	−1	− 6
		1	0	−1	−10
1/2	3/2	2	0	−1	− 6
		1	0	−1	−10
1/2	1/2	1	0	−1	−10
		0	0	1	−10

p^5p

j_p	j_d	J	$F^2/175$	$-G^1/225$	$-G^3/1225$
3/2	5/2	4	10	90	15
		3	−22	−54	71
		2	− 4	27	92
		1	28	− 9	−84
3/2	3/2	3	7	9	9
		2	−21	3	63
		1	7	−11	189
		0	35	15	315
1/2	5/2	3	0	0	25
		2	0	0	175
1/2	3/2	2	0	25	0
		1	0	−25	0

pd

j	j'	J	$F^2/25$	$F^4/49$	G^0	$G^2/1225$	$G^4/441$
5/2	5/2	5	100	1	−1	−100	− 1
		4	−140	− 7	1	−140	− 7
		3	−116	19	−1	116	−19
		2	28	−21	1	28	−21
		1	184	− 6	−1	−184	6
		0	280	42	1	280	42
5/2	3/2	4	70	0	0	− 30	− 1
		3	−154	0	0	− 46	− 9
		2	− 28	0	0	47	−36
		1	196	0	0	− 21	−84
3/2	5/2	4	70	0	0	− 30	− 1
		3	−154	0	0	− 46	− 9
		2	− 28	0	0	47	−36
		1	196	0	0	− 21	−84
3/2	3/2	3	49	0	−1	− 49	0
		2	−147	0	1	−147	0
		1	49	0	−1	− 49	0
		0	245	0	1	245	0

dd'

When neither of the electrons is in an s state, (jj) coupling is not realized in the extant spectral data. In configurations like p^5d, the greater effective nuclear charge for the equivalent electrons augments one of the parameters of magnetic coupling, but the other remains small so that the four groups overlap in pairs. Comparison with experiment is therefore possible only after an extension of the results to intermediate coupling, similar to that which follows.

ENERGY IN INTERMEDIATE COUPLING

5. Combined perturbations.[10] In intermediate coupling, the perturbation potential is a sum of two terms depending differently on the coordinates, $H'=v+w$. v and w are the spin-orbit and the electrostatic interaction. Among atoms with the same optical-electron configuration, the unperturbed wave functions differ from one atom to another in their radial parts, from one state to another in their angular parts. The secular determinant is then

[9] Laporte and Inglis, Phys. Rev. **35**, 1337 (1930).

[10] This is a more detailed formulation of the method of Goudsmit[3] than that given by him.

$$| Av_{ij} + Bw_{ij} - \epsilon\delta_{ij} | = 0. \tag{5}$$

Here A and B are radial integrals, and are considered as parameters that differ among the atoms, while the matrices v_{ij} and w_{ij} are the same for all the atoms considered. (5) may be written

$$\epsilon^N - \epsilon^{N-1}(At_{10} + Bt_{01}) + \epsilon^{N-2}(A^2t_{20} + ABt_{10} + B^2t_{02}) - \cdots = 0. \tag{6}$$

The roots ϵ_k are functions of the parameters A and B. The coefficients t_{kl} are sums of products of v_{pq} and w_{rs}. The integrations involved are to be avoided by determining the coefficients from a knowledge of the energies in extreme couplings.

6. Determination of the coefficients. From consideration of one perturbation at a time, we know the energies near extreme couplings (B/A or A/B small). In (jj) coupling (small B/A) we know the first two coefficients of the Taylor expansion

$$\epsilon_k(A, B) = \alpha_k A + \beta_k B + \cdots, \tag{7.1}$$

the first from the vector model, the second from the calculations of this paper. In (LS) coupling (small A/B) we have similarly

$$\epsilon_k(A, B) = b_k B + a_k A + \cdots. \tag{7.2}$$

Here the coefficients b_k come from the Slater calculation, and express the separation of the multiplets from one another, while a_k constitute the familiar interval rule. In (6) the coefficient of $(-)^n\epsilon^{N-n}$ is the sum of all products of n roots (7.1):

$$\sum_{j=0}^{n} A^{n-j}B^j t_{n-j\,j} = \sum_{pq\cdots}{}'(\alpha_p A + \beta_p B + \cdots)(\alpha_q A + \beta_q B + \cdots).$$

Assuming convergence of (7.1) for some finite B, we equate the coefficients of the same powers of B. If we know only the first two terms of (7.1), we get only the relations

$$t_{n,0} = \sum_{pq\cdots s}{}'\alpha_p\alpha_q \cdots \alpha_s \qquad (n \text{ factors}) \tag{8.1}$$

$$t_{n-1,1} = \sum_{pq\cdots s}{}'\beta_p\alpha_q \cdots \alpha_s. \quad (n \text{ factors, one of them } \beta) \tag{8.2}$$

An identical treatment of the case of small A/B gives

$$t_{0,n} = \sum_{pq\cdots s}{}'b_p b_q \cdots b_s \qquad (n \text{ factors}) \tag{8.3}$$

$$t_{1,n-1} = \sum_{pq\cdots s}{}'a_p b_q \cdots b_s \quad (n \text{ factors, one of them } a) \tag{8.4}$$

N is the number of states in the set with the same value of J. n has any value from one to N. For $N=3$, (8) are 12 equations. The fact that $t_{1,0}$ and $t_{0,1}$ are determined in each extreme is equivalent to a well-known energy sum rule. For $N>3$, not all the t_{ij} are determined.

7. Example of intermediate coupling, the configuration p^3. This configuration is easily determined both because of its few states and because of

the small number of parameters of equivalent electrons. The various levels in extreme couplings, and the corresponding large and small energies, are indicated in Table III. The central level has been selected as reference level.[11]

TABLE III.

J	(jj) α	β	J	(LS) b	a	
3/2	3	1/3	3/2	2	0	^2P
			1/2	2	0	
1/2	0	2				
5/2	0	0	5/2	0	0	^2D
3/2	0	−5/3	3/2	0	0	
3/2	−3	1/3	3/2	−3	0	^4S

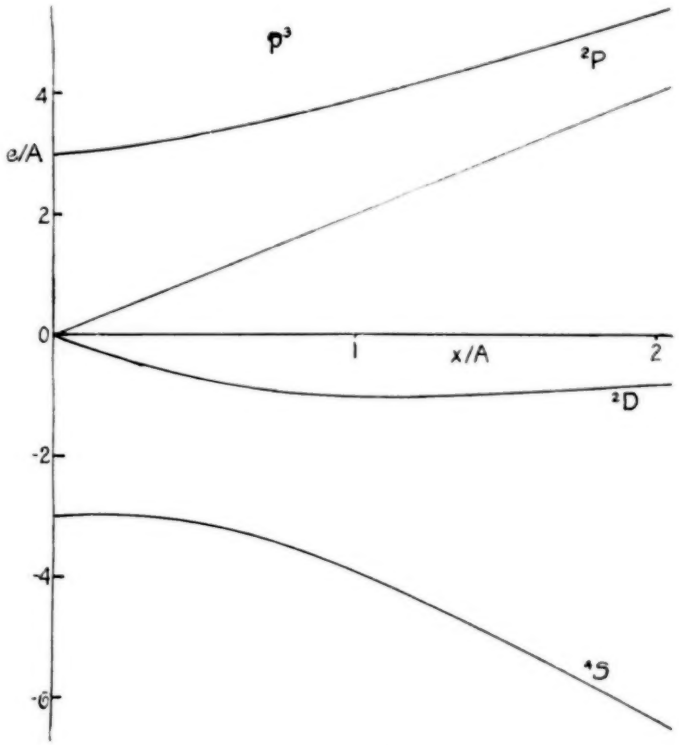

Fig. 2.

Here B = Goudsmit's $X = (3/25)F^2(n1, n1)$. Using Slater's results, b, and the results of the vector model, a, and α, Goudsmit[3] has determined:

$$(jj): t_{2,0} = -9 \qquad (LS): t_{0,1} = -1$$
$$t_{1,0} = -1 \qquad t_{0,2} = -6$$

[11] A linear transformation of the variables ϵ, A, and B, leaves the form of (6) unaltered. Here we subtract from ϵ the energy of the state with $J=5/2$, which is a linear function of A and B.

and the other t's equal to zero, except $t_{2,1}$. Using in addition the values of β in (8.2), we get $t_{2,1}=15$, thus completing the determination of the equation

$$\epsilon^3 + \epsilon^2 B - \epsilon(9A^2 + 6B^2) - 15A^2B = 0.$$

For the sake of plotting in two dimensions, either A or B is taken as unit of energy, making the levels converge in (jj) or (LS) coupling, respectively, as in Fig. 2 and Fig. 3. In Fig. 3 a comparison of the theory with the experimental data is indicated, in the manner of a previous paper.[9]

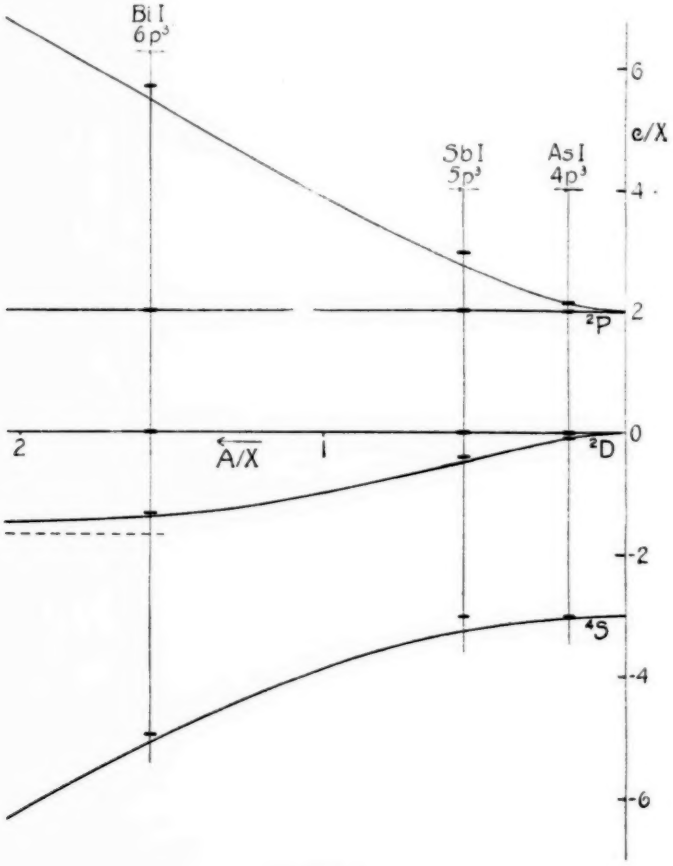

Fig. 3.

Such an extension to intermediate coupling is more difficult for configurations having non-equivalent, non-s-electrons. The first difficulty is introduced by secular equations of higher order, which cannot be treated by this method, but require more direct quantum mechanical methods, involving non-diagonal matrix elements. A second difficulty is that several radial integrals appear as paramaters, so as to render impossible any simple graphical representation of the solutions.

I thank Professors Goudsmit and Uhlenbeck for their instigating interest.

ULTRA-IONIZATION POTENTIALS IN MERCURY VAPOR

By A. G. Shenstone
Princeton University

(Received July 20, 1931)

Abstract

It is shown that Takamine's new $^3P_2{}^0$ level in Hg I is probably the lowest level from the structure d^9s^2p. The positions of the other levels are discussed and it is shown that some of them will be negative. The phenomenon of auto-ionization is described and its effect on the negative terms is suggested as the cause for the existence of ultra-ionization potentials. Some remarks are made regarding perturbed series.

THE discovery of a new $^3P_2{}^0$ term in the spectrum of Hg I by Takamine and Suga[1] and its verification by Paschen[2] leads to a probable explanation of the hyper-ionization potentials in mercury, first found by Lawrence[3] and afterwards extended by a number of others. The results are collected and compared with his own by P. T. Smith.[4] The explanation depends on the identification of the new term as $5d^96s^26p^3P_2{}^0$ and the observation that auto-ionization is effective in atomic spectra.

The new term $X^3P_2{}^0$ is at $\nu = 15295$. If it is due to the structure mentioned above, its value, measured from its own ion is $\nu = 15295 + 35514 = 50809$, since the difference $d^{10}s - d^9s^2$ of Hg II is 35514. A comparison with spectra in which similar structures occur, for instance Cu II, Au II, Ni I, Pd I, Pt I, shows that the value is a very reasonable one. The Rydberg denominator is 1.4692.

Some idea of the positions of the other levels of d^9s^2p may be obtained by an examination of d^9p of Au II.[5] The levels in both cases include[3,1] P^0, D^0, F^0. The total span should be somewhat greater than twice the $d^9s^2\ ^2D$ difference, i.e. about 30,000, so that the highest levels of the group will extend to about -15000. The lowest level is almost certainly the $^3P_2{}^0$ already found and above it by quite closely 2000 units should be $^3F_3{}^0$. In the neighborhood of 10,000 higher should come $^3F_4{}^0$, $^3D_3{}^0$, $^3D_2{}^0$, $^3P_1{}^0$. The remaining levels including the singlets and the last levels of the triplets should extend from about zero to -15000. In combination with known terms, $^3F_3{}^0$, $^3F_4{}^0$, $^3D_3{}^0$ and $^3D_2{}^0$ can produce only lines of very long wave-length. $^3P_1{}^0$, on the other hand, will have a combination with $^3S_1$ of wave-length around λ6000 to 7000. Its value is possibly 7272, calculated from the two possible combinations λ6868 $2^3S - X^3P_1{}^0$ and λ18127.5 $3^3D_2 - X^3P_1{}^0$. Of the higher group, $^1D_2{}^0$ and $^3D_1{}^0$, in combination with ^3D and ^1D, should give lines in the region around λ4500 to

[1] Takamine and Suga, Sci. Pap. Inst. Phys. and Chem. Res. Tokio **13,** 1 (1930).
[2] Paschen, Ann. d. Physik **6,** 47 (1930).
[3] Lawrence, Phys. Rev. **28,** 947 (1926).
[4] P. T. Smith, Phys. Rev. **37,** 808 (1931).
[5] McLennan and McLay, Proc. Roy. Soc. Canada **22,** 103 (1928).

λ6000; but it is doubtful whether the high F^0 and P^0 levels can be found, as will appear from the following discussion of the effect of auto-ionization.

Auto-ionization

There is a well-known effect in band spectra which is called predissociation. The effect is an automatic dissociation of a molecule when the sum of its vibrational and electronic energies exceeds the energy necessary for dissociation in some lower electronic system. Kronig has shown theoretically[6] that such radiationless transitions can take place only under very stringent quantum conditions.

Professor Wigner has suggested to me that certain peculiarities of the copper arc spectrum may be logically explained on the assumption that a parallel action can take place in an atom.

Beyond the ionization limit of any ion, there lies a continuum of possible energy states. That continuum may be considered to be composed of a set of continua, each one of which corresponds to an extension of an ordinary term sequence and retains the characteristic quantum numbers of that sequence i.e. for Russell-Saunders coupling the numbers L, S, J and the parity. But it is possible for an atom, by the excitation of two electrons, to exist in a state of energy-content more than sufficient to ionize it by the removal of the first electron. In such a state, there is the possibility of a radiationless transition carrying the excited atom into the state where it exists as an ion plus an electron. A comparison of this case with that of predissociation, dealt with theoretically by Kronig, makes it very probable that such transitions from a given state can occur if there exists a continuum characterized by the same L, S, J and parity as the state in question. This effect has been referred to as the Auger effect from its analogy to the effect in x-rays discovered by Auger; but I believe that it could much more logically be called auto-ionization. In the spectrum Cu I, the effect is very marked and it will be discussed more fully in a later paper in connection with the experimental results obtained in that and other spectra.

From the discussion of the terms from the structure d^9s^2p of Hg I, it will be seen that $^1P_1^0$, $^1D^0$, $^1F^0$, $^3D_1^0$, $^3F_2^0$, $^3P_0^0$ all probably lie above the ordinary ionization limit of the spectrum. They are therefore energetically in a position to show the effect of auto-ionization. But the continua following the limit correspond to *odd* P and F terms and *even* D terms. Therefore, we would expect the D^0 levels to possess lives of the ordinary magnitude, and the P^0 and F^0 levels to exist for much shorter times and to pass over into ionization automatically. The effect on the spectrum will be that lines from the negative P^0 and F^0 levels will be extremely diffuse, if they exist at all. By analogy with Cu I, it would be expected that the lines would be emitted only at very high vapour densities.

Ultra-ionization Potentials

In experiments on ultra-ionization potentials, the observation is that ions

[6] Kronig, Zeits. f. Physik **62**, 300 (1930).

are detected when the bombarding electrons attain certain particular velocities greater than that corresponding to the ordinary series limit. I suggest that those ions are not a direct result of the electron impact, but that the primary process is one of excitation to a negative level, followed by auto-ionization. One would expect such a critical potential for each possible negative S, P^0, D, F^0, etc., level. The potentials observed near the ordinary I. P. are probably due to the terms from the structure d^9s^2p but many higher ones could exist. For instance, $d^9s^2s\ {}^3D_1{}^1D$, the lowest even terms based on the ^2D ion, should show the effect. On the other hand $d^{10}p^2\ {}^3P$ should not give any ultra-ionization potentials and $d^{10}\ p^2\ {}^1S$ and ^1D should.

It should be noticed that, on this explanation, the observation of ultra-ionization potentials cannot be of much aid in the discovery of new levels because such potentials correspond to levels which are very unlikely to produce spectrum lines.

The $d^{10}p\ {}^3P^0$ sequences of Hg I show marked irregularities. The ${}^3P_0{}^0$ sequence is quite "Ritzian" but the ${}^3P_1{}^0$ shows a marked perturbation about the 4th and 5th terms and the ${}^3P_2{}^0$ sequence at the second term. The cause is not far to seek. The ${}^3P_2{}^0$ sequence is perturbed by $X{}^3P_2{}^0$ and ${}^3P_1{}^0$ by the corresponding ${}^3P_1{}^0$ which possibly has the value 7272. In the former case, the perturbation is of such a magnitude that it is impossible and perhaps meaningless to assign one of the levels to the ordinary sequence and the other to d^9s^2p. The evidence of the line intensities, such as it is, would indicate that possibly the present choice is the less reasonable.

R. M. Langer has shown[7] that the quantum mechanics leads, in such a case as that under consideration, to a series formula in which $n^*=n+\mu+\dot{p}/(\nu_0-\nu_n)$, in which p is a constant and ν_0 is the wave-number of a term foreign to the sequence. The ${}^3P_2{}^0$ sequence may be fitted to such a formula with reasonable accuracy, using either one of the possible levels as the second member. Such perturbations are closely analogous to the phenomenon of auto-ionization, and should be governed by similar quantum conditions i.e. the terms must all have the same L, S, J and parity. Kronig, in the paper referred to above, has dealt with the parallel case in band spectra.

Langer remarks in his letter that 'The chief contribution of this work is the satisfaction one gets from the elimination of an apparent flaw in our notions of line spectra.' Professor H. N. Russell and I have indeed felt that relief while recently making a survey of all the known preturbed series which have been so troublesome in the past.

[7] R. M. Langer, Phys. Rev. **35**, 649 (1930).

EXCITATION PROBABILITIES FOR ELECTRONS IN HELIUM, NEON, AND ARGON

By L. C. Van Atta
Washington University

(Received June 12, 1931)

Abstract

Electrons scattered inelastically in the forward direction in helium, neon, and argon have been studied by means of an electrostatic analyzer. Energy distribution curves revealed the 21.11 and 22.96 volt losses in helium, the 16.6 and 18.5 volt losses in neon, and the 11.6 and 13.9 volt losses in argon. Careful measurements of the principal energy losses gave $21.13 \pm .04$ volts, $16.64 \pm .05$ volts, and $11.53 \pm .05$ volts. The relative probability as a function of electron energy was determined for the 21.11, 16.6, and 11.6 volt losses for electron energies between 100 and 300 volts. The 21.11 and 16.6 volt losses increased with electron energy showing maxima at 200 and 160 volts respectively. The 11.6 volt loss decreased sharply between 100 and 150 volts and then remained constant. Special study of ionization losses in helium showed that an ionizing electron may lose as much as half its remaining energy to the ejected electron, but that smaller losses are preferred.

Introduction

THE study of the scattering of electrons by gas molecules may be divided into two fields, elastic scattering and inelastic scattering. As elastic scattering predominates at finite angles, attention has been concentrated hitherto on this field. The determination of the absorption coefficient at different electron energies gives an approximate measure of the probability of elastic scattering as a function of electron energy, the angle of scattering being integrated from 0 to 180°. The dependence of this probability on scattering angle has recently been studied at large angles with very interesting results.[1,2,3]

In the case of electrons scattered inelastically experimental difficulties are increased because of lack of intensity, so that the measurement of their distribution in angle has not been extended to large angles. Harnwell[4] and McMillen[5] traced angular distribution curves as far as 20° and 35° respectively, and found them to drop sharply toward the zero axis. However, for the particular scattering angle, $\theta = 0 \pm \alpha$(α is small), the intensity is sufficient to permit the accurate measurement of relative probabilities, provided that a suitable method for velocity analysis is employed. The purpose of the present investigation was to determine the relative probability for inelastic scattering of electrons in the forward direction as a function of electron en-

[1] E. C. Bullard and H. S. W. Massey, Proc. Roy. Soc. **A130,** 579 (1931).
[2] F. L. Arnot, Proc. Roy. Soc. **A130,** 655 (1931).
[3] J. M. Pearson and W. N. Arnquist, Phys. Rev. **37,** 970 (1931).
[4] G. P. Harnwell, Phys. Rev. **34,** 661 (1929).
[5] J. H. McMillen, Phys. Rev. **36,** 1034 (1930).

ergy. Helium, neon, and argon were chosen for study because of their many experimental conveniences, and because of previous work that has been done with these gases.

METHOD

Electrons from a hot filament are accelerated to the desired energy and pass into a field-free space where collisions with gas molecules may occur. Those continuing in the foward direction pass into an analyzing chamber so that the resulting energy distribution may be determined.

An electrostatic means of energy analysis was adopted because of its obvious advantages over magnetic methods. The theory of the method was developed by Hughes and Rojansky[6] and the results tested experimentally by Hughes and McMillen.[7] Electrostatic analyzers have since been employed by McMillen[5] and Rudberg[8,9] with satisfactory results.

An inverse first power electrostatic field will cause an electron entering the field perpendicularly to move in a circular path whose center is at the axis provided that

$$V_D = (2 \log r_2/r_1) \cdot V \tag{1}$$

where V is the electron energy in volts and V_D is the deflecting potential applied in the analyzer between cylindrical plates of radii r_1 and r_2. Due to the magnitude of α, the half-angle within which electrons are collected by the analyzer, and due to the finite dimensions of the slits, the energy distribution curve for a strictly homogeneous electron beam will be found to be a peak with a base of finite width. The expression for the maximum value of this width is given by Rudberg:[8]

$$\Delta V/V = 4/3\alpha^2 + \tfrac{1}{2}(L_1 + L_2)/\pi r_0^2 + (W_1 + W_2)/r_0 \tag{2}$$

where L_1, L_2, and W_1, W_2 are the lengths and widths respectively of the entrance and exit slits of the analyzer, and r_0 is the radius of the circular path. Small errors in aligning the slits will decrease their effective area and hence the value of $\Delta V/V$. The departure from homogeneity in the electron beam was due almost entirely to the thermal distribution of velocities. Calculations from thermionic data showed that 95 percent of the electrons had initial energies less than 0.75 volt, and graphical tests indicated that this distribution would not appreciably widen the base of the peaks.

Errors due to constant contact differences of potential, C, between the filament and the analyzer, may be avoided since V_D is a measure of the true voltage applied to the electrons. The relation between V_D and this true voltage may be found by using two different accelerating voltages and finding the corresponding deflecting voltages necessary to bring unscattered electrons to the collector. Substitution into an equation of the type

[6] A. L. Hughes and V. Rojansky, Phys. Rev. **34,** 284 (1929).
[7] A. L. Hughes and J. H. McMillen, Phys. Rev. **34,** 291 (1929).
[8] E. Rudberg, Proc. Roy. Soc. **A129,** 628 (1930).
[9] E. Rudberg, Proc. Roy. Soc. **A130,** 182 (1930).

$$V_D = k(V_A + C) \tag{3}$$

and elimination of C gives the factor for converting deflecting volts into true accelerating volts. Errors in the determination of the separation between two peaks due to variable contact differences of potential may be eliminated by alternating in reading the positions of the peaks, and then averaging.

Apparatus

A diagram of the experimental arrangement, together with the electrical connections, is shown in Fig. 1. The electron gun, bombarding chamber, and collector were made of brass, while the analyzing chamber and plates

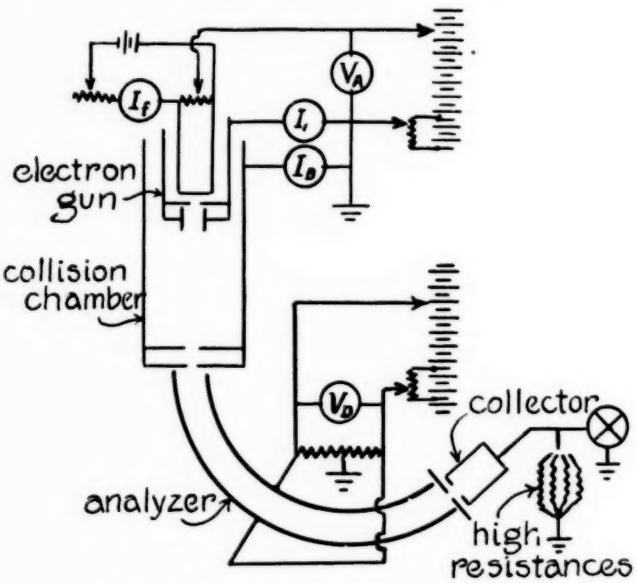

Fig. 1. Diagram of electrical connections.

were cast of special aluminum alloy. Electrons from an oxide-coated filament were accelerated to a platinum disc having a 2 mm circular hole. A short 6 mm cylinder established the energy of the electrons more definitely. The bombarding chamber fixed the electron path length in the gas at 10 cm. The effect of the earth's magnetic field was annulled with a pair of Helmholtz coils. The effect of the magnetic field due to the filament current was minimized by bringing the leads in close together, and by having a return path for the current close behind the filament.

From the bombarding chamber electrons passed into the analyzing chamber through a pair of slits separated by 2 cm. The first slit (1 mm$\times$5 mm) fixed α at 1°40′. The second slit (0.05 mm$\times$5 mm) was made very narrow so that the pressure in the analyzer might be kept low. To ensure this condition a high speed diffusion pump was connected directly to the analyzer by a short length of large tubing. The mean radius of curvature of the plates was 4.4 cm and their separation 0.80 cm. The final slit of the analyzer had dimensions 0.3 mm by 7.5 mm. The entrance slit to the collector (2 mm$\times$10 mm) was

large enough to admit all electrons leaving the analyzer, but small enough to prevent an appreciable number of secondary electrons from escaping.

We are now in a position to calculate from equations (1) and (2) that

$$k = 2 \log r_2/r_1 = 0.365$$

and that

$$\Delta V/V = 0.0009 + 0.0040 + 0.0080 = 0.0129.$$

Experimental determinations of k, as described above, gave 0.371 in good agreement with the calculated value. ΔV was determined experimentally by measurement of the base of several peaks, average values being 1.5 volts for $V_A = 100$ and 2.4 volts for $V_A = 200$.

The essential electrical connections are indicated in Fig. 1. The accelerating potential was applied to the center of the filament, while the electron gun and bombarding chamber were kept at ground potential. The deflecting plates were shunted by a high resistance with center grounded, so that the energy of electrons entering the analyzer midway between the plates would not be altered. Coarse variations in accelerating and deflecting voltages were obtained by variable taps on lead storage cells, and fine variations by potentiometer changes.

Filament emission was of the order of 1 milliampere and bombarding currents of the order of 0.5 microampere. Currents to the collector were sufficient to permit the use of a Compton electrometer under positive control (2500 mm/volt) with a high resistance shunt. The high resistances, ranging from 2×10^8 to 3×10^{11} ohms, were prepared by cathodic sputtering of platinum on soft glass.[10] A stable steady-deflection method for measuring electrometer currents was essential for rapidly locating peaks and for securing quantitative results.

Gas pressure in the bombarding chamber was maintained by a steady flow method. Pressure was controlled by varying the helium pressure in the storage bulb by means of a U-tube of mercury, and by varying the rate of pumping by means of a series of holes of different diameters in the cut-off.

Procedure

The exact procedure followed in taking the readings will merit some consideration. The first step was to obtain energy distribution curves for the inelastically scattered electrons, the purpose being to identify positively the inelastic peaks with known energy losses and to ascertain whether the resolving power of the analyzer was sufficient to isolate peaks for individual study. The energy distribution curves were obtained by fixing the accelerating voltage and the gas pressure at given values and measuring collector current as a function of deflecting voltage. The difference between any inelastic peak and the elastic peak in deflecting volts was translated into energy loss in volts by means of equation (3). Each energy loss was then determined more accurately by reading alternately the positionof the elastic peak and that of the

[10] L. C. Van Atta, Rev. Sci. Instr. **1**, 687 (1930).

inelastic peak, and taking the average difference. This study was repeated for several accelerating potentials between 75 and 300 volts.

Having positively identified and definitely isolated a certain peak, its relative probability as a function of voltage was determined in the following way. The accelerating voltage was varied in 25 volt steps from 75 to 300 volts, the bombarding current being kept constant by altering the filament current as required. For each accelerating voltage several different readings were taken. The deflecting voltage was adjusted to put the maximum of the elastic peak at the collector, and was recorded together with the collector current. The deflecting voltage was then altered to bring the maximum of the inelastic peak to the slit, the electrometer shunt being changed to give increased sensitivity, and the position and height of the inelastic peak were recorded.

The justification for using the height of the peak instead of the area as a measure of the probability lies in the fact that the peaks for any given accelerating voltage were roughly isosceles triangles with fixed base. The area was thus proportional to the height. After every alteration in the apparatus a test was made to ascertain that collector current was directly proportional to bombarding current. Each collector current measurement was divided by the corresponding bombarding current to correct for small fluctuations.

A graph of the height of the elastic peak as a function of accelerating voltage was plotted to obtain a correction to apply to the height of the inelastic peak because of the fact that the apparatus favored the collection of faster electrons. Since the elastic peak was composed almost wholly of electrons which had not suffered a collision of any kind, the height of this peak (when reduced to unit bombarding current) gave a measure of the efficiency of the apparatus for collection of electrons. The correction was made by dividing the inelastic peak (I. P.) by the elastic peak (E. P.) of the same energy. Since the inelastic peak at a particular accelerating potential is composed of electrons having an energy less than the accelerating potential by the amount of the energy loss, the elastic peak to use for correction must be read from the graph at a correspondingly lower accelerating voltage. Thus the I. P. obtained at an accelerating potential of 200 volts in helium is composed of electrons which, having lost 21 volts, retain an energy of 179 volts. The correction to this I. P. is made by dividing by the E. P. obtained for an accelerating potential of 179 volts, as read from the E. P. against V_A curve.

Taking I. P./E. P. as a measure of the relative probability of a loss involves the assumption that the peaks are affected to the same extent by a number of factors: (1) Variation of absorption coefficient with electron energy; (2) Residual magnetic fields; (3) Redistribution of intensity in the electron beam with changing potential; (4) Varying space charge conditions; and (5) Contact potential differences at the edges of slits (especially of the narrow slit at the entrance to the analyzing chamber). It does not seem likely that this assumption is exactly realized for any one of the factors, but in each case the effect on the peaks would certainly be in the same direction.

Results and Discussion

A. Energy distribution curves.

Typical energy distribution curves are shown in Figs. 2–7. In the case of helium no evidence was found for the 19.76 or 20.54 volt losses though both

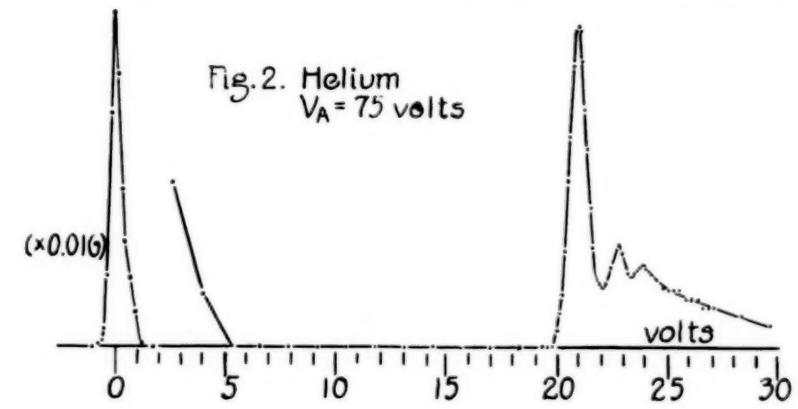

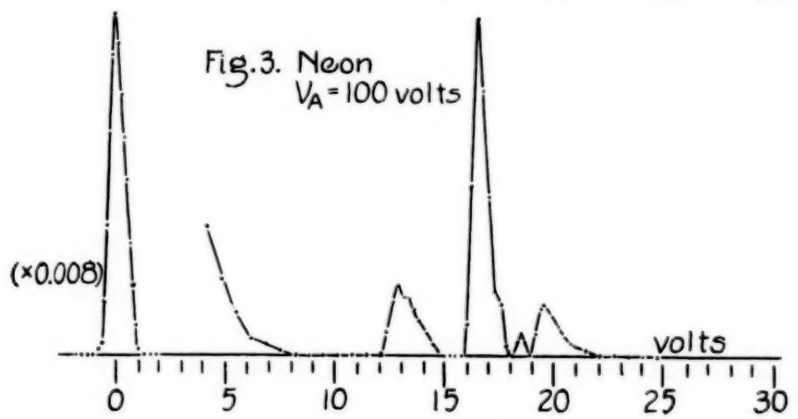

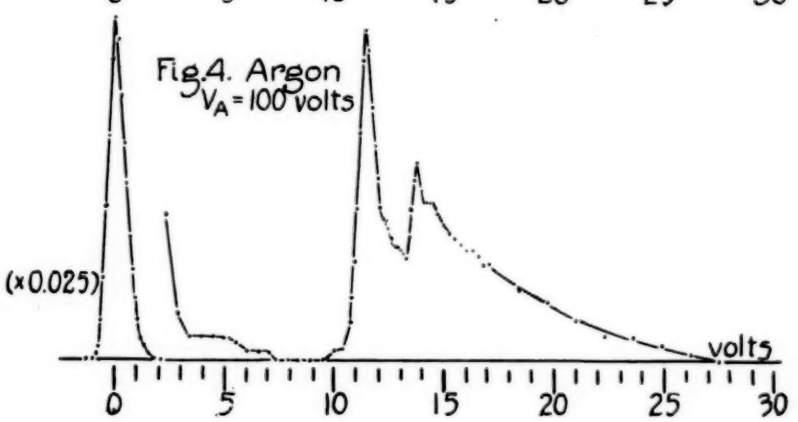

would have been well resolved for an accelerating potential of 75 volts. In Fig. 2, the 21.11 and 22.96 volt losses corresponding to the first two terms of the singlet principal series ($1^1S - m^1P$) are resolved. The third peak is com-

posed of all higher excitation losses unresolved. In Fig. 5, the 22.96 volt loss is merged with higher losses due to the decreased resolving power at 200 volts.

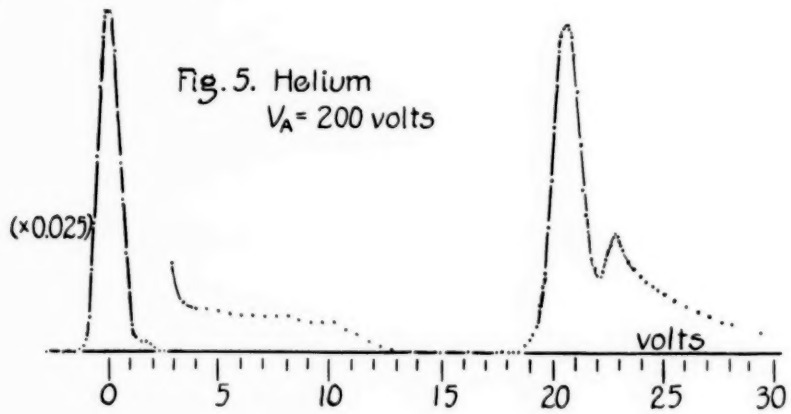

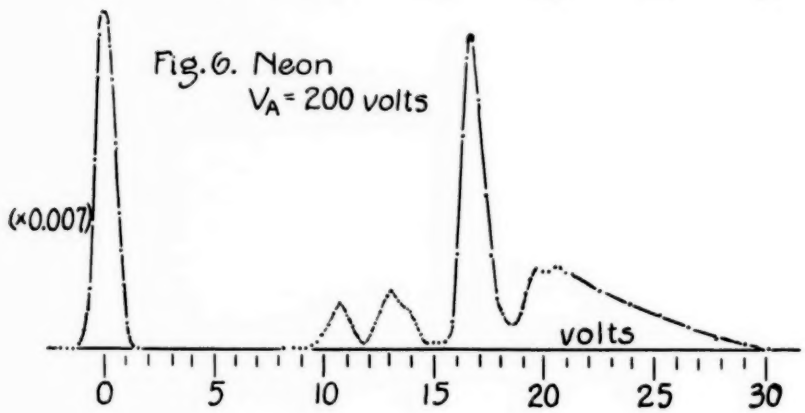

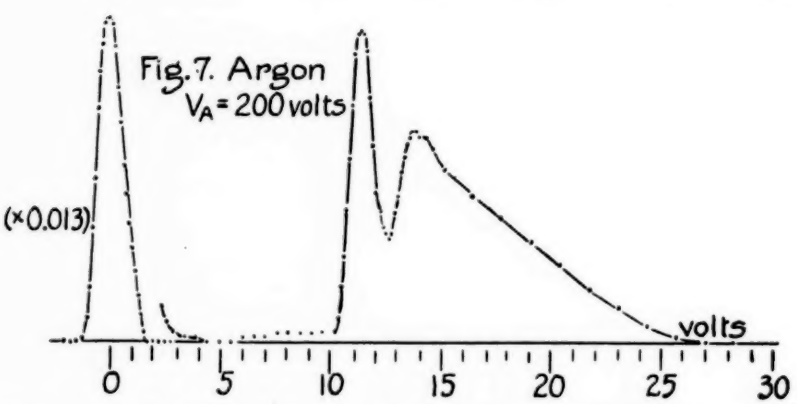

Figs. 2, 3, 4, 5, 6, 7. Electron energy distribution curves in helium, neon and argon.

The 16.6 ($1^1S_0 - 2^3P_1$) and 18.5 volt losses in neon appear in Fig. 3. The peak indicating higher energy loss is probably the higher excitation losses unresolved. The broad hump, indicating lower energy loss, would require the

existence of energy levels not given by spectroscopic data. A comparison with Fig. 4 would suggest argon as an impurity. To test this point Geissler tubes of the neon were prepared by Mr. R. L. Womer and spectrographs were taken by Miss Geneva Miller, but no argon lines were found. The question is left temporarily since it interferes in no way with the study of the probability of the principal loss. A distinguishing characteristic of the neon curves is the size of the 16.6 loss in comparison with other excitation and ionization losses.

In Fig. 4 the 11.6 and 13.9 volt argon losses appear prominently, while the 13.0 volt loss is barely discernible. The higher excitation losses are so prominent that it seemed worth while to measure their combined probability as well as that for the 11.6 volt loss.

The principal energy loss for each gas was determined with as great accuracy as possible. In the course of the probability determinations the position of a peak was recorded each time its height was measured. Since these measurements were made by alternating rapidly between the elastic and inelastic peaks, errors due to changing contact potential differences were minimized. In addition some special measurements were made on helium, using a slightly altered scheme for applying and measuring the accelerating and deflecting voltages. The deflecting potential method consists in fixing V_A and finding the decrease in V_D necessary to move from the elastic to the inelastic peak, and then using equation (3) to calculate the corresponding energy loss. The accelerating potential method consists in fixing V_D and finding the increase in V_A necessary to move from the elastic to the inelastic peak, thus avoiding the use of equation (3). The results are given in Table I. The spectroscopic values to be compared with these are given in Table II.

TABLE I. *Energy losses in He, Ne and A.*

Gas	Average value	No. of determinations	Method	Final value	Estimated uncertainty
Helium	21.12	17	Defl. pot.		
	21.19	17	" "		
	21.10	22	Accel. pot.		
	21.14	9	" "	21.13	±.04
Neon	16.65	18	Defl. pot.		
	16.63	18	" "	16.64	±.05
Argon	11.58	11	Defl. pot.		
	11.48	12	" "	11.53	±.05

TABLE II. *Spectroscopic values corresponding to energy losses in Table I.*

Gas	Transition	Potential	Reference
Helium	1^1S-2^1P	21.11 volts	
Neon	$1^1S_0-2^3P_1$	16.68 "	11
		16.58 "	12
Argon		11.57 "	12

[11] W. Hanle, Zeits. f. Physik **65**, 512 (1930).

[12] G. Hertz and J. C. Scharp de Visser, Zeits. f. Physik **31**, 470 (1925).

In a number of curves the elastic peak was asymmetrical, Fig. 2 being the most marked example. This same feature is to be observed also in curves obtained by Rudberg with nitrogen.[8] It may be explained as due to small energy losses at slit edges, to a special type of small energy loss in the gas, or to a departure from perfect refocussing in the analyzer. Calculations show that the last explanation probably is not sufficient. The question of small energy losses in gases (of the order of half a volt) is soon to be made the subject of a separate experiment.

A special study was made of energy distribution curves in helium above the ionization potential with a view to ascertaining how much energy beyond that required for ionization is given up by an ionizing electron. Accelerating

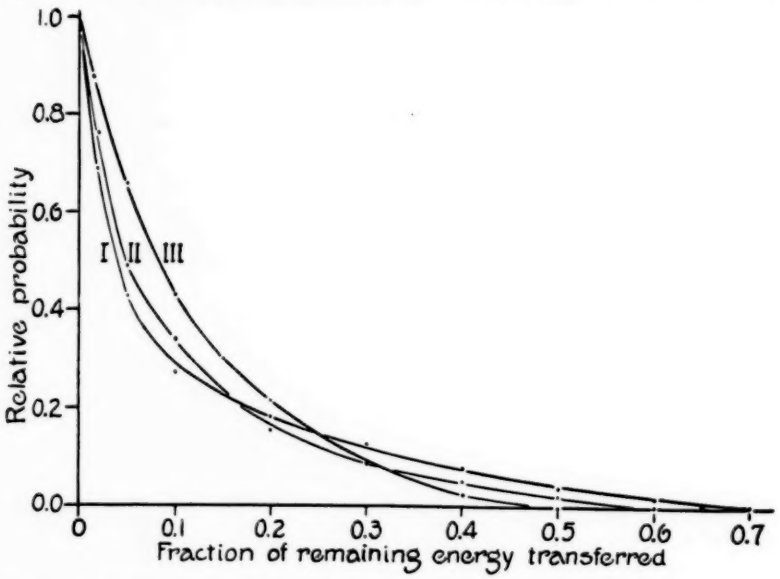

Fig. 8. Sharing of energy by ionizing electrons in helium. I, $V_A = 300$ volts (corrected); II, $V_A = 200$ volts (corrected); III, $V_A = 100$ volts (uncorrected).

potentials of 100, 200, and 300 volts were used, so that the ionizing electrons had 75, 175, and 275 volts respectively to share with the ejected electrons. The results were put in the form shown in Fig. 8 for comparison. The abscissae represent fractions of the energy of the bombarding electrons in excess of that necessary for ionization, and the ordinates give the number of bombarding electrons which surrender these fractions to ejected electrons. Slight corrections have been added to the 200 and 300 volt curves to compensate for the fact that the apparatus favored the collection of faster electrons. This correction in the case of the 100 volt curve was somewhat uncertain and therefore was not applied, but the effect would have been to raise the curve especially at the lower end. It appears that an ionizing electron in helium may lose any fraction of its remaining energy up to at least half, but that the loss of smaller fractions is much more probable. This is not in agreement with results obtained by others with mercury. Arnot[13] found that 80 volt electrons

[13] F. L. Arnot, Proc. Roy. Soc. **A125,** 660 (1929).

which are scattered at $\theta = 10°$ on ionization lose only 10.4 volts. On the other hand, Foard[14] found that ionizing electrons between 10 and 40 volts scattered in the forward direction may lose any fraction of their remaining energy, with the larger losses definitely preferred.

B. Relative probability curves.

To indicate the type of curves obtained for the variation of elastic peak and inelastic peak with accelerating potential, Figs. 9 and 10 for helium have

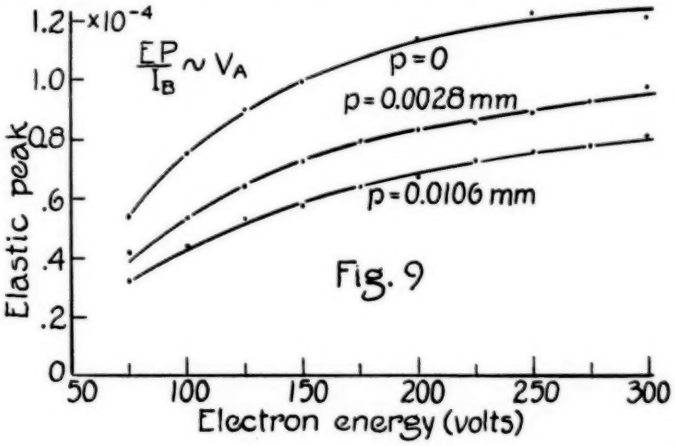

Fig. 9

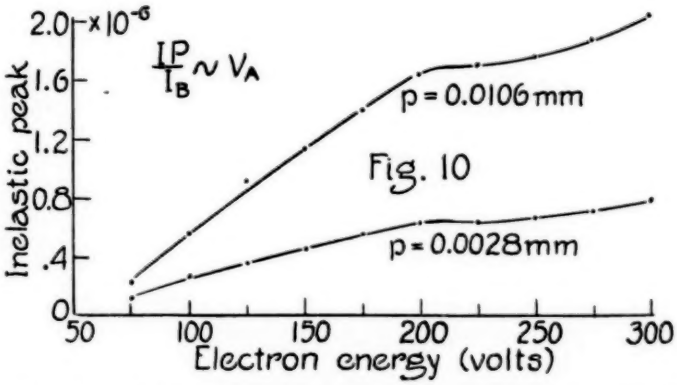

Fig. 10

Figs. 9, 10. Variation of elastic and inelastic peaks with accelerating potential for helium.

been included. It is apparent from Fig. 9 that a correction to curves for the inelastic peak is necessary. From the drop in the E. P. (composed almost entirely of unscattered electrons) with increased pressure it should be possible to calculate the absorption coefficient for the gas. The difference between the curves $p = 0$ and $p = 0.0028$ mm gives too large a value for α, and can be explained only as due to a "contamination" of slit edges by the introduction of gas into the apparatus. Using the equation

$$I_2 = I_1 \exp\left[-\alpha(p_2 - p_1)L\right],$$

[14] C. W. Foard, Phys. Rev. **35**, 1187 (1930).

the *difference* between the curves for $p=0.0028$ and $p=0.0106$ mm gives α as a function of electron energy in satisfactory agreement with Normand's values.[15] A comparison of the two curves of Fig. 10 shows that the inelastic

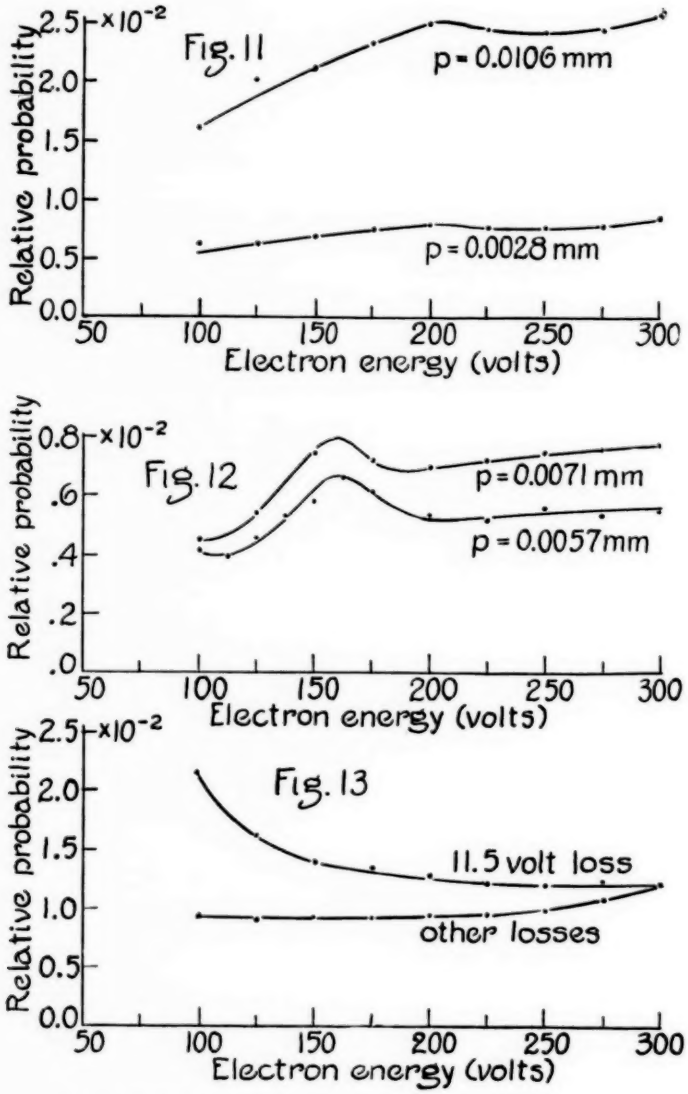

Fig. 11. Relative probability of 21.11 volt loss in helium.
Fig. 12. Relative probability of 16.6 volt loss in neon.
Fig. 13. Relative probability of 11.5 volt and other losses in argon ($p=0.0034$ mm).

peak was proportional to the pressure for the pressures used. It is desirable, of course, that this condition be fulfilled, since it may be taken as a criterion for single scattering.

[15] C. E. Normand, Phys. Rev. **35**, 1217 (1930).

The relative probability curves are shown in Figs. 11–13. The curves for helium and neon are somewhat similar, while that for the 11.5 volt loss in argon seems to be quite different from these. It is of interest to compare the curves in Fig. 11 for the 1^1S-2^1P loss in helium with the curves obtained by Michels[16] for the optical excitation function of the 2^1S-3^1P and 2^1S-4^1P transitions. He found that the principal series curves after the drop following the initial sharp maximum rose steadily, reaching the height of the initial maximum at about 100 volts. The curves of Fig. 11 might be considered an extension of his, though the comparison would be more exact if the relative probability were measured with the scattering angle integrated from 0 to π.

There is a suggestion of a minimum at about 100 volts in neon. One is tempted to explain this as a faint indication of the marked rise toward lower electron energies seen in the upper argon curve. Bullard and Massey[1] (working at finite angles of scattering) do not find the 11.6 volt argon loss and conclude that the corresponding level must be metastable. While this loss behaves quite differently from the others, it is still the most prominent at 200 volts. To correlate these results with those of Bullard and Massey one must assume either: (a) that electrons which lose this energy are not scattered appreciably; or (b) that the probability drops again suddenly between 100 and 40 volts.

The second curve in argon represents the average relative probability for higher losses which come into greater prominence as the accelerating voltage is increased. This is in agreement with certain optical excitation function data which show higher losses favored at higher electron energies.

The writer takes this opportunity to acknowledge his indebtedness to Professor A. L. Hughes, who proposed the problem and offered many helpful suggestions during the course of the work.

[16] W. C. Michels, Phys. Rev. **36,** 1362 (1930).

THE EFFECT OF TEMPERATURE ON THE CONTINUOUS BAND SPECTRUM OF MERCURY VAPOR

By Walter M. Nielsen
Duke University

(Received July 17, 1931)

Abstract

The continuous bands of mercury vapor at 4850A and 3300A were excited by electron impact in the vapor at high pressures (1 to 10 mm of mercury) and low electron currents (1×10^{-6} amperes). Under such conditions the luminous regions are limited to striations. The potential difference between striations corresponds to approximately five volts. Under the experimental conditions the excitation of the lower excited states of the mercury atom appears to be essential for the emission of the bands. A complementary variation in intensity of the two bands is observed. The 3300A and 4850A bands are more intense at the cathode and anode respectively than they are in other portions of the discharge space. The variation in intensity of 2537A parallels that of the 3300A band. A measurement of two temperatures enabled the calculation of the temperature at the different striations from which the relative numbers of atoms in the $^3P_1$ and $^3P_0$ states are determined from well-known properties of resonance and metastable atoms. It is shown that the ratio of the intensity of the 4850A band to that at 3300A is directly proportional to the ratio of the population of the $^3P_0$ and $^3P_1$ atomic states. The conclusion is that the excitation of the $^3P_0$ state is essential for the radiation of the 4850A band and that the $^3P_1$ state is associated with the 3300A band.

IT IS well known[1] that when dense mercury vapor is excited either by electron impacts or by the absorption of certain spectral lines or bands that two broad and apparently structureless bands are observed in the emitted radiation. One of these bands is in the visible portion of the spectrum and has a maximum intensity at about 4850A. A similar band having an intensity maximum at 3300A is observed in the near ultraviolet. With prolonged exposure, these two bands merge and the continuous radiation is observed to extend from the red to the mercury resonance line at 2537A where it abruptly ends.

It is the purpose of this paper to present some new observations on the effect of temperature on the relative intensities of the 4850A and 3300A bands of mercury vapor and to suggest an interpretation of their origin based on the results here recorded and the known properties of excited atoms as obtained from other studies on the quenching of resonance radiation and the life of metastable states.

Experimental

The experimental tube is shown in Fig. 1. Radiation was excited in the spherical Pyrex vessel A, to which was attached another spherical vessel B,

[1] See Finklburg, Phys. Zeits. **31**, 1 (1930) for a résumé of work done on the band spectrum of mercury.

which served as a liquid mercury reservoir. The two spheres were exhausted of air through a tube C, and were heated by separate electric furnaces, the temperatures being controlled by thermoregulators in such a way that the temperatures were kept constant to within 0.1°C throughout a run. To insure an accurate knowledge of the vapor pressure in the discharge sphere A, the sphere B was always maintained at a lower temperature, and a steel ball at E was pulled up by means of a wire into the ground concave surface at D. This motion was effected by means of a small electromagnet and a soft iron plunger attached to the other end of the wire.

Electrons from an oxide-coated equipotential cathode F_1 were accelerated by means of a potential difference, V_a, towards a similarly formed electrode F_2 from which the oxides were removed before assembly. The separation be-

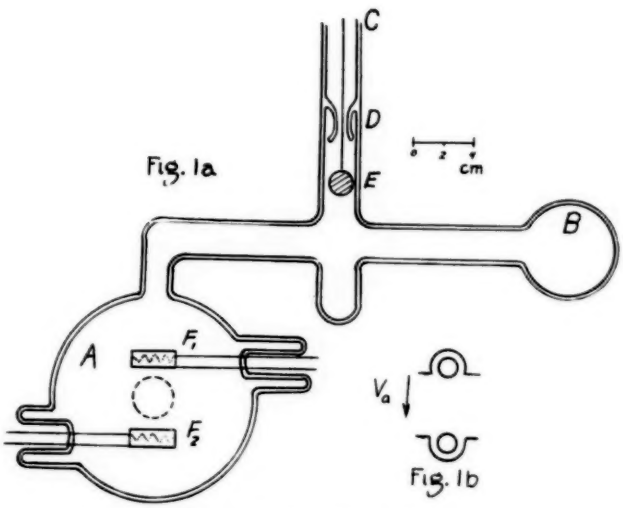

Fig. 1. Experimental tube.

tween cathode and anode was 2 cm; in the figure this distance is multiplied by two. The cathode and anode assembly is more completely displayed in Fig. 1*b*. As indicated, a thin sheet of nickel partially surrounded the two filaments and was formed in such a way as to tend to make the electric field between cathode and anode more uniform. These sheets of nickel were always maintained at the same potential as the cylinders of F_1 and F_2 respectively.

The residual gas pressure was not detectable on a McLeod gauge reading to 10^{-5} mm of mercury and the degassing of the filament assemblies was carried to a stage such that at the end of a series of exposures (1–8 hours) no gases were detectable when the steel ball was lowered and the gases trapped by means of a mercury seal and a reading taken on the McLeod gauge.

With the fairly dense mercury vapor (pressures of 1 to 10 mm of mercury) as here employed, and low electron currents (1×10^{-6} amperes), the emitted radiation appeared in well-defined striations between F_1 and F_2. Such radiation was photographed by means of a small Hilger quartz spectrograph through a quartz window shown by the dotted circle in Fig. 1. The radiation

was condensed onto the slit of the spectrograph by means of a quartz lens, in such a way that the slit of the spectrograph was in the image plane of the plane defined by the two electrodes F_1 and F_2.

Results and Discussion

Typical spectrograms obtained under the conditions outlined above are reproduced in Fig. 2. Visually the radiation appears as striations and the

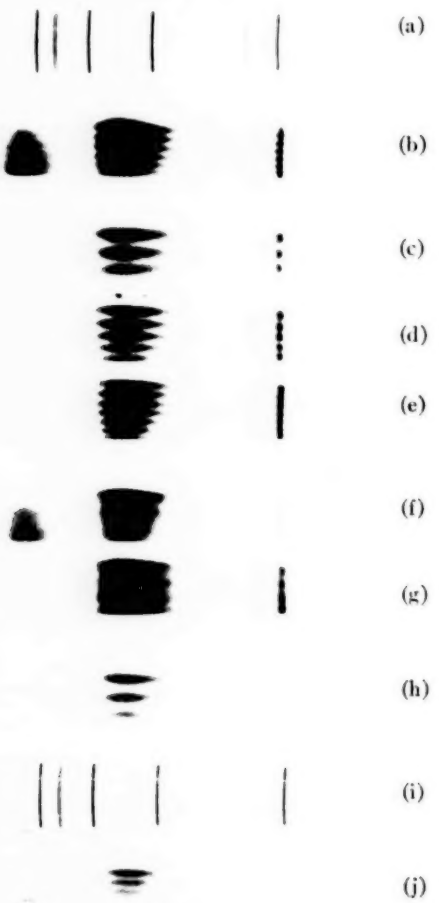

Fig. 2. Typical spectrograms of radiation emitted in striations with mercury arc spectrum at (*a*) and (*i*).

spectrograms such as (b) of Fig. 2 show that the radiation emitted by mercury vapor under such conditions is confined to the broad visual band at 4850A, the ultraviolet or 3300A band, and what is apparently the resonance line of mercury at 2537A, but which may also be made up in part of the 2540A band of mercury. For our purposes, there are several significant features of the spectra to be here considered, (a) the variation in the number of striations with applied voltage, (b) the sharpness of the striations, (c) the appearance

of the continuous and absence of arc radiation except 2537A, and, (d) the complementary variation of the intensity of the 4850A and 3300A bands.

Spectrograms (c), (d), and (e), show the effect of a variation of the applied voltage V_a on the number of such striations. The applied voltages were 23, 33 and 43 volts respectively. The corresponding number of striations are 3, 5 and 7. Apparently an increase of 10 volts in each case increases by two the number of observed regions in which radiation is produced. With extremely low currents and moderately high pressures it was possible to detect photographically as many as 16 striations without any deviation from the linear relation between the increase in the number of such striations and the increase in the applied potential difference. The variation in the number of such striations for changes in the value of V_a is such that we infer the difference in potential between adjacent striations to be very nearly 5.0 volts. This result

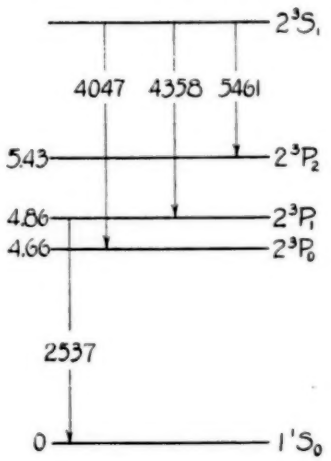

Fig. 3. Energy levels of mercury atom.

is in agreement with the observation of Grotrian[2] who measured the potential difference between such striations under conditions which approximate those of the present experiments and who found that the potential difference between striations to be approximately 4.9 volts.

We may infer from the sharpness of such striations that practically all of the electrons must make an inelastic collision in traversing a relatively short distance in the forward direction of the electric field. This is very definitely demonstrated by the absence of radiation corresponding to the higher excited states as would be expected from a consideration of the energy diagram of Fig. 3, in which a few of the lowest energy states are indicated. This fact, together with the linear dependence of the number of striations on applied voltage and the well-known results obtained in the determination of the resonance potentials in mercury vapor[3] makes it plausible to assume that in the present experiment, the primary process is the excitation of the $^3P_1$ and

[2] W. Grotrian, Zeits. f. Physik **5**, 148 (1921).

[3] Ruark and Urey, Atoms, Molecules and Quanta, p. 70.

$^3P_0$ states of the mercury atom. Now the $^3P_0$ state is metastable and we would in general expect the transition probability to this state by light absorption to be small compared to those transitions ending on the $^3P_1$ state. In the case of excitation by electron impact, such forbidden transitions may be more probable, due to the inhomogeneous field at impact.[4] In spite of this fact, it is generally believed[5] that such transitions when induced by electron impact are less probable than those ending in a radiating state such as $^3P_1$. As we shall see later a metastable atom produced by electron impact may receive energy from a collision with a normal atom and thus rise to the $^3P_1$ state and that consequently the relative numbers of atoms in these states will be affected by secondary processes such as collisions between normal and excited atoms.

As previously mentioned, one of the striking features of the observed spectra is the large amount of continuous radiation compared to the radiation emitted at wave-lengths normally associated with the mercury atom. By far the greater portion of the emitted radiation is in the form of continuous bands. Now Franck and Grotrian[6] have pointed out the possibility of the formation of an excited molecule by the combination of an atom in an excited state with an atom in the normal state. Houtermann[7] in his study of the fluorescence radiation of mercury vapor assumes such processes to take place, and by a measurement of the intensity of the green and ultraviolet bands emitted by a moving column of vapor as a function of distance from the point of initial excitation by the 2537A line, inferred that the green band is to be associated with the $^3P_1$ state and that the ultraviolet band is to be associated with the $^3P_0$ state. He assumed that when such an excited molecule dissociates, the frequency of the light emitted may be expressed by the equation

$$E = D_{S_0} + V_r + h\nu$$

where E is the energy of the activated molecule, V_r is the relative translational energy of the atoms on dissociation, D_{S_0} is the heat of dissociation of the normal molecule and ν is the frequency of the radiation accompanying the process. The above conclusion of Houtermann that the green band is associated with a molecule formed by a normal and a $^3P_1$ atom, and that the ultraviolet band is to be correlated with a molecule formed by a normal and a $^3P_0$ excited atom was based on the observation that in his work the intensities of the two bands did not decay at the same rate. It is very questionable if great significance can be placed on such observations for the relative intensity of the two bands can be affected by agencies other than the time required for the excited vapor to move from the point of initial excitation to the point of observation. As observed by others[1] and as should be quite apparent from the results herein presented the relative intensity of the two bands in question are greatly affected by temperature. We shall therefore next consider in some detail the complementary variation in intensity of the two bands.

[4] Franck and Jordan, Anregung von Quantensprüngen, p. 170.
[5] Ruark and Urey, Atoms, Molecules and Quanta, p. 477.
[6] J. Franck and W. Grotrian, Zeits. f. Physik **4,** 89 (1921).
[7] F. G. Houtermann, Zeits. f. Physik **41,** 140 (1926).

An examination of (b), (c), (d), (e), and (h) of Fig. 2 shows that, in general at the cathode the green band is quite faint, if at all detectable, and that towards the anode where the temperature must be very nearly that of the walls of the tube, the green band becomes progressively more intense. The intensity of the ultraviolet band undergoes a similar variation, but in the reverse direction—relatively very intense at the hotter portion of the tube near the cathode and weak at the anode. In order to be certain that this variation in intensity is due to the temperature of the vapor and not something else, the lower element F_2 was heated. The exposure (f) was taken when no current was flowing in the heater of F_2 and is to be compared with (g) where the temperature of the anode was considerably more than that of the cathode. In addition to the destruction of the visible band at 4850A and a complementary enhancement of the ultraviolet band, the resonance line at 2537A undergoes an enhancement parallel to the variation in intensity of the 3300A band. One would normally expect the pattern in the resonance line to be quite blurred due to absorption and re-emission. The fact that it is not, in general, indicates that the vapor must be quite transparent to at least a portion of the radiation at this wave-length, due possibly to the fact that the temperature of the discharge space was higher than the temperature of the walls of the tube. This fact must be taken into consideration when interpreting the variation in intensity of the radiation in this region. It is important to observe, however, in this connection that the general background, that is, the radiation between striations, is also more intense at the hotter positions in the discharge space, as I hope will be clear in the reproduction of (g), so that it appears as though there is a real parallelism between the variation in intensity of the 3300A band and that of the line at 2537A. Additional evidence for this will be given later. The complementary variation in the intensity of the 4850A and 3300A bands and the variation of the intensity of the resonance line suggests that the 3300A band may be in some way associated with the $^3P_1$ state of the mercury atom, and that the green band is in some manner connected with the metastable $^3P_0$ state.

In addition to the qualitative observations so far considered, an attempt was made to obtain a more quantitative estimate of the effect of temperature on the relative intensity of these two bands. For this purpose, the cathode temperature was reduced to 540°C as measured by means of a L. & N. optical pyrometer. A low cathode temperature was employed so as to enhance the intensity of the green band. The radiation observed under such conditions is shown in (j) of Fig. 2. Microphotographic records of (j) in the region of the maxima are shown in Fig. 4. A Moll microphotometer was used. The point of maximum intensity was chosen in order to obtain information on as many striations as possible. Densities calculated from such records were converted into relative intensities by means of a $D-\log E$ curve for these two wavelengths constructed from the density marks on a plate of the same emulsion number and developed at the same time as (j). Neutral plates of known density were used in the plate calibration. The results of such measurements are given in Table I. The striations are numbered from the cathode to the anode.

TABLE I. *Intensities of the violet and green bands at various temperatures.*

	I_V	I_G	T	α	x
Cathode	—	—	813°K	—	0
Striation No. 1	5.66	—	745	30	21.5
Striation No. 2	4.69	2.06	677	42	40.5
Striation No. 3	2.91	2.47	616	62	57.
Striation No. 4	2.24	2.67	559	90	71.
Striation No. 5	1.84	3.01	522	124	80
Anode	—	—	447	—	89

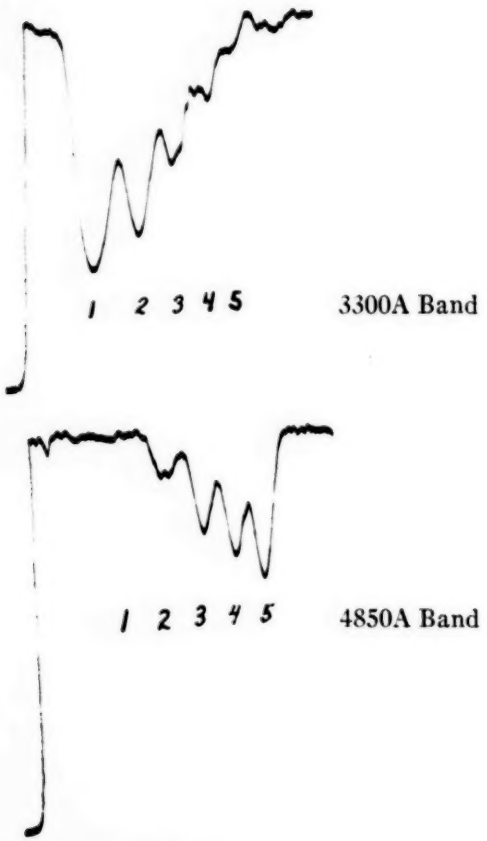

Fig. 4. Microphotograms from (*j*).

The numbers in the second column give the relative intensities IC, of the striations in the ultraviolet band, and those in the third column refer to the relative intensities I_G, in the green band. The sixth column are numbers which are proportional to the distance x, between the cathode and the various striations. Such numbers were obtained from a measurement of the position of the centers of the striation on the photographic plate. The fourth column gives the temperature in absolute units at the various striations. These temperatures were calculated in the following manner.

For purposes of simplification we assume the temperature to be constant

in planes perpendicular to x, where x is defined above. When equilibrium is attained, the temperature at any point must be constant so the equation of heat flow becomes

$$\frac{\partial}{\partial x}\left(K\frac{\partial T}{\partial x}\right) = 0. \tag{2}$$

The conductivity K is not constant in this case, for from kinetic theory

$$K = \tfrac{1}{3}Nm\bar{c}\lambda CV \tag{3}$$

where N is the number of atoms per cc, m is the mass of the atom, $\bar{c}$ the average speed of the atoms of the vapor, λ the mean free path and CV the specific heat of the gas. In the steady state the pressure will be constant and therefore N is proportional to T^{-1}. The mean free path is proportional to N^{-1} and therefore to T, and the average speed will vary as $T^{1/2}$. The other factors entering into K may be regarded as constants so that we infer that the heat conductivity will be proportional to the square root of the absolute temperature and write (2) in the form

$$\frac{\partial}{\partial x}\left(T^{1/2}\frac{\partial T}{\partial x}\right) = 0.$$

If one writes this in the form

$$\frac{\partial^2}{\partial x^2}(T^{3/2}) = 0 \tag{4}$$

the solution is readily seen to be

$$T^{3/2} = a + bx \tag{5}$$

where the constants a and b are obtainable from the assignment of the temperature at two values of x. This has been done assuming the anode temperature in the exposure (j) to be the same as the temperature of the walls of the tube which in this case was 477°K. The cathode temperature was 813°K as previously stated. The values of T given in column 4 of Table I were calculated from (5) for the various values of x given in column (6).

Before we proceed to a comparison of the observed intensities at various values of T it will be interesting to recall some of the effects of temperature on the relative populations of atoms in the $^3P_0$ and $^3P_1$ states. Such calculations have been given by others[8] and we give here briefly a restatement of the essential of the argument as treated by Gaviola.

We shall assume that the primary process occurring in the striations is the excitation by election impact of the mercury atom to the resonance state. Atoms may leave the $^3P_1$ state and enter the $^3P_0$ state by collisions of the second kind. If under equilibrium conditions N_1 is the population of the $^3P_1$ state and N_0 is the population of the $^3P_0$ state and if E_1' is the efficiency factor

[8] See for example P. D. Foote, Phys. Rev. **30**, 288 (1927); M. W. Zemansky, Phys. Rev. **34**, 213 (1929); E. Gaviola, Phys. Rev. **34**, 1373 (1929).

for collisions of the second kind, then the number of collisions per second producing $^3P_0$ atoms is

$$N_1 Z' E_1' \tag{6}$$

where Z' is the total number of collisions suffered per second by a $^3P_1$ atom. Now the population of the $^3P_0$ state is given by the product of the number of metastable atoms produced per second and the mean life τ_0 in the metastable state so

$$N_0 = N_1 Z' E_1' \tau_0 \text{ or } N_0/N_1 = Z' E_1' \tau_0. \tag{7}$$

We see that in order to determine the ratio of N_0 to N_1 it is necessary to examine the factors which determine the mean life τ_0.

At low vapor pressures the life τ_0 is limited by the average time required for the metastable atoms to diffuse to the walls where they are destroyed. At higher pressures, such as concern us in this work, the number of metastable atoms destroyed in this manner must be negligible compared to the number which are destroyed by being raised to the $^3P_1$ state by a collision of the first kind. Thus if Z is the number of collisions per second between a metastable and normal atom and if α is the average number of collisions required in order that one collision have sufficient energy to effect the change, and if E_1 is the efficiency factor for such collisions of the first kind then the probability of destruction by this cause is

$$P_1 = ZE_1/\alpha \tag{8}$$

where α is given by the reciprocal of the Boltzmann distribution formula $1/\alpha = e^{-W/KT}$, where W is the energy difference between the $^3P_0$ and $^3P_1$ states.

It is also possible that metastable atoms may be destroyed by collisions with normal mercury atoms or by molecular formation. If we let ZE_2 be the probability of the above two processes

$$P_2 = ZE_2. \tag{9}$$

The probability of the emission of 2656 ($1S_0 - {}^3P_0$) appears to be so small in our work that we shall neglect it. The probability of the destruction of a metastable atom is the sum of the individual probabilities, so

$$P_0 = P_1 + P_2. \tag{10}$$

The mean life τ_0 is the reciprocal of this probability, so, substituting (8) and (9) into the reciprocal of (10) gives

$$\tau_0 = \frac{1}{(ZE_1/\alpha) + ZE_2}. \tag{11}$$

If we now assume that the collision areas of metastable with normal atoms and $^3P_1$ atoms with normal atoms are the same and further if $E_1^1 = E_1$ then substituting (11) into (7) we have for the ratio of the concentrations in the two states

$$\frac{N_0}{N_1} = \frac{1}{(1/\alpha) + (E_2/E_1)}. \tag{12}$$

The results of Zemansky[8] indicate that E_1 is of the order of unity and at the pressures and temperatures employed in our work, E_2 would appear[8] to be small compared to $1/\alpha$ so that we have finally

$$N_0/N_1 = \alpha. \tag{13}$$

The calculated values of α for the various striations are given in column 5 of Table I, and the ratio of the intensity in the green band to that in the ultraviolet is plotted as a function of α in Fig. 5. The closeness with which the points fall on a straight line through the origin must be due in part to a cancellation of errors introduced by the necessary approximations required. The linear dependence between the ratio I_G/IV and α as strongly suggested by Fig. 5 points quite definitely, it would appear, to the conclusion that the states which are responsible for the production of these two bands, obey, in

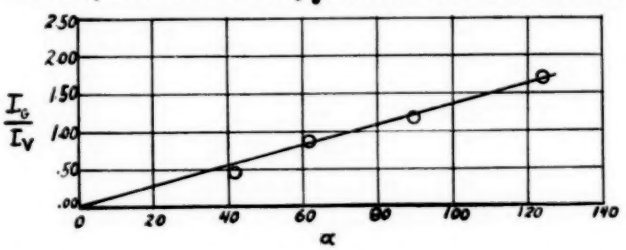

Fig. 5. Relation between the ratio of the relative intensity of green band to relative intensity of ultraviolet and α at the various striations.

the temperature interval thus far considered, the Boltzmann distribution formula and that the energy difference between these states is that corresponding to the energy difference between the $^3P_1$ and $^3P_0$ states of the mercury atom. Granting the original suggestion of Franck and Grotrian as to the formation of excited molecules by the union of normal and excited atoms we conclude that the green band is to be associated with the metastable state of the mercury atom and that the ultraviolet band is to be associated with the $^3P_1$ state.

There is yet to be mentioned one other observation on the variation of the intensity of the 3300A band. With extremely high cathode temperatures such that the striation nearest the cathode was in a region having a temperature of 500°C or more, its intensity under such conditions was less than the intensity of the next adjacent striation. Beyond the second striation the intensity variation was the same as shown in Fig 2. The same phenomena has been observed by others.[1] This variation in intensity is accompanied by a similar variation in the intensity at 2537A. This last observation supports the qualitative inferences previously given on the parallelism between the variation in intensity of this line and the 3300A band. The green band is so weak at these higher temperatures that nothing can be said from this work as to its intensity variation with temperature. Transition probabilities between the

$^3P_0$ and $^3P_1$ states and between excited states and the normal state might be expected to depend in part on the character of the potential energy curves of quasi-molecules formed by collisions between such atoms,[9] and it may be that the explanation of the decrease in intensity of the 3300A band and the 2537A line at the elevated temperatures is connected with the characteristics of such potential energy curves.

In conclusion, I wish to thank Mr. Buttoph of the General Electric Vapor Lamp Company for cathodes used in the present work and to acknowledge my indebtedness to Dr. W. F. G. Swann of the Bartol Research Foundation where this investigation was carried out for his aid and criticisms, and to the National Research Council and Duke University for making this work possible.

[9] O. K. Rice, Phys. Rev. **37**, 1187 (1931).

SPECTRAL FLUORESCENCE EFFICIENCIES OF CERTAIN SUBSTANCES WITH APPLICATIONS TO HETEROCHROMATIC PHOTOGRAPHIC PHOTOMETRY*

By George R. Harrison, Massachusetts Institute of Technology
and Philip A. Leighton, Stanford University

(Received July 23, 1931)

Abstract

In extending the method of fluorescence photographic photometry recently described by the writers from homochromatic to heterochromatic usefulness, experiments have been carried out on the efficiencies of fluorescence of various substances in the visible and ultraviolet regions. A number of substances fluorescing at wave-lengths between the red and the ultraviolet have been tested, and many of these have been found to exhibit the same variation of fluorescence efficiency with wave-length, when in a pure state and in solutions of proper concentration. The intensity of the fluorescence light emitted by them when illuminated with light of constant intensity at different wave-lengths was measured and found to be such that the number of quanta emitted was practically proportional to the number of incident quata over a wide range of wave-lengths. This is in contradiction to certain results previously announced by other workers who found the emitted energy proportional to the incident energy, but is confirmed by other results and by well-known photochemical laws. Small traces of impurities in certain of the fluorescing substances, particularly aesculin, produce large variations in the efficiency of response, which appears to explain the conflicting results previously obtained. The general relation found is applied to the development of a simplified method of heterochromatic photographic photometry useful in the range 3900–2000A, which it is believed can be extended to the Schumann region. The end desired is attained by photographing the fluorescence light emitted when the spectrum is allowed to fall on a plane surface of the substance, or by use of a dry plate with fluorescent coating, which shows not only constant contrast but almost uniform quantum sensitivity over a large spectral region. Small corrections need to be applied for variation in reflecting power of the coated emulsion, but these are all of the type which can be measured and controlled by homochromatic photometry.

I. Previous Data on Fluorescence Efficiencies

TWO of the most arduous requirements of photographic photometry are the calibration and standardization of the photographic plates used, i.e., the determination of the density—log-intensity curves of the emulsion for each wave-length desired, and the measurement of its variation in sensitivity from one spectral region to another. If a dry plate could be developed which showed uniform contrast at all wave-lengths, and which obeyed some general law of sensitivity variation both problems would be greatly simplified. The experiments described here were undertaken with a view to developing such a plate by making use of certain properties of fluorescent substances.

* Much of the material discussed in this paper was presented at the Cleveland meeting of the American Physical Society, December 1930.

We have recently shown[1] that ordinary dry plates coated with certain fluorescent oils show constant contrast at all wave-lengths lying in the region of continuous absorption of the oil used, which in certain cases extended from 3300A to at least 900A. We have since[2] eliminated the variation in surface sensitivity occasioned by the flowing of the oils, together with the necessity of removing the oil from the surface of the emulsion prior to development, by using a fluorescent layer consisting of a coating of aesculin dissolved in gelatine which was allowed to dry on the original emulsion. In this way constant contrast was obtained at all wave-lengths below 3900A at least as far down as 2300A, and probably as far down as the plates are sensitive, the lower wave-length limit being presumably set by the absorption of the gelatine.

Anderson and Bird[3] found that they obtained exact agreement in the region 3350A to 2537A between spectral energy measurements made by means of a thermopile and by means of an optical fluorescence photometer employing aesculin, fluorescein, or uranium glass. Their results led us to expect that fluorescence methods of the type we had been studying would show uniform sensitivity at all wave-lengths for which they are suitable. In making the tests described below on this point, however, we found that curves which were expected to be horizontal straight lines were in fact hyperbolic, and such as to indicate that a uniform quantum efficiency rather than a uniform energy efficiency existed, a result much more in accord with the present picture of the quantum mechanism of fluorescence. From the known laws of photochemistry it appears more reasonable to suppose that the same number of fluorescence quanta will be emitted per 100 incident quanta no matter what the size (within limits) of the latter than that this fraction will vary in just the proper way to keep the amount of emitted energy proportional to the amount of incident energy. We accordingly investigated the literature further, and found that Nichols and Merritt[4] had noted a decrease in the energy efficiency of fluorescence of eosin and resorcufin at shorter wave-lengths, and that this decrease appeared about of the magnitude that one would expect to find if a uniform quantum efficiency existed. Wawilow[5] found that fluorescein showed a definite proportionality of the energy efficiency to the wave-length in the region 4047–2537A, indicating a uniform quantum efficiency, while aesculin solutions gave a fluorescence efficiency independent of wave-length in the same region, the former result being in contradiction and the latter in agreement with the results of Anderson and Bird. As the difference in the two results involves a discrepancy of about 40 percent some unknown variable factor appears to be operating. We accordingly determined to make a careful study of the efficiency of fluorescence of various substances in the desired range.

[1] Harrison and Leighton, J.O.S.A. **20,** 313 (1930).
[2] Harrison and Leighton, Phys. Rev. **34,** 779 (1930).
[3] Anderson and Bird, Phys. Rev. **32,** 293 (1928).
[4] Nichols and Merritt, Phys. Rev. **31,** 381 (1910).
[5] Wawilow, Phil. Mag. **43,** 307 (1922); Zeits. f. Physik **22,** 266 (1924); **42,** 311 (1927).

II. Apparatus for Measuring Relative Fluorescence Efficiencies at Different Wave-Lengths

A special monochromator was constructed, having quartz-fluorite achromatic lenses and a Cornu prism. The achromatic feature is very desirable so that a constant aperature may be kept for all wave-lengths, and if a sufficiently wide slit is used the spectral images are all of the same size. When this is the case a single thermopile reading gives the true intensity of a line;

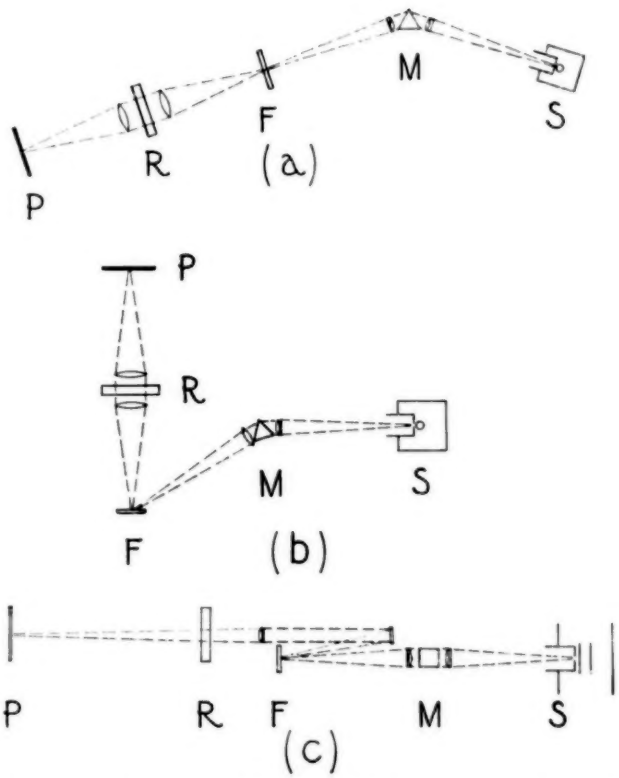

Fig. 1. (a) Quartz monochromator with achromatic lenses arranged to project a spectrum of constant magnification on a fluorescent surface, the resulting "homochromatic spectrum" being then photographed with a camera through the fluorescent material. A thermocouple or pile could be substituted in place of the fluorescent material, so that the energy distribution in the spectrum could be determined. (b) and (c) Alternative arrangements which allow the fluorescence light to be photographed from the front surface of the fluorescing material.

with the monochromators ordinarily used this is not true, and all spectral intensities should be integrated or special corrections applied. We have averaged a large number of runs through the mercury spectrum obtained with our instrument both by integrating and by merely reading maxima, and find no systematic deviations between the two averages. The prism was kept fixed, the thermopile being moved across the spectrum so that the line intensities were measured under exactly the same conditions as were used when they were all allowed to fall simultaneously on different portions of the fluorescent

material. This arrangement of apparatus is shown in Fig. 1 (a). *S* is a quartz mercury arc run from a storage battery under constant conditions at 73 volts and 3.2 amps. Light from this passes through a slit 0.5×3 mm, and the mercury spectrum is spread out by the monochromator *M* in the plane *F*, where a quartz cell with plane windows containing the fluorescent material being studied is placed. From the far side of the cell one sees the spectrum lines, but all below a certain wave-length appear of the same color, the fluorescent light in most of the substances studied comprising a comparatively narrow band of wave-lengths in some portion of the visible spectrum. An image of this "homochromatic spectrum" is now thrown on the photographic plate *P* by means of two quartz lenses whose distance apart can be varied to provide accurate focusing for light from materials which fluoresce with different colors, care being taken that none of the visible light not absorbed by the fluorescent material reaches the plate. *R* represents a filter whose transmission to the fluorescent wave-lengths is known; by photographing the homochromatic spectrum through filters of varying known transmissions data were obtained to calibrate the plate for the fluorescence wave-lengths. The filters were approximately neutral to that part of the spectrum covered by the fluorescent light, and were calibrated in terms of neutral screens in a separate apparatus by means of the fluorescence light itself, for each fluorescent substance.

In order to detect any errors that might be introduced through allowing the fluorescence light to pass through the fluorescent material, the arrangement shown in Fig. 1, (b) was also used. Here a chromatically uncorrected quartz lens is substituted for the camera lens of the monochromator so that the focal plane will not be normal to the optic axis, and the fluorescence light is taken off from the front face of the cell. With this arrangement the spectrum lines are unequally magnified, and a correction for this must be applied.

Still further to insure that unknown errors were not present, the third arrangement shown in Fig. 1, (c) was used to obtain supplementary data. The achromatic camera lens of the monochromator was replaced, and a mirror was introduced into the optical system so that the fluorescence light could still be taken from the front face of *F* while the uniform magnification of spectral lines was kept.

Eastman 36 plates were used for substances giving a blue or violet fluorescence, while Wratten panchromatic plates were found satisfactory when green and red fluorescing substances were being studied. Exposures of from 3 to 10 seconds sufficed for the first, while with the second 20 seconds or more were required.

In order to measure accurately the energy distribution in the spectrum in the focal plane at *F* a number of different thermoelectric devices were used, these being substituted for *C* when desired. One of the most probable causes of error in such work arises from the lack of true blackness of the absorber on the radiometer used. For example, the difference between results indicating an equal energy yield and an equal quantum yield could be entirely caused by a radiometer which had the absorption properties of copper rather than those of a true black body, and many commercial thermocouples are

unsatisfactorily blackened. We accordingly obtained our results in terms of two Moll vacuum thermoelements in quartz, a similar instrument with a fluorite window, and three different Bi-Ag thirteen element thermopiles of our own construction. These all showed substantial agreement.

After a plate was obtained by taking a number of exposures to the homochromatic spectrum through various filters R it was measured on a projection lantern microphotometer and the data were plotted for the various spectrum lines as in Fig. 2, the log intensity values being known from the relative

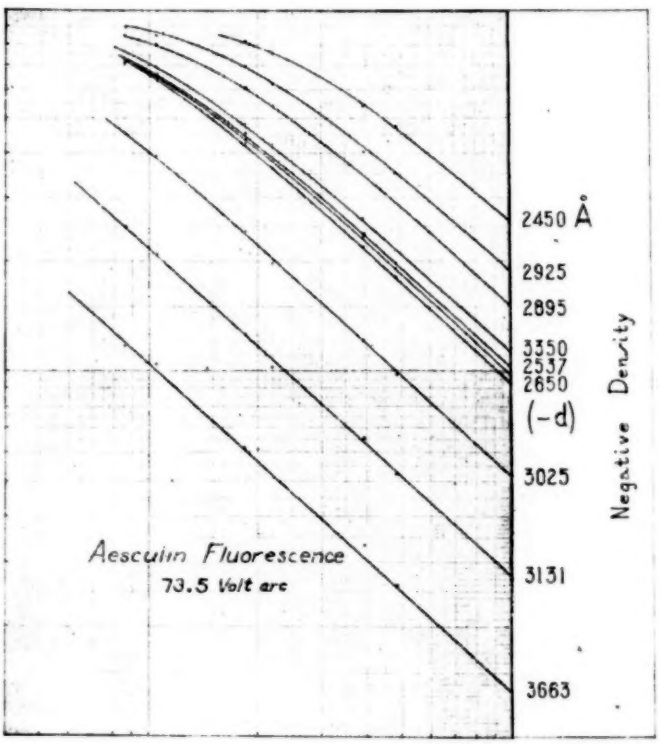

Fig. 2. Calibration curves for the photographic plate when exposed to the fluorescence light from aesculin produced by various incident wave-lengths.

transmission factors of the filters. The curves for the various lines were found to be accurately parallel so long as the fluorescence light did not vary in quality with the color of the incident light, and so long as the number of quanta produced at a given wave-length remained proportional to the number of incident quanta. With the substances tested in the concentrations used these conditions were almost always fulfilled, and any departures from them could be readily detected.

By measuring the horizontal distances apart from the curves for the various lines, one obtains the relative intensities of fluorescence I_f of the lines. The ratio of this quantity to the actual intensity I_i of the incident light, as measured by the thermoelement, then gives a measure of the fluorescence efficiency for each wave-length.

III. Results

In Fig. 3 we show the types of curve obtained for various fluorescent substances when I_f/I_t was plotted against wave-length. Pure aesculin dissolved in water, a standard Wratten filter of aesculin in gelatin, a light machine oil (Cenco pump oil #11021), several standard automobile lubricating oils, chlorophyll dissolved in alcohol, and solid anthracene all showed similar variations in fluorescence efficiency between 3300 and 2400A, though they did not follow the relation found by Anderson and Bird. The strength of many of the solutions was found to have a great effect on the variation of fluorescence efficiency as is of course to be expected; the conditions depicted hold only when all of the incident light is absorbed in a very thin layer of fluorescing material. In chlorophyll this is particularly marked; in solutions of such

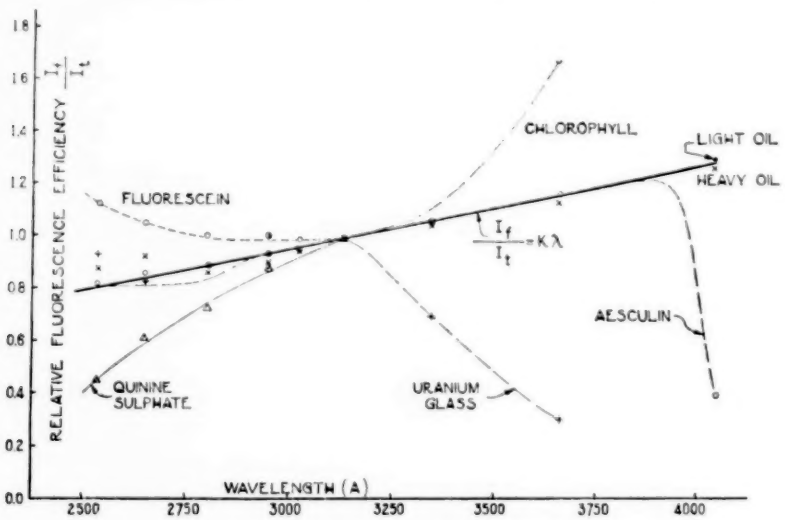

Fig. 3. Curves showing the variation of fluorescence efficiency with wave-length for various samples, the relative efficiency I_f/I_t being set at 1.0 for λ3131.

dilution that a banded structure can be observed in the absorption spectrum, no regularity of response can be expected, of course. Various substances, such as a solution of quinine sulphate in water and calcium tungstate in powdered form, obey entirely different laws in the region tested.

Our results as depicted in Fig. 3 show then, that the conclusion of Anderson and Bird, that in general, fluorescent substances will be found to have a constant fluorescence efficiency at wave-lengths shorter than a certain limit cannot hold. In order to obtain a still further check on the results we set up an optical method of measurement somewhat similar to that used by Anderson and Bird; the arrangement is shown in Fig. 4. Light from the monochromator M passing through the micrometer slit S is made parallel by the lens L, and after passing through the diaphragm D which maintains a constant aperture for all wave-lengths falls on the quartz cell C containing the fluorescent substance. The fluorescent light is taken off at an angle different

from that of the reflected light and passes into the Lummer-Brodhun photometer P where it is compared visually in intensity with light from an incandes-

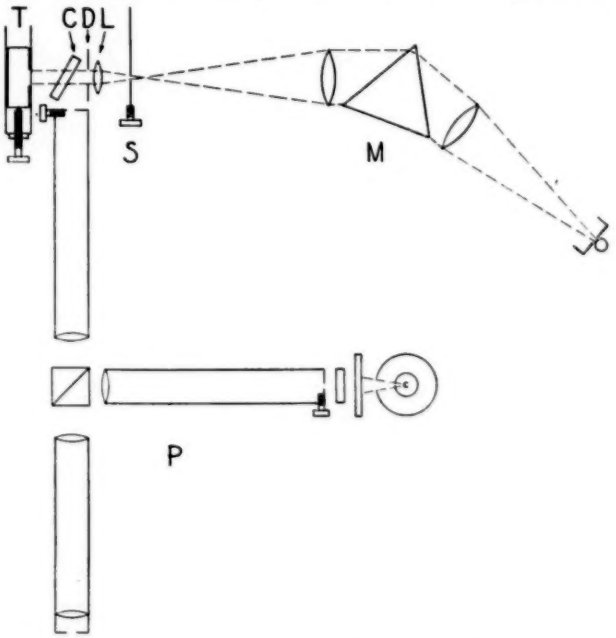

Fig. 4. Lummer-Brodhun photometer arranged to measure fluorescence efficiencies, giving an optical check on the results obtained photographically with the apparatus depicted in Fig. 1.

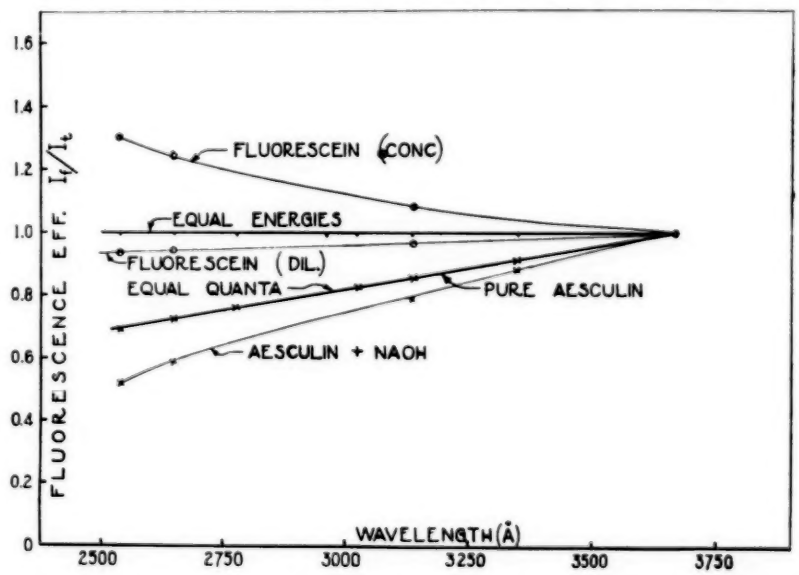

Fig. 5. Variation in fluorescence efficiency for fluorescein and aesculin with different dilutions and degrees of contamination, I_f/I_t being set arbitrarily at 1.0 for λ3663.

cent lamp shining through a filter and a solution of the fluorescent substance being studied, which gives a constant comparison source of the proper color.

By varying slit S the intensity of the light falling on C is varied to give a match in the photometer; the cell is then removed and the incident light allowed to fall directly on the surface thermopile T, where its total intensity is integrated. Results obtained in this way again contradicted those of Anderson and Bird, and showed a linear variation of fluorescence efficiency with wave-length for most substances.

We noted during the course of this part of the work that often the curves for one cell filled with aesculin differed from those of another, and soon found that minute traces of alkaline impurities had a large effect on the result. With fluorescein, also, concentration appeared to play a large part. Fig. 5 shows results obtained with these substances under various conditions, and appears to explain the results of Anderson and Bird for fluorescein, at least.

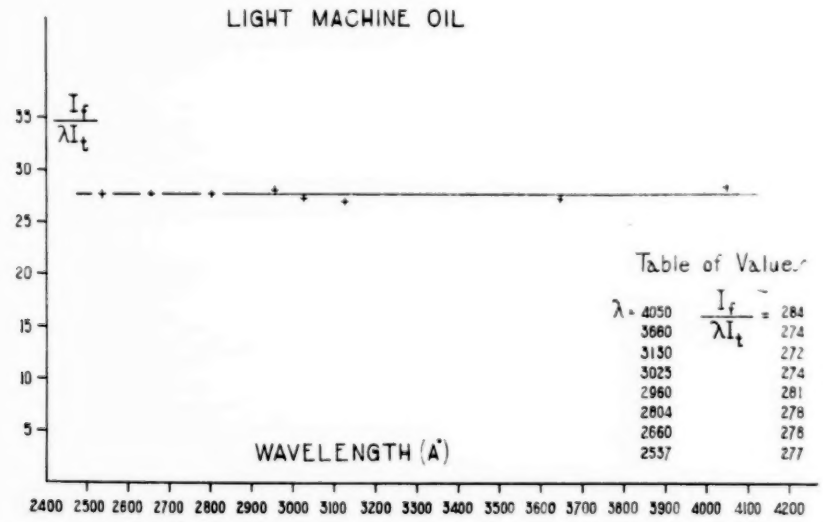

Fig. 6. Curve showing constancy of quantum yield obtained at various wave-lengths with an oil sample of the type used for coating plates.

IV. Conclusions and Application to Photometry

Turning now from the exceptions to the rule to the gratifying number of substances which were found to obey a simple law within a certain spectral range, we see at once that while the uniform fluorescence efficiency does not ordinarily exist, a uniform quantum yield often does. In Fig. 6 we show results (obtained from a single plate) for the type of lubricating oil which we have found most useful for coating plates to produce uniform contrast. Here we have plotted $I_f/\lambda I_t$ against wave-length; obviously, within the range plotted a constant number of fluorescent quanta are emitted per 100 incident quanta.

The greater part of this work was done by the writers at Stanford University during 1929–30; on account of the contradiction between many of the results and those of previous workers a new set-up of the apparatus has

been made at the Massachusetts Institute of Technology by one of us and the work has been repeated by Mr. A. L. M. Dingee, who is continuing and extending it. We are indebted to Mr. Dingee for the data plotted in Fig. 6, which agree entirely with our previous results, and give points lying somewhat closer to the theoretical curve than ours had done, due to the fact that in obtaining them the incident light was varied by means of filters of platinum on quartz, in place of the variation of the fluorescence light by means of the filters *R*. This reduces small errors arising from the non-neutrality of the filters, the platinum filters being calibrated with monochromatic light at each wave-length used.

We turn now to the direct application of these results to heterochromatic photographic photometry. An Eastman 36 plate was coated with the light machine oil and was found to give a response which agreed quite accurately with that expected from the uniform quantum yield law. However, a correction is required here, even when the necessary conditions of layer thickness, etc. have been fulfilled. For there is a variation of the amount of reflection from the air-oil interface with wave-length which may not be negligible. In the cases recorded above, where the oil or other material was enclosed in quartz, the thermopile was also enclosed in quartz, so the variation in loss of light at the air-quartz surface could be neglected. The loss at the quartz-oil surface was found to be exceedingly small, so that its variation was entirely negligible. The magnitude of the correction required for the coated plate at the air-oil face can be readily determined, however, by the methods of homochromatic photometry.

Apparently then, this method can be used in place of a thermopile, provided proper precautions are taken to see that the simple law assumed holds. Otherwise errors similar to or greater than those often made by the gratuitous assumption of the reciprocity law in photographic photometry are liable to occur. The sensitivity of such a coated plate is several hundred times as great as that of a thermopile, and we believe that its greatest application will be, not in supplanting this, but in supplementing it for use with weak spectra and in regions difficult of access, such as the Schumann region. A further advantage is that the coated plate bridges the gap in sensitivity between the thermopile and the photographic plate as ordinarily used; we have found that in order to satisfactorily record directly on a photographic plate a spectrum which was about as weak as could conveniently be measured with the average thermopile-galvanometer combination, and exposure time of about 1/500 second was sufficient. This inconveniently small time of exposure gives inaccurate results with the mercury arc or a similar source due to the flickering which occurs at high intensities. The fluorescence method, on the other hand, bridges the gap, and in addition transforms all energies into a single set of wave-lengths, so that various spectral lines can be reflected or absorbed equally without introducing relative errors. Much higher resolving power can be used than with the thermopile, and very weak lines can be accurately measured.

For many kinds of work a still further simplification would result if the

fluorescent dry plates discussed above[2] should follow the same law. Accordingly photographs of the spectrum were taken on plates prepared with the pure aesculin coating in gelatin as described, and a uniform quantum yield was found within the same limits as for the oil coated plates. We accordingly possess a dry plate which shows uniform contrast and almost uniform quantum sensitivity, which provides a known energy sensitivity distribution if one knows the wave-lengths photographed. We are now investigating further methods of improving the uniformity of this type of plate, and especially of extending the method to wave-lengths shorter than 2000A.

Much of the apparatus used in this investigation was purchased with a grant from the Rumford Committee of the American Academy of Arts and Sciences, which is hereby gratefully acknowledged.

THE EFFECT OF VARYING CONCENTRATIONS OF CERTAIN ELECTROLYTES ON THE VIOLET BAND OF THE RAMAN SPECTRA OF WATER

By C. C. Hatley and Dixon Callihan
Department of Physics, Duke University

(Received June 20, 1931)

Abstract

A Hilger E-1 spectrograph was used to study the Raman scattering by pure water excited by the 3650A group of the mercury arc. Photometric measurements of the plates were made with a Moll microphotometer. The violet band at about 4150A appears to consist of three components. The effect on this band of various concentrations of aqueous solutions of KCl, NaOH, and KOH was examined. In all cases the energy appears to shift toward the long wave-length side and in addition the top of the curves grows sharper with increasing concentrations.

A GREAT amount of work has already been done on the Raman spectra of pure water[1,2,3,4] and a still greater amount has been done on the effect produced on the Raman bands by various concentrations of different substances in aqueous solutions.[5,6,7]

In spite of the amount of work that has been done there is yet quite a bit of uncertainty and some conflicting data as to the structure of these bands. Some have found broad continuous bands[8] showing no real structure while others have found two[9,10] or three[11] and even a higher number[12] of components. Of the bands excited by different lines, Kinsey[13] found the band excited by the 3650A group to be a double band while that excited by the 4047A group was found to be a triple band.

The present work was undertaken with the aim of helping to clarify this situation and to add to the present available data on the changes produced in the water bands by the addition of varying amounts of easily ionized substances.

The major part of the previous work has been confined to the most con-

[1] Raman and Krishnan, Ind. Jour. Phys. **2,** 399 (1928).
[2] Rao, Nature **125,** 600 (1930); Proc. Roy. Soc. **127,** 279 (1930).
[3] Dadieu and Kohlrausch, Naturwissen. **17,** 625 (1929).
[4] Ellis, Nature **123,** 205 (1929).
[5] Carrelli, Pringsheim and Rosen, Zeits. f. Physik **51,** 511 (1928).
[6] Dickinson and Dillon, Proc. Nat. Acad. Sci. **15,** 334 (1929).
[7] Daure, Compt. Rendus **187,** 940 (1928).
[8] Meyer, Phys. Zeits. **31,** 510 (1930).
[9] Dadieu and Kohlrausch, Cf. Ref. 3.
[10] Gerlach, Phys. Zeits. **31,** 695 (1930).
[11] Rao, Cf. Ref. 2.
[12] Ganesan and Venkteswaran, Ind. Jour. Phys. **4,** 195 (1929).
[13] Kinsey, Phys. Rev. **34,** 541 (1929).

spicuous band of water, namely, the one shifted from the exciting line by about 3400 wave-numbers, which corresponds to about 3μ.

The violet band at about 4150A excited by the 3650A group was selected in this work, in spite of its composite nature, because of its intensity and also because fewer data are available concerning this band than concerning the one at about 4700A.

It seemed worthwhile to determine what effect is produced on the water band by a solution of some of the hydroxides. Ten photographs were taken with each of the following as the scattering substance: distilled water, aqueous solutions of KOH varying in concentration from 9.74N to 0.27N, and aqueous solutions of NaOH varying from 13.5N to 1N. In addition three photographs were taken for aqueous solutions of KCl at 2.5N, 0.25N and 0.025N.

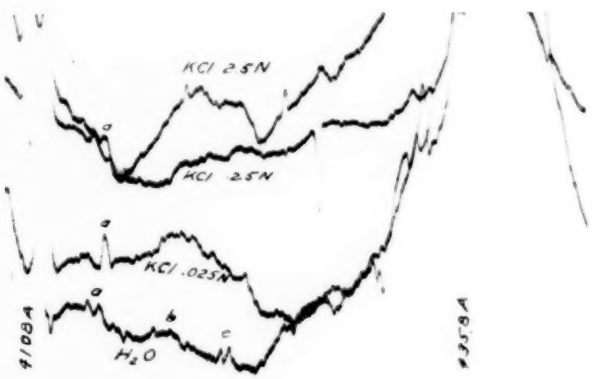

Fig. 1.

The scattering tube and water jacket were of glass. The tube was similar to that described by R. W. Wood.[14] The end farthest from the spectrograph slit was drawn out into a cone, curved upward and painted black. A Hilger E-1 quartz spectrograph was used with special astronomical green sensitive plates. The photometric measurements of these plates were made with a type A Moll microphotometer. The source, for all photographs except those of NaOH, was a Hanovia quartz mercury arc operated at three amperes with 150 volts directly across the lamp terminals. The NaOH photographs were made at an earlier date with the same lamp operating at a lower temperature. The time of exposure for each plate was about 30 hours except in the case of NaOH solutions and in that of pure water where exposures of 48 hours were made. The temperature of the scattering substance was held at 30°C within 2°.

An inspection of the microphotometer curves taken from these plates will give the best idea of the form of the band and also of the effect on the band of various concentrations of the above mentioned substances. It was

[14] R. W. Wood, Phil. Mag. **6**, 729 (1928).

thought best to record a curve for pure water and a number of curves for the same electrolyte at different concentrations on the same microphotometer film. An effort was made to have these curves so placed that corresponding points of all curves on any one film should lie in the same vertical line. How nearly this was accomplished may be judged from the 4108A line near the left in the figures and best seen in the curves for the NaOH solutions. The heavy line seen at the right of the figures is the 4358A line from the arc.

In Fig. 1 the H_2O curve was made from a plate exposed for 48 hours with a spectrograph slit width of 0.02 mm, the microphotometer thermocouple slit being correspondingly narrow. The curve seems to indicate a triple structure

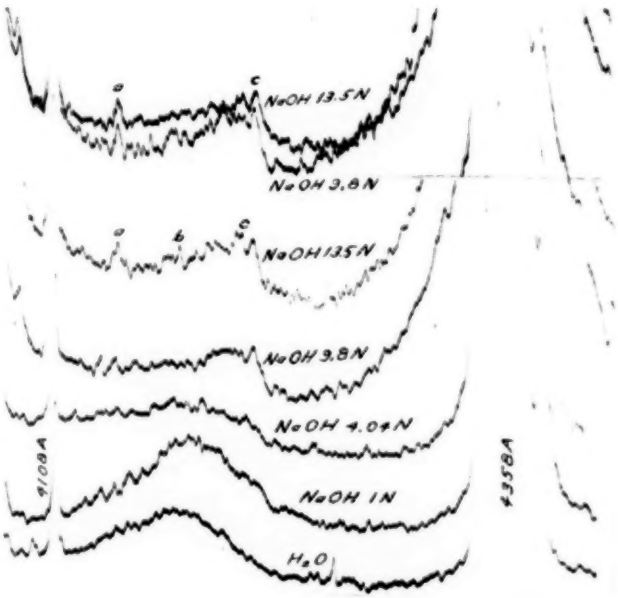

Fig. 2.

for the water band. The components are indicated by letters (a), (b), and (c). These represent shifts from the exciting line of approximately 3228, 3435 and 3624 wave-numbers corresponding to 3.10, 2.91 and 2.76μ. The wave-lengths of the components of the band are 4137A, 4173A and 4206A respectively. This curve shows the components of the water band better than either of the other two curves for water which were made with a wider slit for both spectrograph and microphotometer. Some uncertainty is introduced in regard to component (a) due to the fact that there is in the mercury arc a weak line at 4145A. The gear ratio of the microphotometer for all curves shown was such that 1 mm of film corresponded to 2A closely. The distance between the two outer components measures 35 mm, the inner component being located about midway between the outer ones. The overlapping of the bands due to the different lines of the 3650A group and the general Raman scattering combined with the continuous radiation from the arc make it impossible to determine

the wave-length of the individual components with much precision. However, since a large percent of the energy of this groups is associated with the two closely lying lines 3650 and 3655A, the scattering due to these two lines should stand out prominently.

The other three curves for different concentrations of KCl show that for low concentration, 0.025N, there is an increase of energy in all the components, (a) becoming quite sharp. Further concentration shifts the energy more and more toward the long wave-length component (c) and at the same time renders the peak of the curve sharper. Gerlach[15] has reported a like energy shift for a number of the chlorides including KCl. He also reports the disappearance of the short wave-length component of the 4700A band of water for concentrated solutions. Woodward[16] has recently reported a Raman band

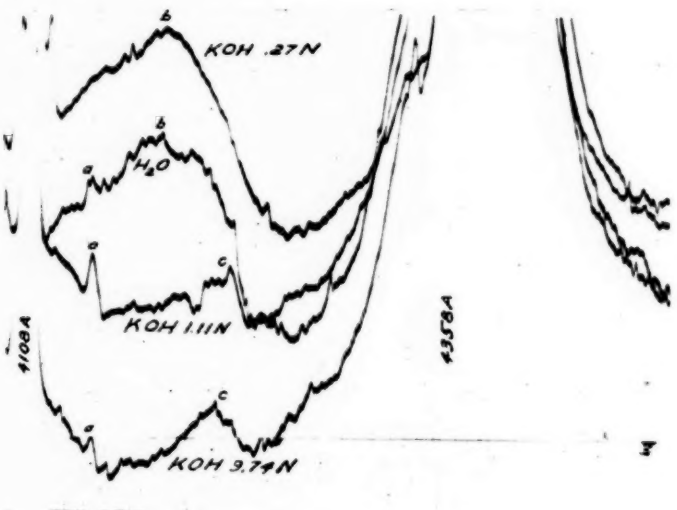

Fig. 3.

which corresponds to a shift of 3615 wave-numbers for very nearly concentrated solutions of both NaOH and of KOH.

In Fig. 2 are shown curves obtained with different normalities of NaOH. At the bottom is shown the poorly resolved curve for water. For 1N the scattering increases while the center of gravity of the curve is shifted toward the long wave-length side. For better comparison the curves for 9.8N and 13.5N are repeated in juxtaposition at the top of the figure. These two curves were made at a later date with a different slit width for the thermocouple. For high concentrations the (c) component becomes most prominent and shows a steep curve on the long wave-length side.

The data are hardly sufficient to enable one to decide whether the individual centers of (b) and (c) shift or whether the energy increase in the locality of (c) shifts the center of gravity of the more or less poorly resolved

[15] Gerlach, Naturwissen. **18,** 68 (1930).
[16] Woodward, Phys. Zeit. **32,** 261 (1931).

curve. It might be pointed out in this connection that the (a) component while suffering a decrease in energy shows little if any shift with change in concentration. With some degree of uncertainty the curves for higher concentrations of NaOH shows signs of the unshifted (b) component.

The effect of different concentrations of KOH is shown in Fig. 3. It can be seen that with increasing concentration there is again a shift of energy away from the center toward the (c) component. The curve for 9.74N, the base of which has been supplied from another curve made from the same plate, shows a marked sharpening of the top of the curve near the location of the (c) component.

The difference in general appearance of the curves for NaOH and those for KOH may be explained in part by the fact that the latter were taken with the arc at a much higher temperature and with slightly wider slit.

Further work along this line is in progress using as a source a helium hot cathode arc described by Wood.[17] It is hoped that with this arrangement, which gives practically monochromatic light, the components of the water band may be located with higher precision and the effect of solutes on this band may be better determined.

[17] R. W. Wood, Phys. Rev. **35**, 670 (1930).

THE SATELLITES OF M-SERIES X-RAY LINES

By F. R. Hirsh, Jr.
Department of Physics, Cornell University

(Received July 20, 1931)

Abstract

Four satellites of the diagram line $M\alpha_1$ have been measured in the range of atomic numbers from U (92) to Yb (70). Two of these satellites have not been reported previously. Three satellites of the diagram line $M\beta$ have been measured in the range of atomic numbers from U (92) to Gd (64). Two of these satellites have not been reported previously. Superposition of the semi-Moseley graphs for the satellites of $M\alpha_1$ and $M\beta$, gives rise to the suggestion that perhaps both x-ray lines are modified by the same optical lines. All these observed satellites obey the "Moseley" law, the data giving a straight line within experimental error. The semi-Moseley graph of the satellite $M\beta^{ii}$ shows a significant break at atomic number 70. The satellites of $M\alpha_1$ vanish at Er (68), coincident with the splitting of the $M\alpha_1$ line into three components at this place, i.e. at atomic number 68. The range of values of $\Delta\nu/R$, between satellite and parent line, is from 0.1 to 2.0, in agreement with the results of previous workers, for the satellites of K and of L series lines. A peculiar continuous spectrum accompanies the satellites of $M\alpha_1$ and $M\beta$ for the elements U (92) and Th (90).

X-RAY "satellites," "spark lines" or "non-diagram" lines, as they have been variously termed, are those relatively faint lines accompanying certain diagram lines in the x-ray spectrum. Their presence cannot be accounted for by the usual energy-level diagrams, consequently they have been described as due to various inner-atomic processes. Among these Wentzel's hypothesis[1,2] of multiple ionization, with a single electron jump, was first advanced as an explanation.

The work of Druyvesteyn[3,4] has shown that the experimental verification of Wentzel's theory is not very satisfactory. Bäcklin[5] has shown that experimental observations of satellite excitation potentials do not confirm Wentzel's hypothesis.

In view of the defects of Wentzel's theory, and because of certain important experimental evidence, F. K. Richtmyer[6] advanced his "double-jump hypothesis" as an explanation of the origin of x-ray satellites. This double-jump hypothesis has an experimental basis in the existence of the quasi-Moseley graphs for x-ray satellites. The hypothesis is adequately explained in a later paper.[7] Briefly, his theory is, that in a doubly ionized atom, simultaneous jumps of two electrons occur. One jump releases an x-ray quantum;

[1] G. Wentzel, Ann. d. Physik **66,** 437 (1921).
[2] G. Wentzel, Zeits. f. Physik **31,** 445 (1925).
[3] M. J. Druyvesteyn, Zeits. f. Phys. **43,** 707 (1927).
[4] M. J. Druyvesteyn, Dissertation, Groningen (1928).
[5] E. Bäcklin, Zeits. f. Physik **27,** 30 (1924).
[6] F. K. Richtmyer, Phil. Mag. **6,** 64 (1928).
[7] F. K. Richtmyer, Jour. Frankl. Inst. **208,** 325 (1929).

the other jump releases the energy of a semi-optical quantum; the total energy of both jumps are emitted from the atom as a single modified x-ray quantum, or satellite quantum.

More data were essential for the testing of this double-jump hypothesis, and for providing an experimental foundation for the building of any explanation of the origin of x-ray satellites. Accordingly, F. K. Richtmyer and R. D. Richtmyer[8] made a survey of the L-series x-ray satellites. Recently, O. R. Ford[9] made a similar survey of K-series satellites. Hence a survey of M-series satellites seemed to promise new and interesting results.

M-series satellites of the diagram lines $M\alpha_1$, $M\beta$ and $M\gamma$ were first reported by Hjalmar.[10,11] Recently Lindberg[12,13] made a re-survey and an ex-

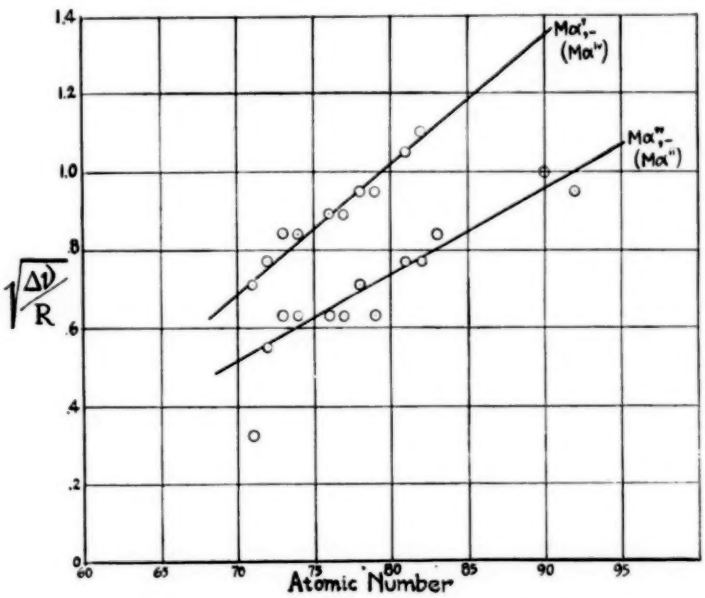

Fig. 1. $M\alpha_1$ satellites (from Lindberg's data).

tension of previous M-series precision wave-length measurements. He noted satellites of the diagram lines $M\alpha_1$ and $M\beta$ only.

The satellite data, secured from the data tables of the articles by Lindberg,[12,13] are plotted as a semi-Moseley graph in Figs. 1 and 2. Lindberg finds two satellites of $M\alpha_1$ and one satellite of $M\beta$, in agreement with the results of Hjalmar.[11] (Hjalmar apparently found three satellites of $M\beta$, but this was for one element only, U(92).)

Especially to be noted in Fig. 2 is *some sort of discontinuity in the semi-*

[8] F. K. Richtmyer and R. D. Richtmyer, Phys. Rev. **34,** 574 (1929).
[9] O. R. Ford, Phys. Rev. **37,** 1695 (1931).
[10] E. Hjalmar, Zeits. f. Physik **1,** 439 (1920).
[11] E. Hjalmar, Zeits. f. Physik **15,** 65 (1923).
[12] E. Lindberg, Zeits. f. Physik **50,** 82 (1928).
[13] E. Lindberg, Zeits. f. Physik **57,** 797 (1929).

Moseley graph at or about atomic number 70. Further mention will be made of this fact.

Experimental Work

In the present investigation a Siegbahn vacuum spectrograph was used. Spectra were recorded on Imperial eclipse plates cut specially for this spectrograph. Three different crystals were used to cover the wave-length range from 3.708A to 10.234A. Calcite was used for the range from 3.0 to 6.0A.; quartz, for the range from 6.0 to 8.0A., and gypsum (selenite), for the range from 8.0 to 10.3A.

The d.c. voltage for the x-ray tube was supplied by a standard high-potential circuit, using kenotrons and condensers in the usual manner. A small vol-

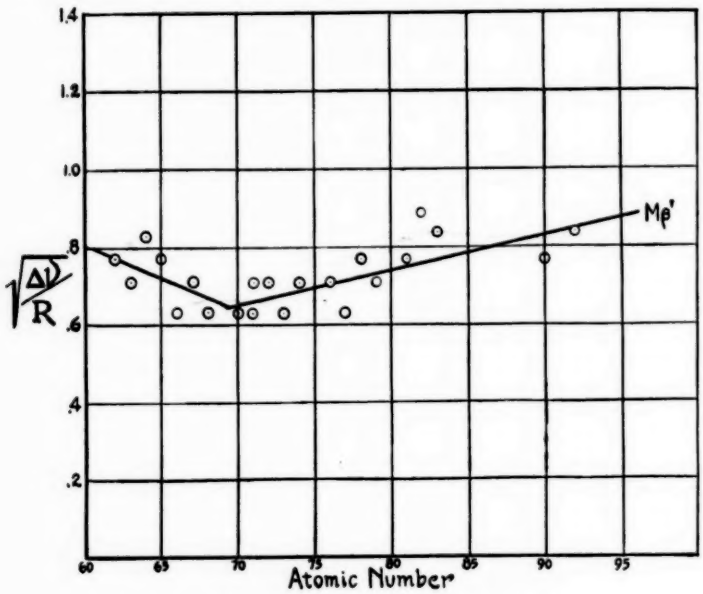

Fig. 2. $M\beta$ satellites (from Lindberg's data).

tage ripple was present. A third kenotron was used as a thermionic valve to limit the current through the x-ray tube to a safe value. This prevented the sudden high-current discharges which are disastrous to milliammeters. The current was read with a standard Weston milliammeter designed for x-ray work. Voltage was measured by means of a repulsion-type, electrostatic voltmeter, which was calibrated by a standard spark gap. The moving member of this voltmeter consisted of two ping-pong balls, coated with india ink and fastened at the ends of a threaded brass tube of small diameter. This device reduced the inertia of the moving member, and the india ink rendered the balls conducting.

Exposures of the x-ray plates, necessary to bring out the satellite structure, varied from one to eight hours, depending on the power which could be safely applied to the anti-cathode wedge and the material fixed on the wedge. The exposure time was considerably reduced in the case of the long wave-

length x-rays, where aluminum leaf was used as the slit covering to exclude light from the plate-crystal chamber of the spectrograph. Ordinary typewriter carbon paper proved satisfactory for the slit covering, when wavelengths of from 3 to 5A were being used. However, in the region of from 7 to 12A this absorbed practically all the radiation which should have passed through to the crystal and plate.

In Table I, is given the form in which each element was used as an anti-cathode material, and the metal which composed the wedge supporting the material. Wedges were prepared by roughening the metal surface with a pointed tool, and the material to be used as an anti-cathode was forced on to the roughened surface. Such wedges would often last three hours, with the x-ray tube running at 8 kv and 12 to 13 ma.

TABLE I. *Form in which each element was used as anti-cathode, and the wedge material.*

Element	Used in form of	Wedge material
U	Yellow Oxide, UO_3	Cu
Th	White Oxide, ThO_2	Cu
Bi	Metal	Cu
Pb	Metal (commercial solder)	Cu
Tl	Metal	Cu
Au	Metal	Cu
Pt	Metal	Cu
Ir	Metal (powdered)	Al
W	Metal (flat spiral)	Al
Ta	Metal	Al
Hf	White oxide	Al
Lu	Oxide, mixed with BeO	Al
Yb	Oxide, mixed with BeO	Al
Er	Oxide	Al
Dy	Oxide, mixed with BeO	Al
Gd	Oxide	Al

The potential, at which the x-ray tube was run, was always maintained at least twice the excitation voltage for the parent line, for the purpose of having the satellites as intense as possible.

While most metals can be hard soldered to copper, for use as x-ray targets, tungsten and tantalum are notable exceptions. Neither metal is wetted by molten solder and hence cannot be secured by this method. A flat spiral of tungsten wire was made, and this was pounded into an aluminum wedge which served satisfactorily for an anti-cathode wedge. A small piece of sheet tantalum was likewise pounded into a piece of aluminum and thus firmly secured for use as a target.

Although tungsten spirals are convenient for use as x-ray tube filaments, they usually coat the anti-cathode with tungsten, a very objectionable feature. This can be avoided by using oxide filaments, which, however, are relatively short lived.

The wave-lengths of the lines accompanying a given diagram, (or "parent"), line, were determined by means of comparison with the known wavelengths of the parent lines.

Satellites of the diagram lines $M\alpha_1$ and $M\beta$ were measured for sixteen elements in the range of atomic numbers between U(92), and Gd(64).

Satellites of the diagram line $M\alpha_1$ were present at U(92) and vanished at Er (68). Satellites of the diagram line $M\beta$ were present at U(92) and continued to Gd(64), where the last remaining satellite was so faint that observations beyond this point must be considered as somewhat doubtful.

A careful search was made for satellites of the diagram line $M\gamma$ (previously reported by Hjalmar).[11] Faint lines accompanying $M\gamma$ were observed, but they were identified as higher order reflections of known L-series lines.

Another investigation was carried out in the M-series spectrum of Bi(83), for the purpose of detecting satellites accompanying diagram lines other than $M\alpha_1$ and $M\beta$. The results were negative. Satellites, if present, must be so faint as to avoid detection. Perhaps all diagram lines are modified by optical

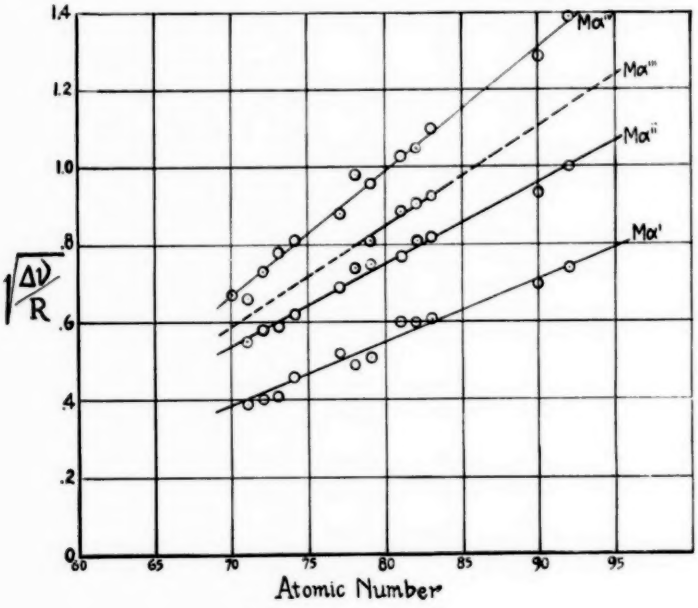

Fig. 3. $M\alpha_1$ satellites.

lines, so as to have satellites. The modified part of the parent line (the satellite) will be much fainter than the parent line and accordingly the satellite will be readily observable only for the stronger diagram lines which for the M-series are $M\alpha_1$ and $M\beta$.

Experimental Results

In Table II is given the results of the study of the $M\alpha_1$ lines and their accompanying satellites. The terminology of F. K. Richtmyer has been used for satellite designation. The satellites have been called $M\alpha^{i}$, $M\alpha^{ii}$, $M\alpha^{iii}$ and $M\alpha^{iv}$, where $M\alpha^{i}$ is the satellite nearest the peak of the parent line, and the others are located successively towards shorter wave-lengths.

In Tables II and III, values of $\Delta\lambda$ are the differences in wave-length between the satellites and the parent lines, ($M\alpha_1$ or $M\beta$), and are determined by direct measurements on the spectrum plates. $\Delta\nu/R$ and $(\Delta\nu/R)^{1/2}$ are then

TABLE II. *Data on satellites of $M\alpha_1$ lines.*

M line	U (92)	Th (90)	Bi (83)	Pb (82)	Tl (81)	Au (79)	Pt (78)	Ir (77)	W (74)	Ta (73)	Hf (72)	Cp (71)	Yb (70)	
$M\alpha_2$	3.9146	4.1416	5.1181	5.2845	5.4543	5.8372	6.0440	6.2581	6.9763	7.2440	7.5308	—	8.1359	λ Wave-length values (angstroms)
$M\alpha_1$	3.9010	4.1290	5.1070	5.2730	5.4430	5.8270	6.0330	6.2480	6.9670	7.2350	7.5230	7.8230	8.1240	
$M\alpha^{i}$	3.8920	4.1198	5.0961	5.2626	5.4319	5.8164	6.0236	6.2364	6.9562	7.2248	7.5128	7.8136	—	
$M\alpha^{ii}$	3.8843	4.1114	5.0878	5.2537	5.4237	5.8055	6.0113	6.2292	6.9469	7.2148	7.5035	7.8029	—	
$M\alpha^{iii}$	—	—	5.0821	5.2486	5.4174	5.8014	—	—	—	—	—	—	—	
$M\alpha^{iv}$	3.8690	4.0890	5.0724	5.2400	5.4083	5.7922	5.9950	6.2153	6.9330	7.1998	7.4897	7.7937	8.0917	
$M\alpha_2$	233.71	220.91	178.76	173.13	167.74	156.74	151.38	146.20	131.14	126.30	121.49	—	112.45	ν/R values
$M\alpha_1$	234.53	221.59	179.16	173.50	168.10	157.04	151.65	146.43	131.32	126.46	121.62	116.95	112.62	
$M\alpha^{i}$	235.08	222.08	179.53	173.86	168.46	157.30	151.89	146.70	131.53	126.63	121.78	117.10	—	
$M\alpha^{ii}$	235.53	222.53	179.83	174.15	168.69	157.60	152.20	146.90	131.70	126.81	121.93	117.25	—	
$M\alpha^{iii}$	—	—	180.03	174.32	168.89	157.70	—	—	—	—	—	—	—	
$M\alpha^{iv}$	236.47	223.26	180.37	174.60	169.17	157.96	152.61	147.20	131.97	127.07	122.16	117.39	113.07	
$M\alpha^{i}$	0.55	0.49	0.37	0.36	0.36	0.26	0.24	0.27	0.21	0.17	0.16	0.15	—	$\Delta\nu/R$ values
$M\alpha^{ii}$	1.00	0.94	0.67	0.65	0.59	0.56	0.55	0.47	0.38	0.35	0.31	0.30	—	
$M\alpha^{iii}$	—	—	0.87	0.82	0.79	0.66	—	—	—	—	—	—	—	
$M\alpha^{iv}$	1.94	1.67	1.21	1.10	1.07	0.92	0.96	0.77	0.65	0.61	0.54	0.44	0.45	
$M\alpha^{i}$	0.74	0.70	0.61	0.60	0.60	0.51	0.49	0.52	0.46	0.41	0.40	0.39	—	$(\Delta\nu/R)^{1/2}$ values
$M\alpha^{ii}$	1.00	0.94	0.82	0.81	0.77	0.75	0.74	0.69	0.62	0.59	0.58	0.55	—	
$M\alpha^{iii}$	—	—	0.93	0.91	0.89	0.81	—	—	—	—	—	—	—	
$M\alpha^{iv}$	1.39	1.29	1.10	1.05	1.03	0.96	0.98	0.88	0.81	0.78	0.73	0.66	0.67	
$M\alpha^{i}$	0.0090	0.0092	0.0109	0.0104	0.0111	0.0106	0.0094	0.0116	0.0108	0.0102	0.0102	0.0094	—	Δλ values (angstroms)
$M\alpha^{ii}$	0.0167	0.0176	0.0192	0.0193	0.0193	0.0215	0.0217	0.0188	0.0201	0.0202	0.0195	0.0201	—	
$M\alpha^{iii}$	—	—	0.0239	0.0244	0.0256	0.0256	—	—	—	—	—	—	—	
$M\alpha^{iv}$	0.0320	0.0310	0.0336	0.0330	0.0347	0.0338	0.0380	0.0327	0.0327	0.0352	0.0333	0.0293	0.0323	

Richtmyer Notation: $M\alpha^{ii} = M\alpha''$, $M\alpha^{iv} = M\alpha'$ — Siegbahn Notation

computed from these values of $\Delta\lambda$, taking the values of λ from Lindberg's data.[12,13] The wave-lengths of the several satellites are computed by subtracting from the values of λ^* the corresponding values of $\Delta\lambda$.

The semi-Moseley graph for the $M\alpha_1$ satellites is given as Fig. 3. From the graph, it is seen that there are four distinct satellites of $M\alpha_1$. $M\alpha^{i}$ and $M\alpha^{iv}$ are relatively faint lines, while $M\alpha^{ii}$ is a relatively strong line. $M\alpha^{iii}$ appears resolved from $M\alpha^{ii}$ only for atomic numbers 79 through 83. By comparison of Fig. 3 with Fig. 1 it can be seen that $M\alpha^{ii}$ and $M\alpha^{iv}$ are the satellites $M\alpha''$ and $M\alpha'$ observed by Lindberg.[12,13]

Thus Lindberg's observations are verified, and, in addition, two new satellites are observed, namely $M\alpha^{i}$ and $M\alpha^{iii}$. Fig. 3 shows a distinct im-

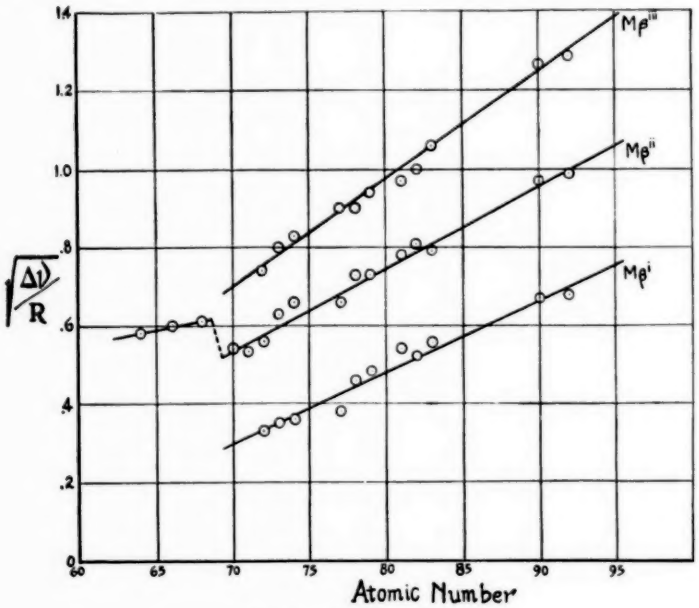

Fig. 4. $M\beta$ satellites.

provement over Fig. 1 in the grouping of the data points about the average straight lines, indicating improved experimental accuracy. The graph shows that $(\Delta\nu/R)^{1/2}$ plotted against Z, atomic number, is a straight line relation within experimental error.

In Table III the results of the studies of $M\beta$ lines are tabulated. The data are again plotted as a semi-Moseley graph in Fig. 4. Three distinct satellites are shown here, and they have been called $M\beta^{i}$, $M\beta^{ii}$ and $M\beta^{iii}$, using the Richtmyer method of designation. As before, $M\beta^{i}$ is the satellite closest to the parent line maximum, and $M\beta^{ii}$ and $M\beta^{iii}$ are successively farther from this peak.

Referring back to Fig. 2, one readily sees that $M\beta^{ii}$ is Lindberg's satellite

* It will be noted that the last figure in each parent line wave-length value is given as zero. Lindberg's data does not give this last figure. It was used merely for convenience in computing the data of the present paper.

TABLE III. *Data on satellites of Mβ lines.*

M line	U (92)	Th (90)	Bi (83)	Pb (82)	Tl (81)	Au (79)	Pt (78)	Ir (77)	W (74)	Ta (73)	Hf (72)	Cp (71)	Yb (70)	Er (68)	Dy (66)	Gd (64)	
$M\beta$	3.7080	3.9330	4.8980	5.0640	5.2380	5.6110	5.8150	6.0240	6.7410	7.0060	7.2890	7.5860	7.8920	8.5760	9.3450	10.2340	λ Wave-length values (angstroms)
$M\beta^{i}$	3.7011	3.9254	4.8901	5.0564	5.2294	5.6030	5.8070	6.0179	6.7344	6.9996	7.2828	—	—	—	—	—	
$M\beta^{ii}$	3.6933	3.9172	4.8795	5.0455	5.2197	5.5929	5.7951	6.0064	6.7188	6.9848	7.2711	7.5697	7.8714	8.5484	9.3101	10.1925	
$M\beta^{iii}$	3.6831	3.9100	4.8687	5.0361	5.2099	5.5807	5.7853	5.9914	6.7072	6.9758	7.2569	—	—	—	—	—	
$M\beta$	246.74	232.63	186.79	180.67	174.67	163.06	157.34	151.89	135.73	130.59	125.52	120.60	115.94	106.66	97.91	89.40	ν/R values
$M\beta^{i}$	247.20	233.08	187.10	180.94	174.96	163.29	157.55	152.03	135.86	130.71	125.63	—	—	—	—	—	
$M\beta^{ii}$	247.72	233.57	187.50	181.33	175.28	163.59	157.88	152.32	136.17	130.99	125.83	120.88	116.23	107.03	98.27	89.74	
$M\beta^{iii}$	248.41	233.99	187.92	181.67	175.61	163.94	158.15	152.70	136.41	131.15	126.07	—	—	—	—	—	
$M\beta^{i}$	0.46	0.45	0.31	0.27	0.29	0.23	0.21	0.14	0.13	0.12	0.11	—	—	—	—	—	$\Delta\nu/R$ values
$M\beta^{ii}$	0.98	0.94	0.71	0.66	0.61	0.53	0.54	0.43	0.44	0.40	0.31	0.28	0.29	0.37	0.36	0.34	
$M\beta^{iii}$	1.67	1.36	1.13	1.00	0.94	0.88	0.81	0.81	0.69	0.64	0.55	—	—	—	—	—	
$M\beta^{i}$	0.68	0.67	0.56	0.52	0.54	0.48	0.46	0.38	0.36	0.35	0.33	—	—	—	—	—	$(\Delta\nu/R)^{1/2}$ values
$M\beta^{ii}$	0.99	0.97	0.79	0.81	0.78	0.73	0.73	0.66	0.66	0.63	0.56	0.53	0.54	0.61	0.60	0.58	
$M\beta^{iii}$	1.29	1.17	1.06	1.00	0.97	0.94	0.90	0.90	0.83	0.80	0.74	—	—	—	—	—	
$M\beta^{i}$	0.0069	0.0076	0.0079	0.0076	0.0086	0.0080	0.0080	0.0061	0.0066	0.0064	0.0062	—	—	—	—	—	Δλ values (angstroms)
$M\beta^{ii}$	0.0147	0.0158	0.0185	0.0185	0.0183	0.0181	0.0199	0.0176	0.0222	0.0212	0.0179	0.0163	0.0206	0.0276	0.0349	0.0415	
$M\beta^{iii}$	0.0249	0.0230	0.0293	0.0279	0.0281	0.0303	0.0297	0.0326	0.0338	0.0302	0.0321	—	—	—	—	—	

Richtmyer Notation, $M\beta^{ii} = M\beta'$, Siegbahn Notation

$M\beta'$. Peculiarly too, the curve for the satellite $M\beta^{ii}$ shows a break at atomic number 70, precisely as is shown in Fig. 2. The satellite $M\beta^{ii}$ is a relatively strong line, while $M\beta^{i}$ and M^{iii} are much less intense. Hence it is not surprising that $M\beta^{ii}$ persists at the lower atomic numbers, where $M\beta^{i}$ and $M\beta^{iii}$ are too faint for detection.

By comparison of Figs. 2 and 4 it can be seen that *$M\beta^{i}$ and $M\beta^{iii}$ are new satellites.*

Obviously now, this question arises: if, according to the double-jump hypothesis, a certain set of semi-optical jumps modify one x-ray diagram line to produce a set of satellites, might not these same jumps modify a second x-ray diagram line and produce another similar set of satellites? To test this sug-

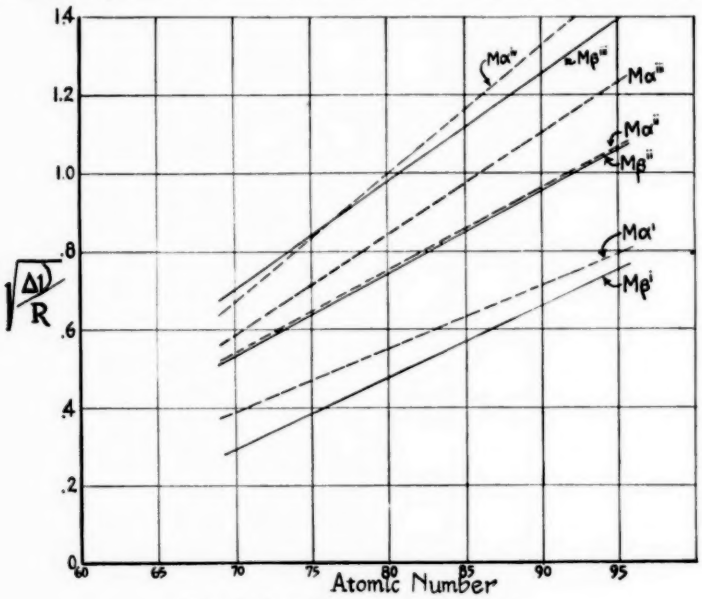

Fig. 5. Sattellites of $M\alpha_1$ and $M\beta$.

gestion, Figs. 3 and 4 are superimposed in Fig. 5. From Fig. 5 it can be seen that the curves for $M\alpha^{ii}$ and $M\beta^{ii}$ are practically coincident; $M\beta^{iii}$ and $M\alpha^{iv}$ while having different slopes, lie in the same region. The lines for $M\alpha^{i}$ and $M\beta^{i}$ lie within a reasonable distance from each other. On the other hand, $M\alpha^{iii}$ has no counterpart in the $M\beta$ series of satellites. The fact that these pairs of lines are not exactly coincident, may be the result of experimental error. On the other hand, there may be some real difference between the satellites of one diagram line and those of a neighboring line. However, the close proximity of the superimposed satellite curves, for two different diagram lines, strongly supports the idea that the same set of optical jumps modifies both diagram lines, to give rise to the observed satellites.

In Fig. 4, the semi-Moseley graph for the satellite $M\beta^{ii}$ shows a definite break in the region of atomic number 69 or 70, with a displacement of the former straight line and a change in its slope. It will be remembered that this discontinuity is present in the curve plotted from Lindberg's data (Fig. 2).

Foote's arrangement of electrons in orbits[14] shows that at atomic number 71, the building of the N_{VII} electron shell is just completed. Conversely, at atomic number 70(Yb) the first of the rare earths, the removal of electrons from the N_{VII} shell starts as we go down the atomic number range. It is known also that the Bohr-Coster diagrams, for the M, N and O, x-ray energy-levels, show similar breaks in the region of atomic number 70. Likewise, curves for the screening constant of the M and N electron shells, show breaks at the region of atomic number 70.

The interpretation of these facts, in terms of the double-jump hypothesis, is obvious. In terms of this theory, the semi-Moseley graphs represent a number of radiated semi-optical lines. A graph, showing a break at atomic number 70, means that the optical frequencies must suffer some change at this place in the periodic table. Since these semi-optical lines originate by electron jumps between two atomic energy levels, it at once follows that either one, (or both), of these energy levels must be one of those which show breaks in the Bohr-Coster diagrams, or which show a change in the screening constant in the region of atomic number 70.

It was observed in this research, that the satellites of the diagram line $M\alpha_1$ vanished at Er(68). Here, according to Lindberg,[13] the $M\alpha_1$ line splits into three components. This splitting was observed, too, by the present author. This fact, on the basis of the double-jump hypothesis, affords a possible explanation of the fading out of the satellites of the diagram line $M\alpha_1$. The semi-optical jumps will now modify all three components of the $M\alpha_1$ line, giving rise to three series of satellites, which being correspondingly broad, and therefore faint, will be difficult to observe.

It is significant that the range of values of $\Delta\nu/R$ for the M-satellites, as shown in Tables II and III, and in Figs. 3 and 4, is very close to the corresponding range for K and L satellites as found by other workers.

The spectrum plates of the diagram lines $M\alpha_1$ and $M\beta$ of Th (90), and U (92), show the *satellites of these lines as superimposed on a sort of continuous spectrum*. This fact has already been noticed and explained by F. K. Richtmyer[7] in the case of some satellites at the high atomic number end of the L-series satellite range.

The double-jump hypothesis opens up a new method of attacking the problem of the origin of x-ray satellites. Briefly, it is this. The Richtmyer double-jump equation (reference 7, page 359) is,

$$h\nu_s = h\nu_i + h\nu_0$$

where ν_s is the frequency of the satellite; ν_i that corresponding to the inner jump, and ν_0 that corresponding to the outer jump. From this equation it is clear that if ν_s and ν_i are known, values of ν_0 are predicted. Thus, for a given satellite, there should occur in the spark spectrum of the particular element, a radiated frequency of value ν_0. Perhaps this may be for a forbidden jump, and we may only observe a term-difference in the energy level diagram for the atom,—which term-difference will be of size $h\nu_0$. Thus the double-jump

[14] Foote, Trans. Amer. Inst. Min. Metal. Eng. **63,** 628 (1926).

hypothesis may be experimentally verified by the appearance of the predicted lines. By simple calculations, it can be found from the data in this article, that these values of ν_0 will predict lines in the soft x-ray, ultraviolet, and ordinary optical regions. Remembering that $c = \nu_0 \lambda_0$, where c is the velocity of light in vacuo, and λ_0 is the wave-length of the semi-optical line of frequency ν_0, which is represented, according to the double-jump theory, by the values of $\Delta\nu/R$, given in Tables II and III, we have

$$\lambda_0 = \frac{c}{\Delta\nu/R}.$$

Using the accepted values for c and R, we find that,

$$\lambda_0 = \frac{911.3 \times 10^{-8}}{\Delta\nu/R} \text{ cm}.$$

From this last relation, the following values of λ_0 are computed from the values of $\Delta\nu/R$ given in Table II for the four satellites of the diagram line $M\alpha_1$ in the spectrum of Bi (83).

Line	$\Delta\nu/R$	λ_0
$M\alpha^{i}$	0.37	2460A
$M\alpha^{ii}$	0.67	1358
$M\alpha^{iii}$	0.87	1046
$M\alpha^{iv}$	1.21	753

The investigation of the possibility of the occurrence of spark lines, as predicted by x-ray satellites, is under way in this laboratory. Preliminary work seems to show promise, and a detailed report will be made later.

If this connection, as suggested by the double-jump hypothesis, does exist, it means that there is a relation, previously unsuspected, existing between x-ray and optical spectroscopy.

In concluding, the writer particularly wishes to express his gratitude to Dean F. K. Richtmyer for suggesting this study, and for his encouragement and advice, without which the completion of this research would have been difficult. The writer also wishes to express his gratitude for the interest of various members of the Cornell University Physics Department. Grateful acknowledgment is hereby made for permission to use certain pieces of experimental x-ray apparatus, purchased by the Heckscher Research Council of Cornell University for investigations being carried out by Dean Richtmyer.

A NEW EFFECT PRODUCED BY ACTION OF X-RAYS ON MATTER

By G. I. Pokrowski[1]
All Union Electrotechnical Institute, Moscow

(Received May 22, 1931)

Abstract

This paper describes an investigation of the weak radioactivity which some heavier elements acquire after being irradiated by x-rays. The first method of investigation of this effect is based on the measurement of the ionization produced by the sample after irradiation. The second method consists in the counting of the scintillations produced by particles emited by the irradiated substance. The combination of these two methods makes it possible to determine the mean energy of each emitted particle. This energy is of the order of 10^{-6} erg. It seems quite impossible that particles of such energy could be emitted from the extranuclear electrons. It is much more probable that they originate in the atomic nuclei. On the other hand it is not possible to explain such results by radioactive contamination. Some possible explanations of the phenomena observed are discussed.

I. The Ionization Effect Afteer X-Ray Irradiation

A. Smits[2] some years ago pointed out, that lead irradiated by relatively very soft x-rays acquires feeble radioactive properties. The following apparatus shown in Fig. 1. was constructed in our institute for a more de-

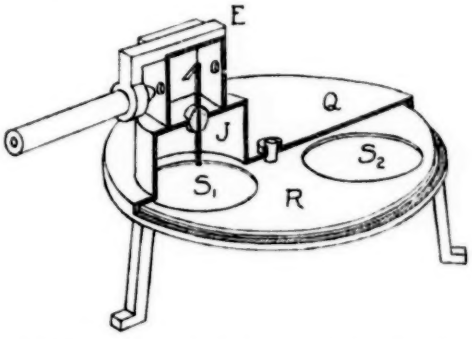

Fig. 1. Diagram of apparatus. E is the electrometer; J, the ionization chamber; R, the rotating disk; S_1 and S_2, the samples.

tailed investigation of this effect under conditions excluding the possibility of spurious effects due to radioactive contamination. It consists of the usual electrometer E for radioactivity measurements connected with a suitable ionization chamber. This chamber is connected with a cylindrical box Q in which is set a perforated resolving circle R for holding the materials to be tested. By revolving the circle any sample can be placed under the ionization

[1] Professor, leader of the theoretical group of the R¨ntgen-technical department.

[2] A. Smits and W. A. Frederikse, Zeits. f. Elektrochemie **34,** 350 (1928); A. Smits and H S. Vening, Meinesz Proceedings, Amsterdam **33,** 1 (1930).

chamber. Since the system is closed as tightly as possible, the testing samples in the cylindrical box are well protected from outside radioactive contamination. It is easy to remove the electrometer and to close the hole in the ionization chamber by means of a special cover, thus making it possible to expose the sample to x-ray irradiation. In addition to this the circle with samples can be revolved in such a manner that the irradiation of all samples will be uniform.

We used for the irradiation a Coolidge x-ray tube with tungsten anode, working at 140 kv_{eff} and 2 m.a. The time of irradiation was 30 minutes; the mean distance from the anode of the tube to the samples was 40 cm. The x-rays passed through the lead cover of the cylindrical box of 2 mm thickness.

After irradiation the instrument was removed to another room; the electrometer was placed back on the ionization chamber and the current in this chamber, produced by the different samples, was measured.

Preliminary experiments showed that, in accordance with the results of A. Smits, light elements like aluminum do not produce any effect. It was therefore possible to determine the zero current of the electrometer by placing an aluminum sample under the ionization chamber.

With that method of working the ionizing power of different elements after irradiation could be investigated. This ionizing power can be expressed as the difference between the ionization currents before and after irradiation produced by a unit of surface (1 cm^2) of the sample and measured by the number of ion pairs formed in unit of time (1 second).

The surface of all investigated samples was cleaned by scraping. Some days before the experiments, the box with the samples was closed and the circle was rotated for a long time. By this means we obtained a uniform distribution of radioactive matter and the dissociation of those contaminations, which are sufficiently unstable.

At first the effect was investigated as a function of time after irradiation. The results for lead obtained by Mrs. H. A. Gordon are given in Table I.

TABLE I. *Results for lead.*

J = ionization current, (ion pairs formed per sec.)	t = time in min. after the end of x-ray irradiation
910	10
560	20
390	33
230	50
110	70
60	90

Table I shows that the diminution of the effect after irradiation is of such a magnitude that the effect can be measured without difficulty. By extrapolating it is possible to determine the value of J directly after the end of irradiation. Mean values of J determined in the above mentioned way with a great number of samples of the several elements are given in the Table II. All these measurements have been made by Mrs. H. A. Gordon.

TABLE II. *Ionization current due to radiations from various metals after x-ray irradiation.*

Element	Atomic number	J
Al	13	no effect
Zn	30	no effect
Sn	50	170
W	74	550
Hg	80	1120
Pb	82	1390
Bi	83	1000

The mean error of J in Table II is about 20 percent. The experiments described did not make it possible to explain the origin of the observed ionization current. For such an explanation it is necessary to investigate the phenomenon from another point of view.

II. SCINTILLATIONS AFTER X-RAY IRRADIATION

The other method used by us is based on the counting of scintillations. Preliminary experiments described in another paper[3] showed, that after x-ray irradiation the heavier elements produce some feeble scintillations similar to the scintillations of α-particles of low energy.

Knowing the number of scintillations produced in 1 second by a unit of surface of a sample it is possible to determine the mean energy of each particle, as well as the energy losses of the particle in the surface layer of the sample. Table III shows the primary energy E of the particles emitted by unit of surface of the sample in 1 second (du/dt) extrapolated to the moment of stopping the x-ray irradiation.

TABLE III. *Energies of particles producing scintillations.*

Element	dn/dt	E
Zn	no effect	
Sn	0.038	0.5×10^{-6} erg.
W	0.087	0.7
Hg	0.095	1.3
Pb	0.090	1.7
Bi	0.089	1.3

The values of E show that the energy of the observed particles is much less than the energy of the α-particles emitted by radioactive substances. For a closer investigation of the scintillation effect we have constructed a specially designed apparatus.

A partial section of this instrument is given in Fig. 2. It consists of a revolving brass cylinder placed in a tight enclosed covering. The cylinder is driven by an electric motor with a suitable transmission. The testing sample put on the cylinder is a ring of suitable size.

The cylinder with the sample can be irradiated by x-rays at one side through an aluminium filter of 1 mm thickness. In these experiments we used an x-ray tube working only at 90 kv_{eff} and 3 m.a. We have determined that when the tension of the current in the tube was lowered from 140 kv to

[3] G. I. Pokrowski, Zeits. f. Physik **63,** 561 (1930).

90 kv the effect changed only very little. On the opposite side of the covering was placed a microscope with a zinc blende screen for counting the scintillations. The x-ray tube and the observer were separated by a wall in which the instrument was placed. Everywhere lead protection was so arranged that the minimal thickness of it met by x-rays should be equivalent to 1 cm of lead.

The inside of the rotating hollow cylinder was also covered with lead so that during the operation of the tube no luminiscence should be observed on the screen used for counting scintillations.

In addition the set was earthed before beginning the experiment. The box with the rotating cylinder and sample was closed for some days and the cylin-

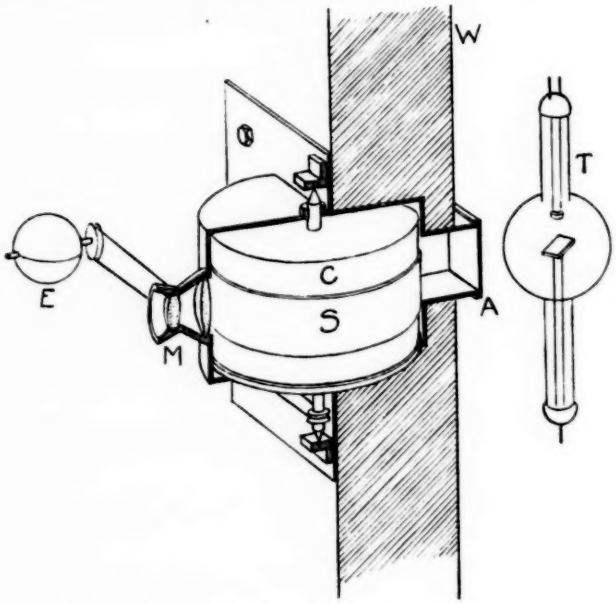

Fig. 2. Diagram of apparatus used in counting scintillations. *C* is the rotating cylinder; *S*, the sample under investigation; *M*, a microscope; *E*, an electric motor; *A*, aluminum window; *T*, x-ray tube; *W*, the wall.

der was rotated for a long time for the same purpose as with the apparatus for ionization measurement.

The principal results obtained as described above could be easily verified with this set.

The results obtained with lead, for instance, are given graphically in Fig. 3. Here dn/dt is the number of scintillations on the screen per second, t being expressed in days. Each point marked with an arrow was obtained during an x-ray irradiation. The number of revolutions of the revolving cylinder was 120 per minute. Thus the lapse of time between irradiation and observation was of the order of 0.25 second. The surface of the screen for counting scintillations was about 3 cm^2.

It is seen from Fig. 3 that in the case of many irradiations each about 2 hours in duration, the lead could be activated for a period of some days and

the effect could be made very large. The curve in Fig. 4 is based on a very large number of observations—approximately 181,000 scintillations. Taking into consideration the relative weakness of the scintillations here observed and the very large field of observation one must state that the experiments described are very laborious.

III. Discussion of the Possible Explanation of the Effect

The results indicate that the ionization effect is probably produced by the particles emitted by heavier elements after x-ray irradiation. These particles are like α-particles. Their energy has an order of 10^{-6} erg. It is quite improbable that particles of such energy could be emitted from the extranuclear

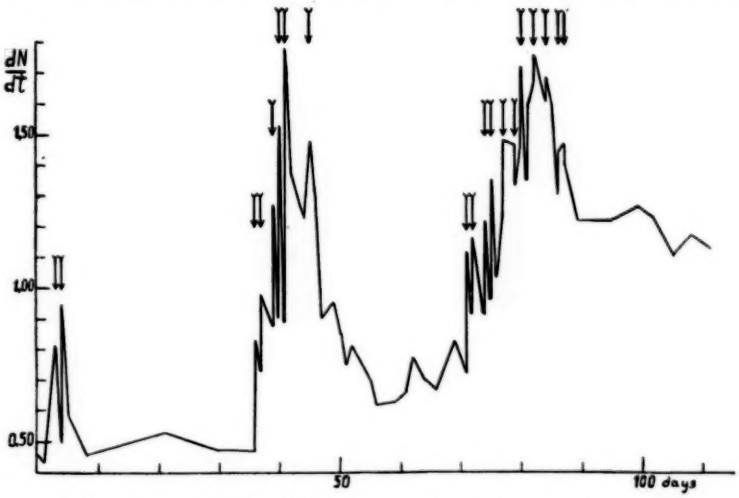

Fig. 3. Number of scintillations per second from lead. The arrows mark observations under x-ray irradiation.

electrons. It seems that the origin of such a phenomenon must be located in the atomic nucleus.

If nuclear transformations are examined from a thermodynamical point of view and if the equivalence of matter and energy is taken into consideration, it will not be difficult to divide all possible phenomena into exothermal and endothermal processes. Thus, if a given nucleus is splitting into two other nuclei and if the sum of their masses is not equal to the initial mass, then either an emission or an absorption of energy will result.

Obviously, when there is a decrease of mass, energy is liberated and, vice versa, energy absorption must be accompanied by a suitable increase of total mass. With the aid of accurate data concerning atomic weights, it can be readily shown that some cases of disintegration are accompanied by the emission of energy. The greatest energy per unit mass will be liberated when α-particles are thrown out of the nuclei the atomic numbers of which are greater than 40.[4]

[4] See G. I. Pokrowski, Zeits. f. Physik **63,** 561 (1930); G. Gamow, Proc. Roy. Soc London **A126,** 632 (1930).

It is possible that the energy necessary for starting such an exothermal process may be relatively very small, and it is therefore quite possible that x-ray quanta can liberate from thermodynamical unstable nuclei particles with energy of a much higher order than that of the quanta themselves. But certainly only very few nuclei, perhaps only an isotope of the activated element, can be thus influenced by means of irradiation. This follows from the weakness of the effect described. A calculation based on the experiments discussed shows that only one nucleus in 10^{15} can be influenced by irradiation.

A more detailed exposition of the theory of the phenomenon is given in another paper.[5]

[5] G. I. Pokrowski, Ann. d. Physik (1931).

AN X-RAY STUDY OF THE MAGNETIC CHARACTER OF LIQUID CRYSTALLINE PARA-AZOXYANISOL AND A COMPARISON WITH THE ISOTROPIC LIQUID

By G. W. Stewart
Laboratory of Physics, University of Iowa

(Received July 20, 1931)

Abstract

The effect of a magnetic field upon the orientation of the liquid crystalline groups in para-azoxyanisol has been studied by means of the angular distribution of x-ray relative diffraction intensities, the magnetic field being oriented perpendicular to the incident x-ray beam and the axis of the spectrometer. The relative number of the large molecular groups in the liquid crystalline condition, oriented perpendicular to the field, was obtained by the application of the Boltzmann distribution law in two theories; one assuming a permanent magnetic moment and the other anisotropic polarization. The latter theory of orientation agrees with the claim of Foex as to the cause of the decrease of the magnitude of the diamagnetic susceptibility in the milky state. Moreover, the experiments, together with general considerations, are in harmony with the second theory. Thus the experiments agree with the contention of Zocher, Jezewski and Foex and are opposed to the conclusions of Kast who favored the first theory. The magnetic effect was decreased in a marked manner by the slow mechanical rotation of the cylindrical vessel containing the liquid crystal and also by the increase of the number of cycles of an alternating magnetic field. In the liquid crystalline state (117.4° to 134°C) the x-ray diffraction intensity at the principal maximum is 10 percent greater than in the transparent liquid (at 143°C). This is explained by the existence of cybotactic liquid groups in the latter case and the grouping of a large number of these "companies" into the large "regiment" which is responsible for the liquid crystalline phenomena. "A theoretical justification is found in Ornstein's and Oseen's theory of the liquid crystalline condition." The marked optical and the small x-ray difference in the two conditions are thus easily explained. The difference between the liquid crystalline and the transparent liquid condition is thus found to be mechanically not so great as optical observations would indicate. In detail using distances small compared to an optical wave-length the liquid is never isotropic but consists of the cybotactic groups oriented in all positions. The effect of the magnetic field upon the transparent liquid is too small to measure. This is explained by the smallness of the cybotactic groups. The view of the author as to the existence of temporary approximate groups (cybotactic) in the transparent liquid is clearly strengthened by the straightforward interpretation of these experiments.

MAUGUIN[1] seems to have been the first to report the effect of a magnetic field in orientating para-azoxyanisol liquid crystals with the optic axis parallel to the magnetic field.

Hückel[2] obtained the x-ray diffraction halos from several liquid crystals. Since the halos were like the "amorphous" ones in the corresponding isotropic fluids, he rightly objected to the use of the word "crystal" in referring to the former condition.

[1] Mauguin, Comptes Rendus **152,** 1680 (1911).
[2] Hückel, Phys. Zeits. **22,** 561 (1921).

W. Kast[3] experimented with a magnetic field applied normal to an x-ray beam passing through a layer of para-azoxyanisol and observed the alteration produced by the field in the x-ray photographic halo. The intensity was diminished in a direction parallel to the field and increased in a direction perpendicular thereto and to the x-ray beam. Kast interpreted these results, taken while the liquid was in a anisotropic, milky state, 117° to 134°C, as indicating a large permanent magnetic moment occasioned by the orderly grouping of the molecules in large numbers. Kast found, by means of dielectric experiments in a magnetic field and Ornstein's[4] theory, that the value of the permanent magnetic moment of the large molecular groups of para-azosyanisol was that of about 10^5 Bohr magnetons, and was independent of the magnetic field.

The conclusions of Kast and Ornstein have been questioned by Zocher[5] and Jezewski.[6] Also Foex[7] has concluded that the more reasonable explanation of the orientation of this substance in a magnetic field rests in the anisotropic diamagnetism found in the crystal, which by orientation produces a diminution of diamagnetic susceptibility in the liquid crystalline condition. His discussion is given at a later point.

A. Van Wyk[8] studied the orienting influence of the magnetic field, the wall and the mutual interacting effect of the "swarms" of the liquid crystal, para-azoxyanisol. He also found the effect of the magnetic field is in better agreement with the interpretation of anisotropic induced polarization (diamagnetism). Freedericksz and Repiewa[9] also reach the same conclusion. Glamann, Hermann and Krummacher[10] have recently extended the experiments of Kast as to the magnetic effect on the x-ray halos of liquid crystalline para-azoxyanisol adding evidence as to the fixed position of the halos observed with and without the application of the magnetic field.

The purpose of the present experiments was to make quantitative measurements on the effect of the magnetic field in orienting the large groups of molecules in liquid crystalline para-azoxyanisol, to point out the bearing of the data upon the interpretation of the magnetic character of this substance and to compare the liquid crystalline and the transparent liquid conditions of para-azoxyanisol.

The diamagnetic explanation already mentioned is based upon the measurements of susceptibility of para-azoxyanisol by Foex and Royer.[11] At the melting point (at 116°C, according to Beilstein, and 117.4°C according to the

[3] W. Kast, Ann. d. Physik **73,** 145 (1924); Ann. d. Physik **83,** 418 (1927); Verh. d. D. Phys. Gesell. **3,** 8, 2–3 (1927). But see also a contribution which has just appeared, Zeits. f. Kristallographie **79,** 161 (1931).

[4] Ornstein, Ann. d. Physik **74,** 445 (1924).

[5] Zocher, Phys. Zeits. **28,** 790 (1927).

[6] Jezewski, Zeits. f. Physik **52,** 268 (1929).

[7] Foex, J. de Phys. et le Rad. VI, X, 421 (1929).

[8] Van Wyk, Ann. d. Physik **5,** 3, p. 879 (1929).

[9] Freedericksz and Repiewa, Zeits. f. Physik **42,** 532 (1927).

[10] Glamann, Hermann and Krummacher, Zeits. f. Krystallographie **74,** 73 (1930).

[11] Foex and Royer, Comptes Rendus **180,** 1912 (1925).

International Critical Tables) there is a sudden decrease of the diamagnetic susceptibility of about 19 percent. As the temperature is raised there is a small gradual increase of the diamagnetic susceptibility, until at the clearing temperature of the liquid, 134°C, there is a very rapid rise to approximately the value occurring in the crystalline state. By undercooling after melting, the curve for decreasing temperatures is extending to about 90°C. Foex[7] found the susceptibility of para-azoxyanisol in the crystalline state at 15°C and for the three principal axes. The values are -6.65×10^{-7} in the direction of the binary axis, and -6.34×10^{-7} and -4.08×10^{-7} in the plane of symmetry. The mean, which would be the observed value for a pulverized crystal, is -5.69×10^{-7}. The observations on the transparent liquid gave the values -5.60×10^{-7} and on the liquid crystal close to the solidifying point -4.59×10^{-7}. Foex opines that the decrease in the liquid crystalline state is caused by the orientation of the molecules, the low values for the susceptibility in the crystalline state, -4.08×10^{-7}, corresponding to the value for the same orientation of molecules in the liquid crystal, -4.59×10^{-7}. The latter orientation is less perfect because of the higher temperature and greater thermal agitation.

Theory

As just shown, there are two contentions. One that there is a permanent magnetic moment in the liquid crystalline form and one that the arrangement of molecules in the large liquid crystalline groups produces a relatively lower value of diamagnetic susceptibility in one direction. According to the latter proposal, such groups would be oriented in a magnetic field as if possessing an induced magnetization. For the purpose of quantitative comparison with experiment, the theories based on these two assumptions will be derived.

A magnetic particle of permanent moment μ, will have a potential energy, $-\mu H \cos\theta$, in a field H, if θ is the angle between the positive direction of the axis of the doublet and the direction of H. Assume this doublet is associated with (or caused by) a group of molecules oriented with their magnetic axes parallel. If we assume the validity of the Boltzmann distribution law, the number of groups having a potential energy—$\mu H \cos\theta$ is

$$A_1 e^{\mu H \cos\theta / kT} 2\pi \sin\theta d\theta \tag{1}$$

where in $2\pi \sin\theta\, d\theta$ is the solid angle concerned. Now A_1 can easily be found if the total number of groups, N, is known. If $b=\mu H/kT$, the value of A_1 is

$$A_1 = \frac{N}{2\pi}\,\frac{b}{e^b - e^{-b}} = \frac{N}{4\pi}\,\frac{b}{\sin hb}. \tag{2}$$

If $H=0$ the number in the solid angle would be $A_0\, 2\pi \sin\theta\, d\theta$ and since

$$2\pi A_0 \int_{0^\circ}^{180^\circ} \sin\theta d\theta = 4\pi A_0 = N$$

$$A_0 = N/4\pi. \tag{3}$$

The number of groups in the solid angle $2\pi \sin\theta\, d\theta$ when $\theta = 90°$, is, from (1)

$$A_1 2\pi d\theta = \frac{N}{4\pi} \frac{b}{\sin hb} 2\pi d\theta. \tag{4}$$

If now H be made zero, the number of groups in the same solid angle is,

$$A_0 2\pi d\theta = (N/4\pi) 2\pi d\theta. \tag{5}$$

The ratio of the former to the latter, R_1 is

$$R_1 = b/\sin hb. \tag{6}$$

In the case of the second theory described above, it is recalled that the diamagnetic susceptibility produced by an electron orbit is proportional to $(1+\cos^2\theta)$ where θ is the angle between the axis of the orbit and the direction of the magnetic field, H. Thus that part of the moment in the direction H which varies with θ is proportional to $H\cos^2\theta$. In a field H the magnitude of the potential energy produced by such a doublet is $-\alpha H^2 \cos^2\theta$, where α is a constant. In the case of the para-azoxyanisol, the polarization is anisotropic because of the differences in diamagnetism in different directions. The net polarization that is effective in orientation can then be considered as a positive induced moment porportional to $H\cos^2\theta$, having a potential energy in the field H of $-\alpha H^2\cos^2\theta$. The number of groups having this potential energy is

$$A_1 e^{\alpha H^2 \cos^2\theta / kT} 2\pi \sin\theta d\theta \tag{7}$$

A_1 is a constant such that

$$2\pi A_1 \int_{0°}^{90°} e^{\alpha H^2 \cos^2\theta / kT} \sin\theta d\theta \tag{8}$$

$\sin\theta\, d\theta$ = total number of groups = N.

This is an integral of the form

$$\int_1^0 e^{bx^2}(-dx),$$

wherein $b = \alpha H^2/kt$ and $x = \cos\theta$. By expanding the integrand according to Maclaurin's theorem and integrating term by term, the value is found to be

$$\int_1^0 e^{bx^2}(-dx) = 1 + \frac{b}{3} + \frac{b^2}{5\cdot 2!} + \frac{b^3}{7\cdot 3!} + \frac{b^4}{9\cdot 4!} + \frac{b}{11\cdot 5!} + \cdots \frac{b^{n-1}}{(2n-1)(n-1)!} + \frac{b^n e^b}{n!(2n+1)}. \tag{9}$$

The last term is an approximation, being greater than the remainder term obtained from Maclaurin's theorem.

A sufficient approximation to the true value of the integral can be made by using the series up to the nth term n being selected so that the remainder is less than one percent.

This approximate value of the integral will be indicated by I. Then from equation (8) we may write:

$$A_1 = N/2\pi I.$$

The number of groups in the solid angle $2\pi \sin\theta\, d\theta$, $\theta = 90°$, is, according to equation (8) and the foregoing

$$A_1 2\pi d\theta = (N/I)d\theta.$$

With $H = 0$, the number of groups in the same solid angle is as already given in equation (5), except now the integration, as in equation (3), should be from 0° to 90° and the result is, $Nd\theta$. The ratio of the former to the latter number, designated as R_2, is

$$R_2 = 1/I. \tag{10}$$

If, then, x-rays are passed through a layer of para-azoxyanisol placed in a magnetic field having a direction at right angles to the beam, it becomes possible to test the correctness of the ratio in equation (6) or (10). This possibility rests upon the assumptions; (1), that in the anisotropic liquid state we have relatively large semi-orderly molecular groups, (2) that these groups act much like powdered crystals in the diffraction of x-rays (3) that the intensity of x-rays at the chief diffraction angle maximum of the liquid is proportional to the number of groups oriented at the correct angle, and (4) that the distribution of orientation of the groups may be determined by the Boltzmann distribution law.

Apparatus and Method

The x-ray diffraction apparatus was the same as used in a series of liquid experiments,[12] but with the addition of a magnetic field having a direction at right angles to the beam. The angle of diffraction and the relative intensities were measured by moving the ionization chamber about the axis of the spectrometer. Comparison is made at a given angle of diffraction, with and without the magnetic field, This permits quantitative (relative) results without elaborate corrections.

If the axis of the effective magnetic doublet corresponds to the length of the molecules in the structure of a group in the anisotropic liquid, and if the chief diffraction-angle intensity maximum is produced by the separation of molecules in a direction perpendicular to their lengths,[13] then the magnetic field should decrease the intensity of this maximum with the above relation of the angle of diffraction and the direction of the field. This decrease does occur. This orientation is also in agreement with the view of Foex.[14]

The temperatures of the liquid were measured with a thermocouple placed in the liquid and just above the path of the x-rays. The heating was accomp-

[12] See references found in Stewart, Phys. Rev. **35,** 726 (1930).

[13] This was asserted by Kast (reference 3), and is in agreement with all the liquid diffraction measurements by the author of chain compounds.

[14] Foex, reference 7, who states that the large axis of the molecule is in the direction of the diamagnetic susceptibility of the least magnitude.

lished by several hot air blasts impinging in such a manner as to produce the least convection and most uniform temperature throughout.

The effect of the magnetic field on the electron beam of the x-ray tube was eliminated by heavy shielding with iron, the elimination being carried to the point where the effect of the field was smaller than that of the observatorial error of the intensity of the x-rays.

While the magnetic field was not homogenous over the entire cylinder, the derivation therefrom was not sufficient to affect the conclusions.

Experimental Results

1. At a temperature of $128° \pm 2.0°$C the relative intensity of diffraction at the principal maximum is shown in the upper curve in Figure 1, marked

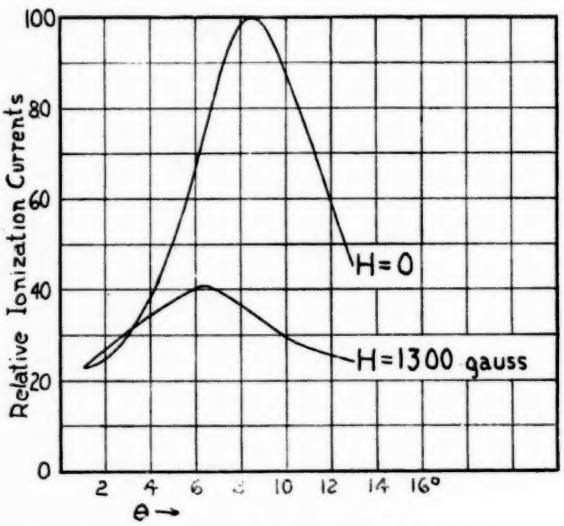

Fig. 1. The influence of the magnetic field at 128°C.

$H = 0$. The cylindrical thin walled glass tube containing the liquid had a diameter of about 1 cm which was less than the optimum thickness of the liquid for the wave-length used, 0.71A. During observation the liquid was not stirred in any manner.

In experiments on chain molecules, the chief diffraction peak is caused[15] by a periodicity that is transverse to the chains. A second peak of much smaller intensity is caused by a longitudinal periodicity. While para-azoxyanisol is not a straight chain molecule, its length is undoubtedly much greater than any other dimension. It is reasonable to assume that the chief peak in Figure 1, is similarly caused by a transverse periodicity, the diffracting "planes" containing the lengths of the molecules. If this be true then the magnetic moment, μ, must be a longitudinal one for this prominent peak disappears under the action of a field which is perpendicular to the x-ray beam and the axis of the spectrometer. As already stated, this choice of dimension agrees

[15] Stewart, Phys. Rev. **35**, 726 (1930) and the literature these cited.

with the results of Kast and of Foex. Figure 2, to be discussed presently, shows that 1300 gauss will produce approximately as great a reduction of this peak as 2200 gauss. Hence, in Figure 1, with 1300 gauss, the number of groups of molecules oriented with lengths perpendicular to the magnetic field and in the spectrometer axis is practically nil. In that case, the residual maximum intensity at 6.4° is clearly caused by different planar separations than the one producing a maximum at 8.4°. The general elevation of the curves is caused by the scattering of the general radiation from the container and from the liquid. In view of the rapid disappearance of the 8.4° peak with increasing field, the doublet orientation is considered complete at 2200 gauss at the x-ray relative intensity shown in Figure 2. This ordinate, 34.5, is taken as the zero value of the 8.4° diffraction intensity produced by the periodicity of separation perpendicular to the axis of the molecules and of the doublet.

2. If the containing tube be rotated, the effect of the magnetic field is

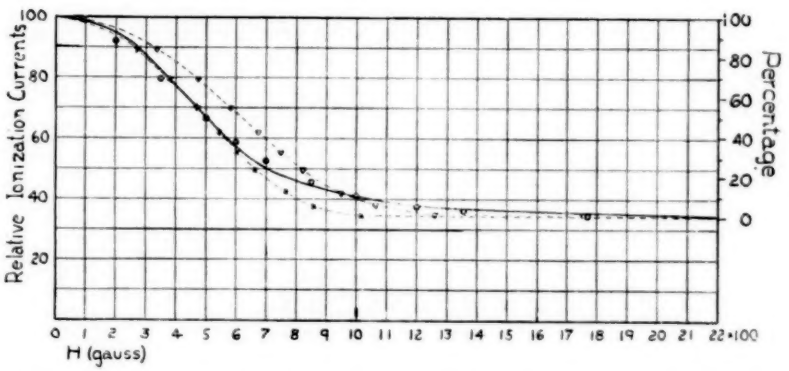

Fig. 2. Comparison of theories and experiment assuming but one size of molecular groups.

very materially altered. When the tube, approximately 1 cm in diameter, is rotated once per second, the effect of the field is reduced to two-thirds. If the rotation is twice per second, only about one-fifth of the effect remains. These results were obtained with a field of 2100 gauss, which, as shown in Figure 2, produced approximately complete orientation of molecules.

3. The diffraction-intensity curve for the transparent liquid at 143°C is practically that shown for the milky liquid at 128°C in Figure 1. But the diffraction intensity of the latter is approximately 10 percent greater throughout the range tested. This indicates greater x-ray coherence in the liquid crystalline condition.

4. The effect of a magnetic field of 2210 gauss upon the chief intensity maximum diffraction, with the transparent liquid at 143°C, and with zero speed of rotation of the sample, was found to be 0.2 percent, an amount less than the error of the experiments.

5. The milky liquid was frozen while in a field of more than 6000 gauss. While in the milky liquid the molecular groups are fully oriented with this magnetic field, yet when frozen there no longer exists any evidence of the effect of the field. This is shown by the fact that the major diffraction peak of

the crystal at 9.25° is the same intensity whether the substance is frozen with or without the presence of the field. On account of chance preferential directions in freezing, this result was derived from the average of ten trials of freezing in the magnetic field.

6. A diffraction intensity curve was made at 122° ± 2.0°C. The intensity at 8.4° was greater at 122°C than at 128°C with $H = 0$, and less with $H = 2100$ gauss. This indicates a difference between the two conditions which should be investigated further but which does not concern the conclusions of this paper, for the diffraction ratio curve for 122°C, with and without the field becomes precisely like that of Figure 1, if allowance is made for a difference in the residual diffraction at 2100 gauss, or in the selection of the observed ratio to be given the value zero.

7. The effect of an alternating field was quite marked. For a given effective current in the electromagnet, making $H = 1100$, the alternations were varied from 18 to 105 cycles. With the former the effect of the magnetic field was 60 percent that obtained with continuous current. With the latter it was 11 percent.

8. The full line curve of Figure 2 is the result of experiments on liquid crystalline para-azoxyanisol at 128°C. The observations of relative ionization [illegible] with the spectrometer at the fixed diffraction angle of 8.4°. With a changing magnetic field this fixed angle would remain the location of the diffraction maximum of the major peak[10] and consequently the observations would give the correct relative values of diffraction intensity. Thus the observations with changing field give the magnitudes of the magnetic effect upon the scattering from the large groups in the liquid crystal condition. This effect is produced by the alteration of the number of groups oriented approximately perpendicular to the field and parallel to the axis of the spectrometer. The percentage of variation of intensity is shown at the right in the figure.

Computed Results

1. Comparison of equations (6) and (10) was made with the experimental data exhibited by the full line curve of Figure 2. The comparison with (6) was obtained by adjusting the value of b at $H = 1000$ gauss to fit the experimental results. At 1000 gauss, the relative intensity is 10.6 percent and this must be equal to $b/\sin hb$. Hence, $b = 4.43$. For this value of b, the values of $b/\sin hb$, or the ratio of intensitives for 200, 350, 500, 600, 700, 850, 1000, 1200, 1355, and 1790 gauss become respectively, 0.880, 0.690, 0.490, 0.376, 0.280, 0.174, 0.106, 0.052, 0.030, and 0.006. These ratios were plotted by the small circles in Figure 2. They agree splendidly with the experimental curve.

2. The third result to be obtained from computations is the value of μ, for, as is clear from Figure 2, the foregoing is decidedly favorable to a permanent moment. At $H = 1000$ gauss, $b = 4.43$. Then since $b = H/kt$, $k = 1.37 \times 10^{-16}$ and $T = 401°$ Abs, $\mu = 24.3 \times 10^{-17}$ or 2.65×10^4 Bohr magnetons. This value of μ is about three times that suggested by Ornstein[4] and also of the same order as claimed by Kast.[3]

3. Similar computations were made from equation (10) except that it is more convenient to make computations for I by assigning values to b. To the latter are given the values of 0.5, 1.0, 1.5, 2.0, 2.5, 3.0, 4.0, 5.0 and 7.0. The The resulting values for the denominator are respectively, 1.19, 1.46, 1.83, 2.36, 3.12, 4.22, 8.21, 17.16, and 86.75 with error in approximation $b^n e^b/n!(2n+1)$ much less than one percent. Comparison of the theoretical variation with the experimental curve was made by assuming the value of H given by the experimental curve for the value of b, 4.00. This value of H is 950 gauss. The other values of H were computed from the variation $b \propto H^2$. The corresponding values of H and the ratio of group numbers, or of intensities, are plotted in Figure 2, with deltas as indicators. A similar curve is also plotted by causing the match of theory and experiment to be at $H = 545$ gauss, $b = 2.0$. The results of comparisons will be discussed later.

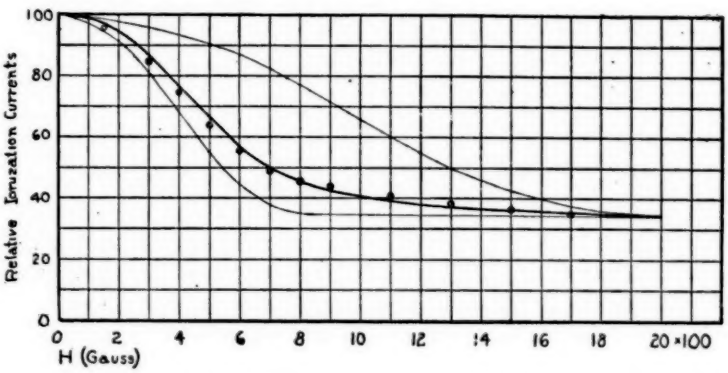

Fig. 3. Comparison of the diamagnetic theory with experiment assuming a mixture of molecular groups of two sizes.

4. But the assumption of groups of oriented molecules that are all alik in size is somewhat unreasonable.[16] Let it be assumed, rather, that there are groups of various sizes and that the theory of anisotropic polarization is to be tested under these circumstances. Fig. 3 shows the original experimental curve and two additional computed curves. The lower one of the latter is plotted with values based upon $b = 2.5$ and $H = 500$ gauss, The upper one with $b = 2.5$ and $H = 1192$ gauss. These adjustments are equivalent to assuming that the group for the lower curve has about 5.7 times the volume of the group belonging to the upper curve. If, using the computed curves of Fig. 3, it be now assumed that the actual groups are a mixture of these two sizes, the ratio of the smaller to the larger being one to three, the number of the larger ones, then the computed resulting relative intensity is represented by the circles, which lie very close to the experimental curve. Obviously the sasumption of these two sizes was made merely to demonstrate the possibility of the theory of the anisotropic polarization satisfying the experimental observations. The results justify the statement that, so far as agreement with experiment is concerned, the induced magnetic moment theory is just as

[16] This point was called to the author's attention by Dr. J. H. Van Vleck.

satisfactory as the one assuming a permanent moment. This will be later discussed.

Discussion and Conclusions

1. In the preceding section on computed results it was shown that the two theories of the magnetic effect had equal sanction so far as these experiments are concerned. But the objection to the permanent magnetic moment theory rests in our general knowledge of magnetism. There are no cases known of permanent moments in organic substances and there is nothing in the magnetic character of the atoms composing the molecule or in the molecular structure that would render the permanent moment theory plausible.

On the other hand, according to the preceding remarks, the decrease in the magnitude of the diamagnetic susceptibility and the induced magnetic moment are fully explained. Now the comparison with experiment in Figure 3, shows agreement of theory and experiment. Consequently, permitting general considerations to decide, it is evident that preference must be given to the theory of anisotropic polarization caused by the orientation of the molecules in groups with their long axes parallel.

2. The similarity of the x-ray diffraction in the milky and transparent condition of the liquid indicates the same cause of intensity distribution in both. But there is 10 percent greater intensity and hence greater x-ray coherence in the former. According to the view of the author presented in a series of papers, the halo in the transparent condition is caused by orderly, unstable molecular groups throughout the liquid. This condition is called "cybotaxis" to distinguish clearly from the orderly grouping in a crystal. These groups do not cause optical anisotropy because they are too small. But they do show structural anisotropy to x-rays in that the separation of planes is not the same in different directions in a group. The optically anisotropic clusters or major groups found in a liquid crystal, are produced by the association in approximate alignment of a number of the cybotactic or "minor" groups such as exist in the transparent state. This increase in size of minor to major groups does not greatly increase the diffraction intensity for the x-rays (10 percent), since the minor groups, although having a general alignment within the major group, producing optical anisotropy, are not sufficiently well aligned with each other to produce coherent x-ray diffraction as in a crystal. This readily explains the difference between the optical and x-ray effects. Here is, then, the picture of the difference between the transparent liquid and the liquid crystal. The cybotactic groups in the liquid form have approximate alignment in the liquid crystal. The aggregation progresses from a little companies to a large regiment.

A recent* discussion of liquid crystals has focussed new attention upon the theory underlying this state of a fluid. Both Ornstein and Oseen** have discussed the kinetic basis of the "swarm" hypothesis. Ornstein's theory may perhaps be more appropriately called a "bundle" hypothesis because it deals

* No. 79, Zeitschrift für Kristallographie, (1931).

** Ornstein, Zeits. f. Kristall, **79,** 90 (1931); Oseen, Zeits. f. Kristall, **79,** 173 (1931).

with groups of molecules having similar orientations rather than similar velocities, Ornstein assumes a molecule with a long axis of symmetry, a potential energy of a molecule proportional to the cosine of the angle between the axes of two molecules and to a function of the relative positions of the two molecules. He develops a "correlation" function, derives a differential equation and gives a solution of this function. From this he obtains the mean value of the radius of a swarm or bundle. It proves to be $r^2 = G^2/[6(kT - F)]$ where k is the Boltzmann constant and T is the temperature. The change with temperature is not a gradual one for there is a temperature below which the formation of the swarm cannot occur. Ornstein does not set forth the theory as complete or adequate. He merely shows that if there is a couple exerted by one molecule upon another, an alignment of molecules and abrupt changes in the extent of this alignment are possible.

Ornstein's discussion by its application to the formation of our cybotactic groups, emphasizes the possibility of these small groups of aligned molecules. That this alignment produces a periodicity, which is essential to the x-ray diffraction effects is fairly clear from a consideration of the high compressibility of the liquid. The distance of separation perpendicularly to the molecular axes in the immediate neighborhood of a point must be approximately the same. The alignment gives an approximately orderly space array producing coherence in scattering in directions normal to the molecular axes. Also, it is clear that a theory similar to Ornstein's is applicable to the formation of the liquid crystal groups from the cybotactic ones. The quantitative x-ray diffraction similarity for the large and the small group shows this to be the case. Moreover, the effect of the magnetic field in almost completely removing the diffraction intensity peak, as described above, shows that the cybotactic groups capable of producing this peak, are practically all included in liquid crystal groups and the intertices between the latter are chiefly the unaligned molecules. It is evident, then, that the view expressed in this paper is consistent with both experimental results and theoretical considerations.

3. The negative results of the impressed magnetic field on the diffraction intensity distribution of the transparent liquid are explained by the smallness of the cybotactic molecular groups.

4. The inability to produce an effect of the magnetic field during the formation of the crystal structure is in harmony with the current conception that the molecules solidify one at a time. But attention should be called to the experience of both Kast and Foex who have found that they could, by freezing, under certain conditions, produce the solid with the same diagmagnetic susceptibility as in the liquid crystalline state.

5. The results of this paper are in harmony with the views of other workers as to the relatively large orderly groups of molecules in the milky state. When these groups are of sufficient magnitude, optical anisotropy appears.

6. A very mild stirring rotation of the container of the milky para-azoxyanisol is sufficient to diminish greatly the orientation of the large groups by the magnetic field. This means that the effect of the rotation is comparable to that of temperature.

7. The results of the experiments are in harmony with the view that in liquids, more especially with molecules not possessing spherical symmetry, there exist groups of molecules with internal regularity sufficient to produce distinct coherence with x-ray diffraction. For the diffraction x-ray intensity curve is practically the same in the milky and transparent conditions and in both cases the principal maximum occurs at nearly the same angle as does the most intense lines of the crystal diffraction curve. The existence of a more extensive molecular orientation in a liquid crystal is evidenced by optical anisotropy. Just as certainly the x-ray diffraction in the transparent liquid indicates the existence of the much smaller cybotactic groups.

8. This x-ray diffraction study was not extended to include the angular range used by Glamann, Hermann and Krummacher. Also, the observations were confined to one orientation of magnetic field and axis of the spectrometer. But the conclusions are not vitiated by these limitations as considerations easily show.

MEASUREMENTS ON THE VAPOR STREAM FROM THE CATHODE OF A VACUUM ARC

By W. E. Berkey and R. C. Mason
Research Laboratories, Westinghouse Electric and Mfg. Co.

(Received July 13, 1931)

Abstract

The velocity of the vapor stream issuing from the cathode region of a vacuum arc between copper electrodes is calculated from (1) the energy received by a vane 3 cm in front of the cathode, as measured by the rate of rise of temperature; (2) the momentum imparted to the vane, as determined by the deflection of the vane. The mass used in the calculations is that of the copper deposited on the vane. The average velocity of the vapor, computed from data obtained by either method, is about 2×10^6 cm per second, confirming Tanberg's momentum measurements. There is some evidence that the vapor is ionized to a considerable degree. Radiation from the arc, or energy of recombination on the vane, can account for only a small part of the total energy received by the vane.

Introduction

TANBERG[1] has calculated the velocity of copper vapor issuing from the copper cathode of a vacuum arc to be over 10^6 cm/sec. The velocity was obtained from measurements of the momentum imparted to (1) the cathode, (2) a vane suspended in front of the cathode. Kobel[2] measured the force of reaction upon the cathode of a mercury arc, from which he calculated a vapor speed of over 10^6 cm/sec. Compton[3] sought to explain the force on the cathode measured by Tanberg with the hypothesis of an accomodation coefficient for the neutralized positive ions. Actually, Compton's calculations substitute a low velocity vapor stream (less than 10^5 cm/sec.) for the high velocity vapor stream of Tanberg. It does not seem that Compton's explanation can apply at the vane.[4]

The results of Tanberg and Kobel are based on momentum measurements involving a mass lifted against gravitational force. It seemed desirable to make an attempt to determine the vapor velocity by measuring the kinetic energy of the vapor stream.

Apparatus

Figure 1 shows a sketch of the apparatus used. Copper electrodes were mounted in a glass desiccator. A flexible coupling allowed the cathode to be brought in contact with the anode to strike an arc. A quartz cylinder surrounding the copper rod cathode, restricted the cathode spot to the end of the 0.55 cm diameter rod

[1] R. Tanberg, Phys. Rev. **35,** 1080 (1930).
[2] E. Kobel, Phys. Rev. **36,** 1636 (1930).
[3] K. T. Compton, Phys. Rev. **36,** 706 (1930).
[4] J. Slepian and R. C. Mason, Phys. Rev. **37,** 779 (1931).

A silver vane 2.5 cm square and about 0.25 mm thick, was suspended 3 cm directly in front of the cathode by a silk thread. Below the vane, a scale was mounted which allowed the deflection of the vane to be observed. A 36 gauge copper-advance thermocuple was soldered to the center of the vane on

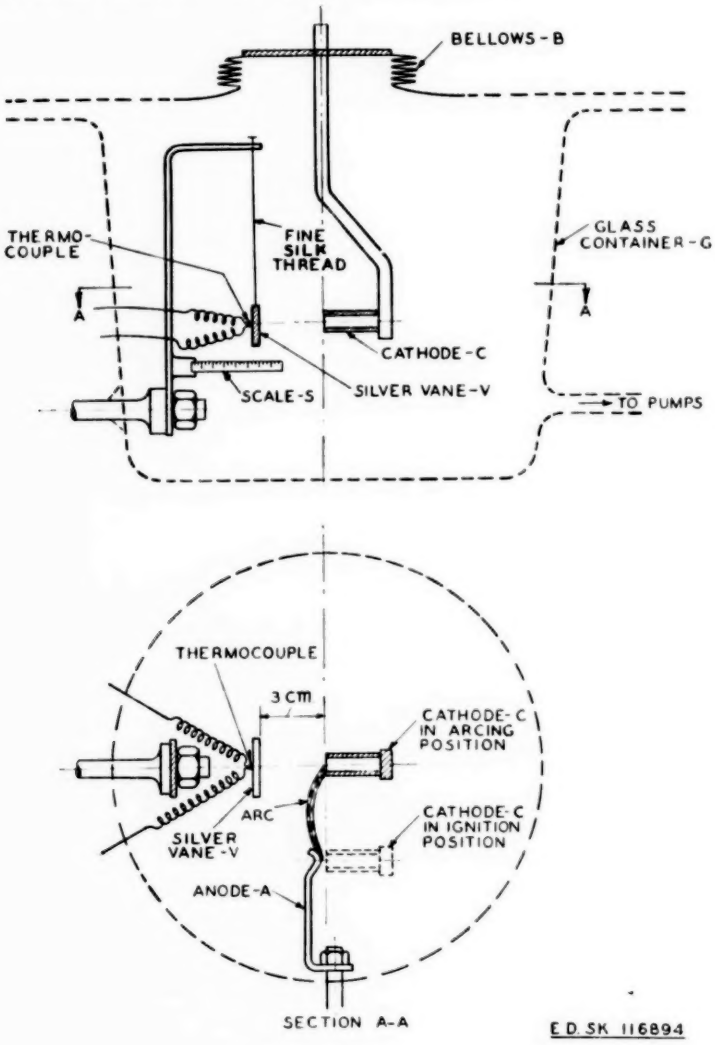

Fig. 1. Apparatus for measurements on cathode vapor stream.

the side facing away from the cathode. The thermocouple leads were coiled so as to offer the least resistance to motion of the vane. A milli-voltmeter was calibrated to give the temperature of the vane in degrees centigrade.

Procedure

With a gas pressure of about 6×10^{-4} mm, an arc was struck and run for a few seconds. During a test the pressure would rise to 20 or 30×10^{-3} mm.

The time of arcing was noted on a stop watch. Readings of the milli-voltmeter were taken at short intervals timed by a second stop watch started upon the ignition of the arc. The deflection of the vane while the arc was running was determined as closely as possible with the eye.

The vane was weighed before and after a series of tests; the mass of the copper deposit was determined from the difference in weights. A check was furnished by removing the copper deposit, and reweighing the vane. The data for a typical test are shown in Table I.

TABLE I. *Data for a typical test.*

Arc current	18.5 amps.
Arc voltage	30 volts
Circuit voltage	220 volts d.c.
Deflection of vane	0.2 cm
Length of vane to support	10 cm
Weight of vane and thermocouple	1.8595 grams
Time of arcing	14.8 seconds
Pressure before test	4×10^{-4} mm
Distance cathode to anode	2 cm
Distance cathode to vane	3 cm
Temperature of cold junction	24°C
Maximum temperature rise of vane extrapolated from cooling curve	163°C

The temperature of the vane reached a maximum a few seconds after the arc was extinguished, and then gradually decreased. The cooling curve was plotted and the temperature of the vane at the end of the arcing period was determined by extrapolation. This temperature and the time of arcing gave the rate of rise of temperature; then from the thermal capacity of the vane, the rate of energy input to the vane was calculated. The rate of cooling was so slow that the vane lost no appreciable energy during the period of arcing.

From the deflection of the vane, the length of support, and the mass of the vane, the force acting on the vane could be found at once.

The mass of copper deposited on the vane per second was determined by averaging the total mass over the sum of times of the individual tests.

An estimate of the amount of radiation absorbed by the vane was based upon a separate experiment. A glass container shielded a blackened silver vane from direct contact with the cathode vapor. The rate of rise of vane temperature when the arc was running gave the energy absorbed by the vane By use of two thicknesses of glass, the absorption by the glass was eliminated, and the total radiation determined. At a distance of 3 cm from the cathode, the radiation amounted to 1.76×10^{6} ergs/cm^2·sec. Since in the vapor velocity experiment a polished silver vane was used, 30 percent of the above radiated energy is probably an upper limit to the radiant energy absorbed. Consequently, a total energy of 0.34×10^{7} ergs/sec is subtracted from the calculated energy input to the vane.

RESULTS

The results of several tests are given in Table II. Column 2 shows the energy input to the vane calculated from thermocouple readings, while in

TABLE II. *Mean velocities of vapor stream from cathode.*

(1) Trial	(2) Measured energy input to vane (ergs/sec)	(3) Corrected energy input to vane (ergs/sec)	(4) Force on vane (dynes)	(5) Avg. mass of copper deposited on vane (gr/sec)	(6) R.M.S. velocity calculated from (3) and (5) (cm/sec)	(7) Mean velocity calculated from (4) and (5) (cm/sec)	(8) Mass calculated from (3) and (4) (gr/sec)
I-1	7.6×10^7	7.26×10^7	—	2.38×10^{-5}	2.46×10^6	—	—
II-1	4.98	4.64	—	2.38	1.98	—	—
II-2	3.93	3.59	53.0 to 70.5	2.38	1.74	2.23 to 2.96 $\times10^6$	3.9 to 6.9 $\times10^{-5}$
II-4	—	—	70.5	2.38	—	2.96×10^6	—
II-5	—	—	70.5 to 88.2	2.38	—	2.96 to 3.7 $\times10^6$	—
III-1	—	—	53.6	2.22	—	2.41×10^6	—
III-2	4.7	4.36	35.8	2.22	1.98	1.62×10^6	1.47×10^{-5}

column 3 the correction for radiation received by the vane has been made. The force on the vane calculated from the observed deflection of the vane is given in column 4. The mass of copper deposited, averaged over several tests, is shown in column 5.

From the mass of copper deposited and the energy input, the r.m.s. velocity of the copper vapor was determined, as given in column 6. The mean velocity of the vapor as calculated from the mass of copper and the observed force is listed in column 7. From the force and energy imparted to the vane, the mass taking part in the reaction can be calculated from

$$\text{Mass} = \frac{\beta^2 (\text{Force})^2}{2(\text{Energy})}$$

where β is the ratio of r.m.s. to mean velocity. For comparison with the mass determined by weighing, the mass of copper calculated on this basis with $\beta = 1$, is given in column 8. The calculated mass, while not checking closely, agrees fairly well with the weighed mass.

The values of r.m.s. velocity calculated from the energy input show close agreement from test to test. The mean velocity calculated from the force shows greater variation than the r.m.s. velocity, but still is of the same order of magnitude. In cases where the deflection could not be determined exactly, upper and lower limits are given for the deflecting force.

The arc did not remain stationary, but wandered about over the small exposed cathode face. When the arc reached the edge of the cathode rod, the space relation of the cathode spot to the vane was changed. This caused variations in the rate of copper deposit and in the vane deflection from test to test. Because of the smallness of vane deflections, the distance from scale to eye and the uncertain retarding force of the coiled thermocouple leads, the force on the vane could not be determined with very great accuracy. More dependence can be placed on the energy measurements. The average of four tests of energy measurements give a velocity of 2.04×10^6 cm/sec.

POTENTIAL ON VANE

There is some indication that the vapor striking the vane is ionized to a considerable degree. An increasing negative voltage was placed on the vane but up to 150 volts, no true saturation current was obtained, At this value,

the current collected was almost as large as would exist if all the copper condensing on the vane were ionized. A positive voltage on the vane gave an increasing electron current. It was not possible to make the vane more than about 30 volts positive with respect to the cathode because of the unlimited current which could be drawn. Hence considerable doubt is thrown on Tanberg's statement of placing 60 volts positive on the vane and consequently on his conclusion that the vapor striking the vane is unionized.

Even if all the copper condensed on the vane came as singly charged copper ions, the energy of recombination would amount to only 0.276×10^{7} ergs/sec, which is less than 10 percent of the total energy received by the vane; so the results given above would not be greatly changed.

It is difficult to devise a mechanism for acquiring such velocities. Tanberg and Berkey[5] have shown that the cathode metal cannot be at a temperature sufficient to account for the vapor speed. Consequently, the vapor stream must acquire its velocity elsewhere in the cathode region.

[5] Tanberg and Berkey, Phys. Rev. **38**, 296 (1931).

ELECTRODELESS DISCHARGE: METHOD OF MEASURING INDUCED CURRENT, VARIATION OF CURRENT WITH PRESSURE FOR VARIOUS GASES

By Charles T. Knipp and Julian K. Knipp
Department of Physics, University of Illinois

(Received July 20, 1931)

Abstract

A special discharge tube has been designed which lends itself readily to the measurement of the *induced gaseous current in the electrodeless discharge*. This apparatus consists of a reentrant tube which describes a circle in the plane of the exciting coil and then goes out and describes a circle perpendicular to the plane of the exciting coil. Thus when a gaseous current is induced in the tube within the exciting coil it must pass through the outside turn before returning and completing the circuit. By placing a conductor of low resistance around the outside turn and connecting it to a radio-frequency ammeter, an induced current in it can be read off which is proportional to the induced gaseous current. This specially constructed tube was connected to an exhaust pump and a McLeod gauge, also to a system of connecting tubes for supplying different gases. The energy to the exciting coil was supplied by a highly damped high-frequency high-voltage source of constant strength, and pressure-current characteristics were obtained for six gases, namely, hydrogen, helium, nitrogen, oxygen, neon, and argon. Relative to these it was found that the induced gaseous current rose to the highest value in oxygen at a pressure of about 0.06 mm Hg; that the maxima in argon and neon were about the same, though for argon the maximum was sharp while for neon it was quite broad, the corresponding pressures being 0.05 and 0.2 mm Hg respectively; that helium and nitrogen were very similar to argon and neon in their behavior but rose to lesser current values with their maxima at about 0.035 mm; and that hydrogen proved to be the most critical of the gases studied, the pressure range was small (between 0.04 and 0.08 mm) and the maximum current 2.4 amperes, which latter is about one fourth that for oxygen. In none of the gases studied did the ammeter show even the slightest current except when there was a "bright glow" indicating that the intensity of the glow is qualitatively a measure of the current induced.

Introduction

THE existence of two types of electrodeless discharge and their main differences in origin have been quite definitely determined.[1] The "dull glow" discharge has been shown[2,3,4,5] to be due to the strong electric field set up by the difference of potential that exists between the ends of the exciting coil. However the "ring" or "bright glow" discharge described by J. J. Thomson[6] has been shown[4,5] to be maintained electromagnetically. In this case the discharge is due, as is well known, to an alternating e.m.f. induced round the

[1] K. A. MacKinnon, Phil. Mag. **8,** 605 (1929).
[2] Townsend and Donaldson, Phil. Mag. **5,** 178 (1928).
[3] C. J. Brasefield, Phys. Rev. **35,** 1073 (1930); **37,** 82 (1931).
[4] C. T. Knipp, Phys. Rev. **37,** 756 (1931).
[5] Smith, Lynch, and Hilberry, Phys. Rev. **37,** 1091 (1931).
[6] J. J. Thomson, Phil. Mag. **32,** 321, 450 (1891); **4,** 1128 (1927).

periphery of the tube by the rapidly changing magnetic field within the coil. The shield experiments of Smith, Lynch, and Hilberry have shown the dependence of the starting of the "bright glow" on the "dull glow" or some ionizing agent. Thomson considered only the "ring" discharge; while Townsend and Donaldson, and Brasefield worked only with the "dull glow" discharge. MacKinnon, Knipp, and Smith, Lynch, and Hilberry have worked with both phenomena.

In this paper we are considering the current induced in the "ring" or "bright glow" discharge. The experiment of Thomson with two bulbs, one inside the other, in which the discharge in the outer bulb shields the inner gas from the inductive effect of the exciting coil, indicates that the gaseous current rises to a high value comparable with the current in the exciting coil. Again, the fact that the current in the exciting coil drops off considerably when the "ring" discharge gets fully under way, conditioned by the pressure

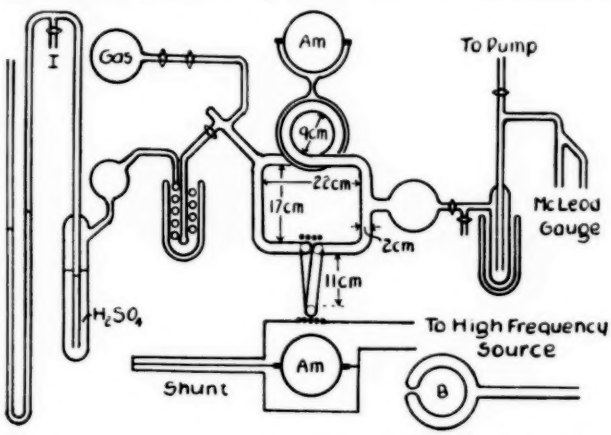

Fig. 1. Sketch of special reentrant electrodeless discharge tube with connections. The approximate dimensions are given. The planes of the two glass circles are at right angles to each other, thus the inductive effect of the energizing coil of four turns on the upper ammeter circuit is eliminated.

in the tube, shows also that the induced gaseous current rises to a high value, i.e., that a strong opposing e.m.f. is induced in the gas in the tube.

Apparatus and Procedure

A diagram of the complete set-up is shown in Fig. 1, and a photograph of the tube used, with the electrodeless discharge passing through it, is shown in Fig. 2. The discharge tube consists of a reentrant tube 2 cm in diameter which describes a discontinuous circle just inside the exciting coil (their planes being parallel to each other and perpendicular to the paper) and then leaves the coil and describes one turn in plane perpendicular to that of the exciting coil (i.e., in the plane of the paper). The total length of the discharge tube is about 155 cm. A heavy copper braid makes one turn round the upper circle of the glass tube and is connected to a Weston radio-frequency ammeter. The discharge tube is shown connected to a 500 cc expansion bulb and on through a liquid-air trap to a McLeod gauge and a mercury vapor pump. Gases are

let in from the other side. Small gas samples in bulbs were connected as shown, while gases in tanks under pressure were let in through the intake I and allowed to bubble through sulphuric acid and a liquid-air trap before entering the discharge system.

As an energy source a motor-generator high-voltage high-frequency set was used, operating at a frequency of about 600 kc. The oscillations were highly damped. The energizing coil used was of 4 turns of copper tubing. Another ammeter is shown connected in a non-inductive shunt for determining the heavy current passing through the energizing coil. Currents as high as

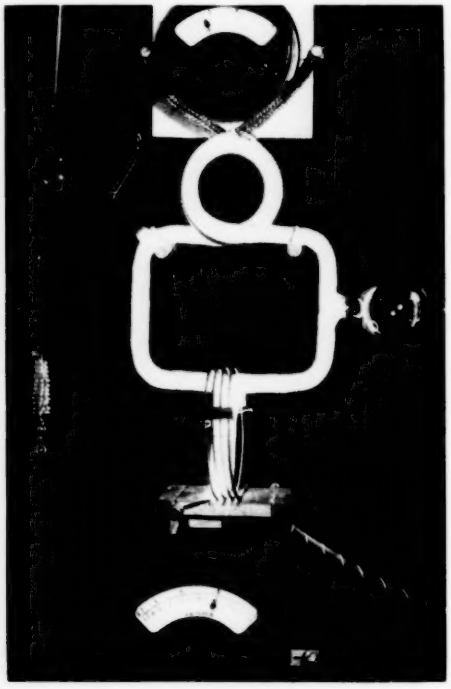

Fig. 2. Photograph of the reentrant electrodeless discharge completely formed by using an energizing coil of four turns. Residual air, pressure about 0.2 mm Hg. Illumination very intense. Time of exposure 6 seconds, followed by a photo-flash to get the apparatus. The energizing current through shunted ammeter shows 8 amperes, while the upper ammeter shows the induced current, due to the gaseous current acting as primary, as 2.6 amperes. The discharge does not enter the expansion chamber.

60 amperes were used. The photograph, Fig. 2, shows the actual deflection of each of the two ammeters as the discharge was passing.

The general procedure with each gas was to pump the system out to a very high vacuum and then wash it out successively with doses of the gas to be studied. After we were sure of the purity of the gas the system was pumped until a stage was reached at which the discharge would just begin (intermittently) to pass, whereupon the pump was shut off. Equilibrium in pressure throughout the system was soon reached after which the coil was again energized and allowed to continue until the two ammeter readings became

steady. The pressure was read before and after the current reading. The system was then exhausted to a new pressure and the readings repeated. As the induced gaseous current increased (as indicated by the ammeter at the top) the current in the energizing coil was observed to decrease, but the frequency remained constant, therefore it was necessary to correct each reading to correspond to a constant energizing current. Following this procedure data for a number of curves were taken for each gas until we were able to reproduce the curves within the errors of observation.

The coupling factor of the upper turn of the discharge tube with the copper braid was investigated by substituting a similar tube filled with about 40 small insulated copper wires with their ends soldered together. It was thought that the wires thus placed would approach the distribution of the gaseous current through the tube. On sending known currents through this improvised primary the coupling ratio, which proved to be strictly linear, was

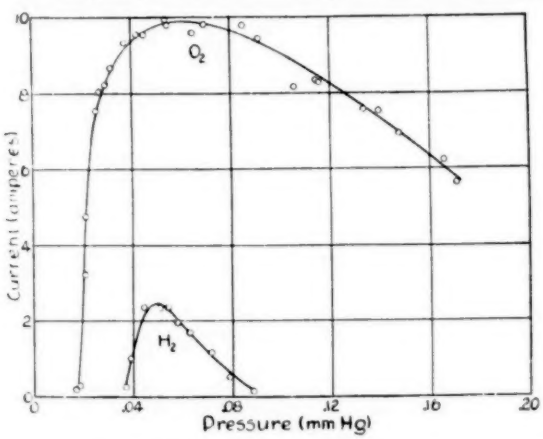

Fig. 3. Currents in the electrodeless discharge in oxygen and hydrogen as a function of the pressure. Exciting current 57 amperes.

found to be 2.84. The resistance of the secondary circuit including the ammeter was 0.033 ohm.

Experimental Results, Pressure-Current Curves

The curves shown are all corrected to a constant exciting current of 57 amperes. The ordinates are the values of the actual gaseous current flowing, obtained by the formula

$$I_p = 2.84 \times I_s.$$

Fig. 3 shows the pressure-current curves that were obtained for hydrogen and oxygen. Hydrogen was found to have the narrowest interval of excitation of any of the gases studied, and the maximum current for this gas was also found to be much smaller than that for any of the other gases, however this maximum was sharply defined. On the other hand the maximum current for oxygen was the largest that we observed for any of the gases. It was broad and its value nearly four times the maximum for hydrogen. Strange enough

these two maxima occurred at nearly the same pressure. The oxygen curve that was obtained was unique in that at the high pressure end it started off very suddenly at a pressure of about 0.172 mm Hg and with an initial current of nearly 6 amperes. At slightly greater pressures the luminous discharge suddenly ceased, the current having dropped to zero.

In general the two points at which any of the curves meet the pressure axis are points at which 57 amperes was the starting current for the "bright glow" for the given gas in this particular tube. It is proposed to use this apparatus for the study of the variation of the induced current with exciting current at constant pressure, to see whether the induced current reaches a saturation value as in the analogous case of the ordinary discharge tube with electrodes.

In Fig. 4 are shown the curves for argon and neon. Both rise to about the same current maxima which is about two amperes less than that for oxygen,

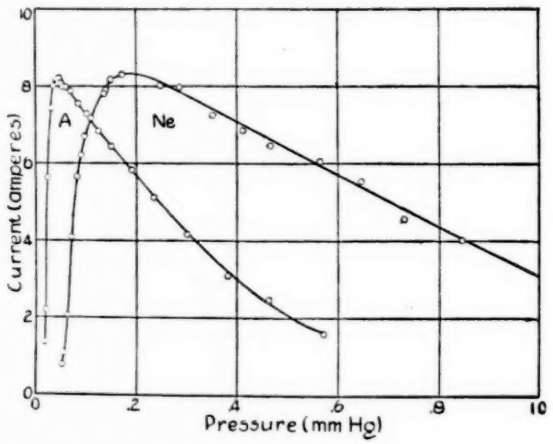

Fig. 4. Currents in the electrodeless discharge in argon and neon as a function of pressure. Exciting current 57 amperes.

however the pressure range is much greater for these two gases, that of neon being particularly large. Note that the maxima come at widely different pressures. To make the comparison with the other gases easier the maxima of these two gases are drawn to the same scale in Fig. 5. The current for neon dropped off to low values long before any of the other gases reached their maxima.

The curves obtained for nitrogen and helium are shown in Fig. 6. They are very similar to each other and in pressure range are similar to hydrogen though their current maxima are each about 2.5 times greater.

Table I gives the value of the maximum current for each gas, the pressure at the maximum, and the approximate pressure range of the "bright glow" discharge. The values tabulated are only useful as a means of comparing the gases since the actual currents and pressures depend on the size and shape of the tube, and on the nature of the source.

Additional interesting points are: Thomson early showed that the dis-

TABLE I. *Maximum current, gas pressure at maximum and pressure range in the electrodeless glow discharge in various gases. Exciting current 57 amp.*

Gas	Maximum current	Corresponding pressure	Pressure range of "bright glow"
Oxygen	9.9 amp.	0.060 mm Hg	0.020–0.172
Hydrogen	2.4	0.052	0.036–0.090
Argon	8.3	0.042	0.020–0.60
Neon	8.4	0.190	0.040–1.00
Nitrogen	5.54	0.032	0.018–0.090
Helium	5.8	0.033	0.017–0.10

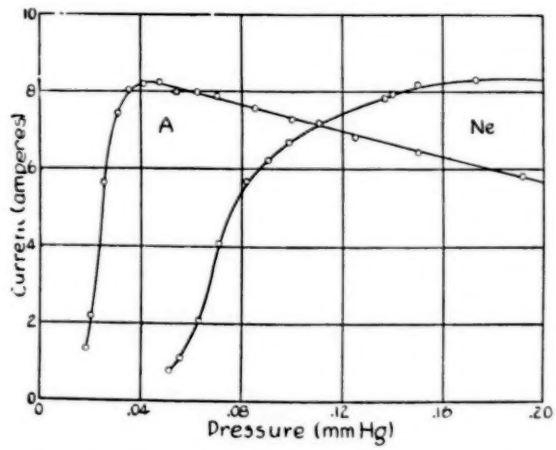

Fig. 5. Same as Fig. 4 except plotted to the same pressure scale as in Fig. 3.

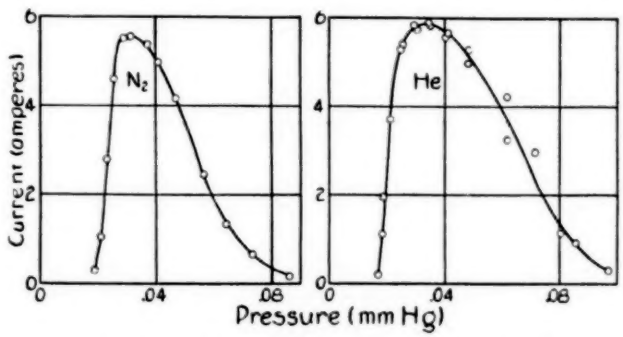

Fig. 6. Currents in the electrodeless discharge in nitrogen and helium as a function of pressure. Exciting current 57 amperes.

charge would pass only when the tube formed a closed path, i.e., when it was reentrant. This observation was confirmed by the use of a non-reentrant tube *B*, Fig. 1. When this tube and the long sinuous one were connected to the system so that each had the same pressure it was observed that a brilliant discharge passed through the reentrant one, but not, in turn, through *B*. The conditions for no current in the former may be approached by increasing its gas and inductive resistance, i.e., increasing its length. Thus the ease with which the induced gaseous current passes is inversely proportional to the

length of the reentrant tube, and directly as the cross-sectional area. Hence reentrant tubes of this design should be of short length.

The character of the discharge as the exhaustion proceeded presented an interesting sequence. It began gradually by a succession of flashes that went all the way round the discharge tube. These became more frequent and more luminous as the pressure decreased, finally filling the entire circuit with a brilliant glow. As the exhaustion proceeded the brilliancy reached a maximum and began to fall off, slowly at first, then rapidly dropped to an occasional flash confined to the lower turn of the tube, in sharp contrast to the flashes that went all the way round at the beginning. It should also be mentioned that at no time was there any indication of a current in the upper ammeter except when a luminous discharge was observed. This indicates quite clearly, as was expected, that no current passed when the "dull glow" alone was observed in the tube.

Again, the discharge, even at its greatest brilliancy did not overflow into the expansion chamber or into the gas supply branch as may be seen by inspecting Fig. 2. Also at no time in the process of exhaustion, even in the case of nitrogen, was there any marked indication of an after-glow, which in itself is an indication of the purity of the gases studied. When the maximum induced gaseous current was allowed to pass for 4 to 8 seconds the reentrant tube warmed up quite preceptably throughout its length. When the upper ammeter was replaced by a 3 cm length of No. 30 nichrome wire it could readily be fused by the inductive effect of the gaseous current.

The oscillatory electrons do not show centrifugal tendencies at sharp bends and corners. A neon bulb previously sealed off at its most sensitive pressure will light up if inserted in the upper gaseous circle.

LIFE OF METASTABLE MERCURY AND EVIDENCE FOR A LONG-LIVED METASTABLE VIBRATING NITROGEN MOLECULE

By M. L. Pool
Mendenhall Laboratory of Physics, Ohio State University

(Received July 20, 1931)

Abstract

Curves showing the rate of decay of the metastable 2^3P_0 state of mercury atom in a quartz resonance cell, containing carefully purified nitrogen at room temperature, are not accurately exponential. The rate of decay in the neighborhood of 4×10^{-4} sec. after termination of the optical excitation, is more rapid than later. A high concentration of nitrogen molecules excited to the first and second vibrational states of the zero electronic state might be expected, due to collisions of the second kind between normal nitrogen molecules and mercury atoms in the 2^3P_1 or 2^3P_2 states. It is assumed that in addition to diffusion and dissipative impacts with unexcited nitrogen, the decay of the number of metastable mercury atoms may be influenced by dissipative impacts with these excited nitrogen molecules whose number decreases with time by diffusion and by dissipative impacts. An equation for the number of metastable mercury atoms is then obtained of the form $N=N_0\exp\left[-\alpha t+A(\epsilon^{-\beta t}-1)\right]$. Evaluation of the constants from experimental data gives the following: For excited vibrating metastable nitrogen molecule, maximum observed life 0.52×10^{-3} sec.; natural life, infinite; distance between centers at impact, 0.85×10^{-8} cm; probability of dissipative impact, 80×10^{-6}; diffusion coefficient 2.4 $g\cdot cm^{-2}\cdot sec^{-1}\cdot dyne^{-1}$. For the metastable mercury atom, maximum observed life, 2.54×10^{-3} sec.; natural life, infinite; distance between centers at impact, 3.2×10^{-8} cm; probability of dissipative impact, 3.3×10^{-6}; diffusion coefficient, 0.129 $g\cdot cm^{-2}\cdot sec.^{-1}\cdot dyne^{-1}$.

CERTAIN experiments on mercury fluorescence radiation with admixtures of hydrogen and nitrogen,[1] also iodine fluorescence radiation with admixture of helium,[2] and experiments on electron impacts in nitrogen,[3] have been interpreted[4] by assuming a strong persistence of molecular rotational and vibrational states in collisions. A recent treatment by Zener[5] based upon wave mechanics, of the interchange in internal energy of molecules during a collision has strengthened this contention that vibrational and rotational quantum numbers may have a marked reluctance to change. Furthermore, vibrational levels of the normal state of symmetrical molecules are strictly metastable. It was thought, therefore, that if the nitrogen molecule really persisted in a vibrational state for a long length of time, its influence upon the life of the metastable mercury atom might be detected experimentally, and an actual estimate of the life of the vibrating nitrogen molecule made.

[1] E. Gaviola and R. W. Wood, Phil. Mag. **6,** 1191 (1928).
[2] J. Franck and R. W. Wood, Verh. d. D. phys. Ges. **13,** 78 (1911).
[3] W. Harries, Zeits. f. Physik **42,** 26 (1927).
[4] O. Oldenberg, Phys. Rev. **37,** 194 (1931).
[5] C. Zener, Phys. Rev. **37,** 556 (1931).

The life of the metastable mercury atom has been measured by various methods, but the method of interrupted optical excitation[6,7] seems to be the most simple and direct. This method as has been previously used indicates that the concentration of metastable atoms decays approximately exponentially with time. It is the purpose of this paper to show that the decay is found to be not accurately exponential when very pure nitrogen is used and great care is taken in the photometric measurements and that the departure from the exponential may be attributed to the persistence of the nitrogen molecule in excited vibrational states.

Apparatus and Method

Mercury vapor at the saturation pressure corresponding to 21°C and contained in a quartz resonance cell with various pressures of admixed nitrogen

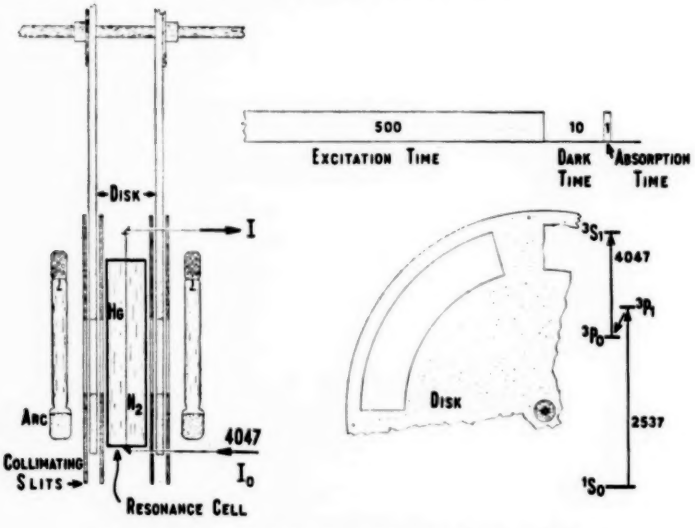

Fig. 1. Apparatus for intermittent optical excitation.

was excited optically by the total radiation from two 110 volt d. c. "Uviarc" quartz mercury arcs. The arcs were water cooled and the discharge pressed against the side of the quartz tube by a magnetic field. A strong air blast was also directed toward the anode of each arc. The position of the resonance cell with respect to the arcs is shown in Fig. 1. It is quite desirable to use two arcs for excitation instead of one, because in later considerations one wishes to assume a uniform concentration of metastable atoms in the resonance cell. But with only one arc it is not possible to get such a concentration, since the absorption coefficient[8] for the 2537 line in mercury vapor is approximately 3×10^{-14}; and therefore the greater number of metastable atoms would be produced within a few millimeters of the wall of the cell. This gradient in the

[6] T. Asada, Physik Zeits. **29,** 549 (1928).
[7] M. L. Pool, Phys. Rev. **33,** 22 (1929).
[8] A. L. Hughes and A. R. Thomas, Phys. Rev. **30,** 466 (1927).

concentration of metastable mercury atoms along a diameter of the cell was noted by Wood[9] and roughly measured by Gaviola[10] in order to get an estimate of the life of the metastable state. However, with two arcs, one placed on either side of the resonance cell, there exists an overlapping of two gradients, giving in the center of the cell a region of comparatively uniform concentration.

The optical excitation of the resonance cell was interrupted by means of two disks, 50.4 cm in diameter and separated from each other by 3.5 cm. Between the disks was situated the resonance cell, 2.15 cm internal diameter and 12.4 cm long. In each disk were cut four sectors of such length that it was possible to excite the resonance cell 70 percent of the time per revolution of the disk. Collimating slits 1×55 mm were placed between the arcs and the resonance cell so that only 5.5 cm of the central portion of the cell would be excited and so that the excitation time would be sharply terminated whenever an opaque portion of the disk came between the arcs and resonance cell.

After the termination of the excitation period the cell remained dark for a short time until two one millimeter holes near the periphery of the disk came opposite two stationary ones. Then a flash of light from a glass 110 d. c. mercury arc, water cooled and magnetically deflected, passed longitudinally through the center of the resonance cell. Five small right angle prisms were used in directing this flash of light from one of the millimeter holes near the periphery through the resonance cell, and then through the other millimeter hole near the periphery. The light then passed through a lens before going into a spectrograph from which the slit was removed. The ratio of the time of flash to the dark time to the excitation time was 1 to 10 to 500.

A mercury diffusion pump slowly circulated the nitrogen through the resonance cell and over phosphorous pentoxide and hot copper and copper oxide for several hours previous to and during all runs in order to remove possible traces of hydrogen, oxygen, and water vapor. This method seemed quite effective because no HgO developed on the sides of the resonance cell even after 1000 hours of illumination. Eastman No. 36 plates were used. Each plate was calibrated with 15 to 20 density markings as obtained with neutral screens[11] mounted on eccentrics and placed between the spectrograph and the disk. A Moll self-recording microphotometer was used to densitometer the plates. Since the speed of the disk was varied over a range from 100 to 1000 r.p.m., the intermittency effect[12] was not constant and was found to vary several percent, depending upon the light intensity and the length of exposure.

Results

For a mixture of nitrogen at a few millimeters pressure and mercury vapor at 21°C in the resonance cell, the mercury line 4047 ($2^3P_0 - 2^3S_1$) always showed marked absorption in the neighborhood of 10^{-4} sec. after the interrup-

[9] R. W. Wood, Phil. Mag. **4**, 466 (1927).
[10] E. Gaviola, Phil. Mag. **6**, 1167 (1928).
[11] G. R. Harrison, J.O.S.A. and R.S.I. **18**, 492 (1929).
[12] C. E. Weinland, J.O.S.A. and R.S.I. **15**, 337 (1927).

tion of the optical excitation. The lines 3650, 4077, 4358, 5461, 5770 and 5790 showed at no time any measureable absorption. An investigation of the amount of absorption of 4047 was made for various time-waits (i.e. for various lengths of the dark period previous to the passage of the flash of light) in order to obtain a measure of the concentration of the metastable 2^3P_0 state. However, the amount of absorption is not directly proportional to the concentration because of the atomic absorption coefficient, μ, defined by $N = N_0 \mu^{-1} \log(I_0/I)$, where N is the number of metastable atoms per cc, I_0 is the intensity of 4047 after passing through previously unexcited resonance cell and I is the intensity after passing through previously excited cell.

The general nature of the rate of decay of absorption with respect to increased time-wait after termination of optical excitation is shown in Fig. 2.

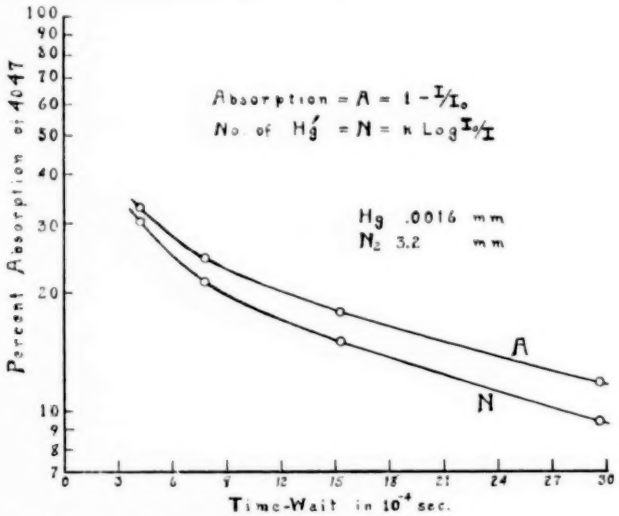

Fig. 2. A, semi-logarithmic plot of percent absorption of 4047 in mercury vapor with 3.2 mm pressure of admixed nitrogen against the time after termination of optical excitation. N, semi-logarithmic plot of the corresponding number of metastable mercury atoms in arbitrary units.

It may be noted that after 3×10^{-3} sec. there still exists over 11 percent absorption. As shown in the figure the effect of the absorption coefficient is to give a decay rate of N somewhat greater than the decay rate of the absorption of 4047. The most important point however, in this figure, is that the N curve is not a straight line but concave upward, indicating that the metastable states decay more rapidly at first and more slowly later. This same character is evident for other pressures as shown in Fig. 3. For nitrogen pressures below 2 mm (not shown in Fig. 3) the curves are straight lines whose negative slope increases with decrease in pressure. Above 2 mm the curves are concave upward with an average negative slope that decreases until a pressure of 5 mm is reached. Beyond 5 mm the average negative slope increases with increased pressure. No measurements were made beyond 50 mm nitrogen pressure.

Two objections might be made against the reality of $dN/dt \neq$ constant as expressed by the fact that the curves of Fig. 3 depart from a straight line. First, N as obtained through the percent absorption and absorption coefficient may not be directly proportional to the number of Hg′ (metastable 2^3P_0 mercury atoms) per cc, because of various factors; namely, absorption coefficient changing[13] with number of Hg′, pressure broadening of absorption line, displacement and dissymmetry in form of absorption line due to admixed foreign gas.[14] In order to test this possible objection, the emission of 2537 was obtained at various time-waits after termination of the optical excitation. It is generally agreed that the intensity of 2537 at any particular instant after

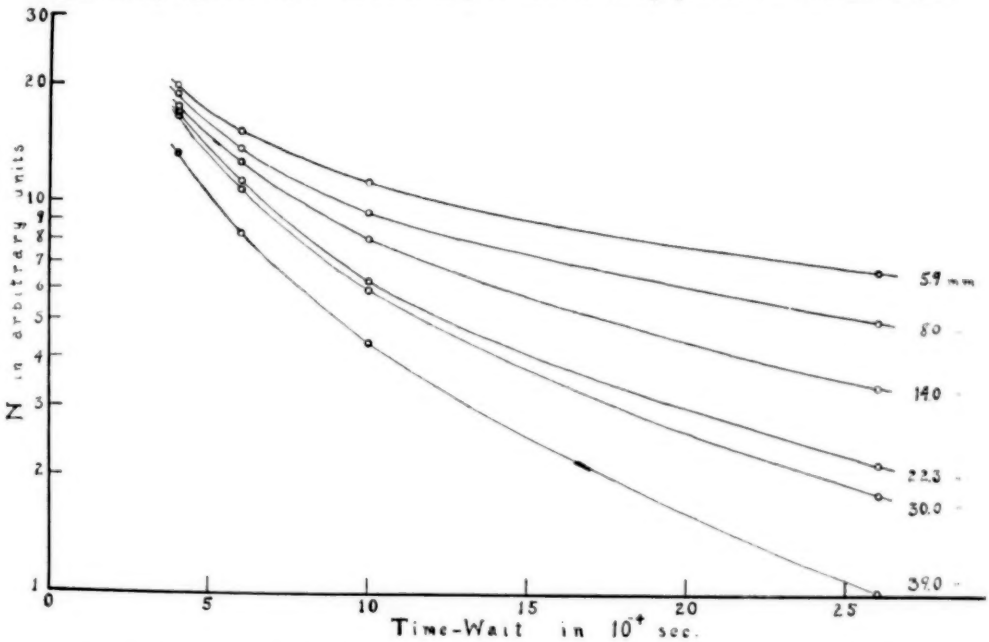

Fig. 3. Semi-logarithmic plot of the number of metastable mercury atoms in arbitrary units for various nitrogen pressures against the time after termination of optical excitation.

optical excitation is directly proportional to the number of metastable 2^3P_0 atoms present at that particular instant provided the concentration of the 2^3P_2 atoms is negligible, which is the case for mercury and nitrogen admixtures as will be pointed out later. Fig. 4 shows the values of the intensity of the emission of 2537 in arbitrary units and also the values of N as obtained from the absorption of 4047 plotted on semi-log paper against the time-wait in 10^{-4} sec. It is seen that the two are in fairly good agreement. It must be, therefore, concluded that the various factors mentioned above change but little when the partial pressure of Hg′ alone changes. One must not, however, conclude that these factors remain constant when the nitrogen pressure is changed. The advantage of running absorption measurements of 4047 in-

[13] A. R. Thomas, Phys. Rev. **35,** 1253 (1930).
[14] P. Kunze, Ann. d. Physik **4,** 500 (1931).

stead of emission measurements of 2537 is that an exposure of 4047 could be obtained in a few minutes while one of 2537 necessitated an hour. As it is de-

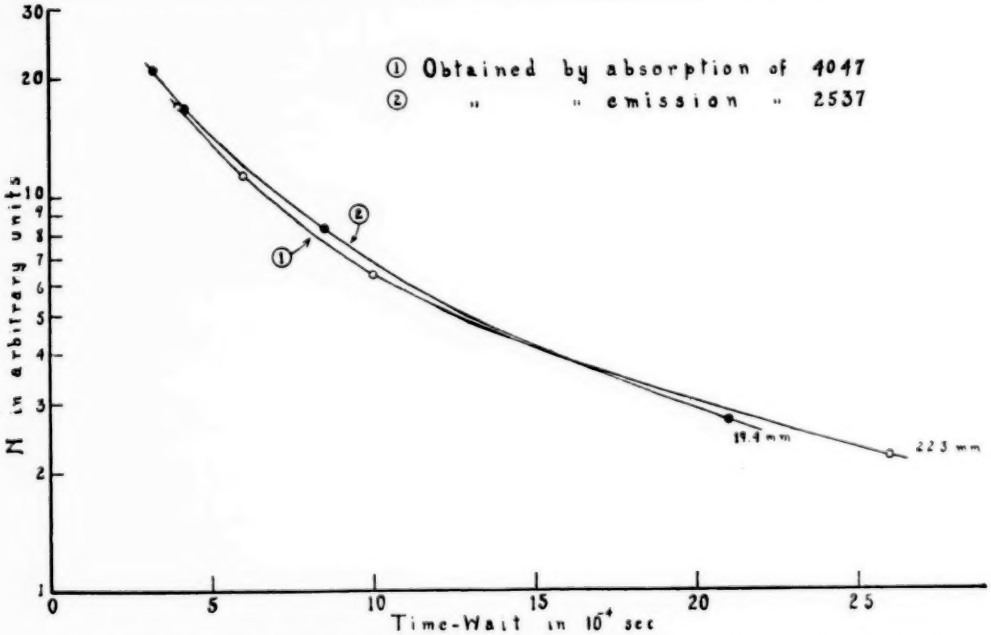

Fig. 4. Semi-logarithmic plot of the number of metastable mercury atoms as obtained from absorption of 4047 and from emission of 2537 against time after termination of optical excitation.

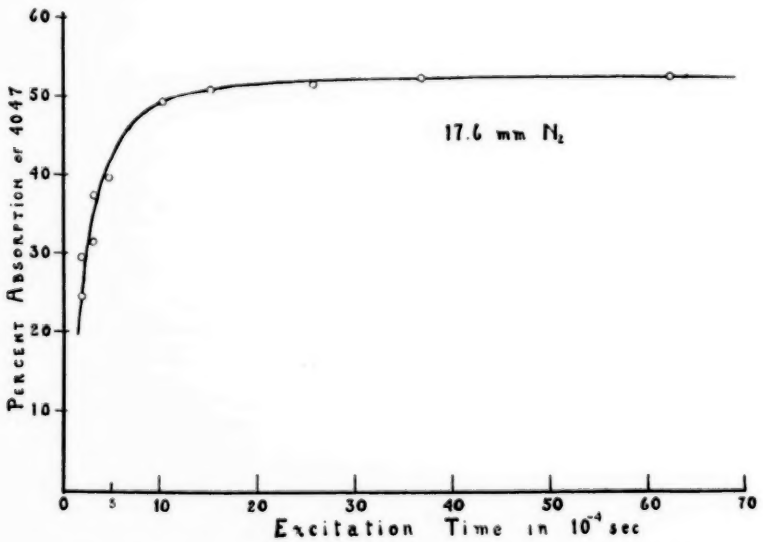

Fig. 5. Percent absorption of 4047 plotted for various time-waits after the beginning of optical excitation.

sirable to have at least ten exposures on a plate, preferably twenty or more, it is very difficult to keep conditions constant for so long a time.

The second objection is that the concentration of Hg′, when the disk is running at high speed, might not be the same as when it is running at low speed. This point was checked by taking absorption measurements at various instants during the excitation period. Fig. 5 shows a typical curve obtained. The percent absorption is plotted against the time after the beginning of the optical excitation. The shortest excitation period used in the regular runs was 16×10^{-4} sec. It is seen from the figure that the concentration of Hg′ has practically reached a constant value by then. It may be added, parenthetically, that the life of the metastable mercury atom was also measured by a series of rate of formation curves for various pressures of nitrogen. The results are in general agreement with those obtained from the rate of decay curves, although not as accurate.

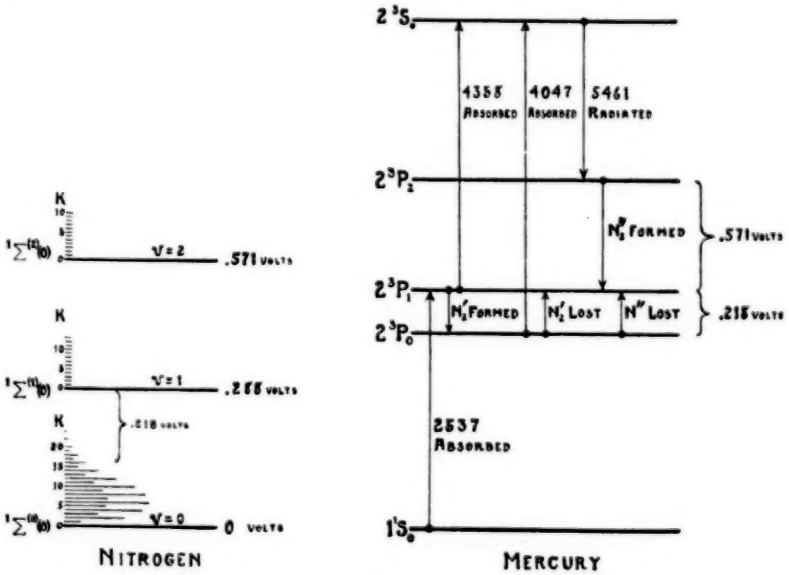

Fig. 6. Schematic diagram of a few of the energy levels of the mercury atom and of the nitrogen molecule.

Discussion

It has been known for some time that nitrogen as well as a few other gases has a marked ability in producing a high concentration of 2^3P_0 states in optically excited mercury vapor. This ability seems to be connected with the energy difference between the 2^3P_1 and 2^3P_0 states of mercury and the possible vibrational energies of the molecule.[15] In the case of nitrogen the first excited vibrational state has an energy of 0.288 volts, and the second an energy of 0.571 volts. The energy difference between the 2^3P_1 and 2^3P_0 states of mercury is 0.218 volts and between the 2^3P_2 and 2^3P_1 states 0.571 volts. Fig. 6 is a schematic drawing of a few of the energy levels in mercury and nitrogen. Several of the rotation levels for nitrogen are plotted above each of the first three vibrational levels. At 20°C a greater percent of the nitrogen mole-

[15] M. W. Zemansky, Phys. Rev. **36**, 919 (1930).

cules (11.2 percent, in fact) are in the sixth rotational state ($K=6$) than any other rotational state, as is represented by the horizontal length of the level. The lengths of the adjacent levels also bring out the fact that the statistical weight of the even levels is twice that of the odd levels.

When a mercury atom is excited to the 2^3P_1 state any one of a number of things might subsequently take place, as indicated in Fig. 6. The electron might be lifted to the 2^3S_0 level by absorption of 4358 or dropped to the 2^3P_0 level by a collision of the second kind with a normal nitrogen molecule. It has been suggested by Beutler and Rabinowitsch[16] that the nitrogen takes on vibrational energy in this type of collision. It is difficult to see how this interaction takes place unless it is the nitrogen molecules in the sixteenth or higher rotational level that are put into the first excited vibrational state by the available 0.218 volts, the amount lost by the mercury. The sixteen or more units of rotation lost by the nitrogen molecule are conserved perhaps by the $Hg-N_2$ system. Although only a little over two percent of the molecules are in the sixteenth level, the large cross section for collisions involving resonance as pointed out by Kallman and London[17] makes these few molecules very effective. Let $^2\Sigma^{(1)}$ represent a nitrogen molecule in its first excited vibrational state.[18] From the 2^3S_0 level the electron might drop to the 2^3P_2 level by emission of 5461. Since this level is also metastable we might expect the electron to remain there until a collision with a normal nitrogen molecule drops the electron to the 2^3P_1 level, and leaves the nitrogen in its second excited vibrational level, $^1\Sigma^{(2)}$. This is, within a few frequency units, a case of exact resonance and would be expected to take place very readily. From the 2^3P_0 level the electron might be lifted to the 2^3P_1 level by absorption of 0.218 volts from the vibrational energy of either a $^1\Sigma^{(1)}$ or $^1\Sigma^{(2)}$ molecule during the impact of a metastable mercury atom with an excited nitrogen molecule.

In the fact that there exists nearly exact resonance in the energy difference between the $^1\Sigma^{(2)}(k)$ and $^1\Sigma^{(1)}(k)$ states of nitrogen and the energy difference between the 2^3P_2 and 2^3P_1 states of mercury, probably lies the reason that no evidence for a long life 2^3P_2 metastable state has been found—even though the emission of 5461 during optical excitation is exceptionally strong.

The usual removal of the electron from the 2^3P_0 state by collisions of the first kind, diffusion to the walls, and natural decay has not been represented in Fig. 6. We see that in addition to diffusion and dissipation impacts with unexcited nitrogen, the rate of decay of the number of metastable mercury atoms may be accelerated by dissipative impacts with these excited nitrogen molecules whose number and influence also decrease with time by diffusion and by dissipative impacts.

With these ideas in mind let us consider a long cylindrical tube of radius $r=a$ filled with both normal and excited nitrogen molecules and mercury atoms. Let N'_2 be the number of nitrogen molecules per cc in the $^1\Sigma^{(1)}(k)$ and

[16] H. Beutler and E. Rabinowitsch, Zeits. f. physik. Chem. **B8,** 403 (1930).

[17] H. Kallman and F. London, Zeits. f. physik. Chem. **B2,** 207 (1929).

[18] Prof. R. T. Birge suggested to me the symbol $^1\Sigma^{(v)}(K)$ to represent a molecule in the $^1\Sigma$ state with v units of vibration and K units of rotation.

$^1\Sigma^{(2)}(k)$ states; D is the diffusion coefficient of a metastable mercury atom, and D_2 is that of an excited nitrogen molecule; C is the number of collisions per sec. experienced by Hg′ with N_2 that are effective in removing the mercury atom from the metastable state; C_2 is the number of collisions per sec. per excited nitrogen that are effective in removing the nitrogen molecule from excited state. E is the number of collisions per sec experienced by Hg′ with excited nitrogen that are effective in removing mercury atom from metastable state. One then obtains the relations

$$\frac{\partial N}{\partial t} = D\left(\frac{\partial^2 N}{\partial r^2} - \frac{1}{r}\frac{\partial N}{\partial r}\right) - CN - ENN_2'$$

$$\frac{\partial N_2'}{dt} = D_2\left(\frac{\partial^2 N_2'}{\partial r^2} - \frac{1}{r}\frac{\partial N_2'}{\partial r}\right) - C_2 N_2'$$

We shall assume that $N = N_0 = \text{constant}$ when $t = 0$ and $r = a$; also $N = N'_2 = 0$ for $r = a$ at all time. We may separate the variables in the above equations by putting $N = TR$ and $N'_2 = T_2R_2$ where T and T_2 are functions of the time only, and R and R_2 are functions of the radius only. One then derives

$$\frac{1}{R}\left(\frac{\partial^2 R}{\partial r^2} - \frac{1}{r}\frac{\partial R}{\partial r}\right) = -q^2$$

$$\frac{1}{T_2}\frac{\partial T_2}{\partial t} + C_2 = -q^2 D_2$$

$$\frac{1}{T}\frac{\partial T}{\partial t} + C + Ee^{-\beta t} = -q^2 D$$

where $q = \text{constant}$ and $\beta = C_2 + q^2 D_2$

The solution $J_0(qr) = R$, of the first equation together with the help of the boundary conditions fixes $q = \mu_\nu / a$ where μ_ν is one of the infinite sequence of roots of $J_0(\mu) = 0$. The final solution to a high degree of approximation is arrived at in the form

$$N = N_0 \exp\left[-\alpha t + A(e^{-\beta t} - 1)\right] \tag{1}$$

where $\alpha = C + q^2 D$ and $A = E/\beta$.

By choosing four values of N from any one curve in Fig. 3, it is possible to solve the above expression for the unknown coefficients, α, β and A. The values of α and β are plotted in Figs. 7 and 8 against the nitrogen pressure. In Fig. 7 it is seen that the minimum value of α occurs in the neighborhood of 6 mm admixed nitrogen. For pressures less than 6 mm α increases due to increase in number of collisions of the first kind. In Fig. 8 the minimum for β is shifted to 20 mm nitrogen pressure. A shift to a higher pressure for the minimum of the coefficient for nitrogen might be expected since nitrogen diffuses more rapidly than mercury. The broken line shows an extrapolation of the curves for α and β may reasonably be made to pass through the origin. In other words the data of this experiment are not sufficiently accurate or the ex-

trapolation is too far to indicate a value of α or β different from zero. The interpretation would be that the metastable mercury and nitrogen, contained

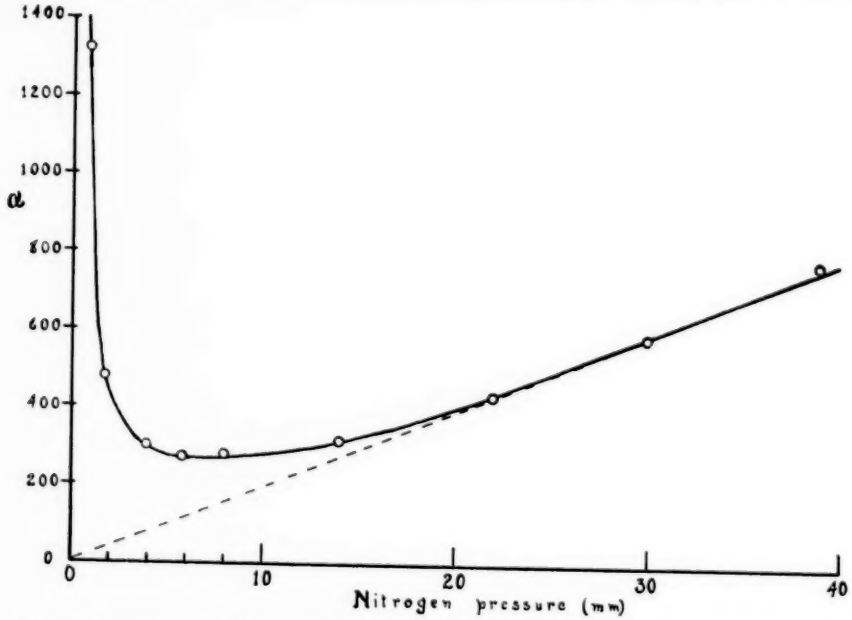

Fig. 7. Decay coefficient, α, for metastable mercury when not influenced by metastable nitrogen plotted against various nitrogen pressures.

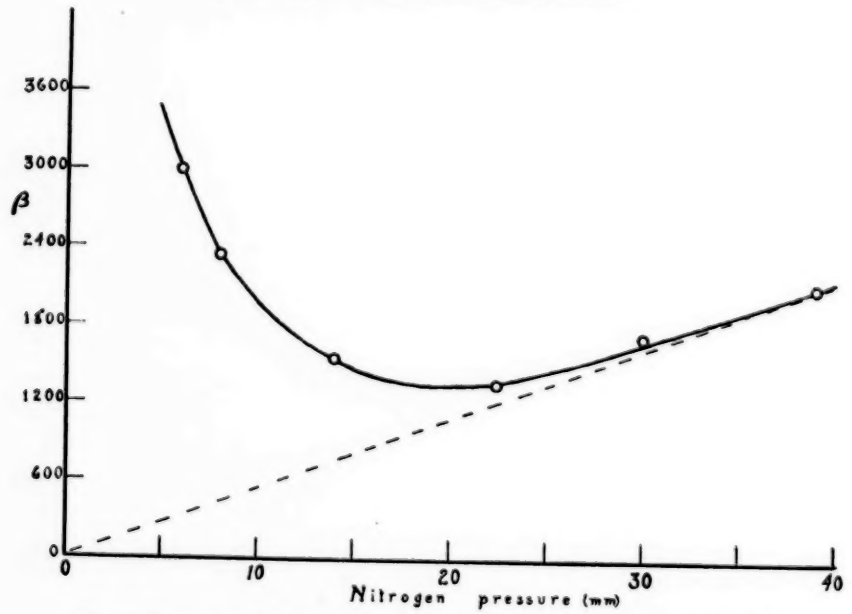

Fig. 8. Decay coefficient, β, for metastable vibrating nitrogen molecule plotted against various nitrogen pressures.

in an infinitely large resonance cell, would have an infinite life at zero nitrogen pressure. This life may be called the natural life.

With the help of the kinetic theory of gases, it is possible by taking the values of α or β at any two pressures in Figs. 7 or 8 to calculate C and D or C_2 and D_2 respectively. From the kinetic theory we may write

$$C = 5.24\gamma\sigma^2 p \times 10^5 \qquad D = 1755/\sigma^2 p$$

$$C_2 = 6.95\gamma_2\sigma_2^2 p \times 10^5 \qquad D = 2320/\sigma_2^2 p$$

where γ is the probability that an impact involving Hg′ be a dissipative one for the Hg′, γ_2 is the probability that an impact involving Hg′ be a dissipative one for the N_2′, σ and σ_2 are distances, expressed in angstroms, between centers at impact for Hg′ and N_2′ respectively, p is the nitrogen pressure expressed in mm of mercury. A summary of the various values calculated from the curves of Figs. 7 and 8 are given in Table I.

TABLE I.

	For Hg′	For H_2′
Prob. that impact be a dissipative one	3.3×10^{-4}	$80.\times10^{-4}$
Distance between centers at impact	3.2×10^{-8} cm	0.85×10^{-8} cm
Diffusion coefficient	0.129 gm · cm^{-2} · sec.$^{-1}$ · dyne^{-1}	2.41 gm · cm^{-2} · sec.$^{-1}$ · dyne^{-1}
Maximum observed life	2.54×10^{-3} sec.	0.52×10^{-3} sec.
Pressure of N_2 for maximum life	6 mm	20 mm
Natural life	∞	∞

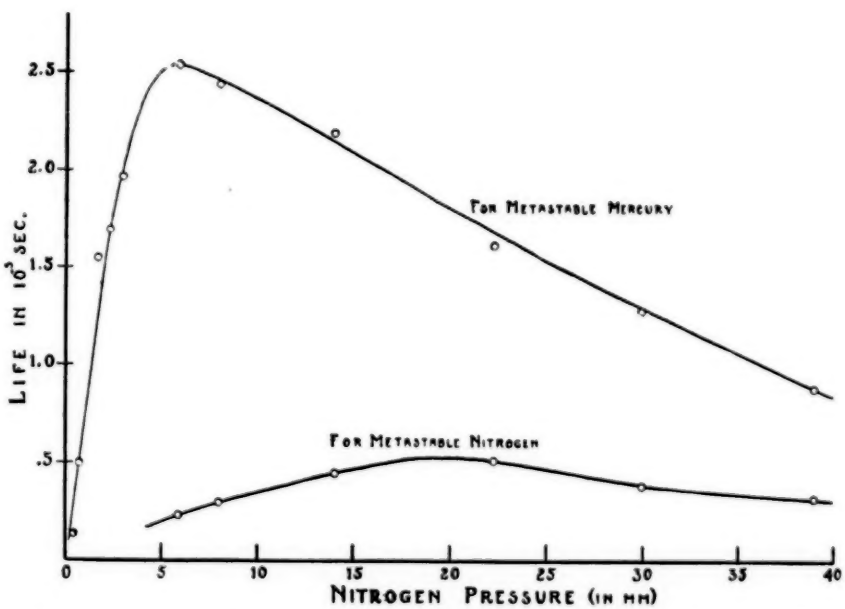

Fig. 9. Life in 10^{-3} sec. for the metastable mercury atom and vibrating nitrogen molecule as a function of various nitrogen pressures.

It must be added that the values quoted for N_2′ are less accurate than those for Hg′, due perhaps to N_2′ (meaning nitrogen in either its first or second excited vibrational state) functions as a second order effect.

The reciprocal of α multiplied $\log_e 2$ gives the half-value time or life of the metastable mercury atom when not influenced by vibrating metastable ni-

trogen molecules. Likewise $(1/\beta) \log_e 2$ gives the life of the metastable nitrogen. Fig. 9 shows a plot of these life times for various pressures of nitrogen. The life of Hg′ increases nearly linearly with small pressures of nitrogen, since the diffusion varies inversely as the pressure. For high pressures the life decreases nearly linearly with pressure, since the number of collisions of the first kind increases directly as the pressure. The maximum life for Hg′ and N_2' is seen to occur for a nitrogen pressure near 6 mm and 20 mm respectively.

If one assumes the distance between the centers for impacts involving Hg′ to be the distance between Hg′ and N_2 and the radius of N_2 is the kinetic theory radius from viscosity, then one obtains the ratio of the radii for Hg′ to Hg to be 0.89 which seems quite reasonable. For the case of N'_2 the distance between the centers at impact is given to be less than the diameter of the normal nitrogen molecule. This is, however, in accord with the recent calculations made by Zener. He calculates, for the simple case of a nitrogen molecule in its first excited vibrational state transferring its energy to a normal nitrogen molecule at room temperature, a cross section for the transfer of $0.0^{14}4\times$kinetic theory cross section; and with increase in mass of the two molecules an increase also in the resonance cross section. It must be remembered that in this experiment with mercury and nitrogen, the excited nitrogen molecule may collide with Hg, Hg′, N_2 or N_2'.

The two main points to be made in this paper are that with careful calibration of photographic plates the decay of the metastable 2^3P_0 state of mercury is found not to be accurately exponential, and that the departure from the exponential can be reasonably attributed to long-lived excited vibrating metastable nitrogen molecules.

THE IONIZATION OF Kr AND Xe BY POSITIVE ALKALI IONS AND THE IONIZATION POTENTIALS OF Ne, A, Kr, AND Xe

By Otto Beeck and J. Carlisle Mouzon
Norman Bridge Laboratory of Physics, California Institute of Technology

(Received July 27, 1931)

THE previous work on the ionization of the noble gases by positive alkali ions[1,2,3,4,5] has been extended to krypton and xenon using velocities up to 600 volts, and the existence of a definite threshold at which ionization sets in has been studied for neon, argon, krypton, and xenon. The original apparatus described by Beeck[4] was used. With respect to the ionization chamber this method is similar to that of Sutton[1] and of Sutton and Mouzon,[2] but the mass spectrograph for ion separation and the use of electrometers instead of galvanometers, which makes the use of lower gas pressures possible, are new refinements. It is, however, noteworthy that the results of both methods are in very good agreement.

Previous work on helium, neon, and argon has given the unexpected result that the alkali ion nearest the noble gas in the periodic system is the most efficient ionizer. In the present work Cs^+ proves to ionize xenon most efficiently. In the case of krypton, however, K^+ seems to ionize equally as well as Rb^+. Also K^+ ionizes xenon more efficiently than Rb^+, while Rb^+ ionizes argon only slightly less than does K^+. These facts indicate that these collision phenomena are even more complicated than was formerly expected. The results show further that the maximum efficiency of ionization for a given accelerating potential increases with the atomic number of the gas. For example, the efficiency (the number of electrons liberated per initial positive ion per cm path per mm pressure) of caesium in xenon at 500 volts is 7.2 while that of potassium in argon is 3.4.

A second new and significant result, which is contrary to expectations based upon previous theories, is that there appears to be a definite threshold at which ionization begins. This was studied in neon, argon, krypton, and xenon. As the accelerating potential is increased from zero the ionization remains zero up to a certain point. Above this point the ionization increases almost linearly showing no indication that it approaches zero asymptotically at the lower voltages. In all cases except that of potassium in krypton it was definitely shown that the ion nearest the noble gas in the periodic system begins to ionize at the smallest voltage. This is in close correspondence with the

[1] Richard M. Sutton, Phys. Rev. **33,** 364 (1929).
[2] R. M. Sutton and J. C. Mouzon, Phys. Rev. **35,** 694 (1930).
[3] Otto Beeck, Naturwissenschaften **18,** 719 (1930).
[4] Otto Beeck, Ann. d. Physik **6,** 1001 (1930).
[5] R. M. Sutton and J. C. Mouzon, Phys. Rev. **37,** 379 (1931).

maximum efficiency of this combination. The observed ionization potentials in volts are given in the table.

	Li^+	Na^+	K^+	Rb^+	Cs^+
Ne	307	175	320	420	437
A	100	105	95	180	(365)
Kr	(420)	(400)	80	100	143
Xe	250	(360)	120	145	105

( ) probable error ± 10 volts.

A detailed account of this work will appear in the "Annalen der Physik" in the near future.

THE AGING OF IONS IN AIR AND NITROGEN*

By John Zeleny
Yale University

(Received July 1, 1931)

Abstract

Previous work on the mobility of aged ions in air has been extended to the measurement in air and in nitrogen of mobilities of ions at different short ages. The ions were produced by alpha-rays directly in the field used for their measurement and the average age was obtained from the time taken by the ions to cross between the two electrodes. In air containing 4 mg of water per liter, both kinds of ions of short age had the same mobility of 2.0 cm²/volt · sec while at an average age of 0.18 sec the negative ions moved 8 percent faster than the positive. In air partially dried by KOH the mobility of the negative ions decreased from 2.3 (above units) at 0.004 sec to 2.1 at 0.34 sec while the positive ion mobility decreased from 2.0 at 0.004 sec to 1.7 at 0.26 sec. In air dried by aid of liquid air traps the negative ion mobility decreased from 2.44 at 0.004 sec to 2.35 at 0.28 sec. The positive ions in this dry air were found to be very sensitive to minute changes in conditions that had no effect on negative ions. These changes are supposed to arise from small traces of some unknown impurity. Positive mobilities as high as 2.3 at 0.05 sec were obtained. The new information is applied to the explanation of the previous results for older ions. No transformation of one type of positive ion into another single type as observed by Erikson was found under the conditions of these measurements. The ions were all found to have the same mobility at the shortest ages but with increase of time the ion mobilities became spread over a range of values, the numbers given above corresponding to the peak of the distribution curves. The nitrogen used contained 0.3 percent of oxygen. The negative ions of short age all had a very high mobility which could only be roughly estimated as of the order of 100. With increase of age these fast ions gradually transformed into slower ions which were not all alike and had a peak mobility that decreased from 3.0 at 0.04 sec to 2.5 at 0.25 sec. The fast negative ions presumably remain free electrons for a large portion of their path and since their mobility does not appear to change with time it is necessary to suppose that these ions alternate frequently between being free electrons and monomolecular ions, but after more molecules become attached, the ion can no longer revert to the electron stage. The positive ions in nitrogen were always contained in one group only, the peak mobility of which ranged from 2.2 at 0.007 sec to 1.8 at 0.17 sec. The slow decrease of mobility of the ions with age and the large effect of slight changes apparently of gas composition upon the rate of this decrease for positive ions especially, indicate that the ions are gradually undergoing change of size owing to the accretion of scarce molecules or the exchange of such molecules for those which first gather about the central charge to form an ion cluster.

I RECENTLY[1] reported the results of some measurements of the mobilities of ions in air which were made with ions about two seconds after they had been formed. These ions were, I believe, the oldest artificially produced ions on which observations have thus far been made. In general the mobilities of

* The first part of this paper dealing with ions in air was read at the March 6, 1931 meeting of the American Philosophical Society and is given here in abstract only. See Proc. Am. Phil. Soc. **70**, 121 (1931).

[1] J. Zeleny, Phys. Rev. **34**, 310 (1929); **36**, 35 (1930).

both kinds of ions in very dry air and in air containing a small amount of moisture were found spread over one more or less extended band of values, although in extremely dry air two groups of negative ions were resolved. The mobility obtained for the peak of the distribution curve of the faster and larger group of negative ions in this very dry air was 2.45 cm^2/volt·sec [cm/sec per volt/cm] and that of the positive ions was only 1.05 cm^2/volt·sec. The corresponding values obtained for air containing about 2 mg of water per liter were 2.08 cm^2/volt·sec and 1.36 cm^2/volt·sec respectively. It is to be noted that in the presence of moisture the mobilities of the negative ions were reduced and those of the positive ions were increased.

Since these values for aged ions differ considerably from those usually given for ions of much smaller age and since the method developed is capable of giving accurate results it seemed advisable to extend the measurements to ions of short age. This was made possible by modifying the apparatus so that the ions could be produced directly in the electric field in which their

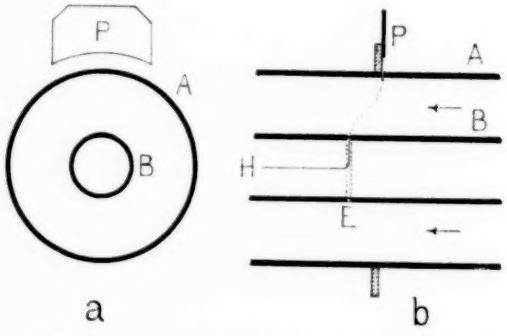

Fig. 1. Sections of apparatus showing how ions were produced in gas stream.

mobility was measured. The method used consists in having ions move under the influence of an electric field from the outer of two concentric cylinders to the inner one and finding how far they are blown down stream during their passage by a slow, nonturbulent stream of air flowing axially in the space between the two cylinders. The distribution of the ions on their arrival at the inner cylinder is found by moving the whole cylinder axially and measuring, for different positions of it, the ion current flowing to a narrow insulated section of the cylinder. A more detailed account of the method and apparatus is given in the previous papers.[1]

Fig. 1 shows the change made in the apparatus to permit the ions to be subjected to mobility measurement immediately after their formation. *a* and *b* represent transverse and longitudinal sections, respectively, of portions of the two cylinders *A* and *B*. The plate *P*, 1 mm thick, has on its lower edge a deposit of polonium, for the preparation of which I am indebted to Professor A. F. Kovarik. Alpha-rays from the polonium produce ions in the air stream close to the inner surface of the outer cylinder, after passing through aluminum covered, 1 mm wide openings made in that cylinder along a circumference. The dotted line in the figure represents the path of the ions

going from the outer cylinder to the insulated section E of the inner cylinder, which the wire II connects to the electrometer. The average age of an ion during the measurement of its mobility, being half the time taken by it to make its journey, was varied from 0.004 sec to 0.34 sec.

It was found that at the shortest ages used, the spreading of the ions along the inner cylinder could be fully accounted for by diffusion effects,[1] indicating that the ions of each sign at these ages all have the same mobility. For older ions this was, as previously, found to be far from true, and when numerical values of mobilities are given it will be understood that these refer in each case to the ions comprising the peak of a distribution curve.

In air partially dried by passage between broken sticks of caustic potash, the mobility of the positive ions was found to decrease with age from 2.0 $cm^2/volt \cdot sec$ at an average age of 0.005 sec to 1.7 $cm^2/volt \cdot sec$. at an average age of 0.26 sec, the rate of decrease being greater in the first part of this range than in the last part. Under the same conditions the mobility of the negative ions diminished from 2.3 $cm^2/volt \cdot sec$ at an average age of 0.004 sec to 2.1 $cm^2/volt \cdot sec$ at an age of 0.34 sec. None of the curves giving the distribution of the positive ions on their arrival at the central cylinder had more than one peak, and accordingly no transformation with time of one definite kind of positive ion into another of lower mobility, such as was found by Erikson,[2] was observed in these experiments.

In air containing about 4 mg of water per liter, the mobilities of the positive and negative ions were found to be identical up to an average age of 0.02 sec. The actual values at these small ages differed somewhat on different days, perhaps owing to changes in the water content of the air used, but averaged approximately 2.0 $cm^2/volt \cdot sec$. For ions older than the age limit just given, the mobilities of the two kinds of ions differed more and more with age owing mainly to the decrease in the mobility of the positive ions; the negative ions having a mobility 8 percent higher than the positive ions at an average age age of 0.18 sec. Here again only one peak was present in the ion distribution curves.

Lastly, many measurements were made in air thoroughly dired by passage first through large jars of granulated calcium chloride and of sticks of caustic potash, and then through tubes and filters immersed in liquid air. The mobilities of the negative ions were found here to decrease but slowly with age, the final average value at an average age of 0.004 sec being 2.44 $cm^2/volt \cdot sec$ and decreasing gradually to 2.35 $cm^2/volt \cdot sec$ at an average age of 0.28 sec. This rate of decrease is nearly the same as that recently reported for both negative and positive ions by N. E. Bradbury.[3]

My own observations show that the positive ions in this very dry air are very sensitive to slight differences in the gas since they were found to undergo marked changes with prolonged use of dry air in the apparatus. The first set of observations with this air gave 2.0 $cm^2/volt \cdot sec$ for the mobility of the positive ions at an average age of 0.005 sec, the value decreasing with the age

[2] H. A. Erikson, Phys. Rev. **24,** 502 (1924).

[3] N. E. Bradbury, Phys. Rev. **37,** 1311 (1931).

of the ions down to 1.4 cm^2/volt·sec for an average age of 0.22 sec. After continued use of dry air, the values obtained increased in magnitude to 2.3 cm^2/volt·sec at an average age of 0.05 sec and to 2.2 cm^2/volt·sec for an average age of 0.1 sec. These values are but little lower than those of negative ions of like age and are much higher than any heretofore reported for positive ions in air. In addition to the peak in the distribution curve corresponding to the above high mobility there was now present also a lower peak of ions of somewhat smaller mobility.

The large influence of the following procedure on positive ions in dry air is significant. The filters and coils used in drying the air had to be disconnected from the apparatus at least every three or four hours to remove the ice crystals that collected and which partly clogged the system. Notwithstanding the great care used to avoid the introduction of any contamination during the operations this involved, when observations were resumed the mobilities of the positive ions were always found to have decreased by 10 to 20 percent from the last previous values and only rose again to the large magnitudes mentioned above after the observations had been repeated over and over again. *A similar procedure had no effect on the results obtained for negative ions.*

It thus appears that positive ions are much more easily influenced than are negative ions by whatever foreign molecules are here involved. A possible source of these molecules which has not been investigated may have been an insulation plug situated some distance down stream from the place where the ions were subjected to measurement and from which some molecules may have diffused and become deposited on the upstream portions of the cylinders while the apparatus was not in use. In any case the amount of this impurity must have been exceedingly small since even in its presence the values of the mobilities obtained were as high as any previously reported.

The great sensitivity to the presence of traces of impurities exhibited by positive ions in air is in accord with the recent similar results of Tyndall and Powell[4] for helium and nitrogen, whose paper was received while this work was in progress.

The very slow decrease with time of the ionic mobilities here observed shows that extremely rare collisions are involved in the growth of the ions. The presence of a very small amount of some impurity whose molecules possess a large polarity would account for the results. The low value of 1.05 cm^2/volt·sec. previously found[1] for the mobility of old positive ions in dry air can on this ground be explained by supposing these ions to consist of a slowly acquired aggregation of such molecules. That the mobility of the positive ions under like conditions was considerably higher in moist air than in dry air may arise from water molecules, owing to their greater number, becoming attached to the ions before these come into favorable collision with molecules of the impurity in question and thus somehow preventing the growth of as large an aggregation as before.

The small group of slow negative ions previously found in dry air may likewise result from the attachment of special impurities to ions of the faster

[4] A. M. Tyndall and C. F. Powell, Roy. Soc. Proc. **A129**, 162 (1930).

group. An adequate explanation is still needed for the greater readiness with which positive ions form clusters.

NITROGEN

The measurements of the mobilities of ions in nitrogen were made with commerical gas prepared from air by the Linde process. The gas contained approximately 0.3 percent of oxygen and may accordingly be considered a mixture like air with the proportion of oxygen present reduced to about one percent of its amount in air. The gas was dried by aid of liquid air traps and filters.

Examples of the ion distribution curves obtained for negative ions in this gas with potentials on the outer cylinder ranging from -200 volts to -10

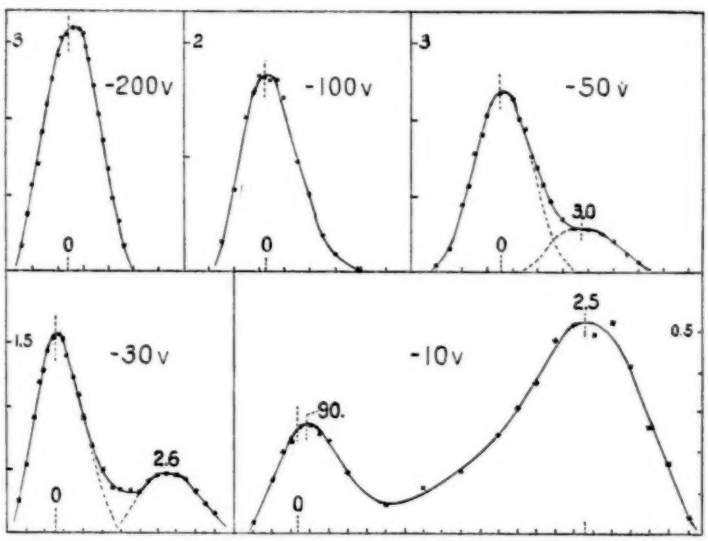

Fig. 2. Distribution of negative ions in nitrogen on arrival at inner cylinder, for different potentials indicated. Ordinates give ion currents in arbitrary units. The abscissas indicate position of ion collecting ring of inner cylinder, the divisions being millimeters. The average gas stream for the 200 v, 100 v, 50 v, 30 v and 10 v curves was respectively 9.65, 9.41, 7.70, 7.71 and 6.07 cm/sec.

volts are shown in Fig. 2. The ordinates represent ionization currents in arbitrary units and are not comparable with one another owing to a change made in the ion source. The scale of abscissas is different for the different curves, but each axis is divided into millimeter units. The vertical broken lines marked by 0 show the position in each case of the experimentally determined peak of the ion distribution curve when no gas stream was flowing, from which the deflection produced by the gas stream is to be measured. The stream velocity was varied and is given in the caption to the figure.

It is seen that with -200 volts on the outer cylinder the negative ions are deflected so little by the slow gas stream used that the distance could not be accurately determined. However, a very high mobility is indicated. As the potential on the cylinder was diminished it is seen that a portion of the ions

retain this high mobility but a larger and larger part of them have their mobility greatly reduced. With -10 volts on the cylinder fully four-fifths of the fast ions have been transformed to a slower type. The time taken by electrons to cross between the two cylinders is in this case about 3×10^{-5} sec.

Not much weight can be attached to the mobility of the group of fast ions computed from the slight but definite deflections produced by the slow gas stream, but the widely differing values obtained have an average approximately of 100 cm²/volt·sec. The largest deflection of 0.42 mm was naturally obtained with -10 volts on the cylinder and this should be reliable to about 10 percent. The mobility computed from it is 90 cm²/volt·sec.

Had these ions remained free electrons for all of their journey they should not have been appreciably deflected by the gas streams used since Wahlin[5] found the mobility of electrons in nitrogen to be about 10^4 cm²/volt·sec for fields of the magnitude here used. On the other hand these ions move far more rapidly than monomolecular ions should go according to any theory yet proposed. It is natural to suppose therefore that they are free electrons for a larger part of their journey and that they consist of electrons attached to molecules of oxygen for the remainder of their path. If an electron continues to adhere to a molecule, once it becomes attached we should expect the fast ion group to become more spread out and its peak mobility to decrease as the time of passage increases because more and more of the electrons will have attached themselves to molecules in the early part of their journey. This does not appear to be the case. The actual results may be explained on the hypothesis that so long as an electron is joined to one molecule only, it may readily become detached and hence that during its passage the ion alternates frequently between being a free electron and being monomolecular. This would account for the mobility of the fast group remaining unchanged with time.

We must suppose further that when the monomolecular ion grows by accretion of more molecules, it can rarely if ever lose the electron that gives it its charge. This would account for the gradual transformation of the fast ions into slower ones.

As regards the negative ions of slower mobility, not only does their number increase with decrease of voltage on the cylinder but the peak mobility decreases as well, as seen by the numbers indicated on the curves. On the -100 volt curve, there is only a suggestion of these slower ions. While the -50 volt curve can be resolved into two simple curves as indicated by the broken lines, this resolution into two symmetrical groups is no longer possible for the -30 volt curve, as shown by the broken lines on that diagram, and even much less so for the -10 volt curve where the slower ions form a group having a very extended distribution of different mobilities. It thus appears from these curves that the ions are not only gradually increasing in size up to the longest time used but also that a number of sizes are present at one time. As indicated on the curves the peak mobility of the slower group of negative ions decreases with the time required for the ions to make the passage, being 3.0 cm²/volt·sec for 0.04 sec and 2.5 cm²/volt·sec for 0.25 sec. The rate of

[5] H. B. Wahlin, Phys. Rev. **23**, 69 (1924).

this change is much larger than that found for air and since oxygen molecules are here present in comparatively small numbers it would seem that these are not primarily involved in this growth of the ions although we have assumed that it is an oxygen molecule that first becomes attached to the free electron since a nitrogen molecule cannot do so.

Samples of the distribution curves for positive ions in nitrogen are given in Fig. 3. Here again the vertical broken lines marked by 0 on the +50 volts and +200 volts curves indicate the position of the peak of the curve obtained when no gas stream was flowing. Taking cognizance of the different scales for the abscissas on the different curves it is seen that the curves become wider as the voltage on the cylinder is decreased and hence as the time of

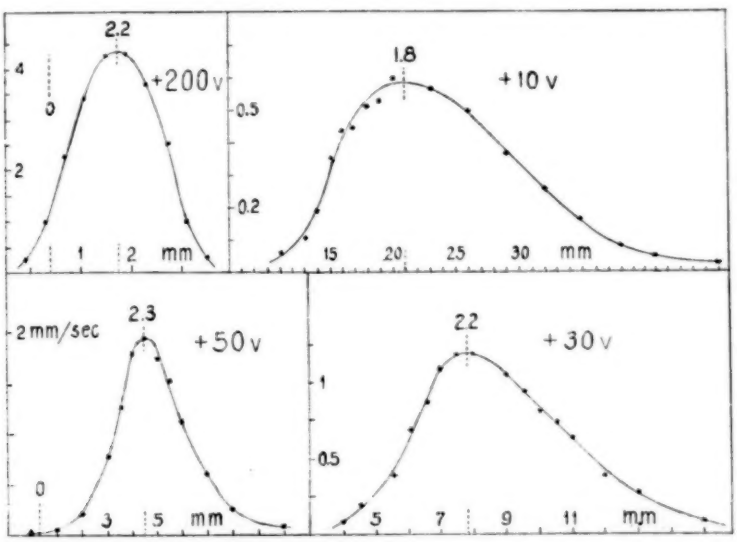

Fig. 3. Distribution of positive ions in nitrogen on arrival at inner cylinder, for different potentials indicated. The average gas stream for the 200 v, 50 v, 30 v and 10 v curves was respectively 9.65, 7.72, 7.86 and 6.12 cm/sec.

passage of the ions is increased. This widening is still very marked after allowance is made for the effects of diffusion and mutual repulsion[1] and shows the presence here also of ions of different mobilities. There is but one peak on each curve and the mobility corresponding to this peak changes from 2.2 cm^2/volt·sec for an average age of 0.007 sec to 1.8 cm^2/volt·sec for an average age of 0.17 sec. The larger value given is even higher than the preliminary value of 2.1 cm^2/volt·sec recently reported by Tyndall and Powell,[4] and is approximately the same as the highest value obtained for positive ions in dry air.

Some measurements were made with nitrogen taken directly from cylinders of the compressed gas, without removing from it the residual moisture it contained. The amount of this moisture was not determined but from other experiments was estimated to be about 0.2 mg per liter. The transformation of the fast negative ions into the slower types was now more rapid than it

was in the dry gas. When -50 volts was used on the outer cylinder about 30 percent of all of the negative ions were of the slower kind, and with -20 volts this fraction had increased to nearly 70 percent. The mobilities of the positive ions obtained with $+200$ and $+20$ volts on the cylinder were about 10 percent smaller than the values obtained for the same potentials when the gas was dried by aid of liquid air.

I am indebted to my assistant, Mr. W. P. Cunningham, for valuable aid with the observations.

REFLECTION OF MERCURY FROM ALKALI HALIDE CRYSTALS

By H. A. Zahl and A. Ellett
Department of Physics, State University of Iowa

(Received July 24, 1931)

Abstract

The distribution of mercury atoms scattered from NaCl, KCl, KBr and KI has been studied by means of an ionization gauge as a function of the angle of incidence and temperatures of scatterer and incident beam. The following facts are observed for the first three crystals: (1) There is a directed beam whose deviation from a specular position increases at smaller glancing angles. (2) The angle between the crystal surface and the direction of maximum intensity in the directed beam becomes less for lower crystal temperature and higher beam temperatures. (3) The relative number of atoms scattered at random increases with decrease in crystal temperature. (4) The directed beam becomes more sharply defined at lower crystal temperatures. Within the limits of error of the present experiments no discernible change is produced by rotation of the scattering crystal about an axis perpendicular to the plane of its face. The above facts are shown to be, qualitatively at least, consistent with a space-grating theory of reflection. In the case of KI the scattering was entirely random, i.e., according to the cosine law. This is also true for scattering by glass.

Introduction

LITTLE is known about the details of the processes by which energy is transferred from a solid to a gas. Previous studies of the scattering of atoms striking the surfaces of solids have shown that the following processes occur.

First, atoms striking the surface of a solid may be adsorbed and subsequently re-evaporated,[1,2] so that all directions of motion of the atoms leaving the surface are equally probable, leading to the familiar cosine distribution. The velocity of the re-evaporated atoms is determined by the temperature of the surface on which they were adsorbed.

Second, the superposition characteristics of the quantum mechanics which find their intuitive expression in the wave concept lead us to expect phenomena analogous to space and surface grating diffraction in optics. The experiments of Knauer and Stern[3] and Estermann and Stern[4] establish clearly the existence of phenomena of the latter type and the experiments of Johnson[5,12] on scattering of atomic hydrogen could scarcely be otherwise interpreted. The existence of specularly reflected beams of atoms[6] together with an apparent velocity selection[7] suggested by the results of double reflection

[1] R. W. Wood, Phil. Mag. **30,** 300 (1915).
[2] I. Langmuir, Phys. Rev. **8,** 149 (1916).
[3] F. Knauer and O. Stern, Zeits. f. Physik **53,** 779 (1929).
[4] I. Estermann and O. Stern, Zeits. f. Physik **61,** 95 (1930).
[5] T. H. Johnson, Phys. Rev. **36,** 381 (1930).
[6] A. Ellett and H. Olson, Phys. Rev. **31,** 643 (1928).
[7] A. Ellett, H. Olson and H. Zahl, Phys. Rev. **34,** 493 (1929).

experiments and of experiments in which the velocities were measured directly has been interpreted by H. F. Olson and the present writers as evidence of a process analogous to Bragg reflection of x-rays.

Any process which is to result in thermal equilibrium between a solid and a gas in contact must provide for the transfer of energy and for the dependence of this energy transfer upon relative temperatures of solid and gas. Obviously the first mechanism discussed, that of condensation and subsequent re-evaporation, is satisfactory from this point of view.

It may be asked whether the two latter mechanisms, surface or space-grating reflection, provide a means for the attainment of thermal equilibrium. Where the effective mass of the crystal is large, i.e., where a large number of atoms scatters coherently so that the resolving power is large, the amount of energy transferred will be very small. The experiments of Stern, Knauer and Estermann show that in those cases of surface-grating diffraction which they have studied the velocity distribution of the scattered atoms is just that characteristic of the gas from which they came. These atoms in rebounding from the crystal have exchanged momentum and consequently energy with the crystal, but the large effective mass of the crystal renders the energy transfer negligible.

That the distribution of intensity in an optical spectrum is determined by the nature of the source rather than by the temperature of the diffraction grating is of course due in the same way to the fact that the effective mass of the grating is large compared to that of a photon. If we could experiment with gratings sufficiently light or photons sufficiently massive we might expect to detect in the spectrum of the grating the influence of the temperature of the grating as well as that of the source.

Similarly with heavy atoms or under circumstances such that the effective mass of the crystal is small we may expect to find evidence of a transfer of energy. The experiments now to be described, on the reflection of mercury atoms from alkali halide crystals, we believe are best understood as a case of space-grating reflection accompanied by an energy transfer by no means negligible.

Method

The distribution of heavy atoms scattered from crystal surfaces has been investigated previously[6,7,8] by condensing the scattered atoms upon a liquid-air cooled surface surrounding the scattering crystal. The use of this method is limited practically to metals which are solid at ordinary temperatures and not too readily oxidized on exposure to air. Even in these cases there is some difficulty in interpretation of the results. Over a limited range of densities microphotometer transmission curves may be used to obtain the relative number of atoms in various parts of the deposit, but of course, heavy deposits are completely opaque while very light deposits on the other hand evaporate so rapidly that it is impossible to obtain significant transmission curves. A further serious difficulty with the deposit method is that the scattering crys-

[8] H. A. Zahl, Phys. Rev. **36**, 893 (1930).

tal must be removed from the apparatus between runs, so that it is not possible to say that its condition is the same in two runs.

In the experiments now to be described the relative numbers of mercury atoms scattered in various directions by alkali crystals were measured by means of an ionization gauge. This made it possible to study the effects of change in the angle of incidence, temperature of the scattering crystal, and temperature of the incident beam all in a single run.

Apparatus

The apparatus used, shown schematically in Figs. 1 and 2, resembles in its general outlines an ordinary x-ray spectrometer, and in fact must be ad-

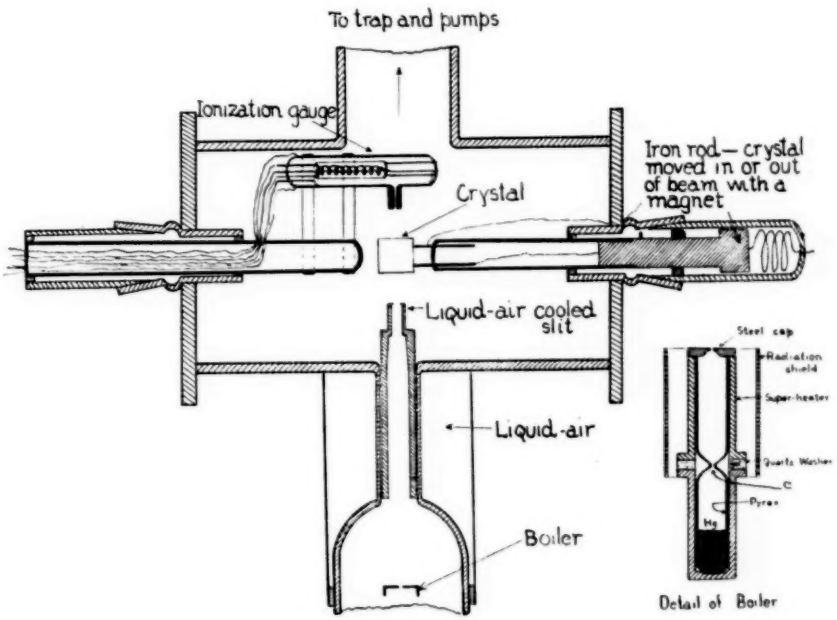

Fig. 1. Diagram of apparatus.

justed just as is such a spectrometer. That is to say the crystal must rotate about an axis in the plane of its face, and this axis must lie in the center of the incident beam of atoms, the latter being defined by the boiler opening and the liquid-air cooled slit just below the crystal. The axis about which the ionization gauge is rotated must be colinear with the axis of rotation of the crystal. These adjustments were effected by placing a closely fitting needle into the projecting aperture of the gauge and adjusting the needle and gauge supports so that the point of the needle appeared to remain stationary when the gauge was rotated about its axis. In a similar manner the crystal mounting was adjusted so that its axis of rotation lay in the plane of the crystal face. Coincidence of the two axes of revolution was then secured by adjusting the supports carrying the ground glass joints by means of which rotation was effected. The adjustment was finally checked optically. A beam of light from a source placed directly below the boiler aperture was reflected from the crys-

tal and must then pass through the aperture of the ionization gauge for all positions of the crystal and proper relative position of the gauge.

The operation of the ionization gauge as a pressure measuring device is too well known to require discussion here. Johnson[9] has considered its application to the measurement of molecular beams but found it unreliable because of difficulties which he ascribed to adsorption. We have had no difficulty with phenomena of the type reported by Johnson provided the gauge is sufficiently outgassed.

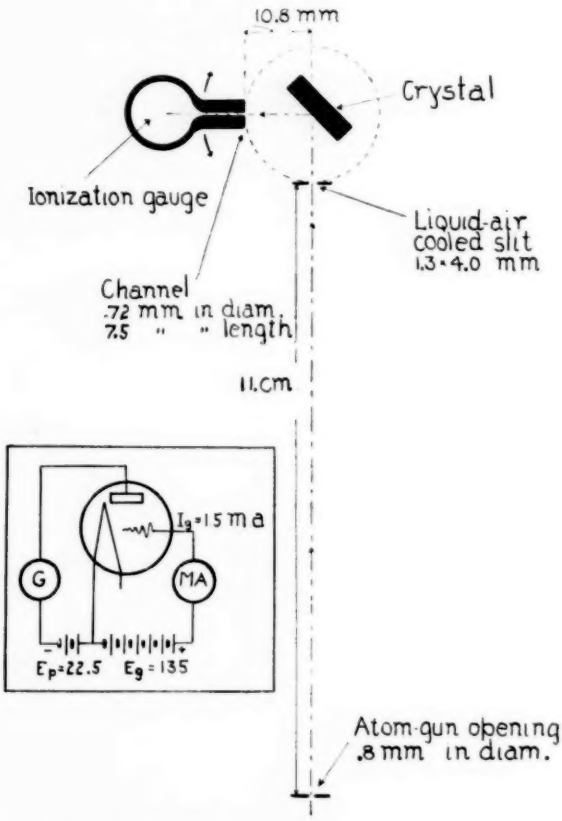

Fig. 2. Essential details of beam system. Insert shows electrical scheme of ionization gauge used.

The elements of the gauge were those of an ordinary 'peanut' vacuum tube with the filament replaced by 1 mil non-thoriated tungsten wire. These were enclosed in a glass envelope having a volume of about 6 cc, to which was sealed a capillary side tube 0.72 mm in diameter and 7.5 mm long. This aperture was arranged so that the atoms of the incident beam struck the opposite glass wall of the gauge instead of striking the metal parts directly. Since the point opposite the aperture is struck by more mercury atoms than any other part of the gauge it is here that adsorption should first occur and as mercury is

[9] T. H. Johnson, Phys. Rev. **31**, 103 (1928).

probably less readily adsorbed on clean glass than on metal the gauge was arranged in this manner.

About the outside of the gauge was wound a heater to aid in out-gassing and to reduce adsorption, but it was not required for the latter purpose as heat generated by the filament kept the gauge sufficiently hot, once it had been well out-gassed. The positive ion current due to residual gas was in all cases less than one half of one percent of that obtained when the gauge was placed into the main beam. That adsorption of mercury on the gauge walls was not appreciable may be seen from the fact that upon removing the gauge from the main beam the galvanometer returned to its zero within thirty to forty seconds. This was with the electron current reduced so that the main beam gave only 500 mm deflection. When the gauge was used for measuring the much less intense scattering its sensitivity was increased by a factor of 2.6 by increasing the electron current.

The gauge aperture offers to the molecular beam entering the gauge no impedance whatever and admits to the gauge the same number of molecules

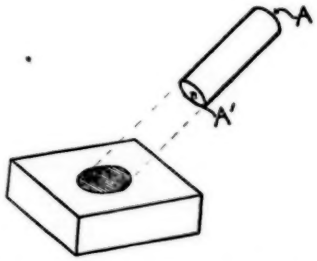

Fig. 3. Illustrating situation when gauge is used to measure the scattering from a crystal.

from the beam as would a thin walled circular aperture of the same area provided the incident beam has negligible divergence. To molecules escaping from the gauge, however, the aperture offers an impedance 9 times as great as would a thin circular aperture of the same area, and the pressure produced in the gauge by a given incident beam of small divergence is increased by just this factor. This of course applies only under circumstances such that the mean free path is long compared to the length of the gauge aperture so that collisions between molecules of the entering beam and molecules escaping from the gauge may be neglected.

The situation when the gauge is used to measure the scattering from a crystal is somewhat more complex and may be more readily discussed with the aid of a diagram, see Fig. 3. Molecules leaving any part of the shaded area within a cone whose solid angle is virtually constant and equal to A/r^2 will enter the gauge without impedance, and in addition some fraction of the molecules coming from this same area with directions lying between this cone and the cone defined by the area A' will also enter. Outside the shaded area the solid angle within which molecules may enter without striking the walls of the gauge aperture drops off rapidly but molecules may of course enter the gauge from parts of the crystal surface from which it is not possible to see

directly into the gauge, and to calculate the fraction of such molecules entering might be rather difficult. This difficulty may be avoided by using a narrow incident beam so that the entire area of the crystal struck by the incident atoms lies close to the axis of the gauge aperture. Otherwise the area of the crystal from which molecules enter the gauge will increase as the gauge is moved away from the crystal normal. With the dimensions of the present apparatus this condition was not met for angles of incidence (measured from the crystal face) less than 25 or 26°.

Fig. 4 shows the distribution of atoms scattered from a heated glass surface when the incident beam made an angle of 31° with the surface. From the surface of an amorphous substance such as glass we would expect random scattering so that the number of molecules scattered into an infinitesimal cone of solid angle $d\omega$ making an angle θ with the crystal surface is pro-

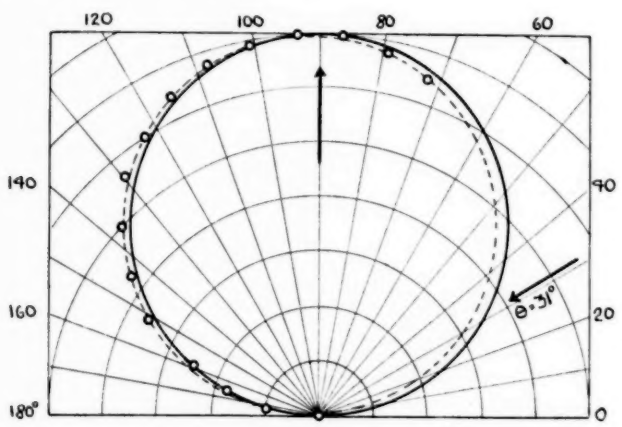

Fig. 4. Distribution of mercury atoms from a glass surface, glass heated to 350°C, beam temperature of 170°C.

portional to sin $\theta d\omega$. That is to say, the readings of the ionization gauge when plotted on polar coordinate paper should lie on a circle whose center is on the normal to the scattering surface. The full curve in Fig. 4 is a circle having its center on the normal to the glass surface. A systematic departure is noticeable, and in fact as the broken curve shows, the observed points lie very closely on a circle whose center is 3° off the normal. This probably does not indicate any such systematic departure from cosine scattering, but merely means that the direction of the normal to the glass surface was not accurately known. This curve represents the first observations made with the apparatus and the optical method of checking alignment had not yet been developed.

Further, if mercury atoms are scattered from glass according to the cosine law the reading of the gauge when standing on the normal to the crystal surface should be the same for all angles of incidence, provided the entire width of the surface struck by the incident beam is equally effective. At small angles of incidence as was mentioned above it is to be expected that the illuminated section of the glass will become so wide that some parts of it will not be effec-

tive, especially when the gauge stands on or near the normal. Figure 5 shows readings of the gauge placed on the normal to the glass surface plotted against the angle of incidence. These readings are constant as far as 30° while at 20° the reading has dropped about 5 percent.

Interpreting gauge readings as in Fig. 4, amounts to assuming that the galvanometer deflection is proportional to the number of atoms entering the

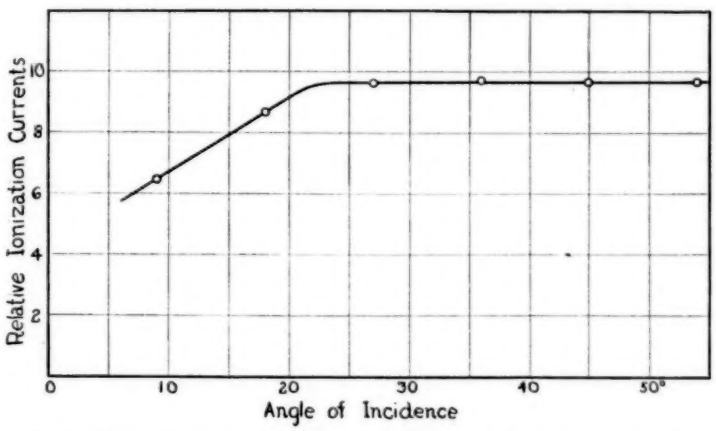

Fig. 5. Readings of gauge when placed on the normal to the glass surface plotted against the angle of incidence.

gauge, and for low pressures this is the characteristic behavior of the ionization gauge. As a check it is worth mentioning that the reading of the gauge when placed in the main beam was proportional to the vapor pressure as calculated from the vapor pressure temperature equation, which is quite accurately known for mercury.

Fig. 6 shows the readings of the gauge as it was swept through the incident beam. This does not give the distribution of intensity in the beam, as the

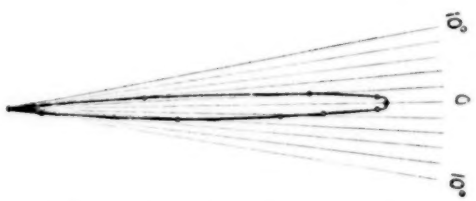

Fig. 6. Direct beam (uncorrected).

center of rotation of the gauge is far removed from the point from which the molecular beam diverges, but the fact that the curve is symmetrical does show that the axis of rotation of the gauge lies near the center of the incident beam. The fact that 6–7° rotation of the gauge away from the maximum is required to bring the gauge reading back to zero does not mean that the incident beam had this great divergence, but merely that the gauge required to be rotated this amount to swing the opening of the gauge channel clear

of the beam, for as long as the channel opening remains in the beam some molecules striking the walls of the channel will enter the gauge.

The width of the incident beam deduced from the movement of the gauge channel opening required to clear it is just what would be expected from the relative sizes and positions of the boiler aperture and upper defining slit. The details of construction of the boiler are shown in Fig. 1. The upper and lower halves insulated by the quartz washer w could be heated separately so that the vapor pressure of the mercury in the boiler could be controlled by regulating the temperature of the lower half of the boiler while the velocity with which the mercury atoms left the boiler could be increased by super-heating the upper half. The constriction c served to reduce diffusion of atoms between the two sections of the boiler so that the vapor in its passage through the upper section might more nearly attain a velocity distribution characteristic of the temperature at which the walls of this super-heater were maintained. It is not to be expected that the molecules escaping from this boiler possess a Maxwell distribution of velocities, for at the pressure maintained in the boiler (4–7 mm Hg) the free path is much shorter than the diameter of the boiler orifice. However, as long as the amount of mercury escaping from the boiler is proportional to the boiler pressure it may be expected that deviations from a Maxwell velocity distribution will not be extremely large, as both the reduction in the quantity of gas escaping and the deviation from the Maxwell distribution are due to the same cause, namely collisions occurring in the vicinity of the orifice.

The results presented in the next section will show that the distribution of atoms scattered by a crystal is affected by the velocity distribution in the atomic beam. That is, the changed velocity distribution brought about by super-heating is immediately evident in the changed distribution of scattered atoms while on the other hand the scattering is not affected by changes in boiler pressure, at least as long as the boiler pressures are kept below the value at which the beam intensity ceases to be proportional to boiler pressure, and this in itself may be taken to indicate that the velocity distribution in the beam is approximately independent of boiler pressure over the range in question.

Experimental Results

(1) *Reflection of Mercury from Rocksalt as a Function of the Angle of Incidence*

Fig. 7(a, b, c, d, e, f, g) represents the results obtained during a single run, the curves therefore being representative of but one crystal. The angle of incidence was changed in 9° steps from 18 to 72° (the angle referred to is always measured from the crystal surface). The circles are single experimental points and could be repeated to within two or three percent. For all the curves the crystal temperature[10] was maintained at 350° C while the incident beam

[10] Ellet and Olson[6] have found that in the region of this temperature outgassing of NaCl seems to be almost complete. J. H. Frazer (Phys. Rev. **34**, 644 (1929)) has also found, in agreement with Ellett and Olson, that at 330°C the thickness of adsorbed gas on the surface of an NaCl crystal appears to have reached a minimum.

was held at 170° C. In the curves the arrows indicate: (1) the direction of the incident beam; (2) the position the maximum of the reflected beam should occupy if the reflection were specular and total; and (3) the normal to the crystal surface.

Consider Fig. 7(a). The beam strikes the crystal at an angle of 18°. A_1 represents the curve obtained by sweeping the gauge over the crystal surface. If we consider the atoms after leaving the crystal surface as a combination of random scattered atoms and those definitely inclined in a specular direction then the experimental curve should allow separation into two such components. Moreover, since the degree to which cosine scattered atoms are present

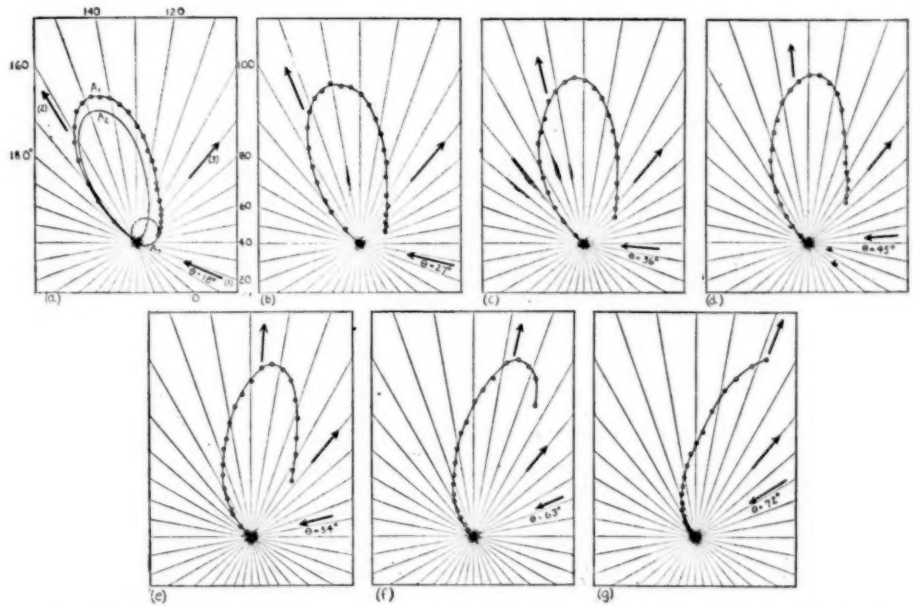

Fig. 7 (a, b, c, d, e, f, g). Distribution of mercury atoms from NaCl as a function of the angle of incidence, crystal at 350°C, beam at 170°C.

is surely limited by the intensity in the regions of the normal and particularly by the intensity on the side of the normal opposite to the reflected beam, an estimate of the cosine scattered atoms can be obtained. The circle marked A_3 represents the estimate of the number of atoms scattered according to the cosine law. Belief in the validity of such a procedure is strengthened when upon subtracting the cosine scattered atoms from the curve A_1 a quite symmetrical curve A_2 is obtained as the second component. It can be seen that the directed curve A_2 obtained after the subtraction is considerably displaced from the position it would occupy if the atoms contributing to this curve were specularly reflected.

For greater angles of incidence, i.e., Fig. 7 (b, c, d, e, f, g) the cosine correction has not been applied since the movement of the gauge was restricted by the upper defining slit and what end points were available in the region of the crystal normal contained increasing numbers of directed atoms making an

approximation to the number of random scattered atoms comparatively uncertain at larger angles of incidence. It is for this reason that most of the work to be described has been done at small angles of incidence.

It should be noted, however, since correcting the experimental curves consisted simply in subtracting the area of the estimated circle, that unless an impossible cosine circle falling beyond the experimental points be chosen the

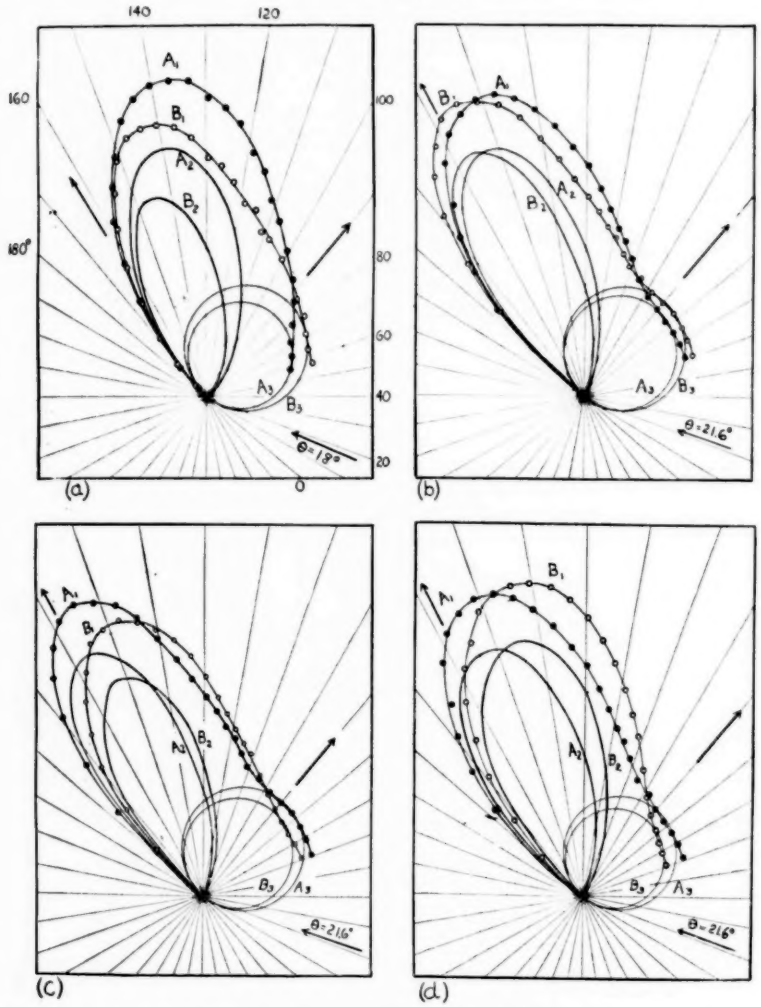

Fig. 8 (a, b, c, d). Distribution of mercury atoms from NaCl as a function of the temperature of the crystal and the temperature of the incident beam:

(a) Curves $A_{1,2,3}$: crystal, 350°C; beam, 170°C; in Table, No. 6
$B_{1,2,3}$: crystal, 50°C; beam, 170°C; in Table, No. 5
(b) Curves $A_{1,2,3}$: crystal, 350°C; beam, 500°C; in Table, No. 4
$B_{1,2,3}$: crystal, 50°C; beam, 500°C; in Table, No. 2
(c) Curves $A_{1,2,3}$: crystal, 50°C; beam, 500°C; in Table, No. 2
$B_{1,2,3}$: crystal, 50°C; beam, 170°C; in Table, No. 1
(d) Curves $A_{1,2,3}$: crystal, 350°C; beam, 500°C; in Table, No. 4
$B_{1\ 2,3}$: crystal, 350°C; beam, 170°C; in Table, No. 3

effect of any such correction applied to curves such as 7(b) and (c) would not move the experimental beam into the specular position. On the basis of the data shown in Fig. 7, and three more similar runs not shown but given equal weight, (it was not deemed advisable to average results since individual crystals showed distinct differences) it appears that up to angles of at least 45° the corrected curve is not specular.

(2) *Effect of Temperatures of Scattering Crystal and of Boiler Upon the Scattering of Mercury Atoms by Sodium Chloride Crystals*

The effect of varying separately the temperatures of crystal and boiler is shown in the four curves a, b, c, d of Fig. 8. In the case of Fig. 8(a) the beam emerging from a boiler at a constant temperature of 170° C was incident at an angle of 18° upon a crystal at 350° C (Curves $A_{1,2,3}$) and 50° C

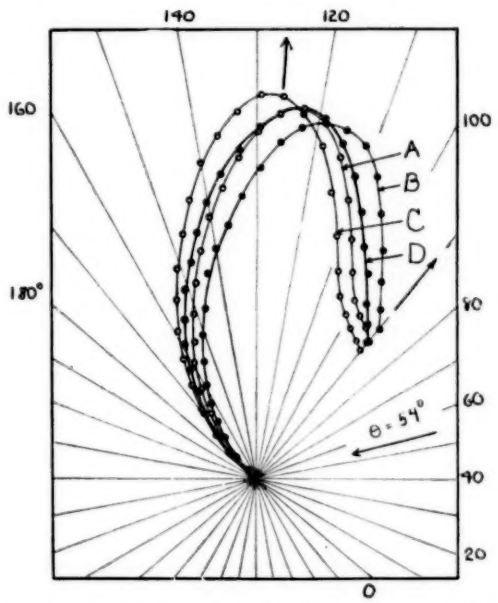

Fig. 9. Distribution of mercury atoms from NaCl as a function of the crystal temperature and the temperature of the incident beam, angle of incidence equals 54°.

Curve *A*: crystal, 50°C; beam, 170°C; in Table, No. 15
B: crystal, 350°C; beam, 170°C; in Table, No. 16
C: crystal, 50°C; beam, 500°C; in Table, No. 17
D: crystal, 350°C; beam, 500°C; in Table, No. 18

(Curves $B_{1,2,3}$). The effect of the same change of crystal temperature when the boiler is maintained at 500°C is shown in Fig. 8(b) in which $A_{1,2,3}$ and $B_{1,2,3}$ are for crystal temperatures of 350°C and 50°C, respectively. The angle of incidence was in this case 21.6°.

The effect of changing the boiler temperature while that of the crystal is maintained constant may be seen in Fig. 8(c and d). In Fig. 8(c), $A_{1,2,3}$ and $B_{1,2,3}$ are for boiler temperatures of 500°C and 170°C with the crystal maintained at 50°C while in 8(d) we have the corresponding situations with the crystal at 350°C.

We note the following changes which have occurred in all cases of NaCl studied: (1) The position of the maximum shifts towards a smaller angle (closer to the specular position) with decrease in crystal temperature. (2) The number of atoms scattered at random increases with a decrease in crystal temperature. (3) The corrected beam definitely becomes narrower with decrease in crystal temperature. (4) The position of the maximum shifts towards a smaller angle with increasing beam temperature.

That the same changes occur at larger angles of incidence may be roughly seen in Fig. 9 (A, B, C, D). Here the incident beam makes an angle of 54°

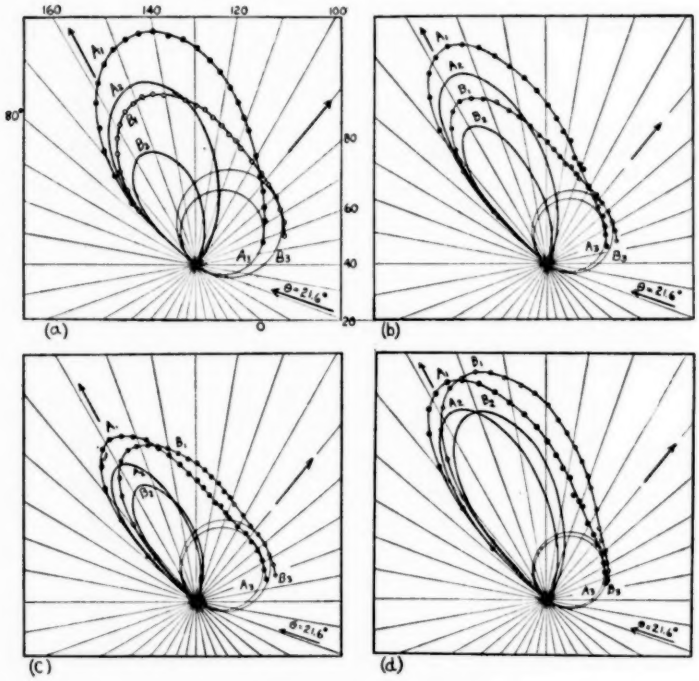

Fig. 10 (a, b, c, d). Distribution of mercury atoms from KBr as a function of the crystal temperature and the temperature of the incident beam.

(a) Curves $A_{1,2,3}$: crystal, 350°C; beam, 170°C; in Table, No. 8
$B_{1,2,3}$: crystal, 50°C; beam, 170°C; in Table, No. 7
(b) Curves $A_{1,2,3}$. crystal, 350°C; beam, 500°C; in Table, No. 10
$B_{1,2,3}$: crystal, 50°C; beam, 500°C; in Table, No. 9
(c) Cruves $A_{1,2,3}$. crystal, 50°C; beam, 500°C; in Table, No. 9
$B_{1,2,3}$: crystal, 50°C; beam, 170°C; in Table, No. 12
(d) Curves $A_{1,2,3}$: crystal, 350°C; beam, 500°C; in Table, No. 10
$B_{1,2,3}$: crystal, 350°C; beam, 170°C; in Table, No. 11

with the crystal surface. The conditions represented by the curves A, B, C, and D are given under the illustration. There has been no attempt to separate these curves into directed and random scattered components but the changes in the positions of the maxima are evidently quite similar to those which occur at smaller angles.

(3) *Reflection of Mercury from KBr and KCl*[11] *as a Function of Temperatures of Crystal and Beam.*

Fig. 10(a, b, c, d) and Fig. 11 are representative of the data available on KBr and KCl. Comparisons are made in the same way as in Fig. 8. The general form of these curves and the effects produced by changing crystal and boiler temperatures are evidently the same as in the case of NaCl discussed in detail above. For KI, however, the situation is quite different.

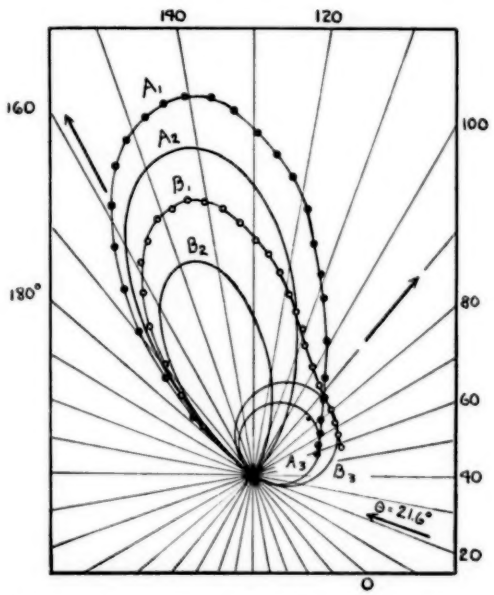

Fig. 11. Distribution of mercury atoms from KCl as a function of the temperature of the crystal.

Curves $A_{1,2,3}$: crystal, 350°C; beam, 170°C; in Table, No. 13
$B_{1,2,3}$: crystal, 50°C; beam, 170°C; in Table, No. 14

(4) *Reflection of Mercury from KI*

A crystal of KI heated to a temperature of 350°C was found to scatter an incident beam of mercury quite closely following the cosine law. In Fig. 12 is shown a case in which a beam of mercury was incident upon the crystal surface at an angle of 36°. The broken line is the circle upon which the points would fall were the cosine law followed. The experimental points through which the full line is drawn suggest that the scattering in this case is of a cosine nature with no indication of directed scattering.

(5) *Calculation of Directed and Random Scattered Atoms*

To obtain the relative number of atoms contributing to the cosine scattered and quasi-specular beam the following procedure was employed.

[11] The crystals of KBr, KCl and KI used in these experiments were kindly furnished us by Professor H. M. Randall of the University of Michigan.

It was found that the corrected beams A_2 and B_2 could be quite well represented by curves of the form

$$I = I_{\max} \cos m\theta$$

where m is some number chosen to fit the particular curve. m was always greater for lower crystal temperatures. These curves with properly chosen

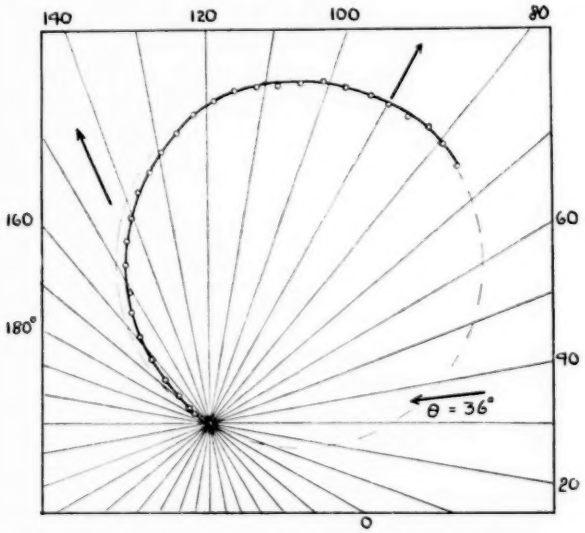

Fig. 12. Distribution of mercury atoms from KI: crystal, 350°C; beam, 170°C.

values of m can be fitted so closely with the experimental curves that intensities obtained from them by integration are considered to be accurate to within the limits of experimental error.

In Fig. 13 is shown a typical case in which cos 3θ has been used to represent a curve obtained with a NaCl crystal at 50°C and a cos 2.5θ curve to represent the case of the same crystal at 350°C. The dots represent the corrected experimental points.

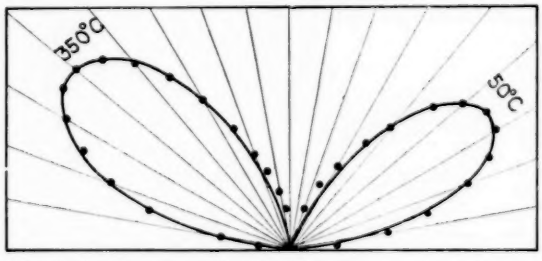

Fig. 13. Typical agreement obtained between corrected experimental curves and curves having form cos $m\theta$.

On the following basis one may write for the total relative intensity of the corrected quasi-specular beam

$$I_2 = 2I_{2(\max)} \int_0^{\pi/2m} \int_0^{\pi} \cos m\theta \sin \theta d\phi d\theta \qquad (1)$$

where $I_{2(\max)}$ is the corrected galvanometer reading on the maximum of the directed curve.

By the same integration we obtain the relative number of atoms contributing to the cosine beam, i.e., I_3, by putting $m=1$ and letting $I_{3(\max)}$ be the diameter of the circle representing these atoms.

To check on the accuracy of such integrations the following procedure is available. If the beam temperature is kept constant and curves are obtained for two different crystal temperatures the total number of atoms scattered must remain the same in both cases since the gauge records all atoms whether in the cosine or directed beam. The degree to which the following equation is true when experimental values are substituted serves as a check on the assumptions made during the integration.

$$I_{A_2} + I_{A_3} = I_{B_2} + I_{B_3} \tag{2}$$

where A and B represent different crystal temperatures, the beam remaining constant.

(6) *Discussion of the Table*

In the Table are presented the results available at this time. In column (1) is given the type of crystal. The numbers to the left of the crystal formula represent different crystals. Strict comparison outside of each parallel set of data is thus permissible only if this crystal identification number is the same, comparison then being restricted to changes in angle and relative percentages in the cosine and directed beam, since in changing the beam temperature it was not feasible to obtain exactly equal vapor pressure at the gun opening for the two different velocity distributions.

In column (2) is given the figure identification. In other words, if there is a number listed in this column corresponding to a certain curve then the experimental points of this run are plotted in one of the illustrations and may be identified by the corresponding number in the figure caption.

Column (4) lists the location of the maximum of the corrected directed beam while in column (6) is given the change in this maximum due to the change in crystal temperature given in column (5).

The value of m for which $\cos m\theta$ showed the best agreement with the directed beam is given in column (8). Columns (9) and (10) list the values of the relative intensities of cosine and directed scattering obtained as explained above. Column (11) shows to what degree equation (2) holds when values listed in (9) and (10) are substituted into this equation, thereby giving an approximation to the magnitude of the error introduced by the integrations.

In column (12) are listed the relative percentages of atoms contributing to the directed beam.

(7) *Reflection of Mercury from NaCl as a Function of the Vapor Pressure at the Gun Opening*

The work discussed up to this point has been done with the same apparatus under essentially constant conditions. Recently, the present writers

TABLE . *Reflection of mercury from crystals of sodium chloride, potassium chloride, potassium bromide and potassium iodide.*

1	2	3	4	5	6	7	8	9	10	11	12
Crystal	Figure Identification Number	Angle of Incidence	Angle of Reflection	Temperature of Crystal	Change in Angle of Reflection Due to Change in Crystal Temperature	Temperature of Mercury Beam	Curve Describing Directed Beam	Intensity of Directed Beam	Intensity of Cosine Beam	Total Intensity	Percent of Atoms Contributing to Directed Beam
(1) NaCl*		21.6°	31.5°	50°C	5.9°	170°C	cos 2.5θ	13.2	23.9	37.1	35.6%
		21.6	37.4	350		170	cos 2.25θ	19.1	19.7	38.8	49.3
(2) NaCl	1	21.6	30.	50	4.5	170	cos 2.9θ	7.	25.65	32.65	21.4
	3	21.6	34.5	350		170	cos 2.5θ	10.55	22.8	33.35	31.7
(2) NaCl		21.6	27.	50	3.5	375	cos 3θ	7.66	25.97	33.63	22.8
		21.6	30.5	350		375	cos 2.7θ	9.85	21.6	31.45	31.3
(2) NaCl	2	21.6	25.	50	2.5	500	cos 3θ	7.87	29.3	37.17	21.2
	4	21.6	27.5	350		500	cos 2.7θ	9.48	26.9	36.38	26.
(3) NaCl		21.6	32	50	4.	170	cos 2.7θ	7.21	35.8	43.01	16.8
		21.6	36	350		170	cos 2.25θ	10.3	32.2	42.5	24.2
(3) NaCl		21.6	29	50	3.5	375	cos 3θ	7.35	30.3	37.65	19.5
		21.6	32.5	350		375	cos 2.7θ	10.15	30.	40.15	25.3
(4) NaCl	5	18	36	50	6.	170	cos 3θ	4.36	21.1	25.46	17.1
		18	42	350		170	cos 2.5θ	7.57	17.9	25.47	29.7
(5) NaCl		18	32	50	5.	170	cos 3θ	7.93	20.6	28.53	27.8
		18	37	350		170	cos 2.5θ	13.2	15.8	29.	45.5
(6) NaCl		18	35	50	6	170	cos 3θ	6.26	19.	25.26	24.8
		18	41	350		170	cos 2.5θ	12.1	11.8	23.9	50.7
(7) NaCl		18	27	50	4	170	cos 3θ	4.16	9.25	13.41	31.
		18	31	350		170	cos 2.5θ	7.7	8.55	16.25	47.4
(8) NaCl		18	27	50	5	170	cos 3θ	4.95	10.3	15.25	32.4
		18	32	350		170	cos 2.5θ	8.75	8.7	17.45	50.1
(9) NaCl		18	40	350		170	cos 3θ	5.73	13.1	18.83	30.4
(10) NaCl		18	38	350		170	cos 2.5θ	10.4	16.7	27.1	38.4
(11) NaCl		18	30	350		170	cos 2.5θ	7.12	10.7	17.82	39.9
(12) KCl	14	21.6	33	50	3.1	170	cos 2.5θ	12.4	33.6	46.	26.9
	13	21.6	37.4	350		170	cos 2.2θ	23.2	26.1	49.3	47.
(13) KBr	7	21.6	27.5	50	5.5	170	cos 2.25θ	8.39	34.4	42.79	19.6
	8	21.6	33	350		170	cos 2θ	15.9	27.	42.9	37.1
(14) KBr	12	21.6	27	50	3.	170	cos 2.8θ	5.9	29.4	35.3	16.7
	11	21.6	30	350		170	cos 2.5θ	11.5	24.5	36.	31.8
(14) KBr	9	21.6	22	50	3	500	cos 3θ	5.8	24.4	30.2	19.2
	10	21.6	25	350		500	cos 2.8θ	8.88	21.5	30.38	29.3
(15) KI	19	36	(Incident beam scattered according to the cosine law)								
(16) NaCl	15	54	55.5**	50	6	170					
	16	54	61.5	350		170					
(16) NaCl	17	54	51.	50	5.5	500					
	18	54	56.5	350		500					
(17) NaCl		45	53	50	5.5	170					
		45	58.5	350		170					
(18) NaCl		45	52.5	50	7.5	170					
		45	59.	350		170					
(19) NaCl		54	49.5	50	6	170					
		54	55.5	350		170					
(20) NaCl		54	54.	50	5	170					
		54	59.	350		170					

* The numbers in column 1 denote different individual crystals. If the crystal position has not been changed the numbers in column 1 are the same. Thus the three sets of data opposite (2) NaCl were taken with the same crystal which was kept fixed while the crystal and beam temperature were varied.

** The remainder of the angles listed in this column represent the peak of the uncorrected beam.

and Mr. R. R. Hancox have experimented with other ionization gauges resulting in the development of a gauge of greater sensitivity which could be used with considerably lower vapor pressures. In brief, with 20 m.a. electron current coupled with increased ionization efficiency, an increase in sensitivity over the old gauge by a factor of about 25 was obtained.

In Fig. 14 is shown a group of curves taken with this new gauge. The reflecting crystal was NaCl, the incident beam making an angle of 20° with the crystal surface. In the case of curves *A* and *B*, the crystal was held at a temperature of 350°C while for curve *C* the temperature of the crystal was approximately 100–150°C. The vapor pressures at the gun opening for *A*, *B* and *C* were 0.5, 2 and 10 mm, respectively.

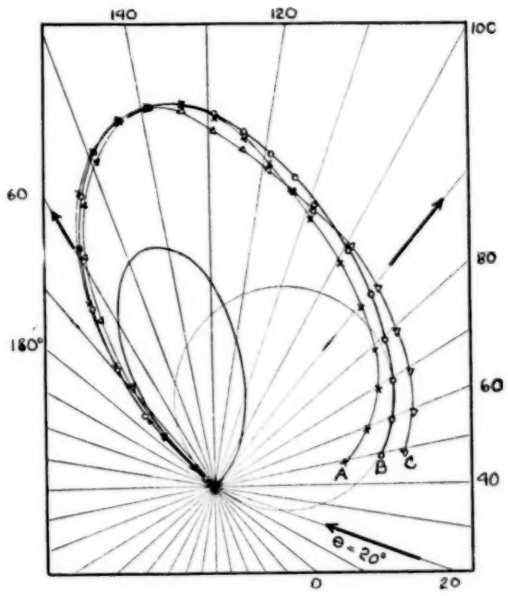

Fig. 14. Reflection of mercury from NaCl as a function of the vapor pressure at the gun opening: *A*, 0.5 mm of Hg; *B*, 2 mm; *C*, 10 mm.

It can be seen that over this range of vapor pressures the general character of the curves remains the same. The curve *C* which is taken at a lower crystal temperature has changed in agreement with the findings discussed earlier. The amount of random scattering in the case of this particular crystal is rather large but other crystals of NaCl have been found which give similar results.

It is evident from Fig. 14, though the mean free path at the gun opening for a pressure of 0.5 mm is small compared to the diameter of the opening, there is little change brought about when the pressure is increased further by a factor of 20. This increases our confidence in the assumption that in the incident atomic beam deviations from a Maxwell distribution of velocities are not great under the conditions described earlier.

(8) *Rotation of the Plane of the Crystal*

A second experiment using the new gauge was as follows: The crystal was mounted so that during a run it could be rotated on an axis perpendicular to the plane of the crystal face. Thus runs could be made under comparable conditions with the crystal oriented so that rows of alternate ions were parallel and perpendicular to the plane of the beam while by a rotation of 45° rows of similar ions could be brought into this position.

In Fig. 15 curve *A*, rows of alternate ions are parallel and perpendicular to the plane of the beam while curve *B* is taken under identical conditions save that the crystal was rotated in its plane through 45° bringing rows of similar ions parallel and perpendicular to the plane of the beam. Curve *C* represents a half-way position. For these data the crystal was held at 350°C, the beam was incident at 19° and the pressure at the gun opening was 1 mm.

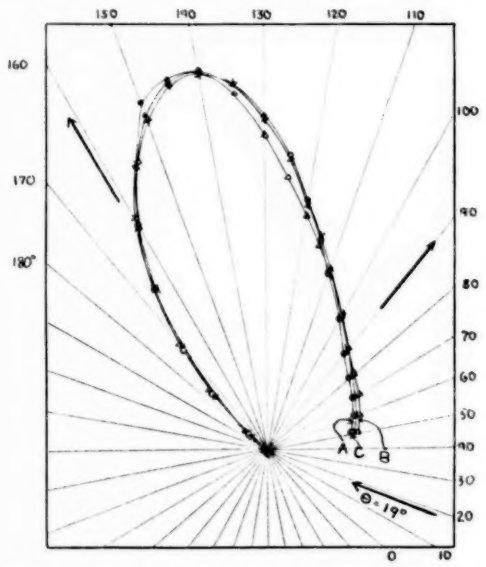

Fig. 15. Distribution of mercury atoms from NaCl as the crystal is rotated about an axis perpendicular to the plane of its face.

Clearly, if there are any changes brought about by change in crystal orientation, they are quite small and beyond the accuracy of the present method of experiment.

Summary and Discussion

Zinc and cadmium atomic beams incident upon rocksalt give rise to directed reflection which for large angles of incidence is specular, at least within the limits of accuracy of the deposit method used in studying the phenomena. Even with these lighter atoms, however, observations at small angles of incidence (6–10°, measured from the crystal surface) have shown unmistakable departures from specular reflection. It seems very probable that the process involved in the reflection of these lighter elements is the same which gives

rise to the various phenomena reported in this paper for the case of mercury. However, the deviation of the directed reflected beam from the direction of specular reflection appears to be considerably greater with mercury than with either cadmium or zinc.

The mechanism involved in the reflection process must then account, qualitatively at least, for the following facts:

(1) The existence of a directed beam.

(2) The deviation of the direction of maximum intensity in this beam from the direction of specular reflection.

(3) The decrease of this deviation with higher beam and lower crystal temperatures and with lighter atoms.

(4) Better definition of the directed beam (narrowing of the beam) at low crystal temperatures, accompanied by an increase in the relative amount of random scattering.

The existence of directed scattering is sufficient to show that the scattering process is not merely condensation and re-evaporation. The possibility of reflection because of the abrupt change in potential energy at the crystal boundary must be considered. Johnson[12] has pointed out that this process is analogous to that of reflection of light from an imperfect (slightly rough) mirror and has considered that the effect of increased thermal agitation at higher crystal temperatures will produce the same effect as increased roughness of the mirror. That is to say it should result in increased random (cosine) scattering. In the present experiments the opposite effect has been observed. That is, the intensity of cosine scattering is always greatest at low crystal temperatures.

Another factor which might enter at low temperatures is the formation of a gas layer on the crystal surface, and this would lead to increased cosine scattering. It would not however account for the fact that the definition of the directed beam is better at low crystal temperatures and this increased definition or narrowing of the beam is quite consistently observed. Neither is it evident how the presence of a gas layer could account for the maximum of the directed scattering being shifted towards the direction of specular reflection.

There remain the possibilities of scattering processes analogous to surface and space-grating diffraction in optics. The wave-lengths of the heavy atoms with which we deal here are so short that we could scarcely expect surface-grating phenomena except perhaps at grazing incidence. At first sight there is the same objection to space-grating phenomena, but we must remember that in this case there occurs in the wave equation a quantity[13,7] whose effect is analogous to that of the refractive index in optical problems. Moreover in the case where the change in potential energy at the crystal boundary corresponds to the existence of repulsive forces the refractive index

$$\mu = (1 - \phi/\tfrac{1}{2}m\bar{v}^2)^{1/2}$$

[12] T. H. Johnson, J. Franklin Inst. **210,** 135 (1930).

[13] Bethe, Naturwiss. **15,** 787 (1927).

is less than unity so that it will operate to increase the apparent wave-length inside the crystal. This perhaps requires us to imagine that the atoms reflected from the crystal penetrate through several layers of the crystal lattice, and to this we must admit an intuitive repugnance. However, the chief basis of this reaction may be merely our intuitive "billiard ball" picture of the atom, leading us to imagine that such a process must lead to disruption of the crystal.

If we may be permitted to lay aside this objection for the moment we can show that the space-grating picture possesses certain advantages in that it appears to give a fairly good qualitative representation of the experimental facts, for it is apparent that for suitably small values of the refractive index there might arise phenomena closely analogous to the familiar Bragg reflection of x-rays, and this is the most obvious explanation of the existence of specular reflection. The concept of the resolving power of the crystal for de Broglie waves, determined essentially by the number of crystal planes effective in scattering, appears as a possible explanation of the fact that the directed beam is more sharply defined and relatively less intense at lower crystal temperatures, for decreased thermal agitation of the crystal should increase its resolving power in this case just as in the optical case. The fact that the direction of maximum intensity in the directed beam does not coincide with the direction of specular reflection suggests that the effective refractive index may be a complex quantity as it is in the optical case when absorption is taken into account.

The ideas advanced by Duane[14] and Compton[15] in connection with x-ray diffraction may lead to a clearer picture, as the emphasis is placed on the particle rather than the wave aspect of the situation and the application of our ordinary notions of conservation of momentum and energy is more evident. The relative translatory motion of a crystal and an atom is periodic as displacement through a distance equal to the lattice space brings the system back to its initial configuration. The quantization[16] of such a periodic motion leads at once to equations which have the form of Bragg's x-ray equation if h/mv is interpreted as a wave-length.

The mass of the crystal entering into the equations expressing the laws of conservation of energy and momentum is the mass of that part which behaves as a rigid body, i.e., suffers no distortion. Scattering in which momentum and energy are communicated to a group of atoms acting as a rigid body has been called by Williams[17] coherent scattering or the atoms are said to scatter coherently. This is a convenient term, suggesting as it does the close connection between the wave and the particle aspects of the situation. From the equations of conservation of energy and momentum it is at once evident that the larger the portion of the crystal which scatters coherently the less

[14] W. Duane, Proc. Nat. Acad. Sci. **9**, 158 (1923).

[15] A. H. Compton, Proc. Nat. Acad. Sci. **9**, 359 (1923).

[16] P. Jordan, Zeits. f. Physik **37**, 376 (1926).

[17] E. J. Williams, Proc. Camb. Phil. Soc. **24**, 343 (1928).

will be the energy communicated to the crystal and the more nearly will the direction of rebound of the reflected atom make an angle with the crystal surface equal to the angle of incidence. Increased thermal agitation of the crystal at higher temperatures will reduce the size and mass of the coherently scattering groups, and the reflection will depart more and more from the specular direction. It is evident too that for a given size of coherently scattering groups the deviation from the specular direction will be less for light atoms, all of which is in accord with observation.

THE LOW TEMPERATURE ROTATIONAL HEAT CAPACITIES AND THE RELATIVE AMOUNTS OF THE NUCLEAR SINGLET, TRIPLET AND QUINTET SYMMETRY MODIFICATIONS OF METHANE

By D. S. Villars and G. Schultze
Research Laboratory, Standard Oil Company (Indiana)
and School of Chemistry, University of Minnesota

(Received July 11, 1931)

Abstract

There should be three noncombining varieties of methane, the nuclear singlet, triplet and quintet, and two of ammonia, the nuclear doublet and quadruplet, just as there are two of hydrogen, the nuclear singlet and triplet ("para" and "ortho" hydrogen). In this paper the statistical weights of the rotational states have been evaluated and used in conjunction with the Raman spectra data to calculate the heat capacities of each separate variety of methane, of the true equilibrium mixture and of the "frozen equilibrium" mixture. The feasibility of demonstrating experimentally the existence of these different varieties of methane is discussed in the light of the present calculations.

THE elegant experiments of Bonhoeffer, Harteck[1] and co-workers and of Eucken[2] who experimentally verified the predicted[3] existence of the two symmetry modifications of hydrogen, nuclear singlet and triplet (commonly designated by the perverted[4] nomenclature, para and ortho-hydrogen) led one to immediate speculations[1] concerning similar modifications of other compounds containing more than one hydrogen atom to the molecule. Owing to a discovery by one of us[5] of some peculiar differential vapor pressure effects with methane at liquid air temperature treated with and without active charcoal, it was deemed desirable to make calculations of the relative amounts of the different forms, their specific heats and the average specific heat of the mixture in true equilibrium and of the one in the frozen metastable equilibrium, since it was by such differences that Bonhoeffer was able to make his

[1] Bonhoeffer and Harteck, Naturwiss **17,** 182 (1929); Zeits. f. phys. Chem. **B4,** 113 (1929); Sitzb. Preuss. Akad. Wiss. **103,** (1929). Abhandl. a. d. Kaiser Wilhelm nst. f. Phys. u. El. Chem. **12,** 121, 129, 305 (1929).

[2] Eucken, Naturwiss **17,** 182 (1929); Eucken and Hiller, Zeits. phys. Chem. **B4,** 142–157 (1929).

[3] Heisenberg, Zeits. f. Physik **41,** 239 (1927); Hund, ibid. **42,** 93 (1927).

[4] Cf. Eucken and Hiller, Zeits. f. phys. Chem. **B4,** 142 (1927) their footnote 4; Mulliken, Trans. Faraday Soc. **25,** 634–645 (1929), especially p. 638 his footnote 16.

[5] G. S. These experiments were first made during the winter of 1929–30. Later experiments more carefully performed showed that the observed differences in vapor pressure might be ascribed to delay in reaching equilibrium between liquid and vapor as well as to a change from the "frozen" to the pure equilibrium which was at first postulated. A minor effect may still be found to exist by means of an improved differential method for determining the vapor pressure which we intend to apply. In the meanwhile Harteck and Schmidt (Naturwiss. **18,** 282 (1930) have looked unsuccessfully for such an effect in nitrogen, methane and chlorine.

famed experiments. In this paper we wish to present the results of this calculation, reserving for a possible subsequent one the description of the experimental work which has been in progress now for over a year.

THEORETICAL

In order to calculate the heat capacity of a gas, it is necessary to know the energy levels ϵ_i and their *a priori* probabilities. When these are known, use is made of the familiar equations:

$$n_i = n_0 p_i e^{-\epsilon_i/kT} \tag{1}$$

$$E = N \frac{\sum_i n_i \epsilon_i}{\sum_i n_i} \tag{2}$$

$$MC_v = \partial E/\partial T. \tag{3}$$

If we neglect stretching effects, the rotational levels are given by the formulae

$$\epsilon_j = j(j+1)h^2/8\pi^2 I \tag{4}$$

if the molecule is rod-shaped, or

$$\epsilon_{j,\tau} = (h^2/8\pi^2)\left[j(j+1)/A + (1/C - 1/A)\tau^2\right] \qquad \tau \leq j \tag{5}$$

if it is shaped like a symmetrical top.

The *a priori* probabilities measure the degeneracy of the energy levels and may be looked upon as the number of levels which happen to have exactly the same energy. The vector model of the molecule is an accurate guide in simple cases for finding the number of these levels, for it is the number of quantized orientations which the angular momentum may take on in a force field, $(2j+1)$ for the rod shaped molecule or $(2j+1)^2$ for the symmetrical top, if we lump all possible values of τ associated with each j. The rigorous rule is to be found from the application of the Pauli principle in quantum mechanics. The *a priori* probability is the number of *different ways* of combining subsidiary eigenfunctions to get a total eigenfunction completely antisymmetric[6] in the protons. The total eigenfunction may be ordinarily[7] taken as a product of the electronic, vibrational, rotational and nuclear eigenfunctions, which we call subsidiary.

$$\psi = \psi_{\text{el}}\psi_{\text{vibr}}\psi_{\text{rot}}\psi_{\text{nuclei}} \tag{6}$$

[6] An antisymmetric function, A, is defined as one which has its sign changed by interchanging the designations of two like particles; a symmetric function, S, is defined as one which suffers no change from such an interchange. If the like particles are electrons, we speak of symmetry characteristics in (regard to) the electrons; if the like particles are protons, symmetry in the protons; if the like particles are nuclei, symmetry in the nuclei. Symmetry in the electrons is of interest to a discussion of the electron multiplicities. In the present problem we are interested only in the symmetry characteristics in the nuclei (or protons—the designations are equivalent for hydrogen) and hereafter shall be understood as referring only to the latter type.

[7] Hund, Zeits. f. Physik **43,** 805 (1927).

If the molecule is in its lowest electronic and vibrational state, they may be disregarded since they are symmetric (exceptions occur when there is an extra unlike atom in the molecule, with the result that the lowest vibrational state may be double, both A and S) and do not change the symmetry character of any function which they multiply. In the case of two equal nuclei, the products obey the rule

$$\left.\begin{aligned} S \times S &= S \\ S \times A &= A \\ A \times A &= S \end{aligned}\right\} \tag{7}$$

As an illustration of how these rules are applied to the problem of *a priori* probabilities, let us review the case for hydrogen. Hund[8] has shown that the even numbered rotational states are S in the nuclei and the odd ones are A. There are $(2j+1)$ different eigenfunctions which belong to each ϵ_j rotational level. For each successive value of j, there are therefore, beginning with zero, $1S$, $3A$, $5S$, $7A$, etc. eigenfunctions. Since to obey the Pauli principle, the total eigenfunction (6) must be A, each S eigenfunction listed above may combine with only an A function of the nuclear spin (and not with a S one) while each A above must combine with a S nuclear spin function. If we represent[9] the two spin eigenfunctions (corresponding to the two orientations) by α and β, we have the following possible combinations,

$$\left.\begin{aligned} &\alpha_1\alpha_2 \\ &\alpha_1\beta_2 + \alpha_2\beta_1 \\ &\beta_1\beta_2 \end{aligned}\right\} S \quad \alpha_1\beta_2 - \alpha_2\beta_1\, A \tag{8}$$

and see that there are $3S$ and $1A$ ones. This means that the *a priori* probabilities of the successive rotational states of hydrogen are 1, 3×3, 1×5, 3×7, 1×9, etc. and since there is very little coupling force to re-orient the nuclear spins in the molecule, a system of nuclear triplet molecules will act as a distinct molecular species entirely independently of a system of nuclear singlet molecules. If the temperature is lowered greatly, the triplet molecules fall into their lowest rotational state ($j=1$) and the singlet molecules into their lowest ($j=0$) and only after a catalytic action which involves a dissociation of the molecules into atoms will the triplet kind change into the singlet variety[10] until equilibrium is established.

When we wish to extend these considerations to the case of three like atoms, we find eigenfunctions which are not completely symmetric or antisymmetric, occurring along with those which are. Hund[11] has introduced the

[8] Hund, Zeits. f. Physik **42,** 93 (1927).

[9] Pauli, Zeits. f. Physik **43,** 601–623 (1927).

[10] We hold with Rodebush that there are only two varieties of hydrogen and that the definition of Giauque (J. Am. Chem. Soc. **52,** 4812, 4822 (1930); Giauque and Johnston, ibid. **50,** 3221 (1928) which calls each molecule in a different energy level a different kind is an unjustified distortion of the word's commonly accepted meaning.

[11] Hund, Zeits. f. Physik **43,** 788 (1927).

term "symmetry character" to designate these different kinds and has discussed the rules of manipulating them. $S(3)$ is an eigenfunction, S in the interchange of two of any three particles; $S(2+1)$ is S in a certain pair but not for any other; and $S(1+1+1)$ is S in none. Hund has also shown that the latter character symmetric in no pair is completely antisymmetric $A(3)$, that the first completely symmetric is antisymmetric in no pair $A(1+1+1)$ and that the second is reciprocal to itself, i.e., is likewise $A(2+1)$.

As an illustration, we take the three different eigenfunctions, a, b, and c as characterizing successively the three equal particles, 1, 2, and 3.

$$\begin{array}{lcccccc} S(3) & = a_1b_2c_3 + a_1b_3c_2 + a_2b_1c_3 + a_2b_3c_1 + a_3b_1c_2 + a_3b_2c_1 \\ S(2+1) & = & - & + & - & + & + \\ S(1+1+1) & = & - & - & + & + & - \end{array} \tag{9}$$

The reader may easily verify the fact that the sign of $S(3)$ remains unaltered on interchanging any two of the three particles, that of $S(1+1+1)$ is changed, and that of $S(2+1)$ remains unaltered if one interchanges particles 1 and 2, but a new function is obtained on interchanging 3 with one of the other two. Hund and others call the latter eigenfunction "degenerate." Whether we should count this degeneracy in computing statistical weights may be seen by setting up the spin functions for three like nuclei, and comparing the results with those given by the vector model, which we know gives the correct multiplicity. Each nucleus has two orientation possibilities. Therefore, there are 2^3 permutations of the eigenfunctions as well as orientations of the component vectors. In the following tabulations it may thus be seen that the complete degeneracy must be counted, otherwise a dissociation of the molecule into separate hydrogen atoms would create new nuclear spin statistical weights, which is impossible.

Three nuclei

$$\begin{array}{lll} \alpha\alpha\alpha & S(3) & \\ \alpha\alpha\beta & S(3) & S(2+1) \\ \alpha\beta\beta & S(3) & S(2+1) \\ \beta\beta\beta & S(3) & \\ \text{degeneracy} & \text{two fold} & \end{array} \tag{10}$$

Four nuclei

$$\begin{array}{llll} \alpha\alpha\alpha\alpha & S(4) & & \\ \alpha\alpha\alpha\beta & S(4) & S(3+1) & \\ \alpha\alpha\beta\beta & S(4) & S(3+1) & S(2+2) \\ \alpha\beta\beta\beta & S(4) & S(3+1) & \\ \beta\beta\beta\beta & S(4) & & \\ \text{degeneracy} & \text{three} & \text{two} & \end{array} \tag{11}$$

The two doublet systems represented are roughly analogous to the different systems of same multiplicity and like L so often encountered in a supermultiplet in electronic spectra. For four nuclei the total number of permutations including degeneracies is 16, as is also the total number of independent orientations of the four nuclei. The symmetry characters with more than two terms in the argument are excluded because, as Hund has shown, these do not occur when the spin can take on not more than two values. The $S(2+2)$ characters are missing from the $\alpha\beta\beta\beta$ case since there is only one pair of different eigenfunctions. How this works out can be seen by writing equation (9) with $b=a$. The function for $S(1+1+1)$ would come out identically zero.

The results of Hund show that in a molecule like NH_3 the number of ψ_{vibr}s of the lowest state are one $S(3)$ and one $S(1+1+1)$. The number and kind of rotational eigenfunctions are given in Table I.

TABLE I. *Rotational eigenfunctions of ammonia.*

τ	$\equiv 0$		$\equiv 1, 2$		$\equiv 3$	
j_{even}	$(2j+1)$	$S(3)$	$2(2j+1)$	$S(2+1)$	$(2j+1)$ $(2j+1)$	$S(3)$ $S(1+1+1)$
j_{odd}	$(2j+1)$	$S(1+1+1)$	$2(2j+1)$	$S(2+1)$	$(2j+1)$ $(2j+1)$	$S(3)$ $S(1+1+1)$

where $\tau \equiv 1$ means $(\tau-1)/3$ is a positive integer (can be zero). For each positive value of τ there is a negative one, which we take account of by the factor 2.

Likewise, the results of Elert[12] show that, in the ground vibrational state of methane, there is one $S(4)$ and one $S(1+1+1+1)$ function. In our discussion we shall discard the use of the "half system" proposed by Hund and used by Elert, and translate the latter's results into terms of the "complete" system, at the same time keeping account of the two different vibrational symmetry characters of the lowest vibrational state. This is less confusing in making the ultimate count of the different ways of getting a completely antisymmetric eigenfunction. As to the rotational states, all three moments of inertia are equal and hence formula (5) applies, giving an *a priori* weight of $(2j+1)^2$ to each j term, the fine structure being completely degenerate. Elert has demonstrated that the following distribution of these $(2j+1)^2$ characters among the different j states holds, at least for the first few states, and believes the rule is general, although he could not prove it.

TABLE II. *Rotational eigenfunctions of methane.*

j	$S(4)$	$S(3+1)$	$S(2+2)$
$\equiv 0$	$(j/6+1)(2j+1)$	$(3j/2)(2j+1)$	$(j/3)(2j+1)$
1	$[(j-1)/6](2j+1)$	$[(3j+3)/2](2j+1)$	$[(j-1)/3](2j+1)$
2	$(1/3)(j/2-1)(2j+1)$	$(3j/2)(2j+1)$	$[(2/3)(j/2-1)+2](2j+1)$
3	$[(j-3)/6+1](2j+1)$	$[(3j+3)/2](2j+1)$	$[(j-3)/3](2j+1)$
4	$(1/3)(j/2+1)(2j+1)$	$(3j/2)(2j+1)$	$(2/3)(j/2+1)(2j+1)$
5	$[(j-5)/6](2j+1)$	$[(3j+3)/2](2j+1)$	$[(j-5)/3+2](2j+1)$

[12] Elert, Zeits. f. Physik **51**, 6–33 (1928).

In order to compute the *a priori* probabilities we now proceed as follows. From (11) we see there are five $S(4)$ spin eigenfunctions, three times three $S(3+1)$ and one times two $S(2+2)$. We desire to count the total number of ways we can combine the functions (6) to get a completely antisymmetric function, $S(1+1+1+1)$. In doing this we must keep in mind that, according to Hund and Elert only one-fourth of the products of two $S(2+1)$ or two $S(2+2)$ functions can be combined to a completely symmetric function and one-fourth to a completely antisymmetric one, while one-ninth of the combinations of two $S(3+1)$ functions multiplied together can be resolved into a completely symmetric function.[13] Table III gives the results, keeping separate those arising from each nuclear spin state, as these form different non-combining varieties of methane, just as they form the two non-combining varieties of hydrogen.

TABLE III. *Rotational weights of different varieties of methane.*

j	$S(4)$ Quintet	$S(3+1)$ Triplet	$S(2+2)$ Singlet
0	5×1	0	0
1	0	$3\cdot3$	0
2	0	$5\cdot3$	$5\cdot2$
3	7	$7\cdot6$	0
4	9	$9\cdot6$	$9\cdot2$
5	0	$11\cdot9$	$11\cdot2$
6	$13\cdot2$	$13\cdot9$	$13\cdot2$
7	15	$15\cdot12$	$15\cdot2$
8	17	$17\cdot12$	$17\cdot4$
9	$19\cdot2$	$19\cdot15$	$19\cdot2$
10	$21\cdot2$	$21\cdot15$	$21\cdot4$

CALCULATIONS

Before making use of Eqs. (1) to (4), we shall introduce the substitution

$$\sigma = h^2/8\pi^2 IkT \tag{12}$$

$$= 0.716\Delta/T \tag{13}$$

where

$$\Delta = 2B = 2h/8\pi^2 cI \text{ cm}^{-1} \tag{14}$$

is the spacing in wave numbers of the lines in the normal band spectrum.

Unfortunately, in the case of methane, we are entangled with an ambiguity in interpretation of the experimental data. Cooley[14] found three different spacings, 5.41 (7.7μ band), 9.77 (3.31μ) and 15.3 cm^{-1} (3.5μ band), of which 9.77 most likely represents the moment of inertia of the molecule (5.66×10^{-40} gm. cm^2). This is near the value obtained from Raman spectra,[15] 5.17×10^{-40} corresponding to an absorption-emission line spacing of $\Delta=2$

[13] Cf. Ludloff, Zeits. f. Physik **57**, 227–241 (1929).
[14] Cooley, Astrophys. J. **62**, 73–83 (1925).
[15] Dickinson, Dillon and Rasetti, Phys. Rev. **34**, 582 (1929).
[16] Mecke, Zeits. f. phys. Chem. **B7**, 108–129 (1930).

$\times 5.363\ \text{cm}^{-1}$, and since this value was capable of the more accurate measurement we shall take it to translate σ into temperature.

$$\sigma = 0.716 \times 10.726/T.$$

Further support for the correctness of this moment of inertia as against that calculated from the other spacings 10.2 and 3.61×10^{-49}, lies in Mecke's[16] comparison of the CH, NH and OH nuclear distances in the free radicals with the corresponding distances in the saturated hydrides. The use of $I = 10.2 \times 10^{-40}$ would give a CH distance out of line with the trend in the other molecules of the series.

Abbreviating the summation of the statistical weights by

$$Q = \sum_i n_i/n_0 = \sum_i p_i e^{-j(j+1)\sigma} \tag{15}$$

and changing the variable from T to σ in (3) we get

$$C_i/R = (\sigma^2/Q_i^2)\left[Q_i d^2Q_i/d\sigma^2 - (dQ_i/d\sigma)^2\right] \tag{16}$$

$$= \sigma^2 d^2 \ln Q/d\sigma^2 \tag{16a}$$

where i refers respectively to the nuclear quintet, triplet and singlet forms. The values of Q_i are to be obtained from (15) and Table III and are, up to the 100σ power in the exponent:

$$^5Q_1/5 = 1 + 7e^{-12\sigma} + 9e^{-20\sigma} + 26e^{-42\sigma} + 15e^{-56\sigma} + 17e^{-72\sigma} + 38e^{-90\sigma} \tag{17}$$

$$^3Q_2 = 9e^{-2\sigma} + 15e^{-6\sigma} + 42e^{-12\sigma} + 54e^{-20\sigma} + 99e^{-30\sigma} + 117e^{-42\sigma} + 180e^{-56\sigma} + 204e^{-72\sigma} + 285e^{-90\sigma} \tag{18}$$

$$^1Q_3 = 10e^{-6\sigma} + 18e^{-20\sigma} + 22e^{-30\sigma} + 26e^{-42\sigma} + 30e^{-56\sigma} + 68e^{-72\sigma} + 38e^{-90\sigma}. \tag{19}$$

The coefficients of the terms in the above expressions as well as of those for the various derivatives are arranged in Table IV, at the bottom of which are given the calculated values of corresponding sums for four different values of σ, chosen to represent temperatures ranging from below the boiling point of liquid hydrogen to those of liquid air and above. In Table V are given the corresponding rotational specific heats obtained by applying Eq. (16). An idea of the rapidity of convergence of the different series for the least value of σ (0.0430) and the consequent accuracy of the summations may be gained from Table VI in which are given the ratio of the next to last to the last term taken and the percent of the whole sum (up to and including the last term) which the last term constitutes. From this we see that the series for Q_1 is still diverging where we stopped off, (although it converges later on) and that for Q_2 is just beginning to converge. At the other temperatures the series are on the whole satisfactorily convergent. The values in parentheses are those for $\sigma = 0.0861$.

TABLE IV. *Summation coefficients.*

	Q_i			$-dQ_i/d\sigma$			$Q_i d^2Q_i/d\sigma^2-(dQ_i/d\sigma)^2$		
	$i=1$	2	3	1	2	3	1	2	3
	÷5			÷5			÷25		
m									
0	1								
2		9			18				
6		15	10		90	60			
8								2160	
12	7	42		84	504		1008		
14								37800	
18								22680	
20	9	54	18	180	1080	360	3600		
22								157464	
26								158760	35280
30		99	22		2970	660			
32							4032	843696	
36								855360	126720
42	26	117	26	1092	4914	1092	45864	1347192	
44								1684800	
48								2274480	336960
50								534600	39600
54							163800	4422600	
56	15	180	30	840	10080	1680	47040		
58								4723920	
62							113256	9807912	976512
68							203280	14636160	
72	17	204	68	1224	14688	4896	88128	1667952	82368
74								8996400	
76							174960	12597120	699840
78								13329360	2962080
84							428400	30844800	
86								12046320	446160
90	38	285	38	3420	25650	3420	307800		
92							413712	49650624	3309696
96								30164400	2681280
98							76440	4127760	152880
Sum									
$\sigma=0.0430$	16.168	145.614	32.239				72999	7543516	314364
.0861	5.970	53.733	11.940				6282.1	540870.	27062
.1937	1.880	16.369	3.576				201.92	10711	388.24
.3873	1.071	6.043	0.987				11.241	328.33	1.6087

$\text{Sum}_i = \sum_i a_i e^{-m\sigma}$ where a is value given in upper part of table.

TABLE V. *Rotational heat capacities of separate forms of methane.*

T	σ	σ^2/Q_i^2			C_i/R		
		$i=1$	2	3	Quintet 1	Triplet 2	Singlet 3
178°K	0.00430	2.834×10^{-7}	8.737×10^{-8}	1.782×10^{-6}	0.5173	0.659	0.5603
89	.0861	8.316×10^{-6}	2.566×10^{-6}	5.196×10^{-5}	1.3059	1.3881	1.4067
40	.1937	4.244×10^{-4}	1.400×10^{-4}	2.934×10^{-3}	2.1433	1.4999	1.1380
19.8	.3873	5.232×10^{-3}	4.107×10^{-3}	1.540×10^{-1}	1.4701	1.3485	0.2477

TABLE VI. *Convergence data for series.*

Ratio $\frac{\text{next to last term}}{\text{last}}$			Percent of whole which last term constitutes	
	$\sigma=0.043$	(0.0861)	0.043	(0.0861)
Q_1	0.98	(2.1)	5	(0.3)
$Q_1d^2Q_1/d\sigma^2-(dQ_1/d\sigma)^2$	7	(9.1)	1.5	(0.3)
Q_2	1.5	(4.7)	4	(0.2)
$Q_2d^2Q_2/d\sigma^2-(dQ_2/d\sigma)^2$	8.	(8.7)	0.8	(0.2)
Q_3	4	(8.4)	2.5	(0.1)
$Q_3d^2Q_3/d\sigma^2-(dQ_3/d\sigma)^2$	20	(21)	0.6	(0.1)

In order to draw curves for the heat capacities we wish to know their asymptotic behavior at very low and very high temperatures. In the former case σ becomes large and the first terms in the series, the coefficients of which are given in Table IV, are the only important ones. Using solely these, the heat capacities were calculated for $\sigma = 0.5$ and 1.0 ($T = 15.4$ and 7.7°K respectively) and the corresponding points were used in plotting the curves.

The extrapolation of the curves in the other direction is more difficult. At high temperatures, σ becomes small and the series may be replaced by integrals

$$Q = \int_0^\infty p(2j+1)e^{-j(j+1)\sigma}dj \tag{20}$$

where $p(2j+1)$ is the number of rotational eigenfunctions of methane given in Table II. Since p is expressed analytically only for every sixth value of j and is a different function depending on whether one starts with 0, 1, 2, 3, 4 or 5 we must split the above integral into six.

$$Q = \int_0 (p_0) + \int_1 (p_1) + \int_2 (p_2) + \cdots \int_5 (p_5). \tag{21}$$

Changing variables in each case, we get for the $S(4)$ functions

$$\begin{aligned}
p_0 &= (j+6)/6 = q+1 \quad & j &= 6q \\
p_1 &= (j-1)/6 = q \quad & j &= 6q+1 \\
p_2 &= (j-2)/6 = q \quad & j &= 6q+2 \\
p_3 &= (j+3)/6 = q+1 \quad & j &= 6q+3 \\
p_4 &= (j+2)/6 = q+1 \quad & j &= 6q+4 \\
p_5 &= (j-5)/6 = q \quad & j &= 6q+5
\end{aligned} \tag{22}$$

and leaving all five intervening terms in the integral, for the other five integrals, $dj \rightarrow dq$ (not$\rightarrow 6\,dq$) we have

$$\begin{aligned}
\int_0^\infty (p_0) &= \int_0^\infty (q+1)(12q+1)e^{-6q(6q+1)\sigma}dq \\
\int_1^\infty (p_1) &= \int_0^\infty q(12q+3)e^{-(6q+1)(6q+2)\sigma}dq \\
\int_2^\infty (p_2) &= \int_0^\infty q(12q+5)e^{(6q+2)(6q+3)\sigma}dq \\
\int_3^\infty (p_3) &= \int_0^\infty (q+1)(12q+7)e^{-(6q+3)(6q+4)\sigma}dq \\
\int_4^\infty (p_4) &= \int_0^\infty (q+1)(12q+9)e^{-(6q+4)(6q+5)\sigma}dq \\
\int_5^\infty (p_5) &= \int_0^\infty q(12q+11)e^{-(6q+5)(6q+6)\sigma}dq.
\end{aligned} \tag{23}$$

It may be shown that

$$\int_0^\infty (q+a)[2(6q+b)+1]e^{-(6q+b)(6q+b+1)\sigma}dq$$
$$= (\tfrac{1}{6}\sigma^{-1})\{ae^{-b(b+1)\sigma} + e^{\sigma/4}\pi^{1/2}\sigma^{-1/2}/12$$
$$- (e^{\sigma/4}/6)[b+\tfrac{1}{2} - (b+\tfrac{1}{2})^3\sigma/3 + (b+\tfrac{1}{2})^5\sigma^2/10 - (b+\tfrac{1}{2})^7\sigma^3/42\cdots]\}. \quad (24)$$

Inserting the appropriate values of a and b from (23) and repeating the calculation in a similar fashion for the $S(3+1)$ and $S(2+2)$ functions we get

$$^5Q_1 = 5(\pi^{1/2}\sigma^{-3/2}/12)\{1+\sigma/4 - 30\pi^{-1/2}\sigma^{3/2} + \sigma^2/32 + 302.4\pi^{-1/2}\sigma^{5/2}\cdots\} \quad (25)$$
$$^3Q_2 = (9\pi^{1/2}\sigma^{-3/2}/12)\{1+\sigma/4 - 74\pi^{-1/2}\sigma^{3/2} + \sigma^2/32 + 840.4\pi^{-1/2}\sigma^{5/2}\cdots\} \quad (26)$$
$$^1Q_3 = (2\pi^{1/2}\sigma^{-3/2}/12)\{1+\sigma/4 - 78\pi^{-1/2}\sigma^{3/2} + \sigma^2/32 + 1094.4\pi^{-1/2}\sigma^{5/2}\cdots\}. \quad (27)$$

Whence we obtain by differentiation of ln Q, remembering that σ is small

$$^5C_1/R = 1.5 - 12.7\sigma^{3/2} + 655.8\sigma^{5/2} \quad (28)$$
$$^3C_2/R = 1.5 - 31.3\sigma^{3/2} + 1817\sigma^{5/2} \quad (29)$$
$$^1C_3/R = 1.5 - 33.01\sigma^{3/2} + 2357\sigma^{5/2}. \quad (30)$$

From these expansions the heat capacities of each form was calculated for $\sigma = 0.01 (T = 768°\text{K})$.

It is possible now to estimate the relative amounts of each form at high temperature from equations 25–7. They are

Nuclear quintet $5(\pi^{1/2}\sigma^{-3/2}/12)/(5\pi^{1/2}\sigma^{-3/2}/12 + 9\pi^{1/2}\sigma^{-3/2}/12 + 2\pi^{1/2}\sigma^{-3/2}/12)$

$$^5F = 5/(5+9+2) = 31.2 \text{ percent} \quad (31)$$

Nuclear triplet $^3F = 9/(5+9+2) = 56.2$ percent

Nuclear singlet $^1F = 2/(5+9+2) = 12.5$ percent.

This relative proportion should remain unaltered if we cool ordinary methane gas down to extremely low temperatures, but should change over into the equilibrium proportion obtaining at that temperature on exposure of the methane to suitable catalysts ("dissociation catalysts"). The latter proportion

$$F_i = Q_i/(Q_1 + Q_2 + Q_3) \quad (32)$$

is to be determined by substituting the appropriate values already calculated.

The results are all summarized in Table VII which gives the relative equi-

TABLE VII. *Heat capacities of frozen and true equilibrium mixtures of methane.*

T	σ	$^5F_1$	$^3F_2$	$^1F_3$	$^5C_1/R$	$^3C_2/R$	$^1C_3/R$	C_v/R frozen	C_v/R equil.
7.7°K	1	80.1	19.5	0.3	0.006	0.488	0.0003	0.28	0.10
15.4	0.5	56.8	37.6	5.7	.626	.902	.0804	.71	.70
19.8	0.3873	43.3	48.8	8.0	1.47	1.349	.248	1.25	1.31
40	.1937	32.0	55.7	12.2	2.143	1.500	1.138	1.65	1.66
89	.0861	31.2	56.2	12.5	1.306	1.388	1.407	1.36	1.36
178	.043	31.2	56.2	12.5	0.517	0.659	0.560	0.60	0.60
768	.01	31.2	56.2	12.5	1.493	1.487	1.491	1.49	1.49

librium proportions of the different symmetry forms, their separate heat capacities, the average heat capacity of the mixture in frozen equilibrium and that of the mixture in true equilibrium. Figs. 1 , 2 and 3 portray the same data graphically. The average heat capacity is calculated from the formula

$$C = {}^5F_1{}^5C_1 + {}^3F_2{}^3C_2 + {}^1F_3{}^1C_3 \tag{33}$$

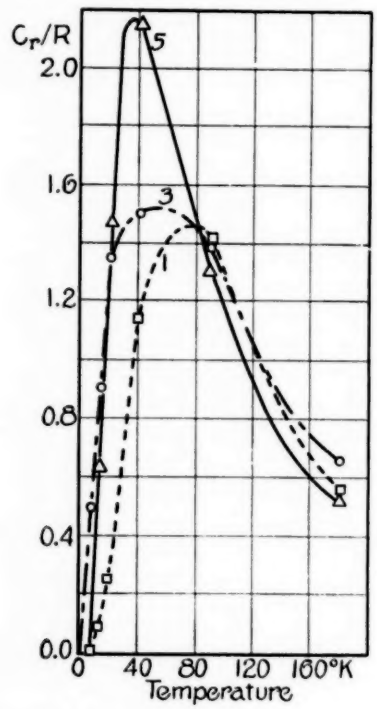

Fig. 1. Rotational heat capacities of methane.
△ Quintet ○ Triplet □ Singlet

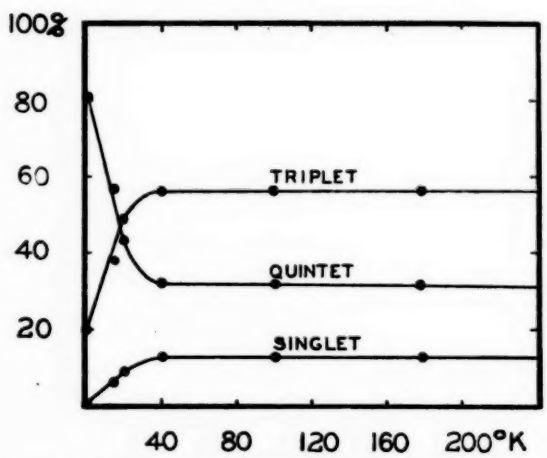

Fig. 2. Equilibrium amounts of different symmetry forms of methane.

Conclusions

A study of Table VII and Fig. 3 shows that according to our calculations, there should be two regions propitious for detecting a change in specific heat after catalytic treatment, were it not for vapor pressure limitations. The more practical would be that at the temperature of boiling hydrogen where the specific heat should increase some five or six percent. The other region should be at the much lower temperature of ~8°K where the heat capacity should

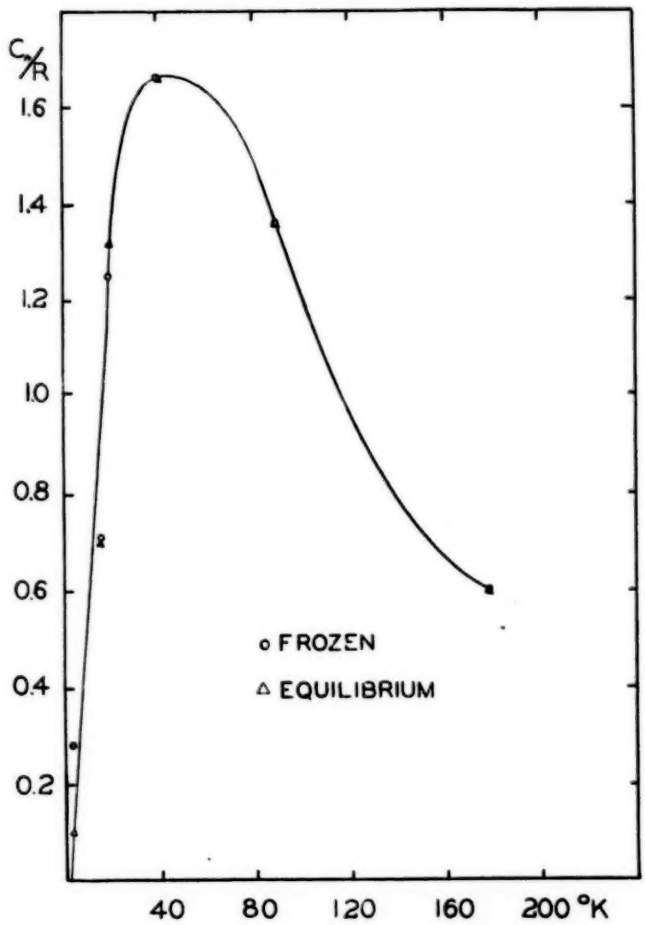

Fig. 3. Average rotational heat capacity of methane.

decrease some 64 percent. The inaccuracies involved in the cessation of our sums at a possibly too early point (Table VI) affect only the values obtained at 178°K, where the frozen equilibrium proportions are practically identical with those at true equilibrium. From the standpoint of these calculations it seems that experimental difficulties of working with methane vapor at such low temperatures would be almost insurmountable in view of the fact that it cannot be held in the gaseous state in concentrations greater than those cor-

responding to its vapor pressure, which indeed must be less than 0.1 mm even at 40°K. Whether the same distribution would hold among the different varieties in the solid crystal as we have calculated for the gas, we are not prepared to state. A catalytic change in the solid state might perhaps be detected by raising the temperature to a test temperature accurately controlled and observing any alteration in the heat capacity of the vapor. Such changes should however be exceedingly minute. These considerations lead one to become exceedingly pessimistic concerning any method of demonstrating the different varieties by means of the specific heats of the vapor.

THE ACOUSTIC RESONATOR INTERFEROMETER: I. THE ACOUSTIC SYSTEM AND ITS EQUIVALENT ELECTRIC NETWORK

By J. C. Hubbard
The Johns Hopkins University

(Received July 27, 1931)

Abstract

The steady state of motion of a fluid between two infinite plane parallel boundaries is found for the case in which one of the boundaries is given a prescribed periodic motion normal to its surface, the other boundary being infinitely rigid or being assigned a coefficient of reflection. The excess pressure at any point in the fluid is found, being of particular interest at the boundary of the source where it has a term in phase with the velocity of the source and one in phase with its displacement. These terms pass through cyclical values as the distance between the source and reflector is increased, the first passing through sharp maxima, the second changing rapidly from negative to positive values at reflector distances of an integral number of half wavelengths in the fluid. Application is made to the case where the source is the surface of a piezoelectric plate maintained in forced vibration. The equivalent electric network of the plate and coupled fluid column is found to be the same as that for the plate alone, with modified resistance and capacity coefficients, making possible consideration of the theory of the acoustic resonator interferometer in conjunction with driving and measuring circuits.

I. Introduction

THE present paper considers the theory of an electro-mechanical system composed of a vibrator such as a piezoelectric plate which is electrically driven by an independent source and to which is coupled a column of fluid set into longitudinal vibration by the plate. This study was undertaken with reference to its application in acoustic interferometry, particularly the measurement of the velocity of high frequency compressional waves in gases and liquids, and their coefficients of absorption and reflection. Mr. A. L. Loomis and the writer[1] in collaboration have applied the piezoelectric resonator to the systematic study of the velocity of high frequency compressional waves in liquids, and the methods have been extended by the writer[2] to the study of gases. In these experiments a piezoelectric plate is maintained in forced vibration by an independent vacuum tube oscillator, while one of the vibrating faces of the plate produces plane compressional waves in the medium in contact with it. If a reflecting plate be set opposite and parallel to the vibrating face of the crystal) multiple reflection takes place and as the reflecting plate is made to approach or recede from the vibrator cyclical changes of phase and amplitude of the forced vibrations occur, the reflector passing through successive positions of resonance in the fluid medium. These changes of phase

[1] J. C. Hubbard and A. L. Loomis, Nature **120**, 189 (1927); Phil. Mag. **5**, 1178–1190 (1928); A. L. Loomis and J. C. Hubbard, J.O.S.A., and R.S.I. **17**, 295–307 (1928). See also E. B. Freyer with J. C. Hubbard and D. H. Andrews, J. Am. Chem. Soc. **51**, 759–770 (1929).

[2] J. C. Hubbard, Phys. Rev. **35**, 1442 (1930); **36**, 1668–1669 (1930).

and amplitude of the vibrator give rise to effects which can be measured electrically and the object of this study is to arrive at expressions for these effects in terms of mechanical and electrical constants of the system.

The theory of the piezoelectric resonator and methods for its study were first treated in the comprehensive paper of W. G. Cady[3] and further extensive analysis has been presented by D. W. Dye.[4] Part I of the present paper consists in a development of the theory of the vibrations of a fluid column and an extension of the methods of Cady and Dye so as to include the reaction of the fluid medium upon the resonator.

G. W. Pierce[5] was the first to develop methods of high frequency acoustic interferometry. He and his collaborators have made use of piezoelectric and magnetostriction oscillators in which the vibrating element serves not only as generator and indicator of acoustic vibrations in a gas, but also maintains electric oscillations in a vacuum tube circuit. The theory of the reaction of the acoustic system upon the circuit developed in the present paper is also

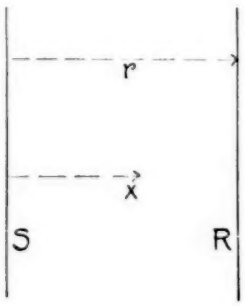

Fig. 1.

applicable in this case, but the problem is complicated by the necessity of considering the characteristics of the vacuum tube and its circuit and calls for separate treatment.

2. The Forced Vibrations of a Fluid Column

Let the space between two infinite, parallel, plane surfaces at normal variable distance r be filled with an elastic fluid of density ρ and isothermal compressibility β. Let the boundary surface S, Fig. 1, be given a normal vibratory motion of infinitely small amplitude by an external agent such that when a steady state of motion is reached throughout the system the motion of S is given by

$$\dot{\xi}_{x=0} = \dot{\xi}_0 e^{i\omega t} \tag{1}$$

and the motion of R is given by

$$\dot{\xi}_r = \dot{\xi}_{r,0} e^{i(\omega t+\delta)}. \tag{2}$$

[3] W. G. Cady, Proc. I. R. E. **10**, 83–114 (1922).
[4] D. W. Dye, Proc. Phys. Soc. Lond. **38**, 399–458 (1926).
[5] G. W. Pierce, Proc. Am. Acad. **60**, 269–302 (1925).

If R is infinitely rigid, $\dot{\xi}_{r,0}=0$ and the surface R is a perfect reflector. Such is the case to a very high degree of precision when the fluid is a gas at ordinary pressures and the reflector is of metal. In the more general case the surface R will transmit motion from the fluid and the reflection coefficient will be less than unity.

It is assumed that the particles of fluid in contact with both S and R have the same motion as those surfaces. Particle velocity in the fluid is propagated with the velocity $v=(K/\beta\rho)^{1/2}$, K being the ratio of specific heats. We shall assume that the velocity is propagated in the fluid with an attenuation α due to absorption, such that

$$d\dot{\xi}/\dot{\xi} = -\alpha dx \tag{3}$$

or

$$\dot{\xi} = \dot{\xi}_{x=0}e^{-\alpha x} = \dot{\xi}_0 e^{-\alpha x}e^{i\omega t}. \tag{4}$$

If we define the coefficient of absorption μ by $I=I_0e^{-\mu x}$, then,[6] since $I=\frac{1}{2}(\delta p_{\max})^2\rho v$, where $\delta p_{\max}$ is the maximum pressure due to particle velocity, and is $\delta p_{\max}=v\rho\dot{\xi}_0e^{-\alpha x}$, we have $\mu=2\alpha$.

At any point x between R and S when the steady state has been reached we shall have at a given time t a total disturbance made up of a term due to particle velocity propagated directly from S, that once reflected from R, that once reflected from R and once from S, that twice reflected from R and once from S, and so on, and in addition a similar series of terms due to the motion, if any, of R. It comes to the same thing if we assume that at each reflection from R the particle velocity term is multiplied by a coefficient γ, the two modes of calculation yielding equations from which the phase and amplitude of the motion of R may be evaluated in terms of the reflection coefficient, or vice versa. The value of the particle velocity at x is thus

$$\begin{aligned}\dot{\xi}_x &= \dot{\xi}_0e^{i\omega t}\{(e^{-(\alpha+i\omega/v)x} + \gamma e^{-(\alpha+i\omega/v)(2r+x)} + \cdots) \\ &\quad - (\gamma e^{-(\alpha+i\omega/v)(2r-x)} + \gamma^2 e^{-(\alpha+i\omega/v)(4r-x)} + \cdots)\} \\ &= \dot{\xi}_0e^{i\omega t}\sum(\gamma^m e^{-(\alpha+i\omega/v)(2mr+x)} - \gamma^{m+1}e^{-(\alpha+i\omega/v)[2(m+1)r-x]}).\end{aligned}$$

The total forward particle velocity at x is

$$\dot{\xi}_x(+) = \dot{\xi}_0e^{i\omega t}e^{-(\alpha+i\omega/v)x}/(1-\gamma e^{-(\alpha+i\omega/v)2r}) \tag{5}$$

and the total backward particle velocity at x is

$$\dot{\xi}_x(-) = -\dot{\xi}_0e^{i\omega t}\gamma e^{-(\alpha+i\omega/v)(2r-x)}/(1-\gamma e^{-(\alpha+i\omega/v)2r}). \tag{6}$$

Boundary conditions: When $x=0$, the total particle velocity is $\dot{\xi}_{x=0}=\dot{\xi}\,e^{i\omega t}$, which satisfies Eq. (1), and when $x=r$

$$\dot{\xi}_{x=r} = \dot{\xi}_0e^{i\omega t}(1-\gamma)e^{-(\alpha+i\omega/v)r}/(1-\gamma e^{-(\alpha+i\omega/v)2r}) = \dot{\xi}_re^{i(\omega t+\delta)} \tag{7}$$

from which the coefficients $\dot{\xi}_r$ and δ may be evaluated in terms of $\dot{\xi}_0$, α, γ and r.

Thus

[6] I. B. Crandall, Vibrating Systems and Sound, p. 92.

$$\dot{\xi}_0(1-\gamma)e^{-(\alpha+i\omega/v)r}/(1-\gamma e^{-(\alpha+i\omega/v)2r}) = \dot{\xi}_r e^{i\delta}$$

from which

$$\dot{\xi}_r = \dot{\xi}_0(1-\gamma)e^{-\alpha r}\left\{1 - 2\gamma e^{-2\alpha r}\cos 2\frac{\omega}{v}r + \gamma^2 e^{-4\alpha r}\right\}^{-\frac{1}{2}} \tag{8}$$

and

$$\tan\delta = \left(\tan\frac{\omega}{v}r\right)(1+\gamma e^{-2\alpha r})/(1-\gamma e^{-2\alpha r}). \tag{9}$$

If $\gamma = 1$, $\dot{\xi}_r = 0$, (gas with rigid reflector). If $r = n\lambda/2$, $\omega r/v = n\pi$ and $\tan\delta = 0$. In resonance positions the phase of the motion of the reflector is the same as that for the vibrator in the even numbered nodal positions, and differs by π in the odd numbered nodal positions.

The excess pressure δp, hereafter referred to as p, in the medium at the point x is given by[7] $\pm v\rho\dot{\xi}_x$ the plus sign being used with the forward particle velocity and the minus sign with the backward particle velocity, thus:

$$p_x = v\rho\dot{\xi}_x(+) - v\rho\dot{\xi}_x(-). \tag{10}$$

Whence

$$p_x = \rho v\dot{\xi}P_x + \rho v\omega\xi Q_x \tag{11}$$

in which, from Eqs. (5) and (6)

$$P_x = \frac{[e^{-x\alpha} - \gamma^3 e^{-(4r-x)\alpha}]\cos(\omega x/v) + \gamma[e^{-(2r-x)\alpha} - \gamma e^{-(2r+x)\alpha}]\cos(\omega/v)(2r-x)}{1 - 2\gamma^2 e^{-2r\alpha}\cos(2r\omega/v) + \gamma^4 e^{-4r\alpha}} \tag{12}$$

and

$$Q_x = \frac{[e^{-x\alpha} + \gamma^3 e^{-(4r-x)\alpha}]\sin(\omega x/v) + \gamma[e^{-(2r-x)\alpha} + \gamma e^{-(2r+x)\alpha}]\sin(\omega/v)(2r-x)}{1 - 2\gamma^2 e^{-2r\alpha}\cos(2r\omega/v) + \gamma^4 e^{-4r\alpha}}. \tag{13}$$

The expressions (12) and (13) take various forms of interest depending upon the conditions to be imposed by experiment. For example if the fluid is a gas, we have at the surface of the source S, $x = 0$, and taking $\gamma = 1$,

$$P_{x=0} = \sinh 2r\alpha/(\cosh 2r\alpha - \cos(2r\omega/v)) \tag{14}$$

$$Q_{x=0} = \sin(2r\omega/v)/(\cosh 2r\alpha - \cos(2r\omega/v)) \tag{15}$$

giving as the excess pressure, $p_{x=0}$, at the surface of S

$$p_{x=0} = v\rho\dot{\xi}P_{x=0} + v\rho\omega\xi Q_{x=0}. \tag{16}$$

The first term on the right of Eq. (16) is in phase with the velocity of the vibrator and is responsible for the transmission of energy into the fluid. This term, as r is varied passes periodically through very sharp maxima, for values of $2r\omega/v = 2\pi n$, or $r = n\lambda/2$, that is, for positions of R, an integral number of half wave-lengths from S. The function $(\sinh 2r\alpha)/(\cosh 2r\alpha - \cos 2r\omega/v)$ is shown graphically in Figure 2 for values of α and ω chosen so as illustrate its general form. It will be seen that as a result of the damping as the path length is increased the maxima, given by $1/\tanh 2r\alpha$ decrease approximately

[7] Crandall, reference 6, p. 93.

along a hyperbola and not logarithmically as seems to have been assumed by several workers with the interferometer.

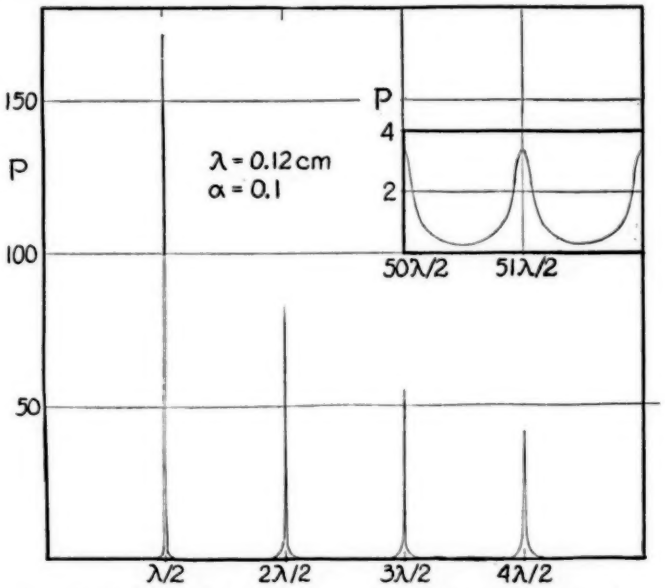

Fig. 2. $P=(\sinh 2r\alpha)/(\cosh 2r\alpha-\cos 2r\omega/v)$ as a function of r. $\alpha=0.1$, $\lambda=0.12$ cm, and $2r\omega/v=4\pi r/\lambda$.

The second term on the right of Eq. (16) is in phase with the displacement and hence is proportional to the reaction of the fluid on the vibrator. The function $(\sin 2r\omega/v)/(\cosh 2r\alpha-\cos 2r\omega/v)$ is shown in Figure 3 as a function of r.

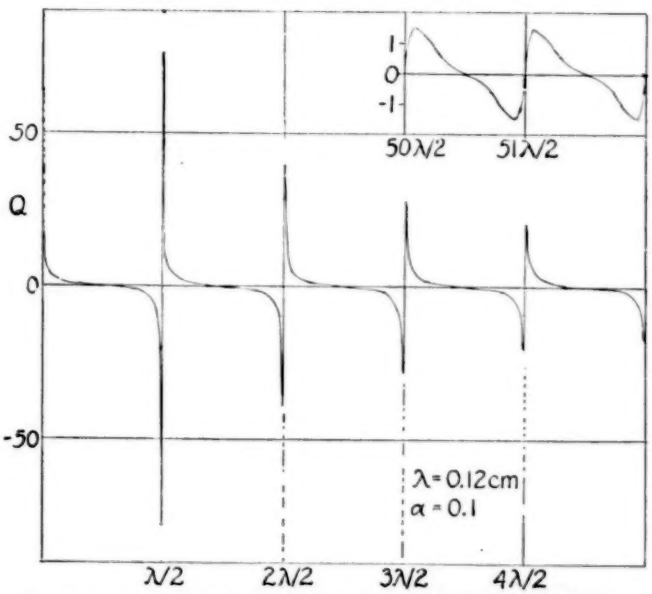

Fig. 3. $Q=(\sin 2r\omega/v)/(\cosh 2r\alpha-\cos 2r\omega/v)$ as a function of r. $\alpha=0.1$, $\lambda=0.12$ cm, and $2r\omega/v=4\pi r/\lambda$.

If the reflector is itself a piezoelectric plate it may be used as a detector of excess pressure variations, and the expression for the latter at its boundary becomes of interest. In this case for a gas, $\gamma = 1$ and $x = r$, and we have

$$P_{x=r} = 2(\cos \omega r/v)(\sinh r\alpha)/(\cosh 2r\alpha - \cos 2r\omega/v) \tag{17}$$

$$Q_{x=r} = 2(\sin r\omega/v)(\cosh 2r\alpha)/(\cosh 2r\alpha - \cos 2r\omega/v). \tag{18}$$

In the case of liquids, except certain solutions and suspensions, α is so small that the decrement is difficult of observation. We may accordingly put $\alpha = 0$. In the case of liquids, however the reflector transmits a measurable part of the wave-motion out of the medium, particularly if the latter is of a density and compressibility of the same order of magnitude as for the substance of the

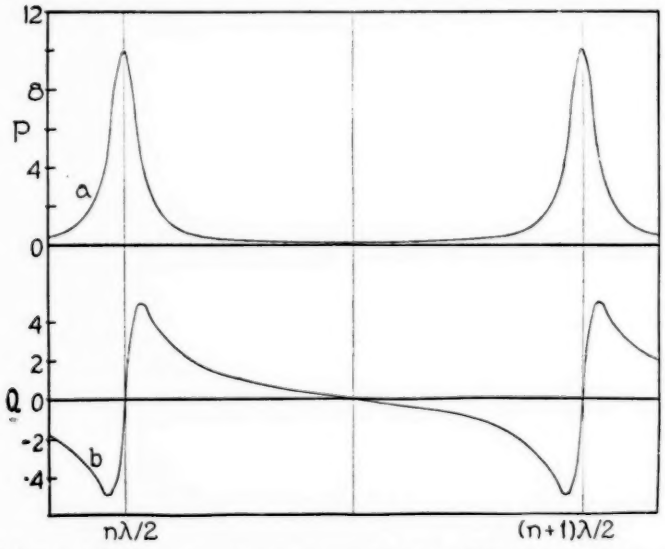

Fig. 4. (a) P and (b) Q as functions of r. $\alpha = 0$ and $\gamma = 0.9$, the fluid being a liquid.

reflector, R. Such a case is that where the liquid is mercury and the reflector is of steel, or if the liquid is water and the reflector glass. In this case

$$P_{x=0} = [1 + \gamma(1 - \gamma) \cos 2r\omega/v - \gamma^3]/(1 - 2\gamma^2 \cos 2r\omega/v + \gamma^4) \tag{19}$$

and

$$Q_{x=0} = [\gamma(1 + \gamma) \sin 2r\omega/v]/(1 - 2\gamma^2 \cos 2r\omega/v + \gamma^4). \tag{20}$$

These functions are shown graphically as functions of r in Fig. 4, at a and b respectively.

3. The Acoustic System and its Electrical Equivalent

If, in the foregoing discussion we limit the planes S and R to the finite area A, then we may ignore the effects of diffraction provided that, compared with the linear dimensions of A, the length of the compressional wave in the fluid is small, and, second, that the path r is not large. Neither of these condi-

tions can conveniently be met in working with audible sound, but are not difficult of fulfillment in ultrasonic interferometry.

Let the vibrator S be a piezoelectric plate provided with electrodes and excited by an independent oscillator. Under these conditions the piezoelectric plate acts as a resonator, the theory of which has been worked out by W. G. Cady.[3] We will now extend this theory to include the combined action of the resonator and the fluid column coupled to it.

Let us assume that we have a plate of piezoelectric quartz with electrode faces perpendicular to an X or electric axis of the crystal. Following Cady's notation, let l, b and e be respectively the length, breadth and thickness of the plate, and let them be parallel respectively to the Y, Z and X axes of the crystal. The equation of motion along the X axis in the neighborhood of resonance is shown by Cady to be represented by

$$M\ddot{\xi} + N\dot{\xi} + G\xi = F \tag{21}$$

where M, N and G are respectively the equivalent mass, resistance, and stiffness of the plate for the mode of motion considered, and F is the equivalent mechanical force exerted by the electric field applied between the electrodes, This field has the value V/e, where V is the instantaneous potential difference of the electrodes, and the mechanical stress in the crystal in the X direction is $X = \epsilon_{11} V/e$, where ϵ_{11} is the piezoelectric constant of quartz for the X axis. The equivalent mechanical force is shown by Cady to be $F = 2beX = 2\epsilon_{11} bV$. Let $V = V_0 e^{i\omega t}$, then, in the steady state

$$\xi = \xi_0 e^{i(\omega t - \theta)} \tag{22}$$

where

$$\xi_0 = 2\epsilon_{11} V_0/\omega \left[N^2 + (M\omega - G/\omega)^2\right]^{1/2} \tag{23}$$

and

$$\theta = \left[\tan^{-1}(M\omega - G/\omega)\right]/N. \tag{24}$$

The leads going to the electrodes of the crystal carry the current i which is made up in part of the current i_1 due to the capacity of the system as a condenser and in part of the current i_2 generated by the crystal itself as a result of the excess of its instantaneous strain due to its motion over that which would be the equilibrium value produced by V itself. The current i_1 will be in phase with V and i_2 will have a phase depending upon the phase of the velocity of extension of the crystal in the direction of its vibration and is shown by Cady to be $i_2 = bl\dot{D}$, where $D = (2\xi - \delta_{11} lv/e)\epsilon_{11}/l$, 2ξ being the total elongation of the crystal, ξ for each face, and ϵ_{11} and δ_{11} being respectively the piezoelectric constant and modulus of the crystal for the axis considered. The equilibrium elongation of the quartz for the potential V is $\delta_{11} lV/e$. Near resonance the crystal reaches great amplitude of vibration and the static elongation may be neglected, giving for the piezoelectric current generated by the crystal $i_2 = 2b\epsilon_{11}\dot{\xi}$. Thus the total current to the electrodes is

$$i = \dot{V}K_1 + 2b\epsilon_{11}\dot{\xi} \tag{25}$$

where K_1 is the capacity of the crystal and its electrodes considered as a condenser, and ξ is subject to Eq. (21).

An examination of Eqs. (21) and (25) shows that the crystal and its electrodes behave as a pure capacity shunted by an effective capacity, inductance and resistance in series, for, substituting $\xi = i_2/2b\epsilon_{11}$ in equation (21) we have, since $F = 2\epsilon_{11}bV$, and putting $4\epsilon_{11}^2b^2 = 1/\mathrm{B}$,

$$Ld^2i_2/dt^2 + Rdi_2/dt + i_2/K = dV/dt \tag{26}$$

where

$$L = BM, \quad R = BN, \quad 1/K = BG. \tag{27}$$

K. S. Van Dyke[8] has shown that the equivalent inductance, resistance, and capacity of the series branch of the equivalent electric network of the crystal have in fact these respective values for the mode of vibration here considered. The crystal and its electrodes may therefore be replaced by the network shown in Fig. 5.

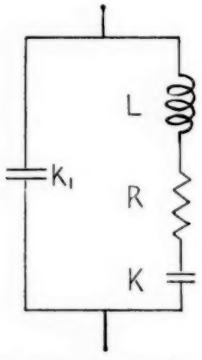

Fig. 5. Equivalent network of piezoelectric plate, and, with modified R and K, of plate coupled to fluid column.

Let us now assume that the electrodes are of negligibly small mass, stiffness, and resistance, and that they are in contact with the surface of the crystal, and that furthermore one of the electrodes serves as the boundary of the fluid medium. Consideration will be given later to the slight modifications introduced by variation of these restrictions. In addition to the force F, we now have the reaction of the excess pressure on the face of the crystal given by Eq. (16), where P and Q have the respective values given by Eqs. (14) and (15) if the fluid is a gas, and by Eqs. (19) and (20) in most cases if the fluid is a liquid. The equation of motion of the crystal is now

$$M\ddot{\xi} + N\dot{\xi} + G\xi = F - Ap \tag{28}$$

where A is the area of the vibrating surface in contact with the fluid. The excess pressure p as has been seen has a term in phase with $\ddot{\xi}$ and one in phase with ξ. We may accordingly write

[8] K. S. Van Dyke, Proc. I. R. E. **16**, 742–764 (1928); See also D. W. Dye, reference 4, p. 401.

$$M\ddot{\xi} + N'\xi + G'\xi = F \tag{29}$$

or

$$Ld^2i_2/dt^2 + R'di_2/dt + i_2/K' = dV/dt \tag{30}$$

where we now have

$$R' = R + AB\rho vP \tag{31}$$

and

$$1/K' = 1/K + AB\rho v\omega Q. \tag{32}$$

It is to be noted that the effective resistance R' and capacity K' of the acoustic system are constants involving the values of α, γ, r, and ω. The acoustic system may thus be represented by the same network as the piezoelectric plate alone (Fig. 5), the resistance R and capacity K of that network being replaced by R' and K' defined respectively by Eqs. (31) and (32). It is often convenient, especially in the interferometry of gases, to work with a transverse face of a crystal instead of with one of the electrode surfaces. In this case the piezoelectric constant and modulus are different, leading to a different value for B in equations (31) and (32) but the form of those equations is unchanged.

In Part II of this paper the acoustic system will be considered in combination with suitable driving and measuring circuits in accordance with the necessities of specific experimental objectives, such as the determination of compressional velocities in liquids and gases, and the absorption coefficients of gases.

ON THE STRAIN-ENERGY FUNCTION FOR ISOTROPIC BODIES

By C. Kaplan*
California Institute of Technology, Pasadena

(Received April 25, 1931)

Abstract

The strain-energy function ϕ is assumed to be made up of a sum of homogeneous polynomials of the first, second, third, etc. degrees in the components of the strain tensor $e_{\alpha\beta}$. The expansion is carried only so far as to include the third degree group of terms and then this expression for ϕ is studied from the point of view of the isotropy of space. Isotropy of space having been defined by means of rectangular trihedrons (or orthogonal ennuples), the effect on the "structure-tensor" $c^{\alpha\beta\gamma\delta\rho\sigma}$ (which forms with $e_{\alpha\beta}$ the third degree terms) of the assumption of isotropy is obtained. It is found that the third degree group introduces, for a completely isotropic state, only two coefficients of elasticity, which when taken together with the corresponding Lame's coefficients λ, μ of the second degree group gives only four elastic moduli in the complete expression for ϕ. The expression for ϕ thus developed is introduced into a set of equations obtained by F. D. Murnaghan connecting the stress and strain components by means of ϕ; and so we obtain relations between stress and strain which are applicable to deformations of higher order than those allowed by Hooke's law. These latter relations are then applied to the case of normal and uniform compression and these further applied to P. W. Bridgman's experiments on the change of volume of sodium under pressure at 30°C. In this application the four elastic moduli are reduced to two.

Introduction

IF THE condition of a body from which the energy of deformation ϕ is reckoned be that of equilibrium under an arbitrary initial stress, then developing this function of the six strain components by Taylor's theorem, we have that[1]

$$\phi = \phi_0 + c^{\alpha\beta}e_{\alpha\beta} + c^{\alpha\beta\rho\sigma}e_{\alpha\beta}e_{\rho\sigma} + c^{\alpha\beta\rho\sigma\gamma\delta}e_{\alpha\beta}e_{\rho\sigma}e_{\gamma\delta} + \cdots \quad (1)$$

where ϕ_0 is an arbitrary constant of no interest as far as the deformations are concerned and the terms following ϕ_0 are respectively homogeneous functions of the first, second and third degrees in the components of the strain tensor $e_{\alpha\beta}$ ($e_{\alpha\beta}=e_{\beta\alpha}$ and $\alpha, \beta = 1, 2, 3$).

Hence, $\partial\phi/\partial e_{\alpha\beta}$ will be a linear function of the strain components together with functions of higher degrees obtained from the third degree, etc. terms. For isotropic bodies the second degree group $c^{\alpha\beta\rho\sigma}e_{\alpha\beta}e_{\rho\sigma}$ takes the simple form

$$2\phi_2 = (\lambda + 2\mu)I_1^2 - 4\mu I_2 \quad (2)$$

where λ and μ are two independent coefficients of elasticity characteristic of the body under consideration; also $I_1 = e_{xx}+e_{yy}+e_{zz}$ and $I_2 = (e_{yy}e_{zz}-e_{yz}^2)$

* National Research Fellow in Physics.

[1] The repeated Greek labels denote summation, each "dummy" label taking all values 1, 2, 3.

$+e_{zz}e_{xx}-e_{zx}^2)+(e_{xx}e_{yy}-e_{xy}^2)$ are the first two fundamental invariants of elasticity theory, the third degree invariant $I_3=e_{xx}e_{yy}e_{zz}+2e_{yz}e_{zx}e_{xy}-(e_{xx}e_{yz}^2+e_{yy}e_{zx}^2+e_{zz}e_{xy}^2)$ not appearing in the theory unless the third degree group of Eq. (1) is taken into consideration. If we further suppose that the initial stress is a uniform hydrostatic pressure P_0, then Eq. (1) becomes (excluding terms beyond the second degree) for isotropic bodies

$$\phi = \phi_0 - P_0 I_1 + \frac{\lambda + 2\mu}{2} I_1^2 - 2\mu I_2 \tag{3}$$

and we obtain Hooke's law of the linear dependence of stress on strain when the latter is small, from the relations

$$X_x = \frac{\partial \phi}{\partial e_{xx}}; \cdots; Y_x = \frac{1}{2} \frac{\partial \phi}{\partial e_{yz}}; \cdots$$

so that

$$\begin{aligned} X_x &= -P_0 + YI_1 + 2\mu e_{xx}; \cdots \\ Y_x &= 2\mu e_{yz}; \cdots . \end{aligned} \tag{4}$$

We shall, in what follows, develop expressions corresponding to Eqs. (3) and (4) for the case where we include the group of terms of the third degree in the expression for ϕ, the strain-energy.[2] For this purpose we introduce an analysis which in reality is the analytical equivalent of the definition of isotropy; that is, the independence of the structure of a substance of the direction in which it is measured.

Analysis of Isotropy[3]

Since the following analysis will not be limited necessarily to a rectangular Cartesian system, we suppose that our space is a Riemannian one of three dimensions. By hypothesis, the energy of deformation $\phi(e_{\alpha\beta})$ is an invariant with regard to changes in the coordinate system used and since the $e_{\alpha\beta}$'s are the components of a covariant symmetrical tensor of rank two, the coefficients $c^{\alpha\beta\gamma\delta\rho\sigma}$ of the third degree group of Eq. (1) are the components of a contravariant tensor of rank six which we shall call the "structure tensor." This tensor $c^{\alpha\beta\gamma\delta\rho\sigma}$ has in general $3^6=729$ components, but because the third degree terms form a homogeneous group and because the strain tensor $e_{\alpha\beta}$ is symmetrical in character, only 56 of these components appear in the expression (1). The additional hypothesis that the body is completely isotropic generates many relations between these 56 coefficients so that the number of independent ones is greatly reduced.

It is in order to find these latter interrelations that we introduce the following analysis. To each point of our space we attach a trihedron, each edge

[2] W. Voigt, Ann. d. Phys. und Chemie, Dritte Folge 2 (**52**) 536 (1894).

[3] The Absolute Diff. Calc.; Levi-Civita; Ch, sec. 2 (we use Einstein's notation h_α^τ instead of the corresponding $\lambda_{\tau/\alpha}$ of Levi-Civita's); C. Kaplan and F. D. Murnaghan; Phys. Rev. **35,** 763 (1930).

of which is presented in the underlying coordinate system (x) by a contravariant tensor of rank one h_r^{α}, the Greek label α denoting tensor character and the Latin letter r the particular edge of the trihedron. Since our space is a Riemannian one it possesses a metric denoted by

$$ds^2 = g_{\alpha\beta}dx^{\alpha}dx^{\beta}.$$

Hence, corresponding to the contravariant components h_r^{α} are the covariant components $h_r{}^{\alpha}$ of the rth edge, with the relations

$$\begin{aligned} h_r{}^{\alpha}h_{\alpha}{}^{s} &= \epsilon_r{}^{s} \quad (= 1 \text{ if } r = s \text{ and } 0 \text{ if } r \neq s) \\ h_r{}^{\alpha}h_{\beta}{}^{r} &= \delta_{\beta}{}^{\alpha} \quad (= 1 \text{ if } \alpha = \beta \text{ and } 0 \text{ if } \alpha \neq \beta) \end{aligned} \tag{5}$$

defining the orthogonality of the trihedron at P and also informing us that the tensor h is a unit one.

By means of the covariant components $h_{\alpha}{}^{r}(=g_{\alpha\beta}h_r^{\beta})$ the contravariant tensor $c^{\alpha\beta\gamma\delta\rho\sigma}$ may be defined by its 3^6 projections along the edges of the trihedron at P. Thus by definition, these projections are given by the equations

$$c^{pqrsmn} = c^{\alpha\beta\gamma\delta\rho\sigma}h_{\alpha}{}^{p}h_{\beta}{}^{q}h_{\gamma}{}^{r}h_{\delta}{}^{s}h_{\rho}{}^{m}h_{\sigma}{}^{n}$$

or

$$c_{pqrsmn} = c_{\alpha\beta\gamma\delta\rho\sigma}h_p{}^{\alpha}h_q{}^{\beta}h_r{}^{\gamma}h_s{}^{\delta}h_m{}^{\rho}h_n{}^{\sigma} \tag{6}$$

where $c^{pqrsmn} = c_{pqrsmn}$ and so for the invariants of the structure-tensor the upper and lower labelling has no meaning except for purposes of notation.

Suppose now that at P we attach a second trihedron whose edges are presented by the covariant or contravariant components ${}^*h_{\alpha}{}^{r}$ or ${}^*h_r{}^{\alpha}$ respectively, and furthermore let us suppose that the contravariant components of the two tensors h and ${}^*h$ are connected by the linear relations

$${}^*h_r{}^{\alpha} = s_r{}^{s}h_s{}^{\alpha} \tag{7}$$

summing over the s's with $r, s, \alpha = 1, 2, 3$. Then, since the ${}^*h$ trihedron is supposed to be orthogonal, the scalar coefficients $s_r{}^{s}$ are the elements of an orthogonal matrix. Indeed if the covariant presentions of the two tensors ${}^*h$ and h are connected by the relations

$${}^*h_{\alpha}{}^{r} = s_s{}'{}^{r}h_{\alpha}{}^{s} \tag{8}$$

then multiplying Eqs. (7) and (8) together and summing over the α's we have that

$${}^*h_s{}^{\alpha}{}^*h_{\alpha}{}^{r} = s_s{}^{p}s_q{}'{}^{r}h_p{}^{\alpha}h_{\alpha}{}^{q}$$

or

$$s_s{}^{p}s_q{}'{}^{r}\epsilon_p{}^{q} = \epsilon_s{}^{r} \quad \text{from} \quad (5)$$

and so

$$s_s{}^{p}s_p{}'{}^{r} = \epsilon_s{}^{r}. \tag{9}$$

Therefore the product of the s and s' matrices yields the unit matrix. We say that the ${}^*h$ configuration is obtained from the h one by a rotation if the

determinant of the matrix s is $+1$ and by a reflexion if this determinant is -1.

The relations between the invariants of the structure-tensor relative to the two trihedrons $^*h$ and h are readily obained; thus

$$^*c_{pqrsmn} = c_{\alpha\beta\gamma\delta\rho\sigma}\, {}^*h_p{}^\alpha\, {}^*h_q{}^\beta\, {}^*h_r{}^\gamma\, {}^*h_s{}^\delta\, {}^*h_m{}^\rho\, {}^*h_n{}^\sigma$$

and

$$c_{pqrsmn} = c_{\alpha\beta\gamma\delta\rho\sigma} h_p{}^\alpha h_q{}^\beta h_r{}^\gamma h_s{}^\delta h_m{}^\rho h_n{}^\sigma$$

and using the relations (7) between the contravariant components of $^*h$ and h, we find that

$$^*c_{pqrsmn} = c_{abcdef} s_p{}^a s_q{}^b s_r{}^c s_s{}^d s_m{}^e s_n{}^f \tag{10}$$

where we sum over the repeated Latin letters, each of which takes all the values 1, 2, 3.

We now define isotropy by saying that a medium is completely isotropic in structure in the neighborhood of a point P, if corresponding components of the invariants $^*c$ and c of the structure-tensor relative to the $^*h$ and h trihedrons are equal; that is

$$^*c_{pqrsmn} = c_{pqrsmn}. \tag{11}$$

These relations, taken together with those of (10) yield the fundamental equations defining isotropy. Thus

$$c_{pqrsmn} = c_{abcdef} s_p{}^a s_q{}^b s_r{}^c s_s{}^d s_m{}^e s_n{}^f. \tag{12}$$

Isotropy with Regard to Simple Rotations

We first consider the effect on the invariants c_{pqrsmn} of a rotation of the $^*h$ configuration through a right-angle in the $h_2 - h_3$ plane, $^*h_1$ and h_1 coinciding. In order to fix our ideas we suppose that the $^*h$ and h systems are right-handed ones and that all rotations take place in a counterclockwise way. The rotation just suggested may then be defined by the following table

	h_1	h_2	h_3
$^*h_1$	1	0	0
$^*h_2$	0	0	1
$^*h_3$	0	−1	0

so that $s_1{}^1 = s_2{}^3 = 1$; $s_3{}^2 = -1$, the other being zero.

When we substitute these values of the s's in equations (12) we find that many of the invariants are zero and that many of them are related. Thus, if $p=2$, $q=3$, $r=1$, $s=1$, $m=3$ and $n=1$, the only term of the sextuple summation of Eq. (12) different from zero is that one for which $a=3$, $b=2$, $c=1$, $d=1$, $e=2$ and $f=1$, so that

$$c_{231131} = c_{321121}.$$

Similarly we find that $c_{321121} = -c_{231131}$ and hence for the two relations to be compatible it is necessary that

$$c_{231131} = c_{321121} = 0.$$

In what follows we shall not make use of the symmetry relations between the invariants c_{pqrsmn} allowed by the fact that in the energy function ϕ the tensor $c^{\alpha\beta\gamma\delta\rho\sigma}$ is summed with the symmetrical strain tensor $e_{\alpha\beta}$, but consider the tensor (and hence its invariants) to be a perfectly general one. Also because the invariants are cumbersome to handle in their present form we introduce a notation defined by the following matrix forms:

$$\begin{pmatrix} 11 & 12 & 13 \\ 21 & 22 & 23 \\ 31 & 32 & 33 \end{pmatrix} \equiv \begin{pmatrix} a & h & g' \\ h' & b & f \\ g & f' & c \end{pmatrix}.$$

Thus instead of writing c_{213233}, say, we write simply $h'f'c$ and so on. When we examine each of the 3^6 invariants with regard to the rotation above, we find that 364 are zero whilst of the remaining 365 only 182 are independent.

If in addition to symmetry of structure with regard to a right-angle rotation in the h_2-h_3 plane, we demand symmetry of structure for a similar rotation in the h_3-h_1 plane, say, we find the conditions on the invariants by simple permutation of the results of the former rotation. Thus the relation $gag = h'ah'$ due to the rotation in the h_2-h_3 plane becomes $gag = g'cg'$ in the h_3-h_1 plane; the combined effect of the two rotations leading to the relations

$$gag = h'ah' = g'cg' = fcf = hbh = f'bf'.$$

Proceeding in this way we find that of the 729 invariants, 546 are zero and of the remaining 183 only 31 are independent. Furthermore, we need no longer distinguish between f, f';g, g';h, h', the reason for doing so in the preceding analysis being one of convenience only. This latter simplification reduces the number of independent invariants to twelve. The following table presents the surviving invariants for combined rotations through right-angles in the h_2-h_3 and h_3-h_1 planes; and also from its symmetry we see that no new conditions are imposed on the 12 independent invariants by including a 90°-rotation in the remaining h_1-h_2 plane.

We consider now a rotation of the $*h$ trihedron through an angle $\theta(\neq 90°)$ in, say, the h_2-h_3 plane. This rotation is conveniently presented by the following table:

	h_1	h_2	h_3
$*h_1$	1	0	0
$*h_2$	0	$\cos\theta$	$\sin\theta$
$*h_3$	0	$-\sin\theta$	$\cos\theta$

so that $s_1{}^1 = 1$; $s_2{}^2 = s_3{}^3 = \cos\theta$; $s_2{}^3 = \sin\theta$; $s_3{}^2 = -\sin\theta$, the other s's being zero.

On substitution of thes values in the fundamental Eqs. (12), taking into

consideration the results embodied in Table I, we obtain the following relations:

$$\begin{aligned} 4bff &= aaa - aab - bab + baa \\ 4ffb &= aaa + aab - bab - baa \\ 4gag &= aaa - aab + bab - baa \end{aligned} \tag{13}$$

and

$$\begin{aligned} baa &= bac + 2aff \\ bab &= bac + 2faf \\ aab &= bac + 2ffa. \end{aligned} \tag{14}$$

This rotation therefore reduces the number of independent invariants from 12 to 6; namely, *aaa*, *aab*, *bab*, *baa*, *bac* and *gfh* (which thus far has not been involved in these simple rotations). In order to find further relations between the invariants, we must consider the most general rotation of the $*h$-frame relative to the h-frame; namely,

	h_1	h_2	h_3
$*h_1$	s_1^1	s_1^2	s_1^3
$*h_2$	s_2^1	s_2^2	s_2^3
$*h_3$	s_3^1	s_3^2	s_3^3

where

$$\sum_{t=1}^{3} s_r^t s_s^t = \epsilon_s^r \left(= \begin{matrix} 1 & \text{if } r = s \\ 0 & \text{if } r \neq s \end{matrix}\right) \text{ and } \Delta = \left\| s_s^r \right\| = +1.$$

Considering Eqs. (12) in conjunction with Table I and Eqs. (13) and (14) we obtain the following pair of relations:

$$\begin{aligned} 3bac + 2(faf + ffa + aff) + 24gfh &= 0 \\ aaa + 2bac + 16gfh &= 0 \end{aligned} \tag{15}$$

thus leaving only 4 distinct invariants, *faf*, *aff*, *ffa* and *gfh*.

The relations between the dependent and independent invariants are:

TABLE I.

	aa	*ab*	*ac*	*af*	*ag*	*ah*	*ba*	*bb*	*bc*	*bf*	*bg*	*bh*	*ca*	*cb*	*cc*	*cf*	*cg*	*ch*	*fa*	*fb*	*fc*	*ff*	*fg*	*fh*	*ga*	*gb*	*gc*	*gf*	*gg*	*gh*	*ha*	*hb*	*hc*	*hf*	*hg*	*hh*
a	*aaa*	*aab*	*aab*				*bab*	*baa*	*bac*				*bab*	*bac*	*baa*																							
b	*baa*	*bab*	*bac*				*aab*	*aaa*	*aab*				*bac*	*bab*	*baa*																							
c	*baa*	*bac*	*bab*				*bac*	*baa*	*bab*				*aab*	*aab*	*aaa*																							
f				*faf*						*gag*						*gag*			*ffa*	*ffb*	*ffb*																	
g					*gag*						*faf*						*gag*							*gfh*													
h						*gag*						*gag*						*faf*					*gfh*														

The empty cells denote zero values.

$$
\begin{aligned}
3aaa &= 4(faf + ffa + aff) \\
3baa &= 2(faf + ffa - 2aff) - 24gfh \\
3bab &= 2(aff + ffa - 2faf) - 24gfh \\
3aab &= 2(faf + aff - 2ffa) - 24gfh \\
3bac &= -2(faf + aff + ffa) - 24gfh \\
bff &= aff + 2gfh \\
ffb &= ffa + 2gfh \\
gag &= faf + 2gfh.
\end{aligned} \tag{16}
$$

We are now in a position to form the group of 3rd degree terms $\phi_3 = c^{\alpha\beta\gamma\delta\rho\sigma} e_{\alpha\beta} e_{\gamma\delta} e_{\rho\sigma}$ in the expression for ϕ, the strain-energy function, for the case of a completely isotropic body. Thus, since ϕ_3 is invariant with regard to transformations of the coordinate system used, we may write

$$\phi_3 = c_{pqrsmn} e_{pq} e_{rs} e_{mn},$$

where

$$e_{pq} = e_{\alpha\beta} h_p{}^{\alpha} h_q{}^{\beta}$$

and using the results embodied in Table I in addition to Eqs. (16), we obtain the following expression for ϕ_3:

$$3\phi_3 = 2(faf + aff + ffa)[3\bar{I}_1\bar{I}_2 - \bar{I}_1{}^3] + 24gfh[\bar{I}_3 - \bar{I}_1{}^3]$$

or, without any loss in generality,

$$\phi_3 = 2faf[3\bar{I}_1\bar{I}_2 - \bar{I}_1{}^3] + 8gfh[\bar{I}_3 - \bar{I}_1{}^3] \tag{17}$$

where

$$\bar{I}_1 = g_{\alpha\beta} e^{\alpha\beta}; \quad \bar{I}_2 = g_{\alpha\beta} g_{\gamma\delta} e^{\alpha\gamma} e^{\beta\delta}; \quad \bar{I}_3 = g_{\alpha\beta} g_{\gamma\delta} g_{\rho\sigma} e^{\rho\alpha} e^{\beta\gamma} e^{\delta\sigma}.$$

For the case of a rectangular Cartesian coordinate system where

$$ds^2 = dx^2 + dy^2 + dz^2$$

these invariants take the following simple form[4]

$$
\begin{aligned}
\bar{I}_1 &= e_{xx} + e_{yy} + e_{zz} \\
\bar{I}_2 &= e_{xx}{}^2 + e_{yy}{}^2 + e_{zz}{}^2 + 2(e_{yz}{}^2 + e_{zx}{}^2 + e_{xy}{}^2) \\
\bar{I}_3 &= e_{xx}{}^2 + e_{yy}{}^3 + e_{zz}{}^3 + 3(e_{xx}e_{zz}{}^2 + e_{xx}e_{xy}{}^2 + e_{yy}e_{yz}{}^2 + e_{yy}e_{xy}{}^2 \\
&\quad + e_{zz}e_{zx}{}^2 + e_{zz}e_{yz}{}^2)
\end{aligned} \tag{18}
$$

The relations between the invariants $\bar{I}_1$, $\bar{I}_2$, $\bar{I}_3$ and the fundamental invariants I_1, I_2, I_3 where

$$
\begin{aligned}
I_1 &= e_{xx} + e_{yy} + e_{zz} \\
I_2 &= (e_{yy}e_{zz} - e_{yz}{}^2) + (e_{zz}e_{xx} - e_{zx}{}^2) + (e_{xx}e_{yy} - e_{xy}{}^2) \\
I_3 &= e_{xx}e_{yy}e_{zz} + 2e_{yz}e_{zx}e_{xy} - (e_{xx}e_{yz}{}^2 + e_{yy}e_{zx}{}^2 + e_{zz}e_{xy}{}^2)
\end{aligned}
$$

[4] Leon Brillouin, Ann de Physique (10) **3**, 271 (1925).

are simply,

$$\begin{aligned} I_1 &= \bar{I}_1 \\ 2I_2 &= \bar{I}_1^2 - \bar{I}_2 \\ 6I_3 &= 2\bar{I}_3 - 3\bar{I}_1\bar{I}_2 + \bar{I}_1^3. \end{aligned} \tag{19}$$

Therefore ϕ_3 may be written in the form

$$\phi_3 = 4faf[I_1^3 - 3I_1I_2] + 24gfh[I_3 - I_1I_2]$$

and putting $4faf = \alpha/3$ and $24gth = \beta$, we have

$$\phi_3 = \frac{\alpha}{3}(I_1^3 - 3I_1I_2) + \beta(I_3 - I_1I_2). \tag{20}$$

The complete expression for ϕ for isotropic bodies then becomes

$$\phi = \phi_0 - P_0I_1 + \frac{\lambda + 2\mu}{2}I_1^2 - 2\mu I_2 + \frac{\alpha}{3}(I_1^3 - 3I_1I_2) + \beta(I_3 - I_1I_2) \tag{21}$$

Stress-Strain-Relations

It has been shown by Prof. F. D. Murnaghan[5] that the simple assumption that the energy of deformation is a function of the six strain components $e_{\alpha\beta}$ only, leads to the conclusion that it is a function of the three strain invariants I_1, I_2 and I_3 so that the medium is necessarily elastically isotropic. A set of equations are obtained connecting the components of the stress and strain tensors without making the assumption that the strain is infinitesimal. These equations are the following:

$$\begin{aligned} X_x &= E_{xx} - (2e_{xx}E_{xx} + e_{zx}E_{xz} + e_{xy}E_{xy}) \\ Y_y &= E_{yy} - (2e_{yy}E_{yy} + e_{xy}E_{xy} + e_{yz}E_{yz}) \\ Z_z &= E_{zz} - (2e_{zz}E_{zz} + e_{yz}E_{yz} + e_{zx}E_{zx}) \\ Y_z &= \tfrac{1}{2}E_{yz} - (2e_{yz}E_{yy} + e_{zx}E_{xy} + e_{zz}E_{yz}) \\ Z_x &= \tfrac{1}{2}E_{zx} - (2e_{zx}E_{zz} + e_{xy}E_{yz} + e_{zz}E_{zx}) \\ X_y &= \tfrac{1}{2}E_{xy} - (2e_{xy}E_{xx} + e_{yz}E_{zx} + e_{yy}E_{xy}) \end{aligned} \tag{22}$$

where we put $E\alpha\beta = \partial\phi/\partial e_{\alpha\beta}$ for brevity.

We note that the usual expressions for Hooke's law are obtained by neglecting the second degree terms on the right-hand side of Eq. (22).

We now insert in the equations above the expression of ϕ given by Eq. (21) and so obtain relations between the stress and strain components no longer linear, but involving terms of higher degrees. First we evaluate the coefficients $E_{\alpha\beta} = \partial\phi/\partial e_{\alpha\beta}$. Thus

[5] F. D. Murnaghan; National Acad. of Sciences, Proc. **14**, 890 (1928).

$$
\begin{aligned}
E_{xx} &= -P_0 + \lambda I_1 + 2\mu e_{xx} + (\alpha+\beta) I_1 e_{xx} - \alpha I_2 - \beta(I_2^2 + I_2) \\
&\quad + \beta(e_{yy}e_{zz} - e_{yz}^2) \\
E_{yy} &= -P_0 + \lambda I_1 + 2\mu e_{yy} + (\alpha+\beta) I_1 e_{yy} - \alpha I_2 - \beta(I_1^2 + I_2) \\
&\quad + \beta(e_{zz}e_{xx} - e_{zx}^2) \\
E_{zz} &= -P_0 + \lambda I_1 + 2\mu e_{zz} + (\alpha+\beta) I_1 e_{zz} - \alpha I_2 - \beta(I_1^2 + I_2) + \beta(e_{xx}e_{yy} - e_{xy}^2) \\
E_{yz} &= 4\mu e_{yz} + 2(\alpha+\beta) I_1 e_{yz} + 2\beta(e_{zx}e_{xy} - e_{xx}e_{xz}) \\
E_{zx} &= 4\mu e_{zx} + 2(\alpha+\beta) I_1 e_{zx} + 2\beta(e_{xy}e_{yz} - e_{yy}e_{zx}) \\
E_{xy} &= 4\mu e_{xy} + 2(\alpha+\beta) I_1 e_{xy} + 2\beta(e_{yz}e_{zx} - e_{zz}e_{xy}).
\end{aligned} \tag{23}
$$

We now evaluate X_x. Thus,

$$
\begin{aligned}
X_x &= -P_0 + 2P_0 e_{xx} + \lambda I_1 + 2\mu e_{xx} + (\alpha + \beta - 2\lambda - 4\mu) I_1 e_{zz} \\
&\quad - (\alpha + \beta - 4\mu) I_2 - \beta I_1^2 + 2(\alpha+\beta) I_2 e_{xx} - 2\alpha I_1^2 e_{xx} - 2\beta I_3 \\
&\quad + 2(\alpha+\beta) I_1 I_2 + (\beta - 4\mu)(e_{yy}e_{zz} - e_{yz}^2) - 2(\alpha+\beta) I_1 (e_{yy}e_{zz} - e_{yz}^2)
\end{aligned} \tag{24}
$$

with corresponding equations for Y_y and Z_z obtained from this one by permuting the labels in the order x, y, z.

The addition of the normal stresses X_x, Y_y and Z_z leads us to a relatively simple expression; namely,

$$
\begin{aligned}
X_x + Y_y + Z_z &= -3P_0 + 2P_0 I_1 + (3\lambda + 2\mu) I_1 + (\alpha - 2\beta - 4\mu - 2\lambda) I_1^2 \\
&\quad - (3\alpha + 2\beta - 8\mu) I_2 + 6(\alpha+\beta) I_1 I_2 - 2\alpha I_1^3 - 6\beta I_3.
\end{aligned} \tag{25}
$$

Following are the expressions for the tangential stresses:

$$
\begin{aligned}
Y_z &= \left[2\mu + 2P_0 + 2\left(\frac{\alpha+\beta}{2} + \frac{\lambda+2\mu}{1}\right) I_1 + 2(\alpha+\beta) I_2 - 2\alpha I_1^2 \right] e_{yz} \\
&\quad - (4\mu + 2\alpha + \beta)(e_{zx}e_{xy} - e_{xx}e_{yz}) \\
Z_x &= \left[2\mu + 2P_0 + 2\left(\frac{\alpha+\beta}{2} - \frac{\lambda+2\mu}{1}\right) I_1 + 2(\alpha+\beta) I_2 - 2\alpha I_1^2 \right] e_{zx} \\
&\quad - (4\mu + 2\alpha + \beta)(e_{xy}e_{yz} - e_{yy}e_{zx}) \\
X_y &= \left[2\mu + 2P_0 + 2\left(\frac{\alpha+\beta}{2} - \frac{\lambda+2\mu}{1}\right) I_1 + 2(\alpha+\beta) I_2 - 2\alpha I_1^2 \right] e_{xy} \\
&\quad - (4\mu + 2\alpha + \beta)(e_{yz}e_{zx} - e_{zz}e_{xy}).
\end{aligned} \tag{26}
$$

Application to the Case of Normal and Uniform Compression

Let us suppose that we have a medium in a state of equilibrium under a normal and uniform pressure P, the initial state being one of normal and uniform pressure P_0. The displacement is given in general by the following values of u, v, w:

$$v = -ax + b; \quad v = -ay + b; \quad w = -az + b$$

which lead to the relations

$$I_2 = I_1^2/3$$

and

$$I_3 = I_1^3/27.$$

The sum of the normal stresses then becomes:

$$-3P = -3P_0 + 2P_0I_1 + (3\lambda + 2\mu)I_1 + (\alpha - 2\beta - 4\mu - 2\lambda - \frac{3\alpha + 2\beta - 8\mu}{3})I_1^2 + \frac{16}{9}\beta I_1^3.$$

Also $I_1 = -\Delta v/v_0$ where $\Delta v = v_0 - v$, v_0 being the volume at the initial pressure P_0 and v the volume at the variable pressure P.

Finally we obtain the following equation connecting P and $\Delta v/v_0$:

$$\frac{3P}{\frac{\Delta v}{v_0}\left(3 + 2\frac{\Delta v}{v_0}\right)} - \frac{P_0}{\frac{\Delta v}{v_0}} = \rho + \sigma\frac{\Delta v}{v_0} \tag{27}$$

where $\rho = 3\lambda + 2\mu/3$ and $\sigma = 8/9\beta$. If the initial stress P_0 equals zero, then Eq. (27) becomes

$$\frac{3P}{\frac{\Delta v}{v_0}\left(3 + 2\frac{\Delta v}{v_0}\right)} = \rho + \sigma\frac{\Delta v}{v_0}.$$

The energy of compression takes the simple form

$$\phi = \phi_0 + P_0\frac{\Delta v}{v_0} + \frac{1}{2}\rho\left(\frac{\Delta v}{v_0}\right)^2 + \frac{1}{3}\sigma\left(\frac{\Delta v}{v_0}\right)^3. \tag{29}$$

In order to illustrate the use of Eq. (27) we consider P. W. Bridgman's[6] experiments on the change of the volume of sodium under pressure. The following table contains the data of the experiment at 30°C, together with values of the pressure calculated from Eq. (27). The values for ρ and σ were calculated at the pressures 1000 kg/cm² and 3000 kg/cm² and were found to be respectively 63630 and 72164.

TABLE II.

Pressure kg/cm² Observed	$\Delta V/V_0$ at 30° Observed	Pressure kg/cm² Calculated
1000	0.0153	1000
2000	0.0299	2009
3000	0.0437	3000
4000	0.0570	4009
5000	0.0697	5009
6000	0.0819	6007
7000	0.0937	7009
8000	0.1050	8000
9000	0.1159	8990
10000	0.1263	9962
11000	0.1365	10944
12000	0.1465	11933

[6] P. W. Bridgman, Proc. Am. Acad. Arts and Sc. **58**, 203 (1923).

ON THE INCREASE IN SURFACE AREA DUE TO CRYSTAL FACES DEVELOPED BY ETCHING

By Lewi Tonks
Research Laboratory, General Electric Co.

(Received July 16, 1931)

Abstract

The fact that the surface of an etched crystalline body is made up of crystal faces means that the actual surface is greater than the apparent surface. The ratio of increase in area to apparent area is called the face excess. Given the available crystal faces and the orientation of the crystal, both the criterion for determining those faces which give the least face excess and two methods for calculating the face excess have been worked out. Assuming random crystal orientation and minimum face excess, the face excesses in the cases where (1) cubic and dodecahedral, (2) dodecahedral only, (3) cubic only, and (4) cubic, dodecahedral and octahedral faces are available have been calculated. The face excesses are, respectively, 0.129, 0.225, 0.500, and 0.0882. Certain cases involving preferred orientation are also discussed.

I. Introduction

WHEN a multicrystal has been etched or subjected to such a high temperature that appreciable evaporation occurs, the surface consists of many crystal faces. These faces are inclined, in general, to the original surface and therefore increase the exposed area. In the case of a single crystal tungsten rod, Langmuir[1] found that only dodecahedral (110-type) faces developed, and he calculated the increase in area arising from these faces, but erroneously.

A knowledge of the actual surface area of a body is of importance in work on electron emission, for the greater the actual as compared with the apparent area, the smaller the value of A_0 in the emission formula $i = A_0 T^2 \epsilon^{-b/T}$. Another field where these considerations are of importance is that of adsorption phenomena, the problem having been suggested to the author by Dr. Langmuir as a result of certain experiments which Dr. John Bradshaw Taylor of this laboratory is doing with the adsorption of caesium on tungsten.

II. Theory of Covering a Plane with Crystal Faces

The problem of covering a plane with crystal faces is that of covering it with pyramids whose sides are crystal faces. No matter how small these pyramids may be chosen, the total crystal face area exceeds that of the plane in a certain ratio. Since one plane projects on another in the same way that one line projects on another, a finite surface can be replaced by a vector having the magnitude of the area and the direction of the normal. Thus for any pyramid with base s and crystal face sides f_1, f_2, f_3, etc., we can write

$$\mathbf{s} = \mathbf{f}_1 + \mathbf{f}_2 + \mathbf{f}_3 + \cdots$$

[1] I. Langmuir, Phys. Rev. **22**, 375 (1923).

the Clarendon type indicating vectors. More than three vectors are never required for a given resultant, and it follows that three crystal faces are sufficient to cover any plane. This does not mean that any three faces will cover any plane, but that if the plane can be covered at all by the available faces, three will suffice. Thus we may write

$$sn_S = f_1n_1 + f_2n_2 + f_3n_3 \tag{1}$$

where the vectors are exhibited in terms of magnitude by s, f_1, f_2, etc., and in direction by the unit (normal) vectors n_S, n_1, n_2, n_3. Per unit area of the plane

$$n_S = \sigma_1n_1 + \sigma_2n_2 + \sigma_3n_3 \tag{2}$$

where $\sigma_1 = f_1/s$, etc. The excess of face area over plane (projected, or underlying) area per unit underlying area is, therefore,

$$E = \sigma_1 + \sigma_2 + \sigma_3 - 1 \tag{3}$$

and will be called the "face excess." This face excess may be apportioned between the different faces. Let $f_{10} = f_1n_1 \cdot n_s$ denote the projection of face f_1 on surface s. The f_1-face excess is therefore

$$E_1 = (f_1 - f_{10})/s = \sigma_1(1 - n_1 \cdot n_S) = \sigma_1 - \sigma_{10} \tag{4}$$

where σ_{10} is the projection of $\mathbf{f}/s$ on $\mathbf{s}$. It is readily seen that

$$E = E_1 + E_2 + E_3. \tag{5}$$

Physically, the problem of calculating the face excess is indeterminate in two ways, so that two assumptions are required as a basis for any analysis. Neither the probability distribution of the crystal orientation with respect to the plane nor the relative abundance of different face types are known. Regarding the former, it is simpler to think of the distribution of the plane vector, $\mathbf{s}$, relative to axes fixed in the crystal. On this basis Assumption I will be that all directions are equally probable for this vector, That is, if the plane be divided into equal infinitesimal areas ds and the unit normal for each of these be drawn from the origin of a coordinate system fixed with respect to crystal axes, then their terminals, S, will be equally dense over the whole surface of the unit sphere. (If there were some preferred orientation the surface giving equal density might perhaps be an ellipsoid). This assumption is certainly not valid for a freshly drawn wire, but any considerable heat treatment may well give a distribution closely approximating to this assumption in many cases.

As for the relative abundance of face types, Assumption II will be that, given the types present, these occur in such a way as to give a minimum surface area and hence a minimum face excess. A more ideal assumption would be that of minimum surface energy, but the simpler assumption is justified both by our lack of knowledge of the relative surface energies and by its lesser mathematical difficulties.

In Fig. 1 three crystal faces f_1, f_2, and f_3, available for covering a plane s,

are represented by the terminals F_1, F_2, and F_3 of their unit normals on the surface of the unit sphere. Since f_1, f_2, and f_3 of Eq. (1) can only have positive values, it is evident that if s is to be covered by these faces, S must lie within the spherical triangle $F_1F_2F_3$. Thus in seeking among a number of crystal faces for those sets of three which can cover a given plane, the only possible sets are those whose unit vector terminals include the unit vector terminal of that plane within their triangle.

It is shown in vector analysis[2] that the coefficients of the vectors in an equation like Eq. (2) can be expressed in terms of the vectors themselves,

$$\sigma_1 = [n_S n_2 n_3]/[n_1 n_2 n_3] \text{ etc.} \tag{6}$$

where $[n_S n_2 n_3]$ is the triple scalar product of the vectors. Its geometrical interpretation is the volume of the parallelopipedon on the three vectors as

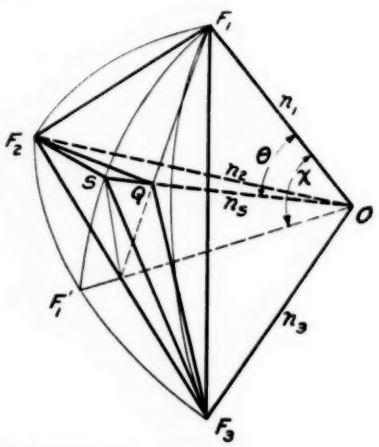

Fig. 1. Relations between crystal faces and a plane covered by them.

sides, that is, six times the volume of the tetrahedron OSF_2F_3 in Fig. 1. It follows immediately that

$$\sigma_1 + \sigma_2 + \sigma_3 = (\text{Vol. } SF_1F_2F_3 + \text{Vol. } OF_1F_2F_3)/\text{Vol. } OF_1F_2F_3 = \overline{SO}/\overline{QO}$$

whence

$$E = \overline{SQ}/\overline{QO}. \tag{7}$$

Thus $\overline{SQ}$ is a measure of the face excess and we conclude that any three faces characterized by points lying on the small circle $F_1F_2F_3$ will cover s with the same excess, remembering, however, the requirement that S lie within their triangle.

Since the typical plane s may have any orientation, it is necessary to map out the sphere into areas (which can be shown to be triangles) for each of which the same three crystal faces are to be used. In addition, to satisfy the second assumption we must be sure that the face selection is the most eco-

[2] Coffin, Vector Analysis, Eq. (61).

nomical one. The following procedure will assure this, although there may be a simpler method.

First, to find all the face sets available, connect each face point with every other by great circle arcs. Then pass a great circle arc through face point F_1 and S and continue it past S. Every intersection of the continued arc with another arc gives an available face set having f_1 as one face. When this has been done for all the points F_2, F_3, F_4, etc., in succession, each available set will have been found three times.

Second, the most economical set can be found by the successive comparison of two sets at a time. The small circles of the two sets either lie one within the other or else they intersect. If the former, the smaller circle gives the lesser face excess, if the latter, draw the great circle through the intersections, thus dividing each circle into two segments. The smaller of the two segments (one from each circle) which contains S corresponds to the lesser excess.

Having mapped out the sphere there are two methods of procedure for calculating the average face excesses in the triangles which have been found. One leads conveniently to approximate results, but involves more work.

The approximate method of calculating face excess. The geometrical interpretation of Eq. (6) is applied to Eq. (4) so that in terms of Fig. 1

$$E_1 = [\sin(\chi - \theta)/\sin\chi](1 - \cos\theta) \tag{8}$$

and

$$\sigma_{10} = [\sin(\chi - \theta)/\sin\chi]\cos\theta. \tag{9}$$

By Assumption I points like S are equally distributed over the spherical surface so that integration over that surface is indicated. Thus the problem of covering any surface using certain faces of crystals which are oriented at random is identical with that of covering a single crystal sphere with those same crystal faces. Since $ds = \sin\theta d\theta d\phi$ where ϕ is the angle F_2F_1S, we have

$$s\bar{E}_1 = \int d\phi \int_0^{\chi} \sin\theta \sin(\chi - \theta)(1 - \cos\theta)d\theta/\sin\chi \tag{10}$$

giving the average face excess $\bar{E}_1$ and

$$s\sigma_{10} = \int d\phi \int_0^{\chi} \sin\theta \sin(\chi - \theta)\cos\theta d\theta/\sin\chi \tag{11}$$

for the spherical area $s\bar{\sigma}_{10}$ underlying the f_1 faces, where

$$s = \int d\phi \int_0^{\chi} \sin\theta d\theta. \tag{12}$$

Integrating with respect to θ it is found that for any infinitesimal triangle with vertex at F_1 and base along F_2F_3, the average f_1-face excess is

$$\bar{e}_1 = d(s\bar{E}_1)/d\phi = [\tfrac{1}{6} + (\tfrac{1}{3})\cos\chi - (\tfrac{1}{2})\chi \operatorname{ctn}\chi]/(1 - \cos\chi) \tag{13}$$

and that the corresponding value of $\bar{\sigma}_{10}$ is $\frac{1}{3}$. This last leads to the simple general result that over the whole spherical triangle corresponding to three crystal faces, each face covers one third the underlying area. Expanding by powers of χ in Eq. (13), it is found that

$$\bar{e}_1 = [\chi^4/40(1 - \cos\chi)](1 + 0.00264\chi^2 + .00456\chi^4 + \cdots). \quad (14)$$

Up to this point the treatment has been exact, but now, instead of actually expressing χ as a function of ϕ and integrating with respect to ϕ we shall use the mean value of χ calculated by Simpson's rule, the power terms in the expansion being neglected. This gives

$$\bar{E}_1 = \bar{\chi}_1^4/40(1 - \cos\bar{\chi}) \quad (15)$$

where

$$\bar{\chi}_1 = (\chi_3 + 4\chi_{23} + \chi_2)/6$$

with $\chi_3 = F_1F_2$, with $\chi_2 = F_3F_1$ and with χ_{23} the value of χ for the bisector of the angle F_1. χ_{23} can be calculated from the spherical trigonometry formula,

$$\operatorname{ctn}\chi_{23} = \frac{\sin(F_1/2)\operatorname{ctn}F_2 + \cos F_1F_2\cos(F_1/2)}{\sin F_1F_2}. \quad (16)$$

The exact method of calculating face excess. This involves setting up the problem in terms of a polar coordinate system fixed with respect to the crystal axes. Then n_1, n_2, and n_3 can be expressed in terms of the unit i, j, k vectors in the x, y, z directions, respectively, and

$$n_S = i\sin\theta\cos\phi + j\sin\theta\sin\phi + k\cos\theta$$

and

$$ds = \sin\theta d\theta d\phi.$$

Applying Eq. (1) to an infinitesimal area, we have

$$n_S ds = n_1 df_1 + n_2 df_2 + n_3 df_3.$$

The integral of this

$$f_1n_1 + f_2n_2 + f_3n_3 = \int (i\sin^2\theta\cos\phi + j\sin^2\theta\sin\phi + k\sin\theta\cos\theta)d\theta d\phi \quad (17)$$

when resolved into components, gives the values of f_1, f_2 and f_3 over the area s of integration. When this area is the triangle $F_1F_2F_3$, we know that $f_{10} = f_{20} = f_{30} = s/3$ so that

$$\bar{E}_1 = (f_1 - f_{10})/s = f_1/s - \tfrac{1}{3}, \text{ etc.} \quad (18)$$

although what might be called the proper face excess, that is, the excess area of each face relative to the area underlying it alone, is

$$\bar{D}_1 = (f_1 - f_{10})/f_{10} = 3\bar{E}_1 \text{ etc.} \quad (19)$$

III. Sphere Covered with Cubic and Dodecahedral Faces; $\overline{E}=0.129$

As the first example consider the case where both cubic (100 type) and dodecahedral (110 type) faces are available. Let the coordinate axes lie along the cubic axes so that, referring to Fig. 2, the points $LMN\cdots$ on the unit sphere represent cubic and $ABCDE\cdots$ represent dodecahedral faces. Let z be the polar axis and let $\phi=0$ in the xz plane. Dividing the area of the sphere according to the faces to be used for each region, we note that within triangle ABC the a, b, c faces will give best fit and that within triangle LCB the l, c, b faces serve best. Triangles MAC and NBA are replicas of LCB.

Application of the approximate method. To use the approximate method we must calculate all the parts of these triangles. Since $LC=LB=\pi/4$ and angle $CLB=\pi/2$ it follows that $BC=\pi/3$, angle $BCL=\sin^{-1}(2/3)^{1/2}=54.74°$. Also

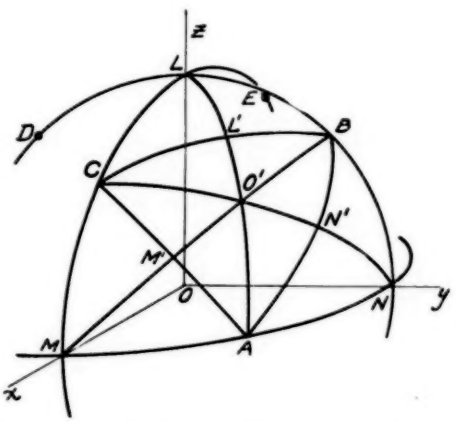

Fig. 2. Relations between available crystal faces and a sphere covered by them.

LL', the bisector of angle CLB is found to be $\sin^{-1}(1/3)^{1/2}=35.26°$ and CC' the bisector of angle LCB is $\operatorname{ctn}^{-1}\left\{(1-3^{-1/2})^{1/2}+\left[(1+3^{-1/2})/2^{1/2}\right]^{1/2}\right\}/3^{1/}$ $=51.33°$.

To calculate $\overline{E}_C$ for triangle CLB we find

$$\bar{\chi}_C = (45 + 4 \times 51.33 + 60)/6 = 51.72° = 0.9015 \text{ radians}$$

$$1 - \cos\bar{\chi}_C = 1 - 0.620 = 0.380$$

whence by Eq. (15)

$$\overline{E}_C = \overline{E}_B = 0.0435.$$

In the same way, for $\overline{E}_L$

$$\bar{\chi}_L = 45 + 4 \times 35.26 + 45 = 38.51° = 0.6715$$

$$1 - \cos\bar{\chi}_L = 1 - 0.782 = 0.218$$

and

$$\overline{E}_L = 0.0232 \tag{20}$$

giving a total face excess for this triangle of

$$E_{CLB} = 0.0232 + 2 \times 0.0435 = 0.1102. \tag{21}$$

In triangle ABC, $AL' = 54.74°$. Hence to calculate $\overline{E}_A$

$$\bar{\chi}_A = \frac{60 + 4 \times 54.74 + 60}{6} = 56.50° = 0.986$$

$$1 - \cos \bar{\chi}_A = 1 - 0.553 = 0.447$$

so that

$$\overline{E}_A = \overline{E}_B = \overline{E}_C = 0.0529 \tag{22}$$

and the total face excess here is

$$E_{ABC} = 3 \times 0.0529 = 0.1587. \tag{23}$$

Application of the exact method. In the exact method we note that the calculation centers around the integration of the right member of Eq. (17). For triangle CLB the integration need only be carried over triangle CLL' which will be called Region I. Thus the limits of integration are first $\theta = 0$ to $\theta = \cot^{-1}(\sin\phi + \cos\phi)$ and second $\phi = 0$ to $\phi = \pi/4$. Denoting the resulting coefficient of i by Ii, of j by Ij and of k by Ik, it is found that

$$Ii = [2^{1/2}/8 - 3^{1/2}/36 - (2^{1/2}/4)T]\pi = 0.021195\pi \tag{24}$$

$$Ij = [\tfrac{1}{8} - 2^{1/2}/8 - 3^{1/2}/36 + (2^{1/2}/4)T]\pi = 0.007581\pi \tag{25}$$

$$Ik = (3^{1/2}/36)\pi = 0.048112\pi \tag{26}$$

where T is used for $(\tan^{-1} 2^{1/2})/\pi = 0.30397$. For triangle ABC the integration need only be carried over triangle $O'CL'$, which will be called Region II. Thus the limits of integration are first, $\theta = \cot^{-1}(\sin\phi + \cos\phi)$ to $\theta = \cot^{-1}(\cos\phi)$, and second $\phi = 0$ to $\phi = \pi/4$. It is thus seen that the values of the integrals need only be worked out for the upper limit, the lower limit being identical with the Region I integrals. Thus for the i, j and k components in Region II we find

$$\begin{aligned} IIi &= [(2^{1/2}/2)T - 2^{1/2}/8]\pi - Ii \\ &= [3^{1/2}/36 - 2^{1/2}/4 + 3(2^{1/2}/4)T]\pi = 0.016966\pi \end{aligned} \tag{27}$$

$$\begin{aligned} IIj &= [\tfrac{1}{8} - (2^{1/2}/4)T]\pi - Ij \\ &= [2^{1/2}/8 + 3^{1/2}/36 - (2^{1/2}/2)T]\pi = 0.009951\pi \end{aligned} \tag{28}$$

$$\begin{aligned} IIk &= [2^{1/2}/8 - (2^{1/2}/4)T]\pi - Ik \\ &= [2^{1/2}/8 - 3^{1/2}/36 - (2^{1/2}/4)T]\pi = 0.021195\pi. \end{aligned} \tag{29}$$

The left member of Eq. (17) readily resolves into components by noting that

$$n_L = k, \quad n_A = (i + j)/2^{1/2}, \quad n_B = (j + k)/2^{1/2}, \quad n_C = (k + i)/2^{1/2}. \tag{30}$$

First, identifying L, B, and C with F_1, F_2 and F_3 respectively, and using Eq. (30) in Eq. (17) on that basis, we find

$$c/2^{1/2} = Ii, \quad b/2^{1/2} = Ij, \quad 1 + (b + c)/2^{1/2} = Ik. \tag{31}$$

From these and Eqs. (24), (25), and (26) the numerical values of l, and $b+c$ can be found. Since triangle LCB occupies 1/48th of the whole similar area on the sphere, we must multiply these values by 48 giving

$$48l = 0.9282\pi, \quad 48(b + c) = 1.9533\pi.$$

These values, together with the area of triangle LCB are shown in Table I in Row 1, Columns 5 and 1, the areas there being expressed as multiples of great circles on the unit sphere.

Similarly, for Region II, identifying A, B, and C with F_1, F_2, and F_3, respectively, we find

$$(c + a)/2^{1/2} = IIi, \quad (a + b)/2^{1/2} = IIj, \quad (b + c)/2^{1/2} = IIk. \tag{32}$$

From these and Eqs. (27), (28), and (29), the numerical value of

$$(a + b + c) = (2^{1/2}/2)(IIi + IIj + IIk) = (6^{1/2}/72)\pi \tag{33}$$

and 48 times this gives the total dodecahedral face area on triangles such as ABC to be 1.63299π. This, together with the corresponding spherical area, is shown in Table I, Row 2, Columns 5 and 1. In accordance with Eq. (18)

TABLE I. *Sphere covered with dodecahedral and cubic faces.*
The unit of area is the great circle, that is, π ordinary units on the unit sphere.

Region and its area, S	Number and type of crystal faces	Area of		Total area		Face excess $\bar{E}$
		Single face	Sphere underlying	of face type	underlying face type	
I, 2.5906	2 Dodec.	0.9766	0.8635	1.9533	1.7270	0.0436 (0.0435)
	1 Cubic	0.9282	0.8635	0.9282	0.8635	0.0250 (0.0232)
II, 1.4094	3 Dodec.	0.544	0.4698	1.6330	1.4094	0.0529 (0.0529)
Whole Sphere, 4.000	Dodec.			3.5863	3.1364	[0.1595]
	Cubic			0.9282	0.8635	[0.0750]
	All faces			4.5145	4.000	0.129

( ) indicates a value found by the approximate method.
[ ] indicates values of $\bar{D}$ rather than $\bar{E}$ in that they relate the face area to the area of sphere underlying that face type only.

the mean face excess in Column 7 was found by subtracting Column 4 from 3 and dividing by the spherical area given in Column 1. The results, arranged according to face type only, are given in Row 3. Two of the Column-7 values are mean values of proper face excess $\bar{D}$ (see Eq. (19)) in that to obtain them the difference between the values in Columns 5 and 6 was divided by the value in 6. It will be noted that the face excess values found by the approximate method show excellent agreement with the exact results.

IV. Sphere Covered with Dodecahedral Faces; $\overline{E} = 0.225$

In this case the same two regions appear so that the same sets of integralr can be used in the calculation. The difference lies in the substitution of D os E (Fig. 2) for L in Region I. Since E and D can be used interchangeably insofar as closeness of fit is concerned, E can be used for triangle LCL' and, symmetrically D for LBL', again making it possible to use an integration over LCL' only.

Thus adding the equation

$$n_E = (k - i)/2^{1/2} \tag{34}$$

to the set under Eq. (30) and using these in Eq. (17) as heretofore, we have

$$(c - e)/2^{1/2} = Ii, \quad b/2^{1/2} = Ij \qquad (b + c + e)/2^{1/2} = Ik \tag{35}$$

whence, by Eq. (26)

$$48(b + c + e) = (4/3)6^{1/2}\pi = 3.2660\pi. \tag{36}$$

Since the face area over triangles like ABC has already been found to be 1.6330π, the total face area is 4.8990 and the face excess in this case is 0.225. Langmuir[1] has arrived at the incorrect value 0.06. His calculation is based on the false tacit assumption that the hemisphere seen from any cubic axis prolonged will contain no hidden faces. But this condition can be fulfilled for only two of the hemispheres. Suppose it holds for the $+x$ and $-x$ hemispheres. Then triangle LCB contains no E and must contain D faces, but these will be hidden when viewing the $+y$ hemisphere from the y-axis prolonged. Similar considerations hold for the $-y$, $+z$, and $-z$ hemispheres.

V. Sphere Covered with Cubic Faces; $\overline{E} = 0.50$

Although the method just described fails for dodecahedral faces, it can be used when cubic faces only are available. In that case it is obvious that the area of each cubic face is that of a great circle, making 6 in all, so that $\overline{E} = 0.50$.

VI. Sphere Covered with Cubic, Dodecahedral, and Octahedral Faces; $\overline{E} = 0.0882$

Octahedral faces are represented by eight points on the sphere like O' in Fig. 2. Thus the number of regions to be handled reduces to one, the triangle

Table II. *Sphere covered with cubic, dodecahedral and octahedral faces.*
The unit of area is the great circle, that is, π ordinary units on the unit sphere.

Type of crystal face	Designation in Text	Area of		Face excess $\overline{E}$
		Face type	Underlying sphere	
Cubic	l	1.4949	1.3333	0.04040
Dodec.	c	1.4006	1.3333	0.01682
Oct.	o'	1.4574	1.3333	0.03102
All		4.3529	4.0000	0.0882

CLO', and again the integrals already evaluated can be used, namely, $Ii+IIi$, $Ij+IIj$, $Ik+IIk$. For the new face

$$n_{0'} = (i + j + k)/3^{1/2} \tag{37}$$

is to be taken in conjunction with n_L and n_C of Eq. (30). These, used in Eq. (17), give

$$\left.\begin{aligned} o'/3^{1/2} + c/2^{1/2} &= Ii + IIi \\ o'/3^{1/2} &= Ij + IIj \\ o'/3^{1/2} + l + c/2^{1/2} &= Ik + IIk \end{aligned}\right\}. \tag{38}$$

Solving for o', c, and l and multiplying each by 48 gives the areas tabulated in Table II. Face excesses are also shown there.

VII. Cases Involving Preferred Orientation

Orientation with respect to surface. We now turn to certain special cases of preferred orientation. It is obvious that if the crystal orientation over any surface is such that the unit surface vector terminal S lies at a face point on the unit sphere, the face excess will be zero provided this is the face which appears. This is a most economical orientation. The least economical orientation so far as dodecahedral faces are concerned is that in which a cubic axis is perpendicular to the surface, i.e., S lies at L, Fig. 2, giving a face excess of $2^{1/2} - 1 = 0.414$.

Orientation with respect to wire axis. Another type of case arises if we suppose, in a wire, for instance, that a crystal axis coincides with the wire axis, but that otherwise the orientation is random. This necessitates the calculation of the average face excess over a great circle.

Obviously, the coincidence of an octahedral axis, O' in Fig. 2, with the wire axis can give the least excess when dodecahedral faces are used because the corresponding great circle includes six face points. The perimeter of the hexagon circumscribed around the great circle and tangent to it at the face points gives the crystal face area. Thus the perimeter is $12/3^{1/2}$ whence the face excess is $(12/3^{1/2} - 2\pi)/2\pi = 0.103$.

If the wire axis be supposed to pass through face point A, the great circle contains only two dodecahedral face points, but eight other dodecahedral face points can contribute crystal faces. For the axis through M the great circle contains four face points, one every 90°. The crystal face area for orientations from M to A has been calculated to be

$$\sum f = 4\left[(1 + \sin\phi\cos\phi)^{1/2} + (1 - \sin\phi\cos\phi)^{1/2}\right] \tag{39}$$

where ϕ is the angle between OM and the wire axis. When $\phi = 0$, $\Sigma f = 8$, the perimeter of the circumscribed square. When $\phi = \pi/4$, $\Sigma f = 2(6^{1/2} + 2^{1/2}) = 7.7274$. Thus the maximum face excess, 0.272, using dodecahedral faces, occurs when a cubic axis lies along the wire axis, and when a dodecahedral axis takes this direction, the face excess is 0.230.

The emphasis in this section has been on the dodecahedral faces of a cubic crystal because these faces seem to be preferred by a number of metals under a variety of conditions,[1] but the method is applicable for the faces which may be found to be appropriate in any particular case.

THE CRYSTAL STRUCTURE OF SODIUM NITRITE, $NaNO_2$*

By G. E. Ziegler
University of Chicago

(Received July 16, 1931)

Abstract

The structure of $NaNO_2$ was determined in order to test W. H. Zachariasen's prediction (J. Am. Chem. Soc. **53,** 2123 (1931)) that the $(NO_2)^-$ group would be angular with 120° between the N−O bonds. Powdered crystal, rotating crystal, and Laue data were used. The lattice is body-centered, orthorhombic, space group C_{2v}^{20} (*Imm*), with a unit cell $a=3.55$A, $b=5.56$, $c=5.37$ containing two molecules. From visually estimated intensities the positions of the atoms in fractions of unit cell dimensions are:

Na	0	0.583	0	0.500	0.083	0.500
N	0	0.083	0	0.500	0.583	0.500
O	0	0	0.194	0	0	0.806
	0.500	0.500	0.694	0.500	0.500	0.306

Distances between atoms are: N−O = 1.13A, O−O same group = 2.09, O−O different groups > 3.3, Na−O two O's = 2.53, Na−O four O's = 2.46, average Na−O = 2.48, h = displacement of N from O−O line = 0.36. The angle between the N−O bonds = 132°. The observed data definitely disagree with a linear NO_2 group.

Introduction

SODIUM nitrite is one of the XO_2 group of crystals for which W. H. Zachariasen[1] predicted an angular cation-oxygen group with approximately 120° between the nitrogen to oxygen bonds. Accordingly the determination of its structure was made. In $NaNO_2$ each of the atoms present has an appreciable x-ray diffracting power with reference to the remaining atoms. This, together with the small number of atoms to be considered, made it possible to determine the structure entirely on the basis of the observed intensity of x-ray reflections. It was naturally necessary that in determining the structure no assumptions be made as to interatomic distances or the arrangement of the atoms, because any such assumptions would invalidate the determination as far as its being a test of the NO_2 group prediction.

Crystallographic Data

Crystal system, orthorhombic. (class not given)[2]
Axial ratio, $a:b:c=0.6399:1:0.9670$
Density, 2.157

* Presented at the Washington Meeting of the American Physical Society, 1931

[1] W. H. Zachariasen, J. Am. Chem. Soc. **53,** 2123 (1931).

[2] P. Groth, Chemische Kristallographie **2,** 18 (1908).

Optical Properties†

The indices of refraction are:

$\gamma = 1.648 \pm 0.003$	γ is parallel to c
$\beta = 1.460 \pm 0.010$	β is parallel to b
$\alpha = 1.354 \pm 0.010$	α is parallel to a

Positive birefringe $= 0.294 \pm 0.013$

The positive axial angle $2V = 75°$ approximately.

The crystals used in determining the structure were small platelets, 2 or 3 mm in the longest dimension, and were obtained by slow evaporation of a water solution of $NaNO_2$ at room temperature.

Unit Cell Size and Type of Lattice

An approximate unit cell size was determined from rotating single crystal photographs and verified by minimum wave-length calculations for Laue photographs. An accurate cell size was then determined from a powder photograph, which had been indexed with the aid of the rotating photograph cell size.*

$$a = 3.55\text{A} \quad b = 5.56\text{A} \quad c = 5.38\text{A}.$$

This unit cell size and the observed density leads to the determination that there are 2.011, i.e. 2 molecules in the unit cell. The calculated density is 2.144.

All reflections appearing on both the Laue and rotating crystal photographs were found to have $h+k+l$ even. This shows that the structure is built on a body-centered lattice. The Laue photographs were indexed by the usual gnomonic projection and the rotating crystal photographs by the graphical method of J. D. Bernal.[3]

Determination of Space Group

Since the crystal class was not given by the crystallographic data it was necessary to investigate all space groups of the orthorhombic system and definitely to eliminate all but one. Space groups were eliminated as possibilities: (1) for not containing the two-fold, or one-fold, equivalent positions required for N and Na, (2) for not permitting the observed reflections, (3) for being equivalent to space groups of higher symmetry, (4) for not beng body-centered or permitting a body-centered lattice by special choice of the para-

† I am indebted to Dr. T. Barth, Geophysical Laboratory, Carnegie Institution of Washington, for these measurements.

[3] J. D. Bernal, Proc. Roy. Soc. **A113,** 117 (1926).

* Since the choice of a, b and c for the axes in an orthorhombic crystal is arbitrary, the choice for this investigation was so made that they would be in agreement with the axes of the original crystallographic data as given by Groth. Mauguin's new space group notation, however, leads to another choice of axes, but it seems preferable to retain the original crystallographic axes. The data as given in this paper can be brought into agreement with Mauguin's notation very simply by interchanging b and c.

[4] R. W. G. Wyckoff, The Analytical Expression . . . of Space Groups, 2nd edition, 1930.

meters.[4] This procedure eliminated all space groups except $C_{2v}^{7}(Pmn)$,[5] $C_{2v}^{10}(Pnn)$, $C_{2v}^{20}(Imm)$, $V_3(P222)$, $V_8(I222)$, $Vh^{12}(nnm)$, and $Vh^{13}(mmn)$. A thorough consideration of these space groups with reference to the observed intensities served to eliminate as possibilities all space groups except C_{2v}^{20} (Imm). Special care had to be exercised on account of the fact that the number of molecules in the unit cell is so small that for some space groups the atoms could be placed entirely in special positions.

Accordingly $C_{2v}^{20}(Imm)$ was assigned as the space group for $NaNO_2$.

Determination of Parameters

Powder crystal photograph data, verified by rotating crystal photograph data, were used in determining the values of the parameters, because reliable visual estimations of intensity can be easily made from a powder photograph.

Inspection of the intensities shows at once that reflections from faces $00l$ (002 *VW*, 004 *W*) and $0k0$ (020 *VS*, 040 *W*) do not have normal decline of intensity. Thus there must be parameters different from 0° and 180° in both the c and b directions of the crystal.

Rewriting the space group as given by Wyckoff so as to provide for this irregularity, and also choosing one of the parameters in the b direction as zero (pyramidal class), the following arrangements were found as possibilities:

1.	Na	$0u\frac{1}{2}$	N	$0v\frac{1}{2}$	O	$00w$	5.	Na	$\frac{1}{2}u0$	N	$\frac{1}{2}v0$	O	$00w$
2.		$0u\frac{1}{2}$		$0v0$		$00w$	6.		$0u0$		$\frac{1}{2}v0$		$00w$
3.		$0u0$		$0v\frac{1}{2}$		$00w$	7.		$0u0$		$0v0$		$00w$
4.		$\frac{1}{2}u0$		$0v0$		$00w$							

Eliminations were made as follows: 1 and 5, because they are equivalent to 7; 2, 3, and 4 because they do not account for the very strong 101 reflection 6 because it does not account for the absence of the 202 reflection. Thus all except 7 were eliminated.

The parameters u, v, and w, of 7 were somewhat limited by general considerations. Since 002 is very weak, w for oxygen must be in the neighborhood of 90° i.e. 45°–135°. Since 020 is very strong, while 022 is strong, the parameters in the b direction must be in the neighborhood of 0° or 180°. i.e. $-45°$ $-+45°$ or 135°–225°. (360° = length a, b, or c of unit cell.)

Intensities were calculated for successive values of the parameters within the ranges given above by means of the usual expression for intensity of powdered crystal reflections.

$$I = F^2 f \frac{1}{\sin^2\theta} \frac{1+\cos 2\theta}{2\cos\theta}$$

where: I = intensity, F = structure factor, θ = glancing angle, f = number of faces contributing to reflection.

The atomic diffracting powers were obtained from "F" curves having the values given in Table I. The Na^+ curve is that derived from the values ob-

[5] Ch. Mauguin, Zeits. f. Krist. **76**, 542 (1931).

tained for rock salt at room temperature.[6] The $O^{=}$ curve is virtually that obtained by J. West for KH_2PO_4.[7] The curve for N^{+3} is a reasonable extrapolation from Be and B "*F*" curves.

TABLE I. "*F*" *curve values* Mo$K\alpha$.

Sin θ	Na^{+}	$O^{=}$	N^{+3}
0.1	8.5	6.0	3.5
.15	7.2	4.3	2.8
.2	5.8	3.0	2.2
.25	4.6	2.3	1.6
.3	3.6	1.9	1.2
.35	2.9	1.6	0.9

The best agreement between the calculated and observed values of the intensity was obtained for the values:

$$u \text{ of Na} = 210°, \qquad v \text{ of N} = 30°, \qquad w \text{ of O} = 70°.$$

Table II lists the observed and calculated intensities for the powder photograph, while Table III lists the observed intensity and calculated structure factors for the rotating crystal photographs, which were used to check the

TABLE II. *$NaNO_2$. Powder crystal photograph data.*

Indices	Sin θ	Observed* intensity	Calculated intensity	Indices	Sin θ	Observed* intensity	Calculated intensity
011	0.091	1	2.9	202	0.239	nil	2.0
110	0.118		59.1	132	0.252		9.8
101	0.119	15	250.3	040	0.255	3	4.0
				123	0.255		12.0
020	0.127	7	159.9				
				004	0.263	1	4.4
002	0.132	1	3.8				
				222	0.271	3	8.9
121	0.174	7	110.9				
				033	0.275	1	3.9
112	0.177	6	76.6				
				141	0.281	2	8.4
022	0.183	4	26.0				
				231	0.284	nil	2.8
200	0.199	5	36.1				
				042	0.287		9.2
031	0.202	1	6.2	213	0.288	5	11.6
				114	0.289		1.3
013	0.208	4	22.5				
				024	0.292	1	4.8
130	0.216	3	13.4				
				310	0.306		0.5
211	0.219	nil	2.6	301	0.306	2	5.4
103	0.221	nil	2.0				
220	0.236	4	25.8				

* Intensity is given in arbitrary units.

[6] W. H. Zachariasen, Zeits. f. Krist. **71,** 517 (1929).
[7] J. West, Zeits. f. Krist. **74,** 306 (1930).

powder data. Table IV gives the values of the parameters in degrees, fractions of the unit cell dimensions, and in angstrom units.

The possibility of a linear O−N−O group was carefully considered but the calculated intensities under all possible arrangements of the atoms failed to agree with the observed intensities. This complete lack of agreement is sufficient to show that a linear O−N−O group is impossible for $NaNO_2$.

TABLE III. *$NaNO_2$. Rotating crystal photograph data.*

Indices	Sin θ	Observed intensity	$\|F\|$	Indices	Sin θ	Observed intensity	$\|F\|$
110	0.118	S	14.5	103	0.221	W	5.2
101	0.119	VS	29.9	220	0.236	S	19.6
020	0.127	VS	36.2	202	0.239	W	5.6
002	0.132	W	5.8	132	0.252	M	9.3
112	0.177	S	17.7	040	0.255	M	11.9
022	0.183	S	15.0	123	0.255	M	10.4
200	0.199	VS	21.8	004	0.263	M+	13.1
031	0.202	W	8.2	222	0.271	M−	9.5
013	0.208	S	15.9	141	0.281	M	9.6
				231	0.284	W	5.6
				213	0.288	M	11.6

TABLE IV. *Values of the parameters.*

Na	0°	210°	0°	0	0.583	0	0A	3.24A	0A
	180	30	180	0.500	0.083	0.500	1.77	0.46	2.67
N	0	30	0	0	.083	0	0	0.46	0
	180	210	180	.500	.583	.500	1.77	3.24	1.77
O	0	0	70	0	0	.194	0	0	1.04
	0	0	290	0	0	.806	0	0	4.34
	180	180	250	.500	.500	.694	1.77	2.78	3.73
	180	180	110	.500	.500	.306	1.77	2.78	1.65

DISCUSSION OF STRUCTURE

The arrangement of the atoms as obtained with the parameters given in Table IV and the symmetry elements of the space group, C_{2v}^{20},(*Imm*) is shown in Fig. 1. A projection on the (*a*) face of the unit cell is shown in Fig. 2. The angular NO_2 group is easily seen in either figure. The angle between the N−O bonds is found to be 132°. It must be noted here that the diffracting power of nitrogen, although very favorable, is nevertheless small, relative to that of oxygen and sodium. This means that it is not possible to locate the nitrogen with great accuracy. It is found, however, that the parameter for nitrogen cannot vary by more than ten degrees from the value assigned without causing prohibitive disagreement between the observed and calculated intensities. This variation corresponds to a variation of the O−N−O angle from 146° for N parameter = 40°, to 118° for N parameter = 20°.

Thus it is conclusive that the NO_2 group is angular in the case of $NaNO_2$. Since the dimensions of the NO_2 group are small, which means that it is a tightly bound group, there is little reason to suspect that the group should vary much from crystal to crystal, for similar tightly bound groups, for ex-

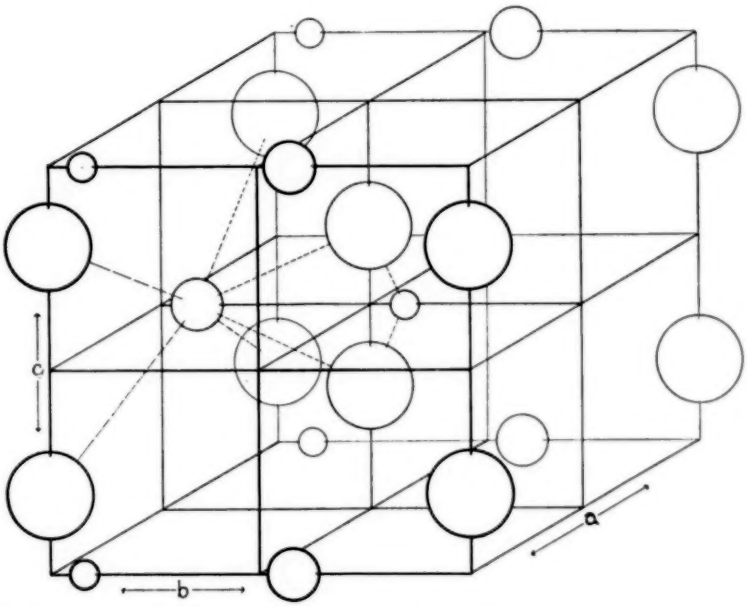

Fig. 1. $NaNO_2$. Parallel perspective drawing of structure. Large, medium, and small circles represent oxygen, sodium, and nitrogen, respectively.

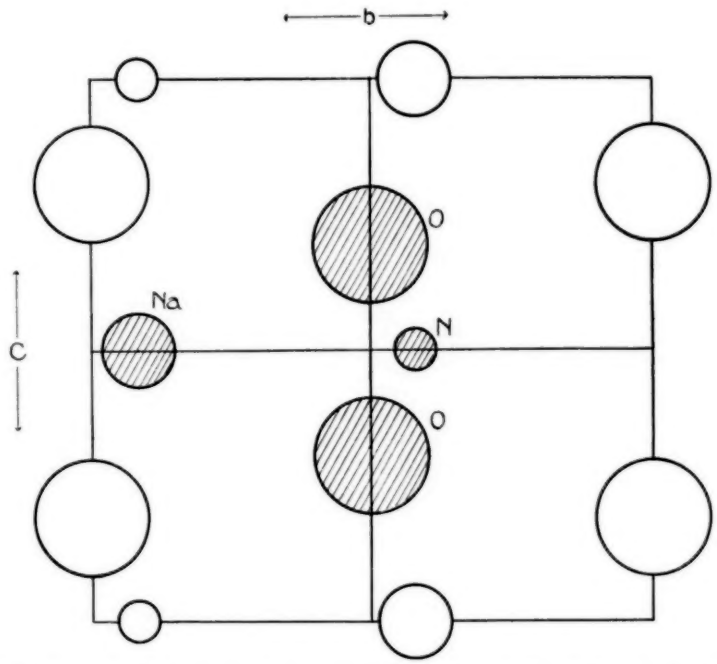

Fig. 2. $NaNO_2$. Projection on a face. Large, medium, and small circles represent oxygen, sodium, and nitrogen, respectively. Clear circles represent atoms placed at $a=0$ and shaded circles atoms at $a=\frac{1}{2}$.

ample the SO_4 group, maintain the same arrangement through a wide range of chemical compounds.

In addition to checking the angular group prediction, the structure of $NaNO_2$ is itself of special value and importance, due to the fact that it is a new type of structure. Since this NO_2 type of structure is new, its characteristics can be compared to those of known structures only to a limited extent. All of the interatomic distances found in the structure are very reasonable when compared to known empirical interatomic distances, and further the structure accounts for the very unusual birefringence.

The interatomic distances are of especial value because in deriving the structure no interatomic distance assumptions were used and further the small number of parameters adds to the certainty of the distances.

The interatomic distances are as follows:

$Na^+-O^=$ two O's	2.53A	$O^=-O^=$ different groups	>3.3A
$Na^+-O^=$ four O's	2.46	$N^{+3}-O^=$	1.13
$Na^+-O^=$ average	2.48	$O^=-O^=$ same group	2.09.

The value 2.48A for the average $N^+-O^=$ C. N. (coordination number) 6 distance agrees very well with the value of 2.46 as found[8] in $NaClO_3$. The minimum $O^=-O^=$ C. N. 6 distance different groups can be compared with the value obtained from W. H. Zachariasen's tables.[9] The value for closest approach from tables = 3.14A while the observed closest approach = 3.3A.

The $O^=-O^=$ distance NO_2 group and the $N^{+3}-O^=$ distance are distinctly new contributions to the available empirical interatomic distances. In comparing them with known distances all that can be said is that they are of the right order of magnitude. For example $N^{+5}-O^=$ C. N. 3 distance is given[10] as 1.22A in $LiNO_3$ while the new $N^{+3}-O^=$ C. N. 2 distance is 1.13A.

Following the method used by W. L. Bragg[11] in his consideration of the refractive indices of calcite and aragonite it is at once apparent from qualitative considerations that the unusually large birefringence is accounted for by the marked difference in the polarizibility of the NO_2 group in different directions. In a future paper quantitative calculations of the indices of refraction will be given, for such calculations should give information regarding the distribution of the outer electrons of oxygen.

For the electric vector perpendicular to the NO_2 group, the polarization is a minimum due to the fact that the induced electric moments oppose each other. This minimum polarization corresponds to the minimum index of refraction. Likewise for the electric vector parallel to the $O-O$ line of the NO_2 group the polarization is a maximum due to the fact that the induced electric moments aid each other. The optical data show that α, 1.354, has the direction of the a axis, which is the direction perpendicular to the NO_2 group,

[8] W. H. Zachariasen, Zeits. f. Krist **71,** 529 (1929).

[9] W. H. Zachariasen, Zeits. f. Krist. in press.

[10] R. W. G. Wyckoff, Phys. Rev. **16,** 149 (1920).

[11] W. L. Bragg, Proc. Roy. Soc. **A105,** 370 (1924); Proc. Roy. Soc. **A106,** 346 (1924).

while γ, 1.648 has the direction of the c axis, which is the direction of the O—O line of the NO_2 group.

Thus the structure as given is in complete agreement with available x-ray and optical data.

I wish to express my best thanks to Dr. W. H. Zachariasen for his interest and advice throughout the course of this investigation.

THE LIGHT OF THE NIGHT SKY

By Joseph Kaplan
University of California at Los Angeles

(Received June 1, 1931)

Abstract

The two lines at 4416A and 4168A, recently reported by Lord Rayleigh in the light of a very bright night sky, are identified as O_{II} lines. A theory is proposed which accounts for the strong excitation of the green aurora line both in the night sky and in the aurora borealis. The theory explains why no O_2+ bands are found in the aurora while N_2+ bands are very strong. Explanations are proposed for the two lines of singly-ionized oxygen and for the continuous spectrum in the night sky. Experiments performed by the writer substantiate the theory.

THE initial purpose of this note was to propose an identification for the two unknown lines recently remeasured by Lord Rayleigh in the light of an exceptionally bright night sky.[1] These lines, which Lord Rayleigh calls X_1 and X_2, have wave-lengths of 4416 ± 2A and 4168 ± 2A and it is suggested that they correspond to two lines of singly ionized oxygen having wave-lengths of 4416.97A and 4169.23A. This agreement is within the errors of measurement. In addition to these two lines the light of the night sky contains the green aurora line and a faint continuous spectrum. The green aurora line is by far the strongest line in the night sky and in most cases it is the only line which is observed.

In trying to understand the possible meaning of the existence of lines belonging to ionized oxygen in the night sky, it occurred to the writer to compare these lines with some of the lines which are observed in the spectrum of the aurora borealis. The reason for this comparison lay in the fact that the green aurora line is a constituent of both the aurora and the night sky spectra. The comparison showed that of eight lines listed by Vegard[2] in the aurora spectrum, five corresponded to lines belonging to singly-ionized oxygen and three are listed either as unidentified nitrogen lines or as singly-ionized nitrogen lines. These identifications were obtained from the Kayser "Tabelle der Hauptlinien" where they are listed both as "luftlinien" and oxygen or nitrogen lines. It is suggested therefore that the method, by which the aurora green line and the other oxygen lines are excited, is essentially the same in both the aurora and the night sky. Furthermore, oxygen molecule-ions, formed by sunlight in the case of the night sky and probably by electrical discharge in the aurora, are the essential elements for the production of the aurora green line. It will be the purpose in what follows, to justify these statements and in that way to explain a most remarkable spectroscopic feature of these two displays, namely, that the only oxygen arc line which is observed in either of the two cases is the green aurora line.

[1] Lord Rayleigh, Proc. Roy. Soc. **131,** 376 (1931).
[2] Vegard, Phil. Mag. **46,** 193, 577 (1923).

We will first point out one other feature of the aurora spectrum which will help us to understand the present problem. The aurora spectrum consists almost completely of the first negative bands of the nitrogen molecule-ion and the green aurora line. Other radiations in the aurora are in general very weak compared with these. In view of the fact that band spectra, which are emitted by ionized molecules, are characteristic of low pressure discharges, it is surprising that the second negative bands of oxygen are completely missing from the aurora spectrum. These bands fall in the red and yellow and are very easily excited in the laboratory discharges in oxygen at pressures around 10^{-2} mm. This fact immediately suggests that the failure of these bands to appear in the aurora, as well as the production of neutral and singly-ionized oxygen atoms, are due to the dissociation of O_2^+. It is proposed therefore to discuss how the dissociation of O_2^+ can result in the formation of oxygen atoms and how this will account for the light of the night sky.

The recombination of an ionized oxygen molecule and an electron can yield a highly excited oxygen molecule with sufficient energy to dissociate into one or perhaps even two oxygen atoms in the $^1S_0$ metastable state on which the green line originates. That this is a process which may well have a very high probability is shown by the following remarkable coincidence. The heat of dissociation of oxygen into two normal atoms is now known to be exactly 5.06 volts;[3,4,5] the energy of the oxygen atom in the $^1S_0$ state is 4.19 volts, so that the energy necessary to dissociate an oxygen molecule into two $^1S_0$ atoms is 13.44 volts. The ionization potential of oxygen, while not definitely known, is generally given as 13.5 volts[6] and it is seen that there is a most striking agreement between the energy required in this process and the most probable value of the available energy.

We can advance another argument to show that the above explanation is probably the correct one. The oxygen molecule is very unstable in its higher energy states. This is shown by the fact that the highest electronic level which has been observed spectroscopically in O_2 lies at 6.1 volts. Thus between 6.1 volts and the ionization potential there are no observed levels of oxygen and in view of the number of energy levels which have been obtained for other diatomic molecules one can certainly take this as an indication that any attempts to excite energy levels higher than the 6.1 volt level, results in a dissociation of the molecule into one or more excited atoms. There is now considerable experimental evidence to show that the failure of a molecule to emit bands in certain energy regions can often be traced either to a predissociation of the excited molecule or to a direct dissociation by electron impact. We thus have another convincing argument for the notion that recombining O_2^+ yields metastable oxygen atoms and the green aurora line.

Direct evidence for the occurrence of the above discussed process has been found by the writer in some current experiments on the aurora spectrum.

[3] R. Frerichs, Phys. Rev. **36,** 398 (1930).
[4] R. T. Berge, Trans. Faraday Soc. **25,** 1929.
[5] F. Paschen, Zeits. f. Physik **65,** 1 (1930).
[6] Franck u. Jordan, Anregung von Quantensprüngen, p. 273.

These experiments are to be reported in detail elsewhere and it will be sufficient to say that it was possible, after the strong O_2^+ bands in the visible were produced, to make them disappear, to be replaced by a strong incandescence of small bits of oxide, indicating the presence of atomic oxygen. Furthermore, collisions of the second kind were observed between $^1S_0$ oxygen atoms and metastable nitrogen molecules, a process similar to the one that takes place in active nitrogen between metastable nitrogen atoms and metastable nitrogen molecules. This process was particularly striking in air at pressures ranging between 10^{-2} mm and 10^{-3} mm. There the oxygen bands failed to appear and the incandescence was quite intense. The nitrogen bands practically duplicated the nitrogen bands of the aurora spectrum so that in effect, this was a reproduction of the aurora spectrum. More will be said about this elsewhere.

We will now discuss a process by which the two lines of singly-ionized oxygen arise in the very bright night sky. A collision between a highly excited oxygen molecule (one which is about to dissociate) and a molecule ion, can result in a dissociation of the molecule ion into an atomic ion and a neutral atom. It is reasonable to assume that this process will be less probable than the recombination and dissociation process mentioned above. Hence only in the brightest night skies are the lines X_1 and X_2 observed. Furthermore, the lines of singly-ionized oxygen are very weak in the aurora.

The night sky which was described by Lord Rayleigh was so bright that the continuous spectrum made it difficult to see the green line. The same explanation that accounts for the green line will also account for a visible continuous spectrum. Thus the energy necessary to dissociate a molecule into an oxygen atom in the $^1S_0$ state and one in the ^1D metastable level is found to be 11.21 volts. The difference between this and the ionization potential will account for a continuous spectrum around 5400A.

It is possible to explain in a similar fashion the failure of nitrogen to play a role in the spectrum of the night sky. Let us assume that nitrogen molecule ions are produced in the upper atmosphere. The recombination of a molecule ion and an electron would produce an excited molecule in some one of the many electronic states which abound in nitrogen. There are at least six levels in nitrogen which are quite stable and either they do not radiate or they emit bands in the ultraviolet. It is quite possible therefore to describe methods by which the decay of nitrogen molecule ions could occur without the radiation of visible lines or bands. Dissociation is highly improbable, as is shown by the difficulty of producing nitrogen atoms in discharge tubes and also by the fact that the N_2^+ bands do appear in the aurora whereas O_2^+ bands do not. If dissociation did occur however, and metastable atoms were produced, their radiation would not be observed because the transition $^2P-{}^2D$, which is the analogue of the green aurora line, lies at about 1μ in the infrared. This fact and the fact that so many stable energy levels exist for N_2, take care of both possibilities, i.e. dissociation or the formation of stable molecules. It seems reasonable to expect the absence from the night sky of nitrogen radiation unless we assign part of the continuous spectrum to nitrogen molecule ions.

At the present stage of this work we don't propose to discuss the production of O_2^+. Whether ozone plays a very significant role in that process is now open to question because the oxygen molecule ions may well be formed by ultraviolet light in the night sky and by electrical discharge in the aurora. Further work will probably shed some light on this question.

THE STABILITY OF THE ATMOSPHERE OF A ROTATING STAR

By Ross Gunn
Naval Research Laboratory

(Received July 13, 1931)

Abstract

It is shown that electromagnetic forces acting on the gaseous ions of a rotating magnetized star can account for its atmospheric stability even when the star proper approaches a condition of rotational instability. Milne's theory of the chromospheric stability is shown to be inconsistent with observation if electromagnetic forces are taken into account. Because the ions are entrapped by the magnetic field the loss of atmosphere by a rapidly rotating star is small and therefore its angular velocity may increase until rotational instability of the entire mass sets in. The considerations of the paper lend considerable theoretical support to the fission theory of multiple stars.

DUE to the opacity of the sun's atmosphere observations thereof are necessarily confined to a relatively thin superficial layer. In this layer the material is highly ionized and the pressure so low that all the ions describe long free paths. The outer layers of this ionized region cannot be in gravitational equilibrium with a supporting gaseous pressure, for eclipse spectra show that surprisingly large amounts of calcium and hydrogen exist several thousands of kilometers above the photosphere. The forces responsible for this departure from the expected equilibrium distribution have not been understood although it has been long recognized that an acceptable mechanism must account for the observed fact that stars which rotate on their axes so fast that their equatorial acceleration approaches zero, do not perceptibly lose their atmospheres. The fission theory of binary stars seems entirely too well founded on observation to deny that rotational break up does not take place, and indeed, Struve[1] has shown that many stars are in a condition of rotation favorable to a shedding of their atmospheric material if an outward supporting force, such as has hitherto been assumed, actually exists.

Effect of a Magnetic Field

The sun is known to possess a general magnetic field which we have shown to have an important influence on solar atmospheric motions. It seems probable that most dwarf stars possess magnetic and electric fields not unlike that of the sun[2] and that theories of electromagnetic solar effects and mechanisms will have direct application to the general case of a rotating star. The magnitude and distribution of the solar magnetic fields are known from direct observation[3] so that the magnetic force on an ion moving as a result of a ther-

[1] O. Struve, Astrophys. J. **72,** 1 (1930); **73,** 94 (1931).

[2] R. Gunn, Phys. Rev. **34,** 335, 1621 (1929).

[3] Hale, Astrophys. J. **38,** 31 (1913); Hale, Sears, Van Maanen and Ellerman, Astrophys. J. **47,** 1 (1918).

mal collision is readily calculable. The magnetic forces are, in general, much larger than gravitational forces and therefore might be expected to determine the stability and motions of the ions that constitute the solar atmosphere.

Page[4] and others have shown that a constant force F acting on ions carrying a charge e immersed in a magnetic field of strength B and executing long free paths *does not cause the ions to move in the direction of the impressed force* but gives rise to a motion with constant velocity $\boldsymbol{u}$ specified by

$$\boldsymbol{u} = \boldsymbol{F} \times \boldsymbol{B}/eB^2 \tag{1}$$

where e and B are in e.m.u. This modifies in an important manner earlier conclusions in regard to the stability of the solar atmosphere. At the solar equator B is northerly and tangential to the surface and any radial force which might arise from gravitational, electric or radiation effects, does not produce a radial motion but superposes a uniform velocity on the ions toward the east or west. We have seen that an electrical force on the ions combined with the known magnetic field will account for the anomalous rotation of the sun[5] if the ions describe mean free paths longer than the radius r of the helix generated by the moving ions. This radius is defined by

$$r = mv/Be = (2mkT)^{1/2}/Be \tag{2}$$

where mv is the ionic momentum in a plane perpendicular to the magnetic field B, e the ionic charge, k the Boltzmann constant and T the absolute temperature. The free paths of the ions are all greater than r at all observable levels of the reversing layer and chromosphere but as B decreases to very small values at the outer boundary of the chromosphere, r probably becomes very large and comparable to the total depth of the chromosphere. In such a circumstance we might expect electromagnetic effects to be unimportant in coronal regions although sufficient data are not yet available to make a definite decision. Except for this outer region of the sun's atmosphere the mean free path is larger than r defined by Eq. (2), and therefore electromagnetic forces and interactions play an important part in determining its equilibrium.

Stability of the Chromosphere

Milne has constructed a theory of the chromospheric stability[6] which depends on the selective absorption of light, emitted at the photosphere, by the ions of the chromosphere. In order to attain even approximate stability and prevent the chromospheric material from being blown completely away by radiation pressure it was necessary for Milne to assume, further, that the motion of the ions away from the sun produced a Doppler displacement of the absorption line and thus modified the incident force. This subsidiary assumption appears to be fatal to Milne's theory, for we have seen that at the equator an outward force does not result in an outward motion of the ion but will produce a tangential drift of the positive ions. Thus the radiation pressure cannot be modified appreciably by Doppler effects and if it actually

[4] Page, Phys. Rev. **33,** 553 (1929).
[5] R. Gunn, Phys. Rev. **35,** 635 (1930); **37,** 1129 (1931).
[6] E. A. Milne, Monthly Notices **84,** 354 (1924).

exists it should produce a *westward* drift of the chromosphere which is not observed. There appears to be no way by which a radiation pressure theory can be brought into agreement with observation when the magnetic forces on an ion are taken into account, and thus Milne's theory could be valid only if there is no magnetic field in the chromosphere. Several lines of evidence show that an appreciable chromospheric magnetic field exists and indeed its value, near the base of the layer, has been measured.[3]

In earlier papers it was shown that the anomalous eastward motion of the solar reversing layer and chromosphere arose from the interaction of ions with the solar electric and magnetic fields. The mechanism is such, that although the electrical force on a positive ion is vertically downward and hence in the direction of the gravitational acceleration, the ions move, not downward, but to the eastward with a definite velocity and are thus "supported." The support of the material evidently depends on its being ionized most of the time and this accounts for the predominance in the chromosphere of spectra arising from ions as well as from the next lower state of excitation, for a captured neutralizing electron does not necessarily occupy the lowest orbit initially but may move down in steps and emit the radiation characteristic of a neutral atom. Ions having high recombination coefficients and high ionizing potentials would be expected to remain neutral most of the time and would therefore be caused to diffuse to lower levels by gravitational forces. If the higher levels are constantly replenished by neutral atoms shot undeviated by the magnetic field to high levels by thermal effects and there become ionized, then, after equilibrium is established, the elements of the solar atmosphere should be arranged into more or less definite layers according to their mass and the fraction of the total time the atoms spend in an ionized condition. The ions having a low recombination coefficient and a low ionizing potential should be found highest in the atmosphere while ions with large coefficients and high ionizing potential will sink deep in the reversing layer or photosphere. The combination of a moderately low ionizing potential coupled with slow recombination is believed to account for the presence of large amounts of calcium and hydrogen in the chromosphere. A suggestion that the ionizing potentials of the elements bears some definite relation to the position of the element in the sun's atmosphere has been made by Nicholson and Perrakis[7] who have pointed out that almost all the elements absent from the solar spectrum have high ionization potentials.

In polar regions the magnetic and gravitational fields are parallel, so that support of the type we have considered above is probably not important and the polar distribution of material in the chromosphere might be expected to differ from that at lower latitudes. A complication enters, however, for unionized matter shot to high levels by thermal processes in lower latitudes becomes ionized and will diffuse along the magnetic field and hence set up an atmospheric circulation toward both poles. The transport of material to the poles and its deposition there at high levels appears to make a prediction of the expected change in distribution quite impossible.

[7] Nicholson and Perrakis, Comptes Rendus **186,** 492 (1928).

Loss of Stellar Atmosphere

The thermal energy of a particle in a typical star's atmosphere is small compared to its negative gravitational potential energy and many writers have shown that the loss of atmosphere by a nonrotating star is quite negligible.[8] Certain stars are known, however, to rotate so rapidly on their axes that they are on the verge of break-up[1,9] and therefore have very small equatorial accelerations. Such stars might be expected to lose their equatorial material and yet retain the atmosphere over the poles because rotation alone would not affect the polar acceleration.

In a criticism of the fission theory of binary star systems, Chamberlin[10] has expressed the opinion that rapidly rotating stars "must shed portions of their matter molecule by molecule" and pointed out that the lost molecules would carry off angular momentum and thus reduce the incipient instability of the system. Chamberlin's position has not been without support, for if Milne's analysis of the chromospheric stability is accepted, then material would be expected to be blown away more rapidly as the surface acceleration of a star approached zero. This is contrary to observation for in an important paper Russel brought forward excellent evidence which showed that the loss of stellar atmospheres by high rotation was quite negligible.[9] Clearly, then, a simple outward radial force on each particle arising from the absorption of radiation cannot support the atmosphere, for that outward force must always just balance a variable surface acceleration which is a function of the rotational velocity of the star. Such a balance seems improbable.

Electromagnetic forces readily account for the observed stability in all cases. In lower latitudes any radial force is at right angles to the star's magnetic field and no matter what the magnitude of the force the ionized atmosphere will be constrained to move to the east or west rather than outward or inward. On account of the spherical symmetry it appears that radial forces acting on the ions are the only ones which could be of importance and it is therefore clear that rapid rotation will not directly disturb the radial equilibrium[5]. However, high speed rotation might affect the equilibrium positions of the neutral material, and the abundance of the elements at various levels of the atmosphere might be expected to change slightly with changes in rotation. This readjustment is not believed to be of great importance.

The presence of a magnetic field in the atmosphere of a star effectively prevents the rapid loss of ionized material at its periphery even if the mass of the star is greatly concentrated toward the center. The ways by which a magnetic star might conceivably lose material are:

(a) by loss of large massive units.

(b) by loss of neutral molecules.

(c) by loss of particles, normally ionized, which succeed by a series of favorable collisions in working their way well clear of the star's magnetic field.

[8] Jeans, Dynamical Theory of Gases (1925).

[9] H. N. Russell, Astrophys. J. **31,** 185 (1910).

[10] Chamberlin, Carnegie Inst. Pub. No. 107, p. 169 (1909).

Loss by method (a) requires no discussion, while the loss of neutral molecules is probably not important except in very cool stars, for it is difficult to see how a single atom could pass through the low pressure regions of a star's atmosphere without becoming ionized and hence subject to magnetic forces. The rate of loss by method (c) is believed to be small but it probably takes place slowly in very hot stars and results in an outer atmosphere whose ions describe individual gravitational orbits about the star.

The evolutionary processes in a star, hitherto assumed to depend only on its physical constitution, are now seen to depend in a large measure on electromagnetic processes. In a preceding paper it was shown that the precise mechanism which prevents the loss of atmosphere adds angular momentum to the star until (if the star has sufficient energy) it breaks up forming a binary pair. It seems clear that evolutionary processes of the type considered by Laplace in his nebular hypothesis has no existence in a magnetized star.

DIELECTRIC CONSTANTS OF CERTAIN ORGANIC LIQUIDS AT MEDIUM FREQUENCY

By W. R. Pyle
Mendenhall Laboratory of Physics, Ohio State University

(Received June 18, 1931)

Abstract

At a frequency of 85.8 kilocycles the dielectric constant was determined at one temperature for each of the following: benzene, 2.279 at 22.9°C; cinnamic aldehyde, 16.918 at 24.2°C; ethyl ether, 4.197 at 26.9°C; methyl cyclohexane, 2.071 at 24.8°C; methyl o-nitrobenzoate, 27.756 at 26.9°C; nitrobenzene, 34.369 at 26.1°C; oxalyl chloride, 3.470 at 21.2°C; n-propyl ether, 3.394 at 25.7°C; iso-propyl ether, 4.449 at 25.9°C; and propylene chloride, 8.925 at 26.1°C. At this same frequency the temperature coefficients of the dielectric constants for ortho-, meta-, and para-xylenes were determined over a temperature range of about 30°C. The data on the three xylenes were tested with the Debye theory.

Introduction and Theory

THE dielectric constant of an organic liquid has been considered to be allied with the other physical properties of the compound such as solvent power and molecular constitution. By methods to be explained later the dielectric constant is used to obtain the electric moment of the molecule and thus account for the symmetry or dissymmetry of its structure.

By a nulled heterodyne method the dielectric constant was determined at a frequency of 85.8 kilocycles and at one temperature for each of the following: benzene, cinnamic aldehyde, ethyl ether, methyl cyclohexane, methyl o-nitrobenzoate, nitrobenzene, oxalyl chloride, n-propyl ether, iso-propyl ether and propylene chloride.

In determining the dielectric constants of some of these compounds it was necessary to fill the test condenser only partially with the liquid under test so that the limit of the capacity of the apparatus was not exceeded. For these cases the following equations were developed with metric units used throughout:

$$h_1 = M'L/V\rho \tag{1}$$

where M' represents the mass of liquid required to fill the test condenser to height h_1 which was just sufficient to null the beat note, ρ the density of the liquid, V the total volume of the test condenser and L its length.

$$h_2 = L - h_1 \tag{2}$$

where h_2 is the height of the air dielectric in the test condenser.

$$C_4 = \frac{(R_1 + C) - (R_2 + Ch_2/L)}{h_1} \tag{3}$$

where R_1 is the reading of the precision condenser with only air in the test condenser, C the corrected capacity of the test condenser with air as the dielectric, R_2 the reading of the precision condenser with h_1 cm of liquid in the test condenser and C_4 the capacity in mmf for each cm of liquid dielectric in the test condenser.

$$\epsilon = LC_4/C \tag{4}$$

where ϵ is the dielectric constant of the liquid under test.

When the test condenser was partially filled with a liquid the air space above the liquid contained some vapor due to evaporation. The dielectric constant of the mixture of air and vapor could not vary much from unity because the dielectric constant of most pure vapors at atmospheric presure and room temperature exceed unity less than 0.5 percent A few pure vapors from liquids with high dielectric constants have dielectric constants which exceed unity by 2.5 percent. Certainly in this work no serious error is introduced by considering the dielectric constant of the mixture of air and vapor equal to unity since only a small amount of liquid could evaporate while pouring sufficient liquid into the test condenser to null the beat note.

At a frequency of 85.8 kilocycles the temperature coefficients of the dielectric constants for ortho-, meta-, and para-xylenes were determined over a temperature range of about 30°C.

For organic liquids whose dielectric constants are only slightly affected by temperature a satisfactory relation is expressed by the simple linear formula

$$\epsilon_t = K_0 - \beta t \tag{5}$$

where ϵ_t is the dielectric constant at temperature t, K_0 the dielectric constant at 0°C and β is the temperature coefficient.

However, nitrobenzene, alcohol, etc., which have comparatively large dielectric constants are considerably influenced by a change in temperature and hence the linear law does not obtain. For these cases Abegg[1] proposed the following formula

$$\log_{10} \epsilon_t = \log_{10} \epsilon_0 - \alpha t \tag{6}$$

where ϵ_0 is the dielectric constant at 0°C and α is the temperature coefficient. Lattey and Gatty[2] have found this equation concordant with their experimental results over a wide temperature range.

In this work the data on o-xylene, m-xylene and p-xylene are tested with the Debye[3] theory. In general Debye's theory has applied only to gases as shown by Zahn[4] and to very dilute solutions of polar compounds in non-polar solvents as found by Stranathan.[5]

[1] Abegg, Wied. Ann. **60,** 54 (1897).
[2] Lattey and Gatty, Phil. Mag. **7,** 985 (1929).
[3] Debye, "Polar Molecules" (Chemical Catalogue Co., New York).
[4] Zahn, Phys. Rev. **24,** 400 (1924).
[5] Stranathan, Phys. Rev. **31,** 653 (1928).

Polar molecules in the gaseous phase or in dilute solution with a non-polar solvent are sufficiently separated to render negligible the mutual interaction due to the overlapping of the electrostatic fields of the molecules.

The well-known Clausius-Mosotti relation leads to the expression

$$\frac{\epsilon - 1}{\epsilon + 2} = \frac{4\pi n}{3}\alpha \tag{7}$$

where the dielectric constant ϵ is expressed in terms of α the molecular polarizability and n the number of molecules per cubic centimeter. If both members of equation (7) are multiplied by the quotient of the molecular weight M and the density ρ, we obtain

$$\frac{\epsilon - 1}{\epsilon + 2}\frac{M}{\rho} = \frac{4\pi M n}{3\rho}\alpha. \tag{8}$$

The right hand member of equation (8) is called P, the molar polarization. Since nM/ρ equals Avogadro's number N (6.06×10^{23}) equation (8) can be expressed thus

$$P = \frac{\epsilon - 1}{\epsilon + 2}\frac{M}{\rho} = 2.54 \times 10^{24}\alpha. \tag{9}$$

From Maxwell's hypothesis the dielectric constant ϵ is identified with the square of the index of refraction r.

Substituting r^2 for ϵ in equation (8) we have the familiar Lorentz-Lorenz relation

$$P_0 = \frac{r^2 - 1}{r^2 + 2}\frac{M}{\rho} = \frac{4\pi N}{3}\alpha \tag{10}$$

where P_0 is called the molar refraction. The molar polarization can be construed as the molar refraction for zero frequency.

Debye[6] expresses the polarizability in the general formula

$$\alpha = \alpha_0 + \mu^2/3kT \tag{11}$$

where α_0 accounts for the distortion effect and $\mu^2/3kT$ takes care of the orientation effect.

Substituting equation (11) in (9) we get

$$P = 2.54 \times 10^{24}\alpha_0 + 2.54 \times 10^{24}\mu^2/3kT \tag{12}$$

where k represents the Boltzmann constant, T the absolute temperature and μ the electric moment of the molecule.

Considering α_0 as an invariable molecular constant we can write equation (12) thus

$$P = A + B/T \tag{13}$$

where A and B are constants for a given dielectric.

[6] Debye, "Polar Molecules," p. 36.

Comparing equations (12) and (13) we see that

$$A = 2.54 \times 10^{24}\alpha_0 \tag{14}$$

$$B = 0.618 \times 10^{40}\mu^2 \tag{15}$$

$$\mu = 1.27 \times 10^{-20}B^{1/2} \text{ e.s.u.} \tag{16}$$

If P is plotted against $1/T$ equation (13) gives a straight line with intercept A and slope B. If the experimental polarization-temperature curve of a substance obeys the linear relationship the slope B may prove to be either positive, zero or negative. If the slope is positive the molecule has an electric moment and it is therefore a polar molecule. If the curve has zero slope the electric moment is zero and the molecule is non-polar. By this method several substances have been definitely classified as polar and non-polar.[7]

If the slope comes out negative the electric moment is the square root of a negative number and is therefore imaginary. This is frequently the case when this simple theory is applied to pure liquid compounds.

Debye[8] quotes an example of the data on liquid ethyl alcohol resulting in an imaginary electric moment. The inadequacy of the theory in the case of pure polar liquids is generally attributed to association and the effect of temperature on the manner and degree of mutual interaction between the molecules.

Source of Liquids

A technical grade of methyl cyclohexane was procured from the Eastman Kodak Company, Rochester, N. Y.

A highly purified sample of each of the following was purchased from the Eastman Kodak Company: benzene, cinnamic aldehyde, ethyl ether, methyl o-nitrobenzoate, nitrobenzene, oxalyl chloride, n-propyl ether, iso-propyl ether, propylene chloride, o-xylene, m-xylene and p-xylene.

Description of Apparatus

The heterodyne arrangement adopted for this work was composed of two high frequency oscillators (Hartley type) and a detector with two stages of audiofrequency amplification. The beat note between the oscillators was picked up by the floating grid of the detector and after amplification was received by the headphones which is similar to the method described by Stranathan[9] and Zahn.[10]

One of the high frequency oscillators was held at the constant frequency of 85.8 kilocycles (3500 meters) by a quartz crystal properly mounted in the grid circuit. This crystal had been carefully calibrated by Dr. Tadashi Fujimoto in this laboratory in 1927. The frequency of the other oscillator was readily altered by variable condensers.

[7] Debye, "Polar Molecules," pp. 40, 50.
[8] Marx, Handbuch der Radiologie **6,** 614 (1925).
[9] Stranathan, Phys. Rev. **31,** 653 (1928).
[10] Zahn, Phys. Rev. **24,** 400 (1924).

At first a 1000-cycle tuning fork coupled electrically to the grid circuit of the second amplifier was used for some preliminary determinations. However, due to harmonics produced by the tuning fork it was difficult to null completely the beat note between the heterodyne of the high frequency oscillators and the tuning fork note. The tuning fork was discarded for subsequent determinations.

The apparatus (Fig. 1) consisted of: one UX-200A tube for the detector, four UX-201A tubes for the oscillators and amplifiers, three Hammarlund variable air condensers, suitable inductance coils, two standard audio frequency transformers and a General Radio Precision Condenser, type 222, with maximum range 1500 mmf.

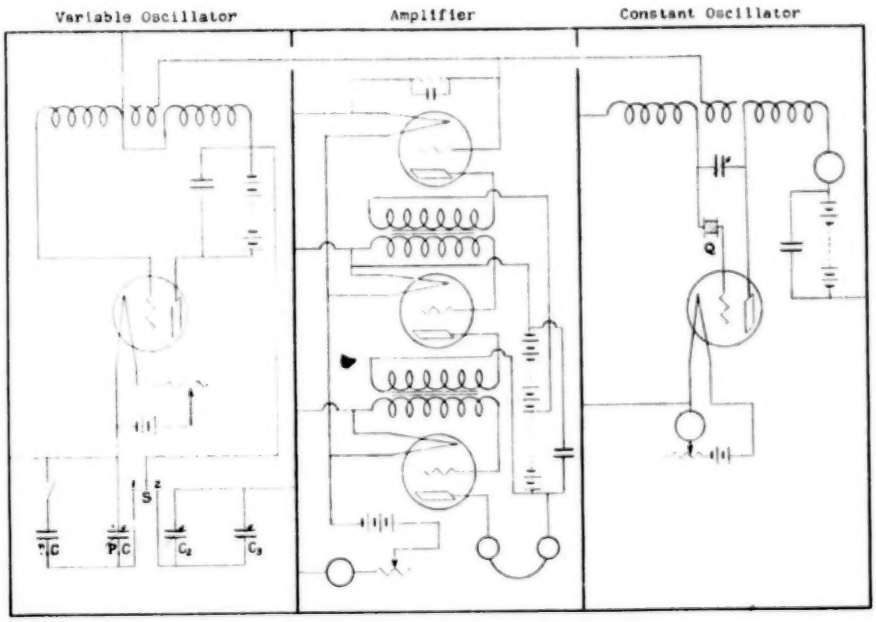

Fig. 1. Diagram of apparatus.

The entire apparatus was shielded with iron sheet and controlled by small wooden pulleys mounted outside the shield. The shield was well grounded thus eliminating the effect of the body capacity of the operator. The three electrical circuits were supplied by independent batteries to eliminate possible synchronizing effects.

In Fig. 1, $T \cdot C$ represents the test condenser, $P \cdot C$ the variable precision condenser, C_2 a variable air condenser of 0.0005 mmf, C_3 a variable air condenser of 0.00014 mmf with vernier attachment and Q a quartz crystal. The conventional symbols of the diagram make the rest of it self-explanatory.

Several test condensers were constructed and tried. The most satisfactory one, designated as condenser No. 2, was made of two coaxial brass cylinders (Fig. 2) cemented with sodium silicate to a ground glass base. The inside of the larger brass cylinder and the outside of the smaller one were gold-

plated to preclude metallic contamination of the organic liquids. The sodium silicate made a rigid bond between the brass cylinders and glass base thus making the condenser fragile to handle. The condenser was insulated with felt three-fourths of an inch thick to retard heat radiation.

Procedure

With S (a mercury switch) in the proper position and test condenser $T \cdot C$ disconnected, the precision condenser $P \cdot C$ was adjusted so that the fre-

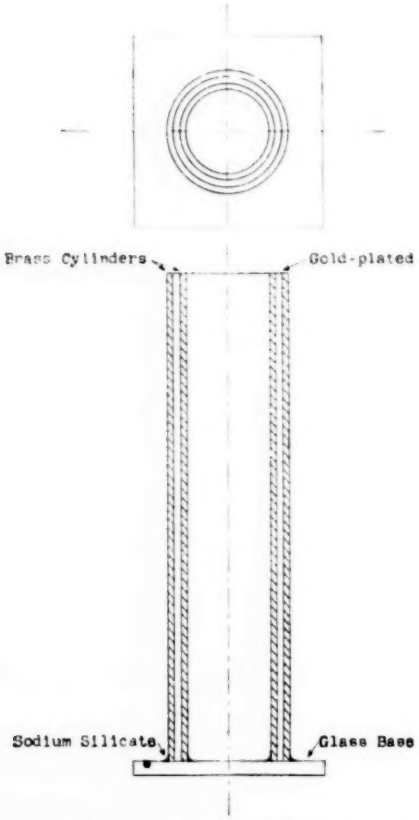

Fig. 2. Diagram of test condenser No. 2

quency of the variable oscillator equalled exactly that of the constant oscillator and under this condition the beat note was completely nulled. The sensitivity of the method was satisfactory because a beat note was heard if the capacity of the variable oscillator circuit was varied 0.2 mmf on either side of the mean nulled position of the precision condenser. The mean nulled position could be determined to within 0.1 mmf.

In making a run S was thrown to position 2, condensers C_2 and C_3 were adjusted so that the beat note was nulled, then S was thrown to position 1 and with $T \cdot C$ disconnected, $P \cdot C$ was adjusted to the nulled position and read. Then $T \cdot C$ was connected in parallel with $P \cdot C$ and $P \cdot C$ was again ad-

justed to the nulled position and read. Then S was thrown back to position 2 to see if any shift in frequency had occurred. The shift, if any, was always very small.

The difference between the two readings of $P \cdot C$ gave the apparent capacity of $T \cdot C$. The apparent capacity of $T \cdot C$ should be corrected for lead capacity, inductance of leads, leakage and stray capacity if the frequency used and the method employed warrant it.

By using two General Radio precision condensers the capacity of dummy leads was measured by a substitution method.

To determine if any appreciable capacity correction due to the inductance of the leads should be taken into account let us consider the following expression

$$L_a = \frac{L(1 - \omega^2 LC_0) - C_0R^2}{\omega^2 C_0^2 R^2 + (1 - \omega^2 LC_0)^2} \tag{17}$$

where L_a is the apparent inductance of the leads, L the calculated inductance of the leads, C_0 the calculated capacity of the leads, R the resistance of the leads and ω equals 2π times the frequency.

We see from equation (17) that terms C_0R^2 and $\omega^2 C_0^2 R^2$ are negligible except when approaching the frequency for which $\omega = 1/(LC_0)^{1/2}$. When just approaching this frequency we have L_a becoming strongly negative. For higher frequencies it remains negative but as the frequency is still increased it approaches zero. This negative value of the inductance indicates that the leads are behaving as a small condenser.

At the frequency of 85.8 kilocycles used in this work and with the short leads employed the terms $\omega^2 LC_0$, C_0R^2 and $\omega^2 C_0^2 R^2$ in equation (17) become negligible. Therefore $L_a = L$ which itself proved to be a negligible positive value. Certainly for frequencies for which the value of the inductance is appreciably negative proper compensation for the capacity should be made.

The nulled heterodyne method can be used satisfactorily to determine the dielectric constants only for liquids with very small conductivity or so-called leakage. Otherwise the leakage sufficiently shortcircuits the condenser so that no beat note is obtainable. This was the writer's experience with acetone and aniline. By bridge methods, however, the power factor of imperfect liquid dielectrics can be measured and the dielectric constant determined.

It is believed that careful grounding and shielding practically eliminated the effect of stray capacities.

The correction of the capacity of the test condenser for difference in density of charge at the ends was considered inappreciable for the slender test condensers used in this work. Attempts to eliminate this end effect by the use of guard rings is described in the Bulletin of the Bureau of Standards, 3,433.

The formula for calculating the capacity of a condenser made of two coaxial cylinders is

$$C = 0.2416L/\log_{10} r_1/r_2 \tag{18}$$

where L is the length of the cylinders, r_1 the radius of the outer cylinder, r_2

the radius of the inner cylinder and C the capacity in mmf. All dimensions are expressed in centimeters.

For the test condenser No. 2, $L = 25.44$ cm, $r_1 = 2.89$ cm and $r_2 = 2.54$ cm. By calculation, the capacity of this test condenser equals 109.6 mmf.

After taking into account the capacity of the leads the capacity of test condenser No. 2 as measured with the precision condenser was found to be 106.9 mmf. Thus the calculated value is about 2.5 percent greater than the measured value.

The calculated value may be in error, (a) due to the cylinders not being exactly coaxial, (b) due to the diameters varying slightly throughout the length of the cylinders and (c) due to small errors in measurement.

The liquid whose dielectric constant was desired was placed in the test condenser and its capacity determined by the compensation necessary on the precision condenser to null the beat note.

For the liquids with high dielectric constants it was necessary to set the precision condenser near its maximum range and partially fill the test condenser until the note was nulled. The mass of the organic liquid required was determined with a balance. The height of the liquid in the test condenser was determined by taking into account the mass and density of the liquid as well as the physical dimensions of the test condenser as already described.

After a run a small glass tube properly bent was inserted to the bottom of the test condenser and the liquid pumped out. The condenser was then filled with ethyl ether which was a solvent for all the liquids used in this work. After a few minutes the ether was pumped out and the condenser was blasted with compressed air and fanned electrically until the ether residue was evaporated. This process was repeated before a new run was made.

Sample calculation of the dielectric constant for oxalyl chloride at 21.2°C

Substituting in Eq. (1)

$$h_1 = \frac{(181.69)(25.44)}{(154.68)(1.488)} = 20.08 \text{ cm.}$$

Substituting in Eq. (2)

$$h_2 = 25.44 - 20.08 = 5.36 \text{ cm.}$$

Substituting in Eq. (3)

$$C_4 = \frac{(265.4 + 106.9) - (57.0 + 22.52)}{20.08} = 14.58.$$

Substituting in Eq. (4)

$$\epsilon = \frac{(25.44)(14.58)}{106.9} = 3.470.$$

Sample calculations of P, P_0 and μ for o-xylene.

From Eq. (9)

$$P = \frac{\epsilon - 1}{\epsilon + 2}\frac{M}{\rho} = \frac{(1.558)}{(4.558)}\frac{(106.08)}{(.879)} = 41.3_4$$

From Eq. (10)

$$P_0 = \frac{r^2 - 1}{r^2 + 2}\frac{M}{\rho} = \frac{(1.265)}{(4.265)}\frac{(106.08)}{(.879)} = 35.8 \text{ cc.}$$

From Eq. (16)

$$\mu = 1.27 \times 10^{-20}[(P - P_0)T]^{1/2} = 1.27 \times 10^{-20}[(5.5)(293)]^{1/2}$$
$$= 0.51 \times 10^{-18} \text{ e.s.u.}$$

RESULTS

In Tables I and II are listed the values of the dielectric constants as found in this work. Figs. 3, 4 and 5 show graphically the values of the dielectric constants at different temperatures for othro-, meta-, and para-xylenes respectively.

TABLE I. *Dielectric constants.*

Organic liquid	ρ	M'	V	h_1	h_2
Cinnamic aldehyde	1.049	9.95	9.49	1.56	23.88
Ethyl ether	.714	67.00	93.84	15.43	10.01
Methyl o-nitrobenzoate	1.284	8.30	6.46	1.06	24.38
Nitrobenzene	1.207	10.85	8.99	1.48	23.96
Oxalyl chloride	1.488	181.69	122.10	20.08	5.36
n-Propyl ether	.747	90.40	123.86	20.37	5.07
iso-Propyl ether	.735	63.21	86.00	14.14	11.30
Propylene chloride	1.166	44.88	37.41	6.15	19.29

Organic liquid	t	R_1	R_2	C_4	ϵ
Cinnamic aldehyde	24.2	267.8	163.5	71.09	16.918
Ethyl ether	26.9	264.3	57.0	17.63	4.197
Methyl o-nitrobenzoate	26.9	264.3	144.8	116.63	27.756
Nitrobenzene	26.1	264.3	57.0	144.42	34.369
Oxalyl chloride	21.2	265.4	57.0	14.58	3.470
n-Propyl ether	25.7	261.9	57.0	14.26	3.394
iso-Propyl ether	25.9	261.9	57.0	18.69	4.449
Propylene chloride	26.1	261.9	57.0	37.50	8.925
Air				4.20	1.000

ρ represents density
M' grams of liquid in test condenser to null beat note
V cc of liquid in test condenser to null beat note
h_1 height of liquid in test condenser to null beat note (cms)
h_2 height of air in test condenser (cms)
t temperature of liquid in degrees centigrade
R_1 reading of precision condenser with only air in T.C (mmf)
R_2 reading of P.C with h_1 cms of liquid and h_2 cms of air in T.C
C_4 capacity per centimeter of liquid in test condenser
ϵ dielectric constant of liquid at 85.8 kilocycles per sec.

TABLE II. *Dielectric constants.*

Organic liquids	t	R_1	R_2	C_5	ϵ
Benzene	22.9	264.3	127.6	243.7	2.279
Methyl cyclohexane	24.8	261.9	147.5	221.4	2.071
o-Xylene	24.2	248.0	81.9	273.0	2.553
m-Xylene	24.1	248.0	101.5	253.4	2.371
p-Xylene	24.3	248.0	112.4	242.5	2.269

t represents the temperature in degrees centigrade
R_1 reading of precision condenser with air in T.C. (mmf)
R_2 reading of P.C. with liquid in T.C. (mmf)
C_5 capacity of T.C. filled with liquid (mmf)
ϵ dielectric constant of liquid at 85.8 kilocycles per sec.

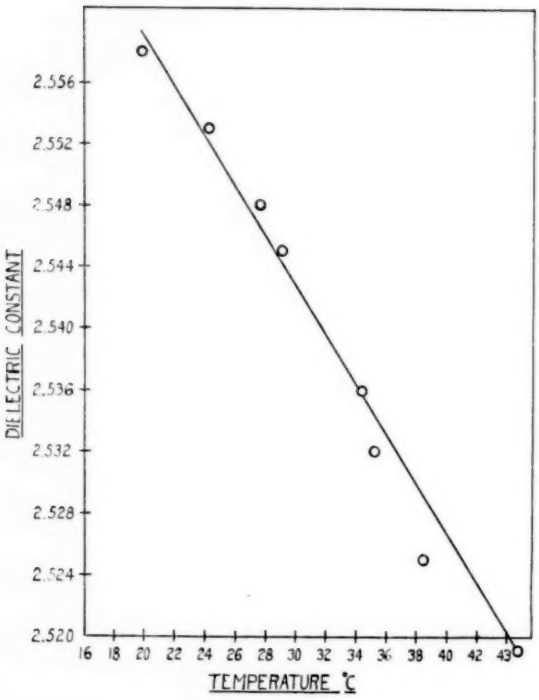

Fig. 3. Dielectric constant-temperature curve for o-xylene.

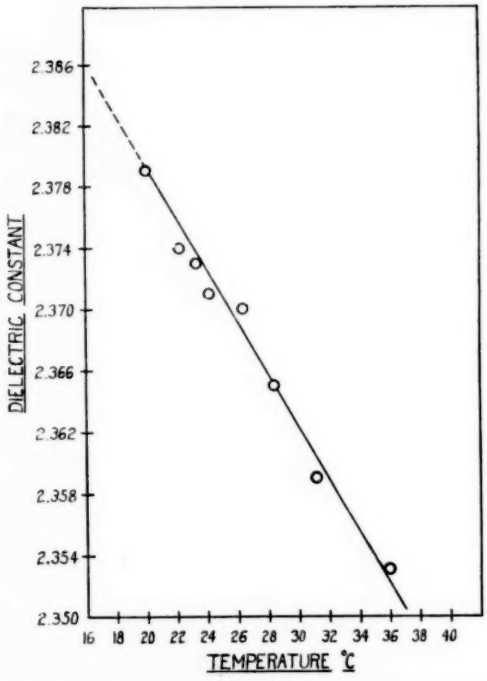

Fig. 4. Dielectric constant-temperature curve for m-xylene.

Table III gives the temperature coefficients of the dielectric constants of the three xylenes for the linear formula and for the formula proposed by Abegg.[11]

TABLE III. *Temperature coefficients.*

Liquid	K_0	β	ϵ_0	$\alpha \times 10^3$
o-Xylene	2.590	0.0016	2.5902	0.270
m-Xylene	2.414	.0018	2.4141	.318
p-Xylene	2.283	.0006	2.2833	.117

Linear formula, $\epsilon_t = K_0 - \beta t$
Abegg's formula, $\log_{10}\epsilon_t = \log_{10}\epsilon_0 - \alpha t$

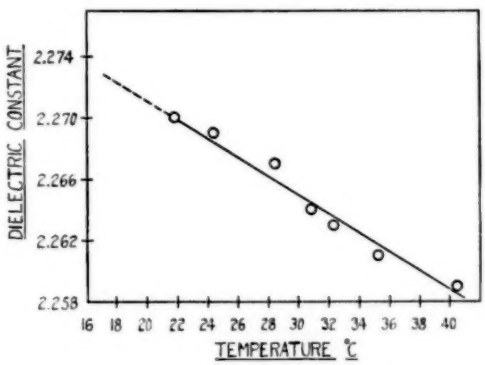

Fig. 5. Dielectric constant-temperature curve for p-xylene.

The density data for the three xylenes were obtained with a Westphal balance. These data are tabulated in Table IV.

TABLE IV. *Density data.*

	o-Xylene	m-Xylene	p-Xylene
T	ρ	ρ	ρ
288	0.883	0.869	0.865
293	.879	.864	.861
298	.875	.860	.857
303	.871	.856	.852
308	.867	.852	.847
313	.863	.847	.843
318	.859	.843	.838

ρ represents density and T absolute temperature.

The values of the polarization P for the three xylenes were calculated for several temperatures from the dielectric constant and density data. These values are plotted in Figs. 6, 7 and 8.

The values of the polarization P_0 for the three xylenes were calculated by substituting optical data in Eq. (10). From the values of P and P_0 the elec-

[11] Abegg, Wied. Ann. **60**, 54 (1897).

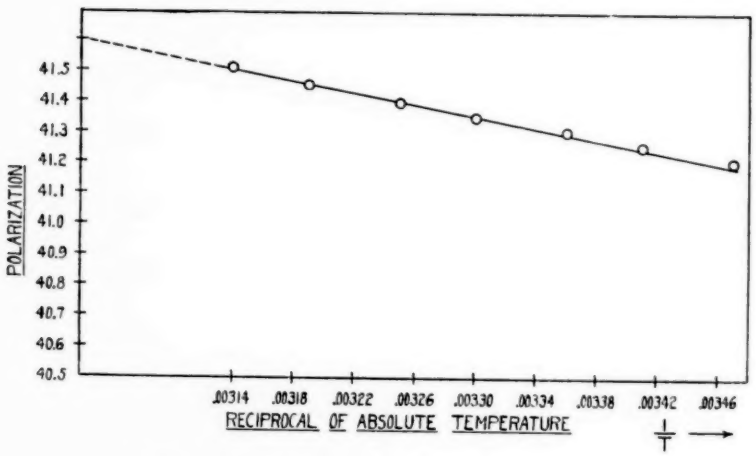

Fig. 6. Polarization-temperature curve for o-xylene.

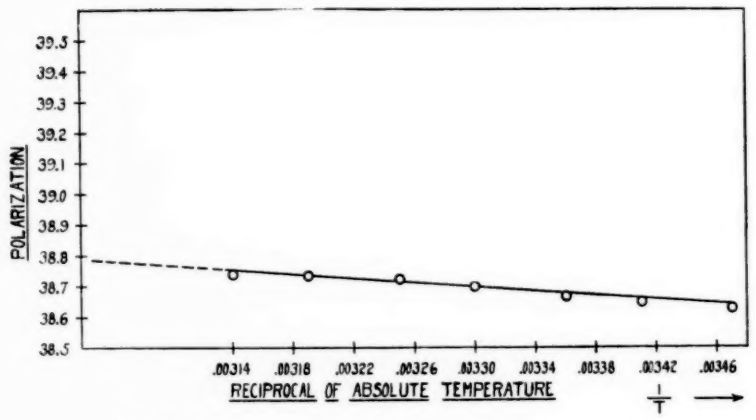

Fig. 7. Polarization-temperature curve for m-xylene.

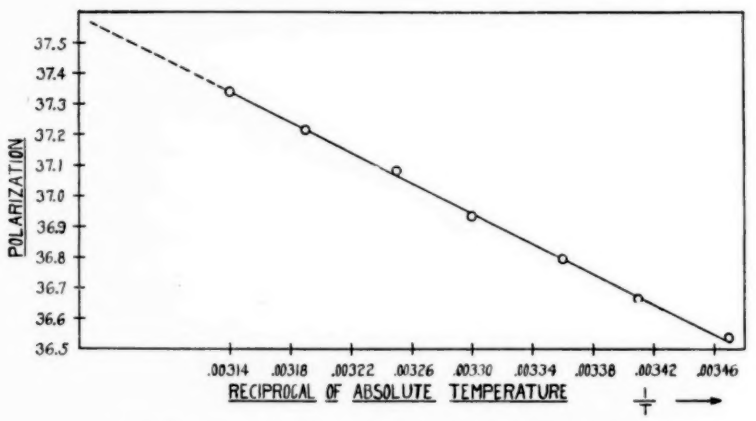

Fig. 8. Polarization-temperature curve for p-xylene.

tric moment μ was calculated for the molecules of each of the three xylenes. P_0 corresponds to the intercept A in Eq. (13). The values of P, P_0 and μ are given in Table V.

TABLE V. *Electric moments of molecules.*

Liquid	r	P	P_0	$(P-P_0)$	$\mu\times10^{18}$ e.s.u.
o-Xylene	1.505	41.3	35.8	5.5	0.51
m-Xylene	1.496	38.6	35.8	2.8	.36
p-Xylene	1.498	36.7	36.1	.6	.17

Symbol r represents the index of refraction
P_0 the polarization calculated from refractive data
μ the electric moment of the molecule
P the polarization at 20°C as determined in this work

Results recorded by Williams and Krchma (14)

Liquid	P	P_0	$(P-P_0)$	$\mu\times10^{18}$ e.s.u.
o-Xylene	40.8	35.0	5.8	0.52
p-Xylene	36.7	35.5	1.2	.06

DISCUSSION OF RESULTS

For a check on the method and technique employed in this work the dielectric constants were determined for ethyl ether, nitrobenzene, benzene, o-xylene, m-xylene and p-xylene and were compared with the findings of several other experimenters. The results were in good agreement considering the different methods used, the experimental error and the inevitable variation in the purity of the organic liquids.

Table III shows that over the temperature range covered that either the linear formula or Abegg's formula is applicable. For large temperature ranges, however, Abegg's formula or the one proposed by Adams[12] are valid. The apparatus at hand did not permit working an extensive temperature range.

The polarization-temperature curves in Figs. 6, 7 and 8 for o-xylene, m-xylene and p-xylene respectively each show a negative slope. Thus the experimental data leads to an imaginary electric moment for the molecules of each xylene. These results illustrate the inadequacy of the simple Debye theory when applied to pure organic liquids where the mutual interaction of the molecules is a dominant factor.

Debye[13] shows that molecules of organic liquids such as toluene $C_6H_5(CH_3)$ with monosubstituents are all dissymmetrical or polar as indicated by the magnitude of the electric moment. For molecules of compounds such as xylene $C_6H_4(CH_3)_2$ and dinitrobenzene $C_6H_4(NO_2)_2$ with two equal substituents the electric moment should be greatest in the ortho position, less in the meta and zero in the para position. The findings in this work on xylene as tabulated in Table V are in accord with this view. For molecules of compounds such as nitrotoluene $C_6H_4(CH_3)(NO_2)$ with two unequal substituents the electric moment is greatest in the para position.

[12] Adams, J. Am. Chem. Soc. **48**, 621 (1926).
[13] Debye, "Polar Molecules," p. 50.

Consulting Table V it is seen that the value of μ for o-xylene accords well with the value found by Williams and Krchma[14] for o-xylene in dilute solution with a non-polar solvent. Also the electric moments for p-xylene are in fair agreement and they are so near zero that p-xylene is considered non-polar.

Conclusions

The writer can find no record of the previous determination of the dielectric constants of cinnamic aldehyde, methyl cyclohexane, methyl o-nitrobenzoate, oxalyl chloride, n-propyl ether, iso-propyl ether and propylene chloride.

It seems reasonable to believe that the values of the dielectric constants are relatively as accurate as the purity of the organic liquids.

The temperature coefficients of the dielectric constants for ortho-, meta-, and para-xylenes have been determined over a temperature range of about 30°C.

The experimental findings which led to negative electric moments further stress the inadequacy of the simple Debye theory when applied to pure organic liquids.

It is indeed a pleasure to give acknowledgment to Dr. F. C. Blake for his constant encouragement and valuable suggestions throughout these experiments.

[14] Williams and Krchma, J. Am. Chem. Soc. **49**, 1676 (1927).

LETTERS TO THE EDITOR

Prompt publication of brief reports of important discoveries in physics may be secured by addressing them to this department. Closing dates for this department are, for the first issue of the month, the twenty-eighth of the preceding month; for the second issue, the thirteenth of the month. The Board of Editors does not hold itself responsible for the opinions expressed by the correspondents.

A Relation Between the Scattering of X-rays by Gases and Crystals

Recently Compton[1] and Jauncey and Harvey[2,3] have obtained formulas for the spatial distribution of the intensity of x-rays diffusely scattered by monatomic gases and by simple cubic crystals respectively. Compton's formula may be written

$$S = 1 + (Z - 1)f'^2/Z^2 \qquad (1)$$

where S is the scattering per electron in terms of the corresponding Thomson value,[4] Z the atomic number of the scatterer, and f' an average atomic structure factor for an atom at rest. The difference between f, the true atomic structure factor, and f' has been discussed by Jauncey[5] and Herzog.[6] The formula of Jauncey and Harvey is

$$S = 1 + (Z - 1)f'^2/Z^2 - F^2/Z \qquad (2)$$

where F is the atomic structure factor of an atom in the crystal lattice and includes the effect of the thermal vibration of the atoms. Woo[7] has also recently obtained a formula for the diffuse scattering from crystals which takes account of the change of wave-length due to the Compton effect. However, if $\alpha(=h/mc\lambda)$ is small, Woo's formula reduces to Eq. (2) provided that $f=f'$.

Wollan[8] and Harvey,[9] respectively working on the diffuse scattering from argon and sylvine, have found that the f' values for argon and sylvine are almost, if not exactly, equal over a wide range of $(\sin\phi/2)/\lambda$. If we

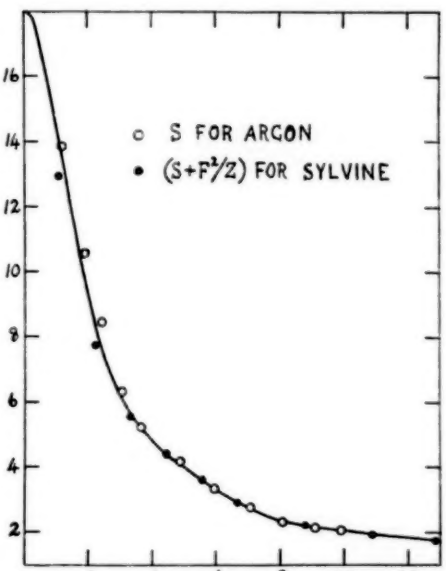

assume this equality to be exact, f' can be eliminated from Eqs. (1) and (2). This elimination leads to

$$S_{gas} = (S + F^2/Z)_{crystal}. \qquad (3)$$

The quantity on the left refers to the gas and the quantities on the right to the crystal, as is indicated by the subscripts.

[1] A. H. Compton, Phys. Rev. **35**, 925 (1930).

[2] G. E. M. Jauncey, Phys. Rev. **37**, 1193 (1931).

[3] Jauncey and Harvey, Phys. Rev. **37**, 1203 (1931).

[4] J. J. Thomson, Conduction of Electricity through Gases, 2nd Ed., p. 325.

[5] G. E. M. Jauncey, Phys. Rev. **38**, 1 (1931).

[6] G. Herzog, Zeits. f. Physik **69**, 207 (1931).

[7] Y. H. Woo, Phys. Rev. **38**, 6 (1931).

[8] E. O. Wollan, Phys. Rev. **37**, 862 (1931).

[9] G. G. Harvey, Phys. Rev. Aug. 15, 1931.

Eq. (3) is a simple and interesting relation connecting the diffuse scattering by monatomic gas, the diffuse scattering by a crystal consisting of the same kind of atoms as the gas, and the Laue scattering (Bragg reflection) from the crystal. The term F^2/Z may be considered as a correction term which eliminates the effect of interference between different atoms in the crystal. Wollan's S values for argon, Harvey's S values for sylvine, and James and Brindley's F values[10] for sylvine were used in constructing the accompanying figure. It is seen how closely the S values for argon and the $(S+F^2/Z)$ values for sylvine fall on the same curve.

G. E. M. Jauncey
G. G. Harvey

Washington University,
St. Louis, Mo.,
July 28, 1931.

[10] James and Brindley, Proc. Roy. Soc. **A121**, 155 (1928).

Reflection of Electrons by a Special Potential Field

In his recent paper on the photoelectric effect, Professor Frenkel[1] has given the formula for the reflection coefficient for a special one-dimensional potential field as derived by the writer. To avoid possible misunderstanding it should be pointed out that the factors A and B in the potential function as quoted on the bottom of page 318 are not absolute constants. The potential function actually used is of the peculiar form $u(x)=0$ for $x\leqq x_1$; $u(x)=W\{1-1/[(x/a)(1-\lambda_1/\lambda_2)-1]^2\}$ for $x_1\leqq x\leqq x_2$; $u(x)=U_2$ for $x\geqq x_2$. Here $a=x_2-x_1$ $\lambda_1^2=h^2/2mW$, $\lambda_2^2=h^2/2m(W-U_2)$. $u(x)$ is a continuous function of x. Naturally this function was used only by accident. It arose in an unsuccessful attempt to solve the problem in which $u(x)$ varies linearly for $x_1\leqq x\leqq x_2$ by approximating $u(x)$ by a step-function. Divide the range (x_1, x_2) into $\mu+1$ elements of lengths $\Delta_1, \cdots, \Delta_{\mu+1}$ by the points $x_0, \cdots, x_{\mu+1}$. The wave-length in the j-th interval is chosen as $\lambda_j=\gamma^{(j-1)}\lambda_1$ and the lengths of the intervals as $\Delta_j=\gamma^{(j-1)}\Delta_1$ with $\sum\Delta_j=a$ and $\gamma=(\lambda_1/\lambda_2)^{1/\mu}$. As $\mu\to\infty$ this step function approximates more and more closely to the function given above. For a finite value of μ, ψ can be written in the form $c_j'e^{i2\pi x/\lambda_j}+c_j''e^{-i2\pi x/\lambda_j}$ in the j-th interval. On fitting up the solutions at the boundaries of the intervals it is found that the linear relations connecting (c_j', c_j'') with (c_{j+1}', c_{j+1}'') do not involve the index j. This allows one to introduce new variables in a manner already described,[2] and the reflection coefficient for the step function can be found. On letting $\mu\to\infty$ the formula quoted by Frenkel results. Since the potential function is of such a special kind it hardly seems worth while to describe the calculations in greater detail. It may be noted that the expression obtained for R actually reduces to that for a single potential discontinuity, namely $(\lambda_1-\lambda_2)^2/(\lambda_1+\lambda_2)^2$ when $a\to 0$. Finally, in calculating some of the numerical values for R from the formula it has been found that the fluctuations exhibited by it are much less pronounced than was originally thought. This has been found also in the accurate calculations on the linear potential function made by Mr. Wetzel which will be published soon.

E. L. Hill

Department of Physics,
University of Minnesota,
August 9, 1931.

[1] J. Frenkel, Phys. Rev. **38**, 309 (1931).

[2] E. L. Hill, Phys. Rev. **37**, 785 (1931).

Quantization of Large Scale Events

The recent letter by Einstein, Tolman and Podolsky (Phys. Rev. **37**, 780, 1931), pointing to an uncertainty in the description of past events required by quantum mechanics, concludes with the following sentence:

"Finally, it is of special interest to emphasize the remarkable conclusion that the principles of quantum mechanics would actually impose limitations on the localization in time of a macroscopic phenomenon such as the opening and closing of a shutter."

It is proposed in what follows to suggest how this unexpected result may have arisen. It should be noted that the system discussed by the authors contains a model of a kind unusual in theoretical physics and it is really this which appears to produce the quantization of the large scale phenomenon. Structures

acting in a narrowly prescribed manner are, it is true, used in the theoretical discussion of physical processes as, for instance, in the Donnan-membrane equilibrium or in the Carnot cycle. How then does the structure used in the present case which consists merely of a box having two openings, a shutter and an ellipsoidal mirror, differ from these other cases?

"The shutter," says the letter, "is arranged to open automatically for a short time and then close again, and the number of particles in the box is so chosen that *cases arise* in which one particle leaves the box and travels over the direct path *SO* to an observer at *O*, and a second particle travels over the longer path *SRO* through elastic reflection at the ellipsoidal reflector *R*."

(The diagram is reproduced here for convenience in discussion.)

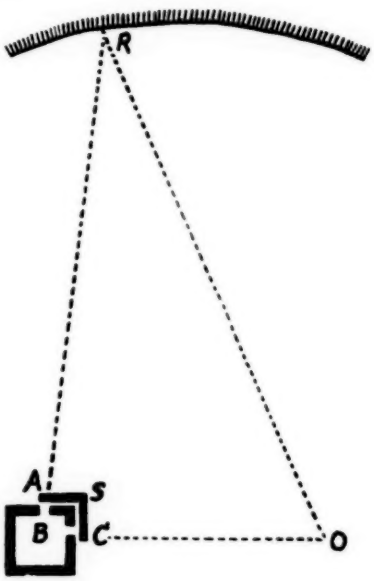

Let us distinguish the two openings in the box as "*A*" and "*C*," "*A*" being that through which the particle of longer path escapes. On opening the shutter, particles will escape through *A* from time to time in arbitrary directions spread through 180°. A large fraction of these, dependent on the angular extent of the ellipsoidal mirror, will be reflected so as to pass the observer at *O*. Those leaving *C*, on the other hand, (that is, reaching the observer by the short "unreflected" path), form a small fraction of all the particles escaping from *C* when the shutter is open.

To discuss the total behavior of such a system, we may suppose the shutter to be opened at random from time to time and the escape of particles duly noted.

Of the various cases arising, we are asked to consider first, those in which particles escape simultaneously, which cases are thus very improbable and, second, of such cases only those in which the *B* particle is directed towards *O*. The relevant cases thus form a small fraction of the class of simultaneous emission, itself a rare case in relation to the totality of observations. Thus the probability of the case with which the argument deals and from which the uncertainty in the description of past events is deduced, is of the second order of infinitesimals.

Doctors Einstein, Tolman and Podolsky do not discuss in how far their conclusion may be due to the selection of this sort of unique happening for their observations. However, some interesting deductions might be made from this view of their discussion. The linking between the large scale event, that is the opening of the shutter, and a microscopic event which is governed by the quantum laws may indeed be due to this virtual waiting for a favorable instant. The deduced and unexpected quantization of the macroscopic phenomenon is due, in part, to the use of the specially devised mechanism in which the large scale event is made to depend on a simple non-statistical quantised atomic effect and, in part, as already indicated, to the choosing of the unique and "improbable" instant when alone this coupling of the two kinds of systems becomes possible. If such coupling has not been noticed before, it may be because structures linking micro- with macro- processes have not been intimately considered in this way.

From an operational point of view, waiting for the favorable event of simultaneous emission may be little different from the assumption that we can observe the ultimate motion of the gas particles and delay the opening of the shutter until we observe two molecules suitably approaching *A* and *C* simultaneously, (the second being directed along the line *CO*). This postulated operation, to some extent, gives us the powers of the Maxwell Demon and may on further examination, be open to similar objections. If this analysis is correct, we may expect the statistical results obtained by the method of Einstein and the others to

be in some way contrary to the spirit of the Second Law. However, as the averaged behavior of the system is not considered, no such anomaly comes to light in the case considered by them.

The initial assumptions of the problem are contrary to the Second Law for a more obvious reason. It is first assumed that the weighing of the box and the observation of the time of arrival and momentum of the unreflected particle could be carried out before the arrival of the second. It is deduced that "It would then seem possible to predict beforehand both the energy and time of arrival of the second particle . . . ." If so, it would surely be possible, using a shutter and two interchangeable receiving vessels at O to separate the gas escaping from A into two portions having different average temperatures, thus realising the conditions of the Maxwell Demon problem, and permitting a violation of the Second Law.

It is therefore not necessary to go to quantum mechanics for evidence that this original train of assumptions is physically unsound—if it is granted that the Second Law applies to the total behavior of the system.

DAVID L. WATSON

Science Service,
Washington, D. C.,
August 6, 1931.

The Emission of Positive Ions from Cu and Ag

By using an electrometer with a sensitivity of 3×10^{-16} amp/mm for measuring the current, it has been possible to detect Cu^+ ions from Cu and Ag^+ at temperatures just below the melting point and above. The results for Cu are in agreement with the findings of L. L. Barnes (Phys. Rev. **37,** 218, 1931). The nature of these ions was determined by a mass spectrograph of the Dempster type. In the earlier work (Phys. Rev. **37,** 467, 1931) when the metals were used as filaments and were heated by electrical conduction, no characteristic positive ions could be detected. This was probably due to the fact that the filaments broke at a temperature below the melting point.

In the present instance the metals were heated in a resistance-wound porcelain vacuum furnace, and a characteristic current was detected. No sudden change in the magnitude of this characteristic current was observed in passing through the melting point.

The current which passed through the slit system of the mass spectrograph was small in each case (of the order of 5×10^{-15} amps for Cu and 10^{-15} amps for Ag at the melting points).

The potassium ion current was several hundred times larger than the characteristic current at these temperatures, and did not decrease appreciably with several hours' heating above the melting point. This may be due to potassium salts from the porcelain passing into solution in the molten metal.

H. B. WAHLIN

Department of Physics,
University of Wisconsin,
August 6, 1931.

The Alternating Intensities of Na_2 Bands

It has generally been supposed that the sodium bands do not show any observable alternation of intensities and that therefore the sodium nucleus must have a large spin. This conclusion depends upon the statement by Loomis and Wood (Phys. Rev. **32,** 223, 1928) that there is no evidence of alternating intensities in these bands. The writer examined their published photograph of one of these bands and came to the conclusion that there might be some slight evidence of alternation of intensities. However, the spectrum is rather messed up by the presence of other lines than those belonging to the bands, and also there may be irregularities in the continuous source used for this absorption spectrum, and no certain conclusion could be drawn by visual observation. This apparently was the method of examination used by Loomis and Wood and probably accounts for their conclusion that there are no alternating intensities.

In order to test this conclusion better I have photographed the reproduction which they gave and have run the negative so secured through a microphotometer. (This method of investigation was suggested to the writer by Professor F. A. Jenkins.) The resulting microphotometer curve shows very strong indications of alternating intensities in these bands. It is the odd-numbered lines

which show the greater intensity, the numbering being that of the $^2\Sigma$ rotational levels.

The P branch lines are resolved from the $P28$ line to the $P57$ line. The height of the peaks on the microphotometer curve measured relatively to an arbitrary base line which was taken as approximately that of the continuous background, are as follows:

Line	Galvanometer Throw	Line	Galvanometer Throw
P28	3.3	P43	4.4
29	4.3	44	2.3
30	2.0	45	3.9
31	3.7	46	3.0
32	2.1	47	4.0
33	3.3	48	3.6
34	1.6	49	4.2
35	3.3	50	—
36	3.8	51	5.2
37	4.7	52	—
38	4.0	53	2.8
39	4.3	54	0.5
40	4.5	55	—
41	5.2	56	—
42	4.1	57	—

It will be noticed that in nearly every case the throw for the even numbered lines is less than the throw for the two neighboring odd-numbered lines and in every case the throw for the even numbered lines is less than the average for the throws of the two neighboring odd-numbered lines. If we sum the throws for the even numbered lines from 28 to 48 inclusive we get 34.3 and for a similar sum of the odd-numbered lines from 29 to 49 we get 45.3 showing that there is a distinctly greater intensity for the odd-numbered lines than for the even numbered lines in this region.

The R and Q branch lines are not well separated. From $R37$ to $R45$ the $R(J'')$ line falls on the $Q(J''-5)$ line and for the higher numbered lines the resolution is imperfect. (The region of the figure containing the lower R lines than $R37$ was not investigated.) No evidence for alternation of intensities is found either in the R or Q branch lines in this region of partial resolution by the method used above for the P branch lines, but I have noticed that the peaks of the partially resolved R and Q lines consist in many cases of one strong peak with a little hump on the side representing the weaker line of the pair. And I noticed that in many cases the odd-numbered line, regardless of whether it was a Q or R branch line, was stronger than the neighboring even numbered R or Q line. The following table gives a list of some 18 pairs of these partially resolved lines. Some such pairs cannot be used because of obvious irregularities in the microphotometer curve. The relative intensities of the two lines are indicated by the inequality sign. In the cases where the microphotometer curve was obviously irregular straight lines have been drawn.

$Q41 > R46$	$Q52 < R57$
$42 < 47$	$53 > 58$
$43 > 48$	$54 — 59$
$44 < 49$	$55 > 60$
$45 > 50$	$56 < 61$
$46 < 51$	$57 — 62$
$47 > 52$	$58 < 63$
$48 — 53$	$59 — 64$
$49 > 54$	$*60 > 65$
$*50 > 55$	$61 > 66$
$*51 < 56$	$*62 > 67$

There are 18 of these double peaks which *seem* to be clear and undisturbed by the presence of other lines. In 14 of these it is the odd-numbered line which is the more intense and in the 4 remaining cases (marked with an asterisk) is it the even numbered line which appears to be the most intense.

It seems to the writer that the evidence from these microphotometer curves indicates very strongly that there is an observable alternating intensity in the sodium bands and that, therefore, the spin of the nucleus is probably 5/2 or less. Also the odd levels of the normal $^2\Sigma$ are the stronger so that Na_2 is similar to H_2 in this respect and the states antisymmetric in the nuclei are those which occur. Experimental work to determine the intensity ratio is in progress in the Columbia University laboratories (Chemistry and Physics) in collaboration with the laboratories of Mr. Alfred Loomis of Tuxedo Park.

HAROLD C. UREY
Department of Chemistry,
Columbia University,
August 7, 1931.

The Red CN Band System

A number of interesting features of this spectrum have appeared in our analysis of its rotational structure from grating plates of high dispersion. It has been known for some

time that the electronic transition is $^2\Pi \rightarrow {}^2\Sigma$, the $^2\Sigma$ state being identical with the lower state of the $^2\Sigma \rightarrow {}^2\Sigma$ violet CN bands. We find close agreement in the constants of the $^2\Sigma$ state as derived from the two systems. Thus in our equation for the band origins,

$$\nu = 14{,}403.22 + 1724.24v' - 12.883v'^2 - 2055.62v'' + 13.176v''^2,$$

the vibrational constants of the final state are close to the accepted values from the violet system: $\omega_0'' = 2055.64$, $x''\omega_0'' = 13.25$. The constants of the rotational energy in the lower state, determined from measurements of the bands (2, 1), (4, 1), (3, 2), (4, 2), (5, 3), (5, 2), and (6, 3), are probably more accurate for the states $v'' = 2$ and 3 than those now known from the violet bands. Our work gives $B_v'' = 1.8904 - 0.0173v''$, while Heurlinger obtained $1.8915 - 0.0173v''$.

The new data on the $^2\Pi$ state are of more importance. The doublet is inverted, with the spin coupling constant $A = -52.2$ cm^{-1}. It presents an interesting example of the intermediate type of coupling between case (a) and case (b), having $A/B_e = -31.4$. In agreement with the general formula for the energy derived by Hill and Van Vleck, a considerable difference is found between the "apparent" constants, $B^*_{v,\Sigma}$ for small rotation, in the two components. Thus, by a graphical evaluation, we find $B^*_{v,-} - B^*_{v,+\frac{1}{2}} = 0.102$, as an average the seven bands measured. This is exactly the difference predicted by the theory. If the true B_v is taken as the mean of the two $B^*_{v,\Sigma}$ values, our data give $B_v' = 1.6554 - 0.01746v'$.

None of the constants, however, shows a perfectly smooth variation with v in the $^2\Pi$ state. Perturbations of both vibrational and rotational energy are especially pronounced for $v = 4$ and 5. These phenomena are caused by the interaction with the higher terms of the $^2\Sigma$ state, which are known[1] to cross the $^2\Pi$ terms in this region, with nearly the same value of B_v. The Λ-doubling becomes very large in the perturbed states, showing an abrupt discontinuity and reversal of sign where the levels of the $^2\Pi$ state are crossed by those of equal J in the $^2\Sigma$ state. For $v' = 2$ and 3, the Λ-doubling is relatively small, and of the expected type. At low J, $\Delta\nu_{de}$ is smaller in the T_1 terms, but takes on considerable negative values as J increases. The T_2 terms show first an increase to a maximum, with $\Delta\nu_{de} = +0.05$ cm^{-1} at about $J = 10$, then a decrease and eventual reversal of sign at about $J = 20$. An analysis of the curves according to the equations of Mulliken and Christy[2] yields $p_0 = +0.0082$, $q_0 = -0.00032$ as mean values for these two vibrational states.

In the bands with $v' = 4$, three large perturbations are found, which by their form and magnitude are evidently due to the crossing of sets of terms. The terms T_{1e} show a discontinuity at $J = 13\frac{1}{2}$, corresponding to the perturbation of the T_2 terms[3] in the $^2\Sigma$ state with $v = 11$. Further perturbations occur in T_{1d} at $J = 25\frac{1}{2}$ and in T_{2d} at $J = 27\frac{1}{2}$. The latter have been predicted by Dr. G. T. Ittmann from a theoretical treatment of perturbations in doublet states[4] as applied to the case of $^2\Pi$ and $^2\Sigma$ in CN. In fact we have found from our data and from those previously given for the violet system[5] that if one assumes a relative position of the $^2\Pi$ and $^2\Sigma$ levels such that T_{1e} crosses T_2 between $J = 12\frac{1}{2}$ and $13\frac{1}{2}$, an extrapolation of the unperturbed levels shows that T_{1d} is crossed by T_1 at $J = 25\frac{1}{2}$, while T_{2d} is crossed by T_2 at $J = 27\frac{1}{2}$. Thus all of the perturbations in the $^2\Pi$ levels are accounted for, as of course are the three corresponding perturbations previously known in the final levels of the violet system.[1]

With the relative position of the $^2\Pi$ and $^2\Sigma$ levels thus fixed to within 1 or 2 cm^{-1}, it appears that the term $^2\Sigma^{(11)}(0)$ lies 57 cm^{-1} below the lowest rotational term of $^2\Pi_{3/2}{}^{(4)}$, while $^2\Sigma^{(12)}(0)$ lies 38 cm^{-1} above the lowest level of $^2\Pi_{1/2}{}^{(5)}$. The $^2\Pi_{1/2}{}^{(5)}$ levels have initially greater spacing than those of $^2\Sigma^{(12)}$, and approach the $^2\Sigma^{(12)}$ levels as far as $J = 12\frac{1}{2}$, then recede again. This explains a remarkably large Λ-doubling found in $^2\Pi_{1/2}{}^{(5)}$, and a corresponding large spin doubling in $^2\Sigma^{(12)}$, previously known.[5] The close approach of the vibrational levels

[1] J. E. Rosenthal and F. A. Jenkins, Proc. Nat. Acad. Sci. **15**, 381 (1929).

[2] R. S. Mulliken and A. Christy, Phys. Rev. **38**, 87 (1931).

[3] In Ref. 1 it was assumed, from the data then available, that the T_1 terms were perturbed at this point. Correcting this shifts the P_1 curve in Fig. 1 of Ref. 1 one J unit lower, and changes its designation to P_2.

[4] G. T. Ittmann, Zeits. F. Physik, in press. We are indebted to Dr. Ittmann for an opportunity to examine this article in MS.

[5] F. A. Jenkins, Phys. Rev. **31**, 539 (1928).

$^2\Sigma^{(11)}$ and $^2\Sigma^{(12)}$ to $^2\Pi^{(4)}$ and $^2\Pi^{(5)}$ respectively, is also probably responsible for perturbations of these vibrational terms, which are shown by a displacement of the bands as a whole some 1 or 2 cm^{-1} from their positions calculated by an equation for origins such as that given above.

F. A. JENKINS, Department of Physics, University of California
YALE K. ROOTS, Department of Physics, Findlay College
ROBERT S. MULLIKEN, Department of Physics, University of Chicago.
August 4, 1931.

Reaction due to Gas Molecules leaving the Cathode of an Arc

Tanberg[1] has published some interesting experimental data which have been interpreted as indicating that a high speed metal vapor jet is ejected from the cathode region of an electric arc drawn from a copper cathode in a vacuum.

Since gas was evolved in the experiment, it is interesting to consider the reaction force produced by the gas molecules leaving the cathode. The relation between vapor pressure and rate of evaporation of a metal[2] is $m=p(M/2\Pi RT)^{1/2}$. In this case, the pressure will be one half that given by the above relationship, since the molecules leave but do not return. We are interested in the force rather than the pressure, so the above equation becomes $m'=2f(M/2\Pi RT)^{1/2}$ or $f=m'(\Pi RT/2M)^{1/2}$, where m' is the actual evaporation in grams per second.

Consider the data from test 356 (Reference 1, page 1081):

Reaction force (uncorrected)	0.485 gm
Electrodynamic force	0.041 gm
Corrected reaction force	0.444 gm

Evaporation from cathode 0.49×10^{-3} gm/sec.

Assuming that the cathode spot has a temperature of 3000°K, as given in a recent paper,[3] the reaction force due to the evaporated copper may be calculated by the equation given above, and is found to be 38.5 dynes or 0.039 gm. There is, therefore, a force remaining to be accounted for of $0.444-0.039$ or 0.405 gm which is $0.405/0.039$ or 10.4 times the force due to the evaporating copper. This force might be due to the gas which is evolved, in which case, assuming that the gas molecules have velocities corresponding to the temperature of 3000°K, it is possible to calculate the ratio of the weight of the gas evolved to the weight of the copper evaporated. This will be called "r." If the gas evolved is molecular oxygen,

$$r = 10.4(32/63.6)^{1/2} = 7.4.$$

If the gas evolved is atomic oxygen,

$$r = 10.4(16/63.6)^{1/2} = 5.2.$$

Test 456 (Reference 1, p. 1087) gives some clue to the amount of gas evolved. Assuming the gas to be oxygen, the weight of the gas evolved is

$$\frac{(56-0.9)V\times 0.00131}{760{,}000}$$

where V is the volume of the vessel. The weight of the copper evaporated is $1.53\times10^{-5}\times2.3\times t$, where t = the duration of the test. Thus

$$r=\frac{55.1\times0.00131}{760{,}000\times1.53\times10^{-5}\times2.3}\frac{V}{t}$$

$$=0.00270\frac{V}{t}.$$

The values of V and t are not given, though Mr. Tanberg states that this test "lasted several seconds," and in the later paper,[3] it is stated that "the arc his never held longer than 5 seconds." Assuming that V is 7000 cm^3 and t is 3 seconds, the value of V would be 6.3, which is seen to be of the same order of magnitude as those calculated above on the assumption that the measured reaction force is produced by a vapor stream and a gas stream both of which have velocity distributions corresponding to a temperature of 3000°K.

It is quite evident that the force due to the gas evolved should not be neglected. For accurate results, the nature and amount of this gas should be determined.

B. WELLMAN
Research Laboratory, General Electric Co.,
August 6, 1931.

[1] Tanberg, Phys. Rev. **35**, 1080 (1930).
[2] Jones, Langmuir, and Mackay, Phys. Rev. **30**, 201 (1927).
[3] Tanberg and Berkey, Phys. Rev. **38**, 296 (1931).

Angular Distribution of Photoelectrons

In his interesting paper (Phys. Rev. July 15, 1931) J. Frenkel proposes an approximate method, very simple indeed, for computing the angular distribution of photoelectrons emitted by a hydrogen-like atom. The result is identical with that obtained by F. Fischer and with the somewhat more general results presented by F. Sauter (Ann. d. Physik **9**, 217, 1931). The remarks of Frenkel about a discrepancy between his formula and that proposed by myself together with G. Schur (Ann. d. Physik **4**, 409, 1930) are evidently erroneous because my formula turns out to be the straightforward approximation of the formulae of Fischer, Sauter and Frenkel, if one expands the latter according to ascending powers of the velocity ratio β and neglects, besides higher powers of β, a term of a relativistic order of magnitude not substantiated by the present treatments.

A. SOMMERFELD

University of Michigan,
August 17, 1931.

Note on "The Effect of Piezoelectric Oscillation on the Intensity of X-ray Reflections from Quartz"

In a paper having the above title, published in the Physical Review **37**, 1622 (1931) Messrs. G. W. Fox and P. H. Carr reported an interesting result of their experiment that the intensity of x-ray reflections from quartz is decidedly increased when the crystal is piezoelectrically oscillated.

It should be noted that a similar experiment was in progress in our laboratory in connection with the effects of heterogeneous strain of a crystal upon its reflecting power of x-rays. A crystal such as quartz has a perfect state of crystallization, and especially in the interior of the crystal the extinction effects, primary as well as secondary, are very large, while in the ground surface the crystallization is made somewhat imperfect so that the effects of both extinctions are reduced in a considerable degree. When a Laue photograph is taken through a quartz plate of the thickness of a few millimeters, each Laue spot splits into two (Fig. 1) showing that the reflection of x-rays takes place only in the thin layers near both surfaces, while the interior part of the plate makes little contribution to the reflection. When, however, the plate is oscillating piezoelectrically, a kind of heterogeneous strain is established in it, and the interior part of the plate can no longer be regarded as a perfect crystal. Hence the extinction effects will be reduced and the interior part will be endowed with a strong power of reflection. In Fig. 2 is given the Laue pattern for the same quartz plate as before but in oscillation. Each splitted spot is now bridged over to form a single spot, the intensity being increased enormously.

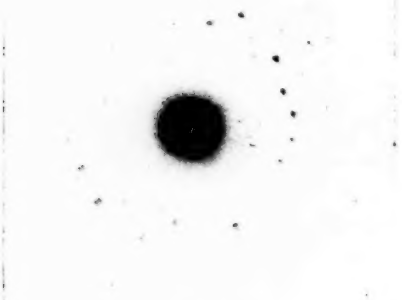

Fig. 1.

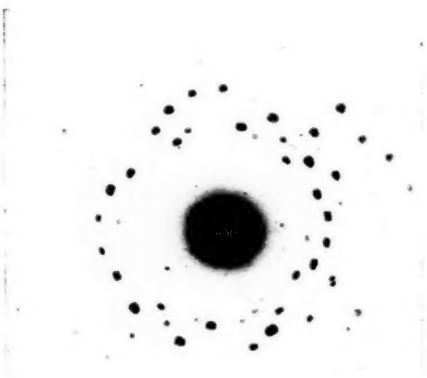

Fig. 2.

A similar effect has been obtained when a

thermal strain was given to the crystal by applying a temperature gradient along a certain direction, of which the experimental result and its interpretation will soon be published. (Proc. of Physico-Math. Soc. of Japan, Ser. III, 13 (1931) 211). Moreover, it was found that, when a mechanical stress is given to the crystal plate so as to produce a heterogeneous strain, a similar effect is also observed. It may be remarked that when the strain is homogeneous as in the case of uniform heating or placing the crystal in a uniform electrostatic field, little effect is produced.

S. NISHIKAWA (Fellow)
Y. SAKISAKA
I. SUMOTO
The Institute of Physical and Chemical Research, Tokyo,
July 26, 1931.

A New Criterion for Predissociation

Nearly a year ago I reported the striking violation of the Franck-Condon principle caused by some of the rare gases in active nitrogen. (Phys. Rev. **36,** 778, 1930) I named this phenomenon "variation of intensity within a progression" since it involved a variation in the relative intensities of bands which are emitted from the same initial vibrational state. In a later paper I briefly discussed the explanation of this phenomenon in terms of Heitler and London levels and I pointed out that the phenomenon could be understood if one considered forced interactions with repulsive energy levels in the molecule. Transitions will not occur not only to the lower levels which are involved in the emission of the group of bands, but radiationless transitions will take place to repulsive energy levels and the predictions of the Franck-Condon principle will not be applicable. That this is true will be seen when one considers that while the Franck-Condon principle will predict the parts of the initial potential energy curve from which the most probable transitions arise, forced transitions to a Heitler and London curve will rob the different parts of the initial potential energy curve of molecules and thus modify the results of the Franck-Condon principle. If the above explanation is correct then we have here a new criterion for predissociation and also the first case of predissociation which is forced by rare gases since the experiments which I first discussed are those reported by Lord Rayleigh in the Proc. Roy. Soc. **A102,** 453 (1922).

It appears that Turner's evidence for forced predissociation is more direct than the present since in his experiment actual dissociation is observed. In some of my work on nitrogen in which the above phenomenon of variation of intensity in a progression was studied, I obtained very intense nitrogen afterglows for the first time in uncondensed discharges. This was reported (Phys. Rev. **37,** 1004, 1931) before the notion of forced predissociation presented itself. Since then I have discussed predissociation in nitrogen in my report on the auroral spectrum (Phys. Rev. **38,** 582, 1931) before the June meeting of the Physical Society in Pasadena. The present ideas regarding active nitrogen and the production of active nitrogen under such unusual conditions, indicate that the forced predissociation in my experiments resulted in an enhanced production of atomic nitrogen. We have therefore another reason for believing that deviations from the Franck-Condon rule may in many cases be indications of predissociation.

JOSEPH KAPLAN
University of California at Los Angeles,
August 18, 1931.

Predissociation in Nitrogen and Excitation of the Green Auroral Line

In a recent note in these columns, L. A. Turner reported the enhanced predissociation in iodine, caused by argon. It is the purpose of this note to report some of my experiments in which some evidence has been obtained corroborating Turner's explanation of the above effect.

Frerichs first pointed out that the green auroral line could be intensely excited in narrow capillary discharges in oxygen. I have recently repeated this in oxygen containing varying amounts of nitrogen, in order to study the modifications in the first positive group of nitrogen bands which might be produced simultaneously with the emission of the green line. A preliminary report of the modification of these bands was published in these columns before the aurora line was observed (Phys. Rev. **38,** 373, 1931), and in that note it was pointed out that it was possible to force the emission of certain "heads" which are not observed under usual discharge tube conditions. The rotational analysis of these bands by Naudé was reported in the name number of the journal in which my note appeared, so that it is now possible to define more clearly

what we mean by "heads" of the first positive group. Naudé's analysis shows that what appears as a "head" under average dispersion, really consists of a group of three P, Q and R branches so that the three strong heads which characterize most of the first positive bands, are really three groups of P, Q and R branches belonging to the transitions ${}^3\Pi_{low} \rightarrow {}^3\Sigma$, ${}^3\Pi_{medium} \rightarrow {}^3\Sigma$ and ${}^3\Pi_{high} \rightarrow {}^3\Sigma$. (The phenomenon of single-headed emission of these bands plays an important rôle in my work on the aurora spectrum.) A forced emission of these heads means a modification of some selection rule for predissociation transitions since their absence under normal conditions can be accounted for by predissociation (Phys. Rev. **37,** 1406, 1931). We will assume that the same selection rules are violated in the forced emission in N_2 and in the emission of the green line in oxygen. Now the normally missing groups in N_2 belong to the transitions from ${}^3\Pi_{high}$ and ${}^3\Pi_{medium}$, and the present effect is to decrease the probability of transitions from these levels to some nearby Heitler and London level. Hence the selection rule which is probably modified is the one which has to do with the angular momentum of the molecule or the atom and this is the one whose modification is proposed by Turner to explain the magnetic quenching of iodine fluorescence as well as the effect of argon on predissociation in iodine. The violation of the selection rule for angular momentum changes in the atom will also account for the emission of the green line.

It is well known that argon and other rare gases play very unusual rôles in the excitation of spectra of molecules and atoms which are mixed with them. The experiments of Turner, the present experiments in which the green line is produced under conditions more readily understood than those produced in argon-oxygen mixtures, as well as other effects of rare gases on the nitrogen spectrum which have been briefly discussed elsewhere (Phys. Rev. **36,** 778, 1930 and **37,** 1406, 1931), all show that at least one of the effects of rare gases in these experiments is to change transition probabilities. It will be interesting to obtain more detailed experimental and theoretical discussions of this important effect.

JOSEPH KAPLAN

University of California at Los Angeles,
August 18, 1931.

BOOK REVIEWS

Numerical Mathematical Analysis. J. B. SCARBOROUGH, Pp. 416, figs. 25. Baltimore, The Johns Hopkins Press; London, Humphrey Milford, Oxford University Press, 1930. Price $5.50.

This is a self-contained and teachable textbook dealing with numerical analysis. The treatment is elementary and suitable for students having the usual first course in calculus. The subject matter is introduced by interesting remarks, the explanations are clear, difficulties are anticipated and pitfalls are pointed out. The text discusses the following: accuracy of calculations; interpolation; numerical differentiation and integration; numerical solution of algebraic, transcendental and differential equations; law of error and least square theory; precision of measurements; and empirical formulas. Numerous examples are worked out and abundant exercises without answers are given.

Several proofs offered seem to the reviewer not conclusive, and some words are not used in their ordinarily accepted technical sense, for example, on Page 140 "An asymptotic series is an infinite series which converges for a certain number of terms and then begins to diverge." The author's meaning in every case, however, is made perfectly clear.

HENRY E. HARTIG
University of Minnesota

Neuere Arbeiten über Quantentheorie des Atomkerns. F. G. HOUTERMANS. A chapter of volume 9 of Ergebnisse der Exakten Naturwissenschaften. Pp. 123–221. Berlin, Springer, 1930.

After reading this interesting review one is left with the feeling that nothing very definite has come of the application of quantum mechanics to the atomic nucleus other than the interpretation of the Geiger-Nuttall law for radioactivity by alpha-particle emission. This topic, the further speculations of Atkinson and Houtermans on atom building, and the various discussions of the theoretical significance of the mass-packing curve are the principal concern of the report. Spectroscopic evidences of nuclear spin from molecular and atomic spectra are not treated.

E. U. CONDON
Princeton University

Über interstellare Massen und die Absorption des Sternlichtes im Weltraum. FR. BECKER, from volume 9 Ergebnisse der Exakten Naturwissenschaften. Pp. 36, 7 figs. 5 tables. Springer, Berlin, 1930.

This is a good summary of existing knowledge and past work on dark matter in space. The first chapter deals with a study of the positions and extent of obscuring matter, "cosmic clouds" as the author calls them. The criteria which lead to a conclusion of the presence of such clouds rather than the absence of stars in certain regions are described, as is the method for measuring their distances. The paragraphs on the reduction of the observations are a trifle obscure. The next chapter treats the evidence for the presence in interstellar space of ionized calcium, recently studied by Struve. It also includes interesting discussions of Trümplers work on galactic absorption, accounting for the dark central bands seen on edgewise oriented spiral nebulae. Chapter three contains an account of Herschel's diffuse nebulosities and a good critique of Hagen's work on cosmic clouds. The summary is clear and concise.

S. A. KORFF
Princeton University

Fünfundzwanzig Jahre Nernstscher Wärmesatz. F. SIMON, from volume 9 Ergebnisser der Exakten Naturwissenschaften. Pp. 222–274. Springer, Berlin, 1930.

The first publication by Nernst of his heat theorem, now called the third law of thermodynamics, was in December 1905. The twenty-fifth anniversary of this event provides a natural opportunity for retrospect and stock taking. This article by Simon deals with this task, giving especial attention to the present state of opinion and the questions now in the focus of discussion, with the proviso that the interest is throughout physical rather than chemical. In two particulars the article lays a different emphasis from many other articles on the same subject, such as those in the Handbuchs. There is in the first place a full discussion of the application of the third law to physical phenomena in systems of a single chemical substance, such as thermal expansion, surface tension, the melting curve of helium, magnetic polarization (diamagnetics, paramagnetics, and ferromagnetics), dielectric polarization, thermo-electric phenomena, and the degeneration of gases. The second special feature is a careful discussion of the implications of many recently discovered quantum phenomena in the neighborhood of 0° Abs, including in particular those interesting effects known as "Umlagerung" phenomena, and the phenomena connected with the transitions between the two varieties of hydrogen at low temperatures. The article closes with a section written in conjunction with K. Wohl on the theoretical calculation of the entropy of gases, with special regard to spin phenomena, and comparison with experiment.

The subject is one in which great progress has been made in the last few years, and is one with which every physicist must be acquainted and with which every student of thermodynamics must be thoroughly familiar. This article, skillfully written by one who has himself made important experimental contributions, affords the pleasantest means to this end that I have yet seen.

P. W. BRIDGMAN
Harvard University